

**PREDISPERSED SOLVENT EXTRACTION OF COPPER
FROM DILUTE AQUEOUS SOLUTION**


by

Alma Isabel Marín Rodarte

Dissertation submitted to the Faculty of the
Virginia Polytechnic Institute and State University
in partial fulfillment of the requirements for the degree of
Doctor of Philosophy
in
Chemical Engineering

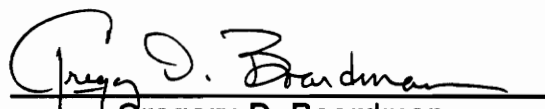
APPROVED:


George B. Wills, Co-Chairperson


William L. Conger, Co-Chairperson


Donald L. Michelsen


Gerhard H. Beyer


Gregory D. Boardman

September 20, 1991

Blacksburg, Virginia

c.2

LD
5655
V856
1991
R622
c.2

**PREDISPERSED SOLVENT EXTRACTION OF COPPER
FROM DILUTE AQUEOUS SOLUTION**

by

Alma Isabel Marín Rodarte

George B. Wills, Co-Chairperson

William L. Conger, Co-Chairperson

Chemical Engineering

(ABSTRACT)

Predispersed Solvent Extraction (PDSE), was used to extract copper ions from dilute acidic aqueous solution. PDSE is based on the principle that there is no need to comminute both phases. All that is necessary is to comminute the solvent phase prior to contacting it with the feed. This is done by converting the solvent into aphrons, which are micron-sized globules encapsulated in a soapy film. Since the aphrons are so small, it takes a long time for the solvent to rise to the surface under the influence of gravity alone. Therefore, the separation is expedited by piggy-back flotation of the aphrons on especially prepared gas bubbles, which are somewhat larger than aphrons and are called colloidal gas aphrons (CGA).

Polyaphrons of various types were studied extensively. The apparatus used to generate the polyaphrons was upgraded. The residence time distribution of a liquid in the polyaphron generator was determined. The particle size distribution of polyaphrons was determined using photo-microscopy and sedimentation among other methods.

Batch tests were done using both conventional and PDSE. Results showed that PDSE approaches equilibrium much faster than conventional extraction. Equilibrium isotherms were drawn and empirical equilibrium relationships were developed. The dynamics of the kinetics of the extraction was modeled using film theory.

Equipment for the PDSE process was built. Experiments were carried out in continuous mode and the process was optimized. An empirical statistical equation was developed for the extraction process in continuous mode. Depending on the aqueous to solvent ration, more than 99% copper can be extracted.

Dedication

I dedicate this dissertation to the memory of my father, Gustavo Arnaldo Marín; my son, Walter Anthony Rodarte; and my late professor, Dr. Felix Sebba. My father taught me to value education and inspired me to go back to school. My son encouraged me to go to school so that I could get a good paying job and buy him "lots of toys". Dr. Sebba gave me the opportunity to pursue a higher degree. His remarkable enthusiasm, unending energy and patience, and invaluable knowledge will always be an inspiration to me. I deeply regret that I was not able to share the joy and pride of completing this degree with them.

I also dedicate this dissertation to my husband, Walter; my daughter, Karla; my mother, Alma; and my brother, Gustavo whose unending love and support has accompanied me always.

Acknowledgements

I would like to thank my committee co-chairmen, Drs. George B. Wills and William L. Conger for their guidance and support during the last two years of this work. Dr. Wills unselfishly accepted to work with me in a project that he had not been involved with previously and he always found the time in his busy schedule to accommodate me. His valuable assistance was essential for the completion of this dissertation. Dr. Conger always managed to find the necessary funds to buy the equipment and supplies needed to do this work and to support me. Whenever I walked into his office to let him know that I needed to buy yet one more thing, he invariably greeted me with a smile and said, "if you need it, buy it." I would also like to thank the other members of my committee, Drs. Donald L. Michelsen, Gerhard H. Beyer, and Gregory D. Boardman for their assistance and helpful comments. Dr. Michelsen always made me feel like a part of his research group. He always invited me to participate in their activities and periodically sent me copies of papers that he felt were relevant to my work. Dr. Beyer's enthusiasm towards my late professor, Dr. Felix Sebba's work is contagious. He is continuously looking for opportunities to inform the public about Dr. Sebba's aphron technology. Dr. Boardman's suggestions were always welcome, not just because of their worth but because they were always made in a manner that reminded me of Dr. Sebba's gentleness and politeness.

Special thanks go to my husband, Walter, who is very much a part of this dissertation. He helped count bubbles, make aprons, and take samples. Also, he took on the household chores of cooking and cleaning house so that I could concentrate on finishing this work.

I am grateful to my friend, Riley Chan, who always went way beyond the call of duty to help me. Whenever a piece of equipment malfunctioned, I needed to use a computer, or any other imaginable problem arose, Riley was always willing to help and he usually solved the

problem. He is also responsible for the drawings of the equipment presented in this dissertation.

I would also like to thank the following persons for providing assistance during the development of this dissertation. Paul Savarese from the Statistics Department for his valuable help with the development of the statistical model of the PDSE process. Dr. Gary Long and Gerald Ducatte from the Chemistry Department for letting me use the AAS. Dr. Long was the first person I found willing to let me analyze kerosene samples with his AAS. I will never forget the first day I showed up with some samples and he told me, "Let me do the first samples. In case we blow up this thing, I would prefer it to be me not you." The personnel of Henkel Corporation who provided the LIX-64N used in this study. Billy Williams and Wendell Brown who provided the support of the Department of Chemical Engineering mechanical shop. Billy built several of the vessels used in this study. Diane Patty, Diane Cannaday, Sandy Simpkins, Sue Stoeckel, and Carol Stables, staff of the Department of Chemical Engineering, who have assisted in many ways over the course of my stay here. Karen Kaster who took on the enormous task of typing the tables and loading this dissertation onto the main frame computer.

As I look back to my years spent at Virginia Tech, I realize that this dissertation is a product of the entire Chemical Engineering Department. At one point or another every research group provided me with the use of a needed piece of equipment, advice, or encouragement. I will never forget the many good friends I have made during my stay here. Thank you Virginia Tech for the opportunity and the wonderful experience.

Table of Contents

1.0 INTRODUCTION	1
1.1 Preamble	1
1.2 Description of the Predispersed Solvent Extraction Process	1
1.3 Research Objectives	3
1.4 Summary of Chapters	4
2.0 LITERATURE REVIEW	5
2.1 Copper	5
2.1.1 Recovery of Copper From Dilute Leach Solutions	5
2.1.2 Copper in Municipal and Industrial Waste Streams	7
2.2 PRINCIPLES OF SOLVENT EXTRACTION OF METALS	10
3.0 EQUIPMENT AND MATERIALS	15
3.1 Continuous Polyaphron Generator	15
3.2 Batch Reactor	15
3.3 Apparatus for Extractions in Continuous Mode	16
3.4 Colloidal Gas Apron Generator	17
3.5 Apparatus used to determine the particle size distribution of the polyaphrons	18
3.6 Atomic Absorption Spectrophotometer	18
4.0 RESIDENCE TIME DISTRIBUTION OF A FLUID IN THE CONTINUOUS POLYAPHRON GENERATOR	24
4.1 Experimental Methods	25
4.1.1 Development of the polyaphron generator	25
4.1.2 Residence Time Distribution	28
4.1.2.1 Tracer Selection	29
4.1.3 Experimental Procedure	30
4.2 Discussion and Results	32
4.2.1 Tracer Selection	32
4.2.2 Operation Difficulties	33
4.2.3 Residence Time Distribution of the Polyaphron generator	34
5.0 DETERMINATION OF THE SIZE DISTRIBUTION OF POLYAPHRONS	47
5.1 Experimental Scheme	47
5.1.1 Design of the Experimental Points	47
5.1.2 Analytical Technique	49
5.1.2.1 Photo-microscopy	50
5.1.2.2 Centrifugal Particle Size Analyzer	51
5.1.2.3 Dynamic Light Scattering	52
5.1.2.4 Coulter Counter	53
5.1.2.5 Lasentec's PAR-TEC 100 Laboratory Analyzer	53
5.2 Discussion and Results	54
5.2.1 Discussion of the Photo-Microscopy Method of Analysis	54
5.2.2 Discussion of the Results from the Photo-Microscopy Measurements	56
5.2.2.1 Effect of mixing rate	57
5.2.2.2 Effect of flow rate	58
5.2.2.3 Effect of phase volume ratio (PVR)	60
5.2.2.4 Effect of surfactant	61
5.2.2.5 Effect of time	62
5.2.2.6 Reproducibility of results	63
5.2.3 Coulter Counter Method of Analysis: Discussion and Results	64

5.2.4	Discussion and Results of Particle Analysis with a PAR-TEC 100 Instrument . . .	65
5.2.5	Discussion of Particle Analysis Using the SA-CP3 Centrifugal Particle Size Analyser	66
5.2.6	Discussion of Results From the SA-CP3 Centrifugal Particle Size Analyser	66
5.2.6.1	Effect of mixing rate	67
5.2.6.2	Effect of feed flow rate	69
5.2.6.3	Effect of the ratio of the volume of the two phases (PVR)	71
5.2.6.4	Effect of surfactant	72
5.2.7	Comparison of the Methods Used to Determine the Particle Size Measurements	73
6.0	CONVENTIONAL VERSUS PREDISPERSED SOLVENT EXTRACTION OF COPPER IN A BATCH REACTOR	121
6.1	Experimental Procedure	121
6.2	Results and Discussion	123
6.2.1	Conventional Extractions	125
6.2.2	Predispersed Solvent Extractions	128
6.2.3	Determination of Equilibrium	131
6.2.4	Correlation of Batch Reactor Data	135
7.0	PREDISPERSED SOLVENT EXTRACTION OF COPPER WITH LIX-64N	221
7.1	Experimental Method	221
7.1.1	Development of Extraction Equipment	221
7.1.2	Design of the Experimental Tests	224
7.1.3	Experimental Procedure	225
7.2	Results and Discussion	228
7.2.1	Determination of Equipment Performance	228
7.2.2	Development of the Statistical Model	231
7.2.3	PDSE Using Different Types of Polyaphrons	234
8.0	CONCLUSIONS AND RECOMMENDATIONS	245
8.1	Conclusions	245
8.1.1	Residence Time Distribution of the Continuous Polyaphron Generator	245
8.1.2	Particle Size Distribution Study	245
8.1.3	Conventional Versus Predispersed Solvent Extraction of Copper in a Batch Reactor	247
8.1.4	Predispersed Solvent Extraction of Copper with LIX-64N	248
8.2	Recommendations for Further Study	249
9.0	SUMMARY	251
9.1	Particle Size Distribution of Polyaphrons	251
9.2	Batch Extractions Using Both Predispersed Solvent Extraction and Conventional Extraction	253
9.3	Predispersed Solvent Extraction of Copper	254
	Literature Cited	255
	Appendix A. Polyaphrons	257
	Appendix B. Colloidal Gas Aphrons	260
	Appendix C. Some Facts About LIX- 64N	263
	Appendix D. Sample Calculation for Determination of Percent of Copper Extracted in the Continuous Process.	265

Appendix E. Sample Preparation for Copper Determination with Atomic Absorption Spectrophotometer (AAS)	267
Vita	268

List of Illustrations

Figure 1. Extraction and Stripping Isotherms for LIX-64N. (Warwick et al., 1970).	14
Figure 2. Schematic of the Continuous Polyaphron Generator.	19
Figure 3. Schematic of the apparatus used to do the batch extractions.	20
Figure 4. Diagram of a trough used in the predispersed solvent extraction process. . . .	21
Figure 5. Schematic of the predispersed solvent extraction process.	22
Figure 6. Diagram of the Colloidal Gas Aphron Generator.	23
Figure 7. Diagram of a typical Continuous Polyaphron Generator	37
Figure 8. Response to the step input into the polyaphron generator for residence time distribution, (A) Test 1, (B) Test 2.	39
Figure 9. Response to the step input into the polyaphron generator for residence time distribution, (A) Test 3, (B) Test 4.	42
Figure 10. Response to the step input into the polyaphron generator for residence time distribution Test 5.	45
Figure 11. Design region of the experimental tests designed. (A) Orthogonal design, (B) non-orthogonal design.	79
Figure 12. Photographs of polyaphron samples from batches (A) B and (B) D.	80
Figure 13. Particle Size Distribution for Batch A (97.9, 9.70, 700), as Determined by Photo-Microscopy. (A) Number of bubbles (%), (B) Weight percent.	81
Figure 14. Particle Size Distribution for Batch B (141.6, 19.1, 700), as Determined by Photo-Microscopy. (A) Number of bubbles (%), (B) Weight percent.	82
Figure 15. Particle Size Distribution for Batch C (197.8, 19.8, 700), as Determined by Photo-Microscopy. (A) Number of bubbles (%), (B) Weight percent.	83
Figure 16. Particle Size Distribution for Batch D (300.0, 29.7, 700), as Determined by Photo-Microscopy. (A) Number of bubbles (%), (B) Weight percent.	84
Figure 17. Particle Size Distribution for Batch E (49.4, 4.9, 1500), as Determined by Photo-Microscopy. (A) Number of bubbles (%), (B) Weight percent.	85
Figure 18. Particle Size Distribution for Batch F (47.2, 4.8, 700), as Determined by Photo-Microscopy. (A) Number of bubbles (%), (B) Weight percent.	86
Figure 19. Particle Size Distribution for Batch G (302.8, 30.0, 1500), as Determined by Photo-Microscopy. (A) Number of bubbles (%), (B) Weight percent.	87
Figure 20. Particle Size Distribution for Batch H (302.4, 20.3, 1500), as Determined by Photo-Microscopy. (A) Number of bubbles (%), (B) Weight percent.	88

Figure 21. Particle Size Distribution for Batch I (302.4, 20.3, 700), as Determined by Photo-Microscopy. (A) Number of bubbles (%), (B) Weight percent.	89
Figure 22. Particle Size Distribution for Batch J (150.3, 30.1, 700), as Determined by Photo-Microscopy. (A) Number of bubbles (%), (B) Weight percent.	90
Figure 23. Particle Size Distribution for Batch K (150.3, 30.1, 1500), as Determined by Photo-Microscopy. (A) Number of bubbles (%), (B) Weight percent.	91
Figure 24. Particle Size Distribution for Batch L (174.5, 20.1, 1100), as Determined by Photo-Microscopy. (A) Number of bubbles (%), (B) Weight percent.	92
Figure 25. Particle Size Distribution for Batch M (174.5, 20.1, 1100), as Determined by Photo-Microscopy. (A) Number of bubbles (%), (B) Weight percent.	93
Figure 26. Particle Size Distribution for Batch N (174.7, 20.1, 1100), as Determined by Photo-Microscopy. (A) Number of bubbles (%), (B) Weight percent.	94
Figure 27. Particle Size Distribution for Batch O (174.7, 20.1, 1100), as Determined by Photo-Microscopy. (A) Number of bubbles (%), (B) Weight percent.	95
Figure 28. Particle Size Distribution for Batch P (46.9, 9.5, 700), as Determined by Photo-Microscopy. (A) Number of bubbles (%), (B) Weight percent.	96
Figure 29. Particle Size Distribution for Batch Q (46.9, 9.5, 1500), as Determined by Photo-Microscopy. (A) Number of bubbles (%), (B) Weight percent.	97
Figure 30. Particle Size Distribution for Batch R (259.2, 25.9, 1500), as Determined by Photo-Microscopy. (A) Number of bubbles (%), (B) Weight percent.	98
Figure 31. Particle Size Distribution for Batch S (267.5, 26.7, 1500), as Determined by Photo-Microscopy. (A) Number of bubbles (%), (B) Weight percent.	99
Figure 32. Particle Size Distribution for Batch A (97.9, 9.7, 700), as Determined by Photo-Microscopy Four Months After the Aphrons Were Made. (A) Number of bubbles (%), (B) Weight percent.	100
Figure 33. Particle Size Distribution for Batch I (302.4, 20.3, 700), as Determined by Photo-Microscopy Four Months After the Aphrons Were Made. (A) Number of bubbles (%), (B) Weight percent.	101
Figure 34. Particle Size Distribution for Batch P (46.9, 9.5, 700), as Determined by Photo-Microscopy Four Months After the Aphrons Were Made. (A) Number of bubbles (%), (B) Weight percent.	102
Figure 35. Particle Size of Polyaphrons, Determined with a Coulter Counter	103
Figure 36. Particle size distribution for Batch H (302.4, 20.3, 1500), as determined by the PAR-TEC 100 Analyzer (A) immediately after testing started, (B) eight minutes.	104
Figure 37. Particle Size Distribution for Batch A (97.9, 9.7, 700), as Determined with the SA-CP3 Analyser. (A) Number of bubbles (%), (B) Weight percent.	105
Figure 38. Particle Size Distribution for Batch B (141.6, 19.1, 700), as Determined with the SA-CP3 Analyser. (A) Number of bubbles (%), (B) weight percent.	106

Figure 39. Particle Size Distribution for Batch C (197.8, 19.8, 700), as Determined with the SA-CP3 Analyser. (A) Number of bubbles (%), (B) weight percent.	107
Figure 40. Particle Size Distribution for Batch D (300.0, 29.7, 700), as Determined with the SA-CP3 Analyser. (A) Number of bubbles (%), (B) weight percent.	108
Figure 41. Particle Size Distribution for Batch E (49.4, 4.9, 1500), as Determined with the SA-CP3 Analyser. (A) Number of bubbles (%), (B) weight percent.	109
Figure 42. Particle Size Distribution for Batch F (47.2, 4.8, 700), as Determined with the SA-CP3 Analyser. (A) Number of bubbles (%), (B) weight percent.	110
Figure 43. Particle Size Distribution for Batch G (302.8, 30.0, 1500), as Determined with the SA-CP3 Analyser. (A) Number of bubbles (%), (B) weight percent.	111
Figure 44. Particle Size Distribution for Batch H (302.4, 20.3, 1500), as Determined with the SA-CP3 Analyser. (A) Number of bubbles (%), (B) weight percent.	112
Figure 45. Particle Size Distribution for Batch I (302.4, 20.3, 700), as Determined with the SA-CP3 Analyser. (A) Number of bubbles (%), (B) weight percent.	113
Figure 46. Particle Size Distribution for Batch J (150.3, 30.1, 700), as Determined with the SA-CP3 Analyser. (A) Number of bubbles (%), (B) weight percent.	114
Figure 47. Particle Size Distribution for Batch K (150.3, 30.1, 1500), as Determined with the SA-CP3 Analyser. (A) Number of bubbles (%), (B) Weight percent.	115
Figure 48. Particle Size Distribution for Batch L (174.5, 20.1, 1100), as Determined with the SA-CP3 Analyser. (A) Number of bubbles (%), (B) weight percent.	116
Figure 49. Particle Size Distribution for Batch P (46.9, 9.5, 700), as Determined with the SA-CP3 Analyser. (A) Number of bubbles (%), (B) weight percent.	117
Figure 50. Particle Size Distribution for Batch Q (46.9, 9.5, 1500), as Determined with the SA-CP3 Analyser. (A) Number of bubbles (%), (B) weight percent.	118
Figure 51. Particle Size Distribution for Batch R (259.2, 25.9, 1500), as Determined with the SA-CP3 Analyser. (A) Number of bubbles (%), (B) weight percent.	119
Figure 52. Particle Size Distribution for Batch S (267.5, 26.7, 1500), as Determined with the SA-CP3 Analyser. (A) Number of bubbles (%), (B) weight percent.	120
Figure 53. Particle size distribution for Batch A (97.9, 9.7, 700), determined with the SA-CP3 Analyzer, 4 months after aprons were generated. (A) Number of bubbles (%), (B) weight percent.	121
Figure 54. Concentration versus time curves of the experimental and film theory values for the conventional solvent extraction of copper in a batch reactor at T=26.0 °C.	142
Figure 55. Concentration versus time curves of the experimental and film theory values for the conventional solvent extraction of copper in a batch reactor at T=26.0 °C.	145

Figure 56. Concentration versus time curves of the experimental and film theory values for the conventional solvent extraction of copper in a batch reactor at T=26.0 °C and pH=2.0.	148
Figure 57. Concentration versus time curves of the experimental and film theory values for the conventional solvent extraction of copper in a batch reactor at T=26.0 °C and pH=2.0.	151
Figure 58. Concentration versus time curves of the experimental and film theory values for the conventional solvent extraction of copper in a batch reactor at T=26.0 °C and pH=2.0.	154
Figure 59. Experimental values of the concentration versus time curves for the conventional solvent extraction of copper in a batch reactor at pH=2.0.	157
Figure 60. Experimental values of the concentration versus time curves for the conventional solvent extraction of copper in a batch reactor at pH=2.0.	160
Figure 61. Experimental values of the concentration versus time curves for the conventional solvent extraction of copper in a batch reactor at T=26.0°C.	163
Figure 62. Experimental values of the concentration versus time curves for the conventional solvent extraction of copper in a batch reactor at T=26.0°C.	166
Figure 63. Concentration versus time curves of the experimental and film theory values for the PDSE of copper in a batch reactor at T=26.0°C and pH=2.0.	169
Figure 64. Experimental values of the concentration versus time curves for the predispersed solvent extraction of copper in a batch reactor at T=26.0°C and pH=2.0.	172
Figure 65. Experimental values of the concentration versus time curves for the predispersed solvent extraction of copper in a batch reactor at T=26.0°C and pH=2.0.	175
Figure 66. Experimental values of the concentration versus time curves for the conventional solvent extraction of copper in a batch reactor at pH=2.0.	178
Figure 67. Experimental values of the concentration versus time curves for the conventional solvent extraction of copper in a batch reactor at pH=2.0.	181
Figure 68. Experimental values of the concentration versus time curves for the conventional solvent extraction of copper in a batch reactor at pH=2.0.	184
Figure 69. Experimental values of the concentration versus time curves for the conventional solvent extraction of copper in a batch reactor at pH=2.0.	187
Figure 70. Experimental values of the concentration versus time curves for the conventional solvent extraction of copper in a batch reactor at pH=2.0.	190
Figure 71. Concentration versus time curves of the experimental and film theory values for the predispersed solvent extraction of copper in a batch reactor at T=26.0 °C and pH=2.0.	193
Figure 72. Experimental values of the concentration versus time curves for the conventional solvent extraction of copper in a batch reactor at pH=2.0.	196

Figure 73. Experimental values of the concentration versus time curves for the conventional solvent extraction of copper in a batch reactor at pH=2.0.	199
Figure 74. Concentration versus time curves of the experimental and film theory values for the predispersed solvent extraction of copper in a batch reactor at T=26.0 °C and pH=2.0.	202
Figure 75. Experimental values of the concentration versus time curves for the conventional solvent extraction of copper in a batch reactor at pH=2.0.	205
Figure 76. Experimental values of the concentration versus time curves for the conventional solvent extraction of copper in a batch reactor at pH=2.0.	208
Figure 77. Equilibrium isotherm for the conventional solvent extraction of copper in a batch reactor at T=26.0°C and pH=2.0.	213
Figure 78. Equilibrium isotherm for the predispersed solvent extraction of copper in a batch reactor at T=26.0°C. and a pH=2.0.	216
Figure 79. Equilibrium isotherm for the predispersed solvent extraction of copper in a batch reactor at T=26.0°C. and a pH=2.0.	219
Figure 80. Schematic of the predispersed solvent extraction process in a batch cell. . .	237
Figure 81. Schematic of the semi-pilot plant unit used for the predispersed solvent extraction experiments.	238
Figure 82. Diagram of the horizontal U-shaped trough used for predispersed solvent extraction tests.	239
Figure 83. Design region of the experimental tests done for the development of a statistical model that predicts the percent of copper extracted.	240
Figure 84. Estimated response surface of the statistical model for the the predispersed solvent extraction process.	241
Figure 85. Actual data values for the tests used to develop a statistical model for the predispersed solvent extraction system.	242
Figure 86. Predicted values from the statistical model for the tests used to develop the model for the predispersed solvent extraction model.	243
Figure A1. Structure of an oil core aphron	260
Figure B1. Structure of a colloidal gas aphron	263
Figure C1. Structure of some LIX molecules	265

List of Tables

Table 1.	Description and Structures of the LIX and KELEX Solvents for Copper Extraction.	13
Table 2.	Description of the tests done for the residence time distribution experiments	38
Table 3.	Concentration readings of the continuous response to the step input into the polyaphron generator for residence time distribution Test 1.	40
Table 4.	Concentration readings of the continuous response to the step input into the polyaphron generator for residence time distribution Test 2.	41
Table 5.	Concentration readings of the continuous response to the step input into the polyaphron generator for residence time distribution Test 3.	43
Table 6.	Concentration readings of the continuous response to the step input into the polyaphron generator for residence time distribution Test 4.	44
Table 7.	Concentration readings of the continuous response to the step input into the polyaphron generator for residence time distribution Test 5.	46
Table 8.	Description of the experimental tests designed to characterize polyaphrons according to size.	76
Table 9.	Average diameter of polyaphron batches determined by photo-microscopy.	77
Table 10.	Density and average diameter of polyaphron batches.	78
Table 11.	Description of copper extraction tests done in a batch reactor using conventional solvent extraction	139
Table 12.	Description of copper extraction tests done in a batch reactor using predispersed solvent extraction	140
Table 13.	Concentration values determined experimentally and calculated from film theory for the conventional solvent extraction of copper in a batch reactor.	143
Table 14.	Concentration values determined experimentally and calculated from film theory for conventional solvent extraction of copper in a batch reactor.	144
Table 15.	Concentration values determined experimentally and calculated from film theory for the conventional solvent extraction of copper in a batch reactor.	146
Table 16.	Concentration values determined experimentally and calculated from film theory for the conventional solvent extraction of copper in a batch reactor.	147
Table 17.	Concentration values determined experimentally and calculated from film theory for the conventional solvent extraction of copper in a batch reactor.	149
Table 18.	Concentration values determined experimentally and calculated from film theory for the conventional solvent extraction of copper in a batch reactor.	150

Table 19. Concentration values determined experimentally and calculated from film theory for the conventional solvent extraction of copper in a batch reactor. . . .	152
Table 20. Concentration values determined experimentally and calculated from film theory for the conventional solvent extraction of copper in a batch reactor. . . .	153
Table 21. Concentration values determined experimentally and calculated from film theory for the conventional solvent extraction of copper in a batch reactor. . . .	155
Table 22. Concentration values determined experimentally and calculated from film theory for the conventional solvent extraction of copper in a batch reactor. . . .	156
Table 23. Experimental concentration values for the conventional solvent extraction of copper in a batch reactor.	158
Table 24. Experimental concentration values for the conventional solvent extraction of copper in a batch reactor.	159
Table 25. Experimental concentration values for the conventional solvent extraction of copper in a batch reactor.	161
Table 26. Experimental concentration values for the conventional solvent extraction of copper in a batch reactor.	162
Table 27. Experimental concentration values for the conventional solvent extraction of copper in a batch reactor.	164
Table 28. Experimental concentration values for the conventional solvent extraction of copper in a batch reactor.	165
Table 29. Experimental concentration values for the conventional solvent extraction of copper in a batch reactor.	167
Table 30. Experimental concentration values for the conventional solvent extraction of copper in a batch reactor.	168
Table 31. Concentration values determined experimentally and calculated from film theory for PDSE of copper in a batch reactor.	170
Table 32. Concentration-time values for the PDSE of copper in a batch reactor.	171
Table 33. Concentration-time values for the PDSE of copper in a batch reactor.	173
Table 34. Concentration-time values for the PDSE of copper in a batch reactor.	174
Table 35. Concentration-time values for the PDSE of copper in a batch reactor.	176
Table 36. Concentration-time values for the PDSE of copper in a batch reactor.	177
Table 37. Concentration-time values for the PDSE of copper in a batch reactor.	179
Table 38. Concentration-time values for the PDSE of copper in a batch reactor.	180
Table 39. Concentration-time values for the PDSE of copper in a batch reactor.	182
Table 40. Concentration-time values for the PDSE of copper in a batch reactor.	183

Table 41. Concentration-time values for the PDSE of copper in a batch reactor.	185
Table 42. Concentration-time values for the PDSE of copper in a batch reactor.	186
Table 43. Concentration-time values for the PDSE of copper in a batch reactor.	188
Table 44. Concentration-time values for the PDSE of copper in a batch reactor.	189
Table 45. Concentration-time values for the PDSE of copper in a batch reactor.	191
Table 46. Concentration-time values for the PDSE of copper in a batch reactor.	192
Table 47. Concentration values determined experimentally and calculated from film theory for PDSE of copper in a batch reactor.	194
Table 48. Concentration-time values for the PDSE of copper in a batch reactor.	195
Table 49. Concentration-time values for the PDSE of copper in a batch reactor.	197
Table 50. Concentration-time values for the PDSE of copper in a batch reactor.	198
Table 51. Concentration-time values for the PDSE of copper in a batch reactor.	200
Table 52. Concentration-time values for the PDSE of copper in a batch reactor.	201
Table 53. Concentration values determined experimentally and calculated from film theory for PDSE of copper in a batch reactor.	203
Table 54. Concentration values determined experimentally and calculated from film theory for PDSE of copper in a batch reactor.	204
Table 55. Concentration-time values for the PDSE of copper in a batch reactor.	206
Table 56. Concentration-time values for the PDSE of copper in a batch reactor.	207
Table 57. Concentration-time values for the PDSE of copper in a batch reactor.	209
Table 58. Concentration-time values for the PDSE of copper in a batch reactor.	210
Table 59. Equilibrium concentrations for conventional solvent extraction of copper in a batch reactor.	211
Table 60. Equilibrium concentrations for the PDSE of copper in a batch reactor.	212
Table 61. Equilibrium parameters for the conventional solvent extraction of copper in a batch reactor.	214
Table 62. Equilibrium parameters for the conventional solvent extraction of copper in a batch reactor.	215
Table 63. Equilibrium parameters for the PDSE of copper in a batch reactor.	217
Table 64. Equilibrium parameters for the PDSE of copper in a batch reactor.	218
Table 65. Equilibrium parameters for the PDSE of copper in a batch reactor.	220

Table 66. Equilibrium parameters for the PDSE extraction of copper in a batch reactor.	221
Table 67. Description of the experiments done to determine a statistical model for the predispersed solvent extraction process.	244
Table 68. Description of the extractions done with different type of polyaphrons.	245

Nomenclature

<i>Arquad 12/50</i>	Trimethyl dodecyl ammonium chloride (Cationic surfactant)
<i>AAS</i>	Atomic Absorption Spectrophotometer
<i>Aq</i>	Aqueous
<i>C</i>	Copper concentration at time <i>t</i>
<i>C_o</i>	Initial copper feed concentration
<i>C_T</i>	Initial tracer concentration
<i>C_{aq}</i>	Copper concentration in the aqueous phase
<i>C_{aqS}</i>	Copper concentration in the aqueous phase determined from a smooth curve drawn through the data points
<i>C_{aq}[*]</i>	Equilibrium copper concentration in the aqueous phase
<i>C_{org}</i>	Copper concentration in the organic phase
<i>C_{orgS}</i>	Copper concentration in the organic phase determined from a smooth curve drawn through the data points
<i>C_{org} (Calc)</i>	Copper concentration in the organic phase calculated by the film theory
<i>C_{org}[*]</i>	Equilibrium copper concentration in the organic phase
<i>D</i>	Diameter
<i>CGA</i>	Colloidal gas aphron
<i>CLA</i>	Colloidal liquid aphron
<i>CSTR</i>	Continuous stirred tank reactor
<i>k</i>	Mass transfer coefficient
<i>K</i>	Equilibrium constant
<i>NaDBS</i>	Sodium dodecylbenzene-sulfonate (Anionic surfactant)
<i>Org.</i>	Organic
<i>PDSE</i>	Predispersed solvent extraction
<i>PVC</i>	Polyvinyl chloride
<i>PVR</i>	Phase volume ratio (volume organic phase/volume aqueous phase)
<i>r.p.m.</i>	Revolutions per minute
<i>RTD</i>	Residence time distribution
<i>Tergitol 15-S-3</i>	Nonionic surfactant

t	time
\bar{t}	Holding Time
V_0	Volume
v	Volumetric flow rate

1.0 INTRODUCTION

1.1 Preamble

Due to depletion of high grade ore reserves, environmental legislation and political factors, increasingly significant proportions of metals production are obtained through hydrometallurgy. In hydrometallurgy, the leaching process is always followed by a separation process to selectively remove components from the mixture. A separation method commonly used is solvent extraction.

In the process of solvent extraction it is important to create a large surface area between the extracting solvent and the feed solution containing the solute in order to achieve rapid approach to equilibrium by facilitating mass transfer of solute across the interface. Although new and improved contactors that employ mechanical energy input to achieve high rates of mass transfer have been developed during the past 40 years, these can be expensive and for very dilute feed solutions the power costs can be significantly high and wasteful. Predispersed Solvent Extraction (PDSE), is a new solvent extraction procedure which has shown promise for extraction from very dilute solution very efficiently and very quickly.

1.2 Description of the Predispersed Solvent Extraction Process

In conventional solvent extraction mass transfer of solute across the interface is achieved by vigorous mixing of the aqueous and solvent phases, followed by a settling stage during which the droplets coalesce; or alternatively by breaking up a stream of one phase as it enters the second. But there is really no need to comminute both phases. In fact, all that is necessary is to comminute one phase and clearly, with energy conservation in mind, that

would be the minor phase, namely the solvent. In PDSE only the solvent phase is comminuted, using mainly surface forces, prior to contacting the feed solution. The process requires the conversion of the solvent into aphrons, (Sebba, 1984), which are micron-sized globules encapsulated in a soapy film which stabilizes them. A concentrate of aphrons containing 90 to 95% oil dispersed in water as the continuous phase is easily made and is known as a polyaphron. Polyaphrons are very stable and can be stored for long periods of time (several years), without deterioration, until they are required for use.

Polyaphrons of high PVR, phase volume ratio, have too much cohesion and take too long to disperse. Therefore, in order to be suitable for PDSE, polyaphrons have to be diluted previously to being used. Since water is the continuous phase in all polyaphrons used so far for solvent extraction purposes, addition of the polyaphron to water breaks it down into individual aphrons that are dispersed in the water.

In the settling stage of conventional solvent extraction the solvent rises because it is lighter than water, and it then coalesces so that in a short time two distinct layers form; the heavier aqueous layer on the bottom with the lighter solvent layer floating on top. In the case of predispersed solvent extraction the solvent is previously aphronized; therefore, the globules are so small that it would take a very long time for the solvent to rise to the surface under the influence of gravity alone. For this reason, separation is expedited by piggy-back flotation of aphrons on specially prepared gas bubbles, which are somewhat larger than aphrons, and are called colloidal gas aphrons (CGA). These, as described by Sebba and Barnett (1981), are 25-50 μm bubbles dispersed to the extent of 60% by volume of gas in water. Since this work was done, an improved method for generating CGA's has been developed by Sebba (1985), using a rapidly spinning horizontal disc mounted between two vertical baffles. The CGA's are made very quickly in this way and can be pumped and metered into the feed solution at any desired rate. They rise more rapidly than aphrons through the aqueous pregnant solution, because of their low density, and in so doing they capture the solvent aphrons which adhere to the outside of the bubble shell. This adherence occurs because the outside of each bubble is hydrophobic because of the orientation of the surfactant molecules

in the encapsulating soap film (Aggarwal et al., 1986). On reaching the surface of the pregnant aqueous phase the bubbles burst, the gas escapes and the solvent remains as a thin layer on the surface.

The possibility of foam formation at any stage of the process can be avoided by an adequate choice of surfactant for the CGA. As reported by Sebba (Nature, 1963), a foam can often be broken by contacting it with a foam of opposite charge. Therefore, taking advantage of this phenomenon, if the polyaphron is made using an anionic surfactant for the encapsulating soapy film, then the CGA that is to be used in the flotation stage should be made with a cationic surfactant. In this manner, the amount of foam that is left floating on the solvent is negligible, provided that the amount of CGA used is not in excess than that necessary to achieve complete flotation.

1.3 Research Objectives

The objectives of this study may be broadly classified as follows:

1. To design and construct equipment used in the predispersed solvent extraction process.
2. To determine the particle size distribution of aphrons.
3. To test the predispersed solvent extraction process as a means of extracting copper ions from dilute aqueous solution.
4. To compare predispersed solvent extraction with conventional extraction.
5. To study the equilibrium and the kinetics of the extraction of copper with LIX-64N.
6. To study the effect of the following process variables on the extraction efficiency of the predispersed solvent extraction process:
 - a. Size of polyaphrons
 - b. Type of surfactant used to make polyaphrons and colloidal gas aphrons
 - c. Volume of polyaphrons added
 - d. Volume of CGA added

1.4 Summary of Chapters

This thesis is divided into 9 major chapters. A summary of the remaining chapters follows.

Chapter 2 contains a review of liquid extraction. The principles of liquid extraction are summarized along with some background and new developments on the recovery of copper.

Chapter 3 gives a description of the apparatus used for predispersed solvent extraction in this study. It also contains a brief description of the instruments used to determine the particle size distribution of the aphrons.

Chapter 4 contains the experimental procedure, results, and detailed discussion of the residence time distribution of a fluid in the continuous polyaphron generator. The chapter also gives a description of the changes made on the polyaphron generator.

Chapter 5 contains the experimental procedure, results, and detailed discussion of the determination of the particle size distribution of polyaphrons. Five different analytical methods are described.

Chapter 6 includes the experimental procedure, results, and detailed discussion of the study of the equilibrium and the dynamics of the approach to equilibrium of the extraction of copper with LIX-64N. The dynamics of the approach to equilibrium are described and modeled using film theory. Equilibrium isotherms are also included.

Chapter 7 contains the experimental procedure, results, and detailed procedure of the predispersed solvent extraction process. A description of the development of the equipment used for the final extraction process is included. Also, the development of a statistical model for the extraction process is described.

Chapter 8 summarizes the conclusions of the study and gives some recommendations for further study.

Chapter 9 contains a summary of the study.

2.0 LITERATURE REVIEW

2.1 Copper

Copper is a useful material with a wide range of applications because of its combination of properties. Because of its excellent electrical conductivity, the electrical industry consumes about 50% of the world copper supply to produce wire for motors, generators, and power distribution and control equipment. As a result of its high thermal conductivity and ease of brazing and soldering, copper is well-suited for radiators, heaters, solar collectors, and heat exchangers. The mechanical properties and corrosion resistance of copper and its alloys make it useful in plumbing and roofing as well as in the chemical, food and automotive industries. Other areas of application are in the fabrication of household articles, art objects, coins and medals, and in military hardware as ammunition.

2.1.1 Recovery of Copper From Dilute Leach Solutions

Copper is produced from three major raw materials: sulfide copper minerals, oxidized copper minerals and scrap metal. These materials are processed pyrometallurgically and/or hydrometallurgically to produce a high-purity electrorefined or electrowon copper containing less than 40 ppm impurities, suitable for all electrical, electronic and mechanical uses. In recent years, in order to avoid air pollution problems posed by conventional smelting operations which are part of the pyrometallurgical process, increased emphasis has been placed on leaching techniques. Since 1965 increased application of leaching technology has had an important impact on copper production. In 1965 leaching yielded approximately 12% of the

United States annual new copper production (Sheffer and Evans, 1968). This increased in 1976 to about 17% (Roman et al, 1980).

The pregnant solutions from leaching operations are of two types according to their copper concentrations: strong, containing 30-50 kg/m³ Cu from vat and agitation leaching, and weak, 1-5 kg/m³ Cu, from in situ, dump and heap leaching. The 30-50 kg/m³ Cu solutions contain copper at sufficient concentration for direct electrowinning of high-purity copper. A more challenging problem is efficient recovery of copper from the weak type of pregnant leach solution since these solutions are too dilute in copper for direct electrowinning of high-purity cathodes. The main method of copper recovery is cementation on scrap steel. This method is simple and efficient but the copper product is impure and it must be sent to a pyrometallurgical smelter for melting and refining.

The development of solvents for extracting copper from acid leach solutions has provided a viable alternative to the cementation process. These solvents permit extraction of copper from dilute leach solutions into an organic phase and production of concentrated copper electrolytes suitable for electrowinning. The electrolytes are prepared by contacting the loaded organics with concentrated sulphuric acid solutions.

Cementation represents a mature technology with almost no effort being made to improve the process except for in-plant operations optimization. Efforts to improve solvent extraction are continuing. These include a search for better organic extractants (e.g., greater selectivity and higher loading capacity for copper, or more rapid phase coalescence) and more effective mechanical systems. In-line motionless mixers are one such mechanical improvement (Merchuk et al, 1980). Alternate copper recovery technologies are also being developed. Possibilities include use of solid ion exchange resins instead of the organic liquids as the copper extractant (Jones and Pyper, 1979), and direct electrolysis of copper from dilute solution. The latter requires cathodes with very high surface areas such as fluidized bed or porous solid cathodes, (Sabacky and Evans, 1979). However, these new approaches have not been commercialized at this point in time.

2.1.2 Copper in Municipal and Industrial Waste Streams

Since copper is such a widely used material, there are many actual or potential sources of copper pollution. Foremost among these are metal cleaning operations, plating baths, and rinses. Copper levels in plating baths can be as high as 50,000 mg/L, while the concentration of the metal in rinse waters is approximately 0.02 to 1% of the process bath concentration (Golomb, 1972).

According to a report prepared by the American Dye Manufacturers Institute (1972), commercial dyes contain from less than 1 to about 80 ppm of tramp heavy metals. These metals get into the dyes from the catalysts that are employed in the preparation of the dyes, and from the raw materials used for synthesizing the dyes. Effluents from textile mills can contain significant levels of heavy metals. The concentration of copper in exhausted dyebath samples taken from several textile mills ranged from 0.03 to 4.2 ppm (Netzer and Beszedits, 1979).

Considerable levels of copper may be present in municipal sewage. The bulk of this copper originates from industrial discharges which find their way into sewage works but Copper piping can also be a significant source. A survey of 100 municipal treatment plants in the states of New York, New Jersey, and Connecticut showed that 5% of the raw waste samples had copper levels eight times higher (i.e., 0.85 mg/L) than the median concentration (Cohen, 1977).

Wastewaters arising from the use of certain wood preservatives also contain copper. For example, copper was found to vary from 0.05 to 1.1 mg/L in the discharge of a wood- preserving plant employing water-based preservatives (Thurlow and Associates, 1977). Effluents from inorganic pigment plants have been found to contain 1.08 mg Cu/L (Barrett et al., 1974).

Numerous techniques are available for the removal of copper from wastewaters. Many of these are established methods, while others are still in the experimental stage. Often a combination of treatment processes is required to obtain the desired quality of effluent. One such system was installed at Beckman Instrument's plant in Porterville, California, which

manufactures printed circuit boards (Warnke et al., 1977). Copper, tin/lead, and gold plating are among the operations at this factory. The treatment system includes pH adjustment, filtration, reverse osmosis, activated carbon adsorption, ion exchange, and solar evaporation. A substantial fraction of the treated effluent is recycled to the plating shop.

Among the experimental methods being presently investigated to remove copper from wastewaters or to recover copper from leach solutions are methods which use liquid membranes. Liquid pertraction or liquid membranes appeared as a prospective separation process relatively recently. Due to its advantages over solid membranes and liquid-liquid extraction, liquid pertraction has attracted the attention of many scientists and engineers. At present there are more than 160 research teams around the world exploring this new, emerging separation operation. The principal idea inherent in liquid pertraction is simple—two completely miscible liquids, the feed and the stripping liquor, are separated by a third immiscible liquid, the membrane phase, usually an organic solvent. The specified component is extracted from the feed due to the favorable thermodynamic conditions set around the feed/solvent interface, and simultaneously stripped by the stripping phase because of the new equilibrium conditions at the solvent/stripping liquor interface.

Liquid-Phase Polymer-Based Retention, a new separation method based on the retention of ions by hydrophilic polymer reagents called polychelators in a membrane filtration system, has been used to successfully separate Cu^{++} ions from other ions at low pH values (Geckeler et al, 1988). Klepac and coworkers (1991) have used ligand-modified micellar-enhanced ultrafiltration as a membrane-based separation technique to selectively remove specific ions from an aqueous solution containing several ions of like charge. In the process surfactant and amphiphilic ligand are added to the contaminated water. The surfactant forms micelles, and the ligand is selected to complex the ion of interest and to solubilize in the micelles. The result is micelles containing a high fraction of the ligand and the target ion. The solution is then passed through an ultrafiltration membrane with pore sizes small enough to block the passage of micelles. Poly[poly(ethylene glycol)phosphate] and poly(ethylene glycol) have been used to develop stable two- component liquid membranes for separating

nickel, cobalt, and copper ions. The properties of these membranes have been compared with the organophosphorous extractants and carriers frequently used in hydrometallurgy (Wodzki et al, 1990).

Several other research groups are investigating the removal of copper from wastewaters by flotation techniques. Caballero and coworkers (1989), have separated Cu from dilute aqueous solution using co-flotation. This process involves the addition of $\text{Fe}(\text{OH})_3$ to the copper solution followed by flotation of the copper with colloidal gas aphanes. The separation is done under basic conditions. Separation yields obtained were higher than those obtained by conventional flotation of solvent sublation. Stalidis et al (1989), have separated copper and zinc as sulfides using precipitate flotation. Precipitate flotation involves the forming of some kind of precipitate and then removing it from the aqueous solution by transferring it to the surface by gas bubbles. Up to 95% of the copper sulfide has been recovered at a high acidic pH region. The concentration of copper, nickel, zinc, and cadmium ions by electroflotation using the ammonium salt of dodecyl dithiocarbamic acid as an anionic collector was examined by Srinivasan and Subbaiyan, (1989). They reported better separation efficiency by this method as compared to column flotation using dodecyl dithiocarbamic acid ligand as a chelating surfactant. The selective precipitation and flotation of copper, zinc, and arsenic ions from dilute aqueous solutions were investigated by Stalidis and coworkers (1989). The ion flotation of copper was carried out by potassium ethyl-xanthate. The air bubbles were generated by dissolved-air flotation, which produces fine bubbles. They reported up to 95% recoveries.

Other researchers are looking into other methods such as anaerobic reduction, and the use of emulsions, zeolites, and silica gel for the removal of copper from wastewaters. The capability of some organisms to anaerobically reduce sulfate to sulphide has been implemented by Barnes et al (1991), to remove heavy metals such as copper from waste waters. The sulphate reducing bacteria is used to convert the water soluble metal sulfates to metal sulphides which precipitate out of the solution. The reactor effluent streams of the process contain H_2S , and therefore require treatment before being discharged. The sludge, which consists of metal sulphides and adhered organisms is treated further to recover the metals

and the sulphur. Vijayalakshmi and coworkers (1990), have shown that it is possible to enhance aqueous metal ion concentrations to a large extent by using suitable microemulsion systems. They extracted bivalent copper into the aqueous core of a water-in-oil microemulsion in equilibrium with an aqueous phase. Kocjan and Przeszlakowski (1989), investigated the sorption of 35 metal ions on silica gel impregnated with a mixture of Aliquat 336 and calconecarboxylic acid. The sorbent was used for the preconcentration of trace amounts of heavy metals from aqueous solutions. They reported that the complexation of metals is relatively rapid, and the relative capacity of the sorbent is different for various metals and increases with pH. The retained metals were eluted from the sorbent with dilute solutions of hydrochloric acid or perchloric acid without elution of the chelating agent.

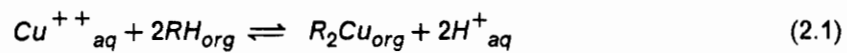
Zeolites from abundant mineral deposits were investigated by the Bureau of Mines for efficiently cleaning up mining industry wastewaters. The zeolites were primarily in the sodium and or calcium form. Aluminum, iron, copper, and zinc were removed from copper mine wastewater to below drinking water standards with clinoptilolite. The calcium content of the wastewater was found to interfere with the uptake of metal ions and greatly increases the amount of zeolite needed to treat a given volume of wastewater. The adsorbed heavy metals were eluted from the zeolite with NaCl solution (Zamzow et al, 1990).

2.2 PRINCIPLES OF SOLVENT EXTRACTION OF METALS

Solvent extraction of metals from solutions received a tremendous impetus from the introduction of selective complexing agents in the 1960's. Today, recovering metals from primary sources and scraps by the use of organic extractants is a well-established process. In the United States, Peru, Chile, and several other countries, solvent extraction is widely used for copper recovery. Consequently, considerable attention has been focused on the use of this technique for the removal and recovery of metals from sludges and even dilute wastewaters.

The most prominent organic solvents for extraction of copper from leach solutions are the LIX reagents produced by Henkel Corporation and the KELEX reagents produced by the Ashland Chemical Company. Both types are chelating agents as is shown by sketches of their structures in Table 1. The solvents are always dissolved (5-20 vol.%) in an organic carrier (e.g. kerosene) to obtain a low viscosity liquid. A modifier is usually added to improve reaction rates or phase separations.

The LIX and KELEX solvents operate by replacing the hydrogen atoms of two solvent molecules with an absorbed copper atom. The general reaction is:



for which the equilibrium constant may be written:

$$K = \frac{C_{R_2Cu}(C_{H^+})^2}{C_{Cu^{++}}(C_{RH})^2} \quad (2.2)$$

or

$$\frac{C_{R_2Cu}}{C_{Cu^{++}}} = \frac{K(C_{RH})^2}{(C_{H^+})^2} \quad (2.3)$$

Equation (3) shows that a low acid concentration (C_{H^+}) in the aqueous phase will result in a high equilibrium proportion of the copper being in the organic phase. A high acid concentration will have the opposite effect. Thus, the organic phase can be loaded with copper from low acid, low copper leach solutions; and stripped of its copper when it is contacted with a concentrated aqueous H_2SO_4 solution. Furthermore, the concentration of copper in the high acid strip solution is many times greater than that in the original leach solution due to the high value of C_{H^+} . This low acid loading and high acid stripping forms the basis of the process.

Figure 1 (A) and (B) show the equilibrium isotherms for LIX-64N under low acid (pH = 2) and high acid ($170 \text{ kg/m}^3 H_2SO_4$) conditions. These isotherms demonstrate numerically the loading and stripping processes for this solvent.

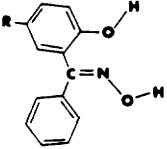
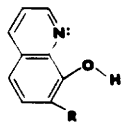
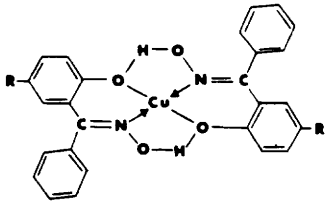
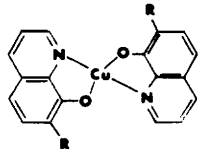
Of equal importance to the equilibrium distributions of copper between the organic and aqueous phases are the rates at which equilibrium conditions are approached and the rates at which the organic and aqueous phases will disengage from the emulsion which is created during the contacting stage. The carriers and modifiers of the organic phase significantly affect these rates.

Equilibrium conditions are closely approached on a laboratory scale after 1-2 min of organic/aqueous mixing. Industrial systems are usually designed to provide 3-4 min of mixing. Rates of approach to equilibrium are increased by raising the temperature of the solutions and by using a carrier of low aromatic content.

The rate of disengagement of the organic and aqueous phases is an important design parameter because it affects the settler area and settling time. Disengagement times are greatly affected by the type of organic carrier and in general, carriers with high aromatic contents (35 vol.%) disengage most rapidly (Murray and Bouboulis, 1973). Disengagement times of 2-6 min and emulsion depths of 0.3- 0.7m provide suitable industrial settling conditions for both the LIX and KELEX systems.

The LIX reagents have been successfully used in industrial practice while the KELEX reagents have only reached the pilot plant testing stage. The development of reagents is continuing with the view of improving extraction and stripping efficiencies. Shimizu and Furuhashi (1984), reported the extraction of copper (II) with 2-(o-hydroxyphenyl)benzothiazole in a water-chloroform system. The extraction constant, K_{ex} , and the rate constant for the reaction were found to be 2.5×10^{-8} and $5.0 \times 10^9 \text{ mol}^{-1} \text{ min}^{-1}$ respectively. Until recently LIX-64N was the most useful for extracting copper from dilute leach liquors. Within the last year, Henkel Corporation replaced the production of LIX 64N for that of LIX-84 and LIX-894 which have been found to extract copper more efficiently.

Table 1. Description and Structures of the LIX and KELEX Solvents for Copper Extraction.

Commercial name	LIX	KELEX
Type	Hydroxy oxime	Hydroxy quinoline
Example	LIX 65N β -hydroxy benzophenone oxime (also the active species in LIX 64N)	KELEX 100 Alkyl- β -hydroxy quinoline (also the active species in KELEX 120)
Molecule (Spink and Okuhara, 1973)	 <p>Molecular weight 339</p>	 <p>Molecular weight 311</p>
Chelated species showing copper position		

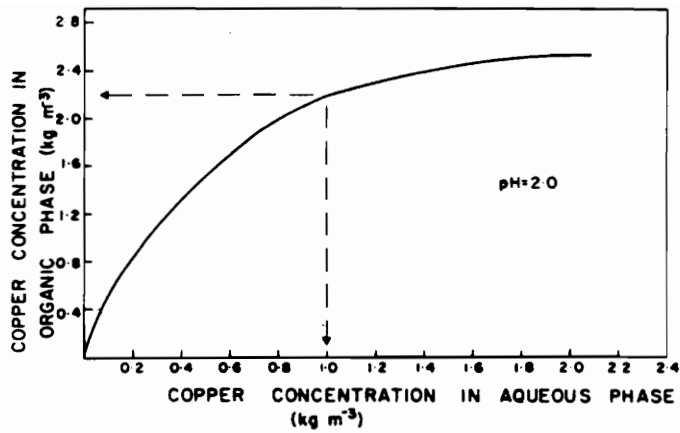


FIGURE (A)

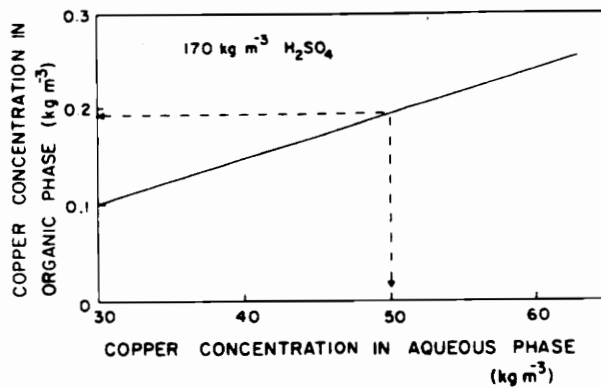


FIGURE (B)

Figure 1. Extraction and Stripping Isotherms for LIX-64N. (Warwick et al., 1970).

3.0 EQUIPMENT AND MATERIALS

3.1 Continuous Polyaphron Generator

The continuous polyaphron generator was fabricated with a 33.0 cm long piece of a 2 3/8 in.-ID, schedule 40 clear PVC pipe. Four feed ports and a vent were located on top of the tube, at 3.5, 9.2, 15.9, 22.9, and 30.6 cm from the end of the tube nearest the feed ports, respectively. An exit port was located below the tube at a distance of 3.2 cm away from the end of the tube furthest away from the feed ports. Four mixing paddles were attached to the 0.25 in. stainless steel shaft. Three of the paddles were 3.8 cm wide and the fourth paddle, positioned closest to the exit port, was 6.3 cm wide. All paddles were long enough so that the outer edges just cleared the tube. The two pumps used to pump the reagents with were Masterflex variable speed peristaltic pumps manufactured by Cole-Parmer. A Masterflex pump head size 13 and one size 16 were used with the aqueous phase pump and the organic phase pump, respectively. A Pacific Scientific 1/2 hp, 2.5 amp motor controlled with a Multi-Drive DC motor speed control was used to rotate the 0.25 in. diameter stainless steel shaft. The shaft r.p.m. were measured with a Metek Digital Phototachometer model 1891. The motor, motor control, and cylindrical tube were supported on a horizontal steel stand. The stand was tilted at an angle of approximately 30 degrees so that the polyaphrons would flow towards the exit port. A schematic of the generator is depicted in Figure 2.

3.2 Batch Reactor

Constant temperature batch extractions of copper were done in the apparatus shown in Figure 3. The apparatus consisted of a 1000 ml two neck round bottom flask immersed in a

water filled refrigerated Fisher reservoir model 730-13R. A model 730, Fisher Scientific constant temperature circulator was added to the reservoir to heat and circulate the water. The mixture in the flask was stirred with a folding, nylon two-blade stirring propeller driven by a stirring motor. Samples were removed from the flask with a Masterflex peristaltic pump and pump head manufactured by Cole-Parmer.

3.3 Apparatus for Extractions in Continuous Mode

The apparatus used to do the predispersed solvent extractions in continuous mode consisted of two identical vessels, an extraction cell and a flotation cell, made of Plexiglas. The cross-sectional area of the ends of the cells was shaped like a trapezoid that measured 58.5 mm on the bottom end, 88.9 mm on the top end and had a height of 152.4 mm and a length of 444.5 mm. The ends of the cells were embedded in rectangular frames 114.3 mm by 203.2 mm. Plexiglas lids 114.3 mm by 470 mm were fixed on top of the frames, above the cells. Six stainless steel tubes were placed inside the cells through holes drilled on the lids. Two of the tubes were J-shaped and one was placed 50.8 mm and the other 101.6 mm from the end of the lid. Each tube was positioned 44.5 mm from opposite sides of the lid. The tubes extended from above the lids to almost the bottom of the cells. Two straight tubes were positioned so that their ends sat about 10 mm above each of the J-shaped tubes. These tubes were used to feed the material into the vessel. All four tubes had 6.4 mm-ID. The other two tubes were placed on the opposite end of the vessel. One, with a 9.5 mm-ID, was placed 38.1 mm from the end of the lid and the other, with a 6.4 mm-ID, was placed 90.0 mm from the end of the lid. Each tube was placed 57.2 mm from the side of the lid. The larger diameter tube extended from above the lid to the bottom of the cell and was used to remove the raffinate. The other tube was long enough to just reach about 25.0 mm into the vessel. This tube was used to remove the extract. Figure 4 depicts a diagram of one of the vessels.

Figure 5 shows a diagram of the entire extraction system. The copper sulfate feed solution was fed through a flowmeter and into the extraction cell through a line that connected to the polyaphron feed line and then divided into two streams before entering the cell through the J-tubes. The diluted polyaphrons were placed in a beaker that sat on a magnetic stirrer. The polyaphrons were also fed through a flow meter and then connected to the feed line. The raffinate was pumped out of the extraction cell through the raffinate tube and into the flotation cell through a line that split into two streams before entering the cell through the two straight tubes. The extract collected from this cell was removed from the process through the extract tube. The surfactant solution used to make the colloidal gas aphrons (CGA) was pumped into the CGA generator through a flowmeter. The CGA were in turn pumped into the extraction cell through a line that split into two streams before entering the cell through the J-tubes. The raffinate and extract were removed from the cell through their respective tubes. All materials were pumped with Masterflex peristaltic pumps.

3.4 Colloidal Gas Apron Generator

To make the colloidal gas aphrons (CGA), a CGA generator such as the one developed by Sebba (1985), was used. The generator consisted of a thin metal disc of approximately 5.0 cm in diameter, mounted horizontally about 2 to 3 cm below the surface of the surfactant solution. The disc was fixed to a vertical shaft connected to an electric 1/2 hp motor. Two rigid baffles made of Plexiglas were mounted vertically and around the disc. The generator is depicted in Figure 6.

To form CGA the disc must spin at more than 4,000 r.p.m.. Once the disc is spinning faster than 4,000 r.p.m., the CGA form almost instantaneously. Thus, the generator can be operated in batch or continuous mode. To operate it continuously all that is necessary are two pumps; one for feeding surfactant solution into the vessel where the CGA are being generated

and the other to remove the newly formed CGA. The vessel can be a 4,000 ml beaker or any other type of container.

3.5 Apparatus used to determine the particle size distribution of the polyaphrons

The particle size distribution of the polyaphrons was measured with the following five apparatus:

A Minolta model M35W 35 mm camera mounted on a Zeiss Axioscope microscope was used to photograph polyaphron samples. A Zeiss MC63A camera control was attached to the camera.

An SA-CP3 Centrifugal Particle Size Analyzer manufactured by Shimadzu Corporation.

A dynamic light scattering system composed of a Lexel Ion Laser model 95, Brookhaven Instruments sample holder assembly model BT-200SM, Detector Unit type TFL serial no. D153, Photo Multiplier Tube RFI-B2F, and a Digital Correlator. The apparatus was mounted on an optical table manufactured by Technical Manufacturing Company.

A Lasentec PAR-TEC 100 Laboratory Analyzer for Particle Size Measurements and an Electrozone-Celloscope model 112LSDADC-80XY manufactured by Particle Data Incorporated. The Electrozone- Celloscope is a coulter counter.

3.6 Atomic Absorption Spectrophotometer

Copper analysis was done with a Buck Scientific M200-A Absorption/Emission Spectrophotometer. The lamp used with the spectrophotometer was a Fisher Type 45458. The lamp cathode was copper and the gas was neon.

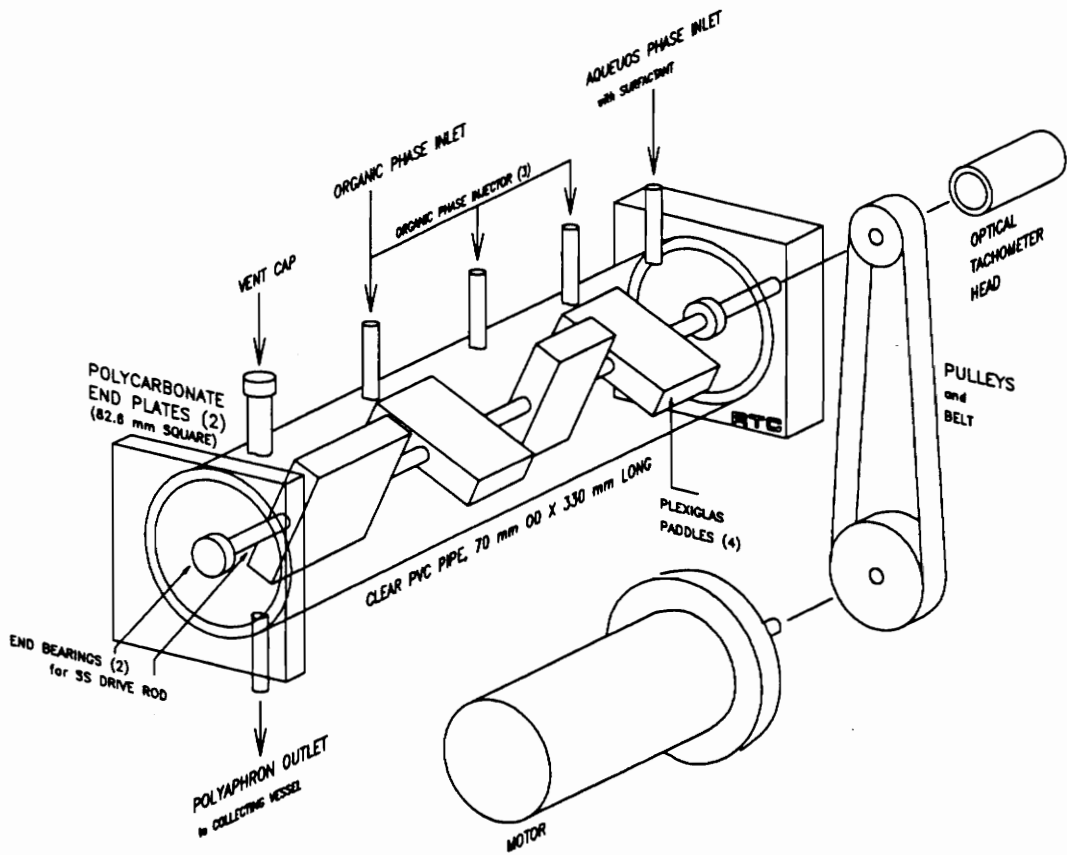


Figure 2. Schematic of the Continuous Polyaphron Generator.

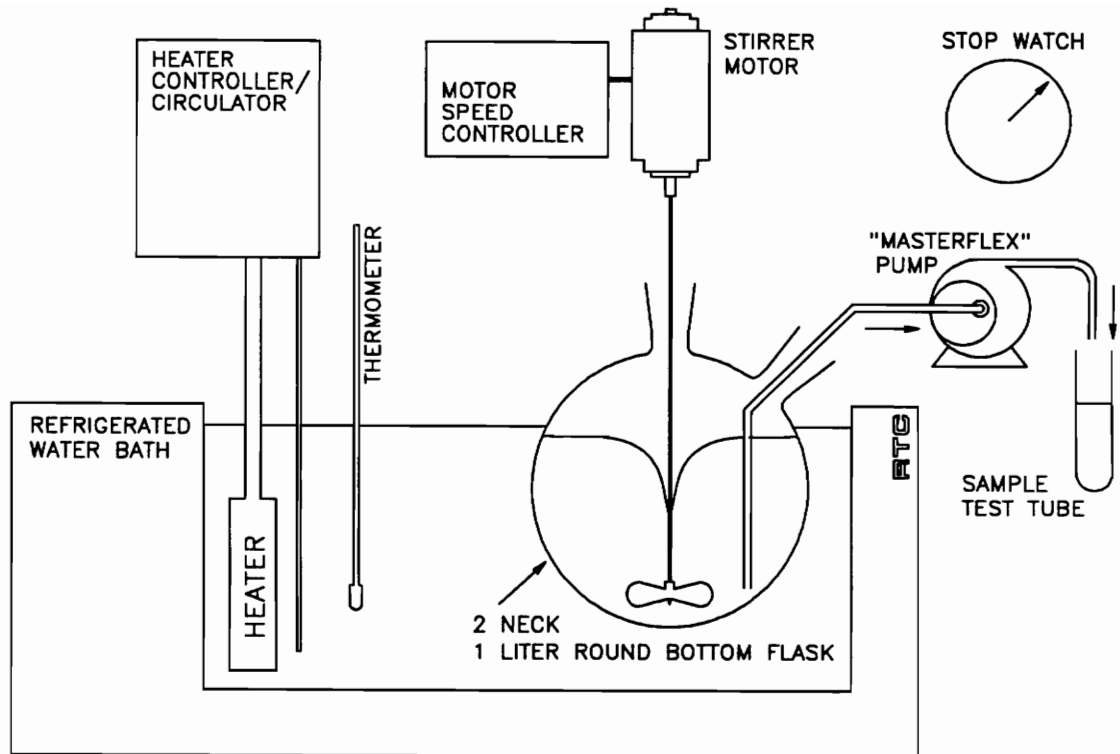


Figure 3. Schematic of the apparatus used to do the batch extractions.

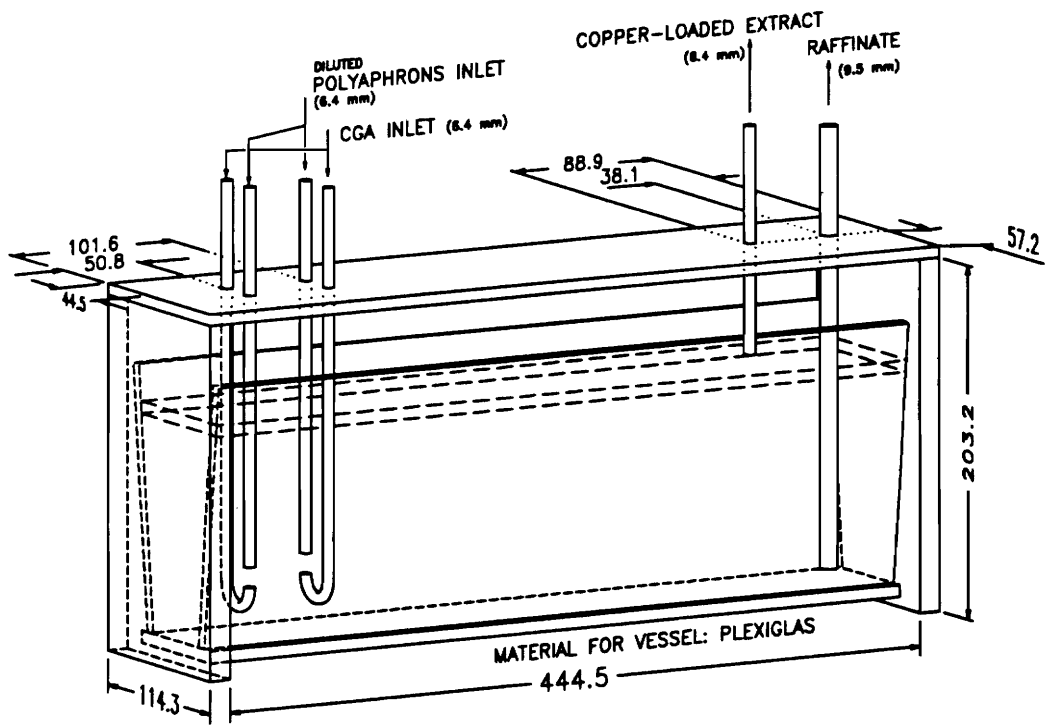


Figure 4. Diagram of a trough used in the predispersed solvent extraction process.

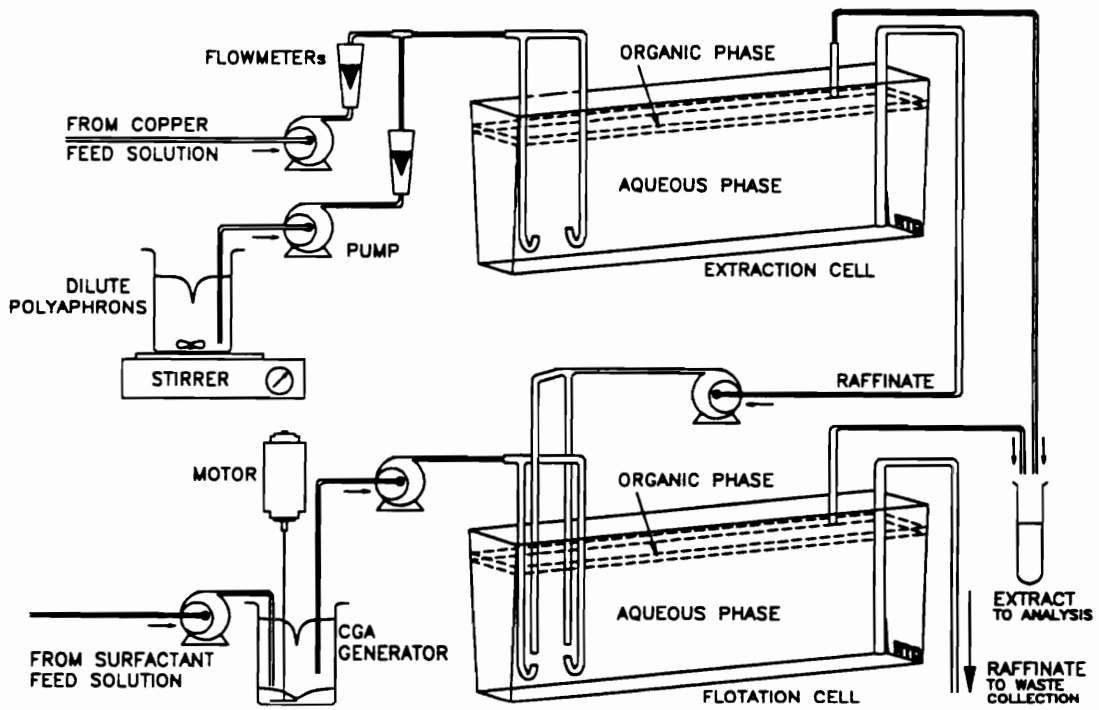


Figure 5. Schematic of the predispersed solvent extraction process.

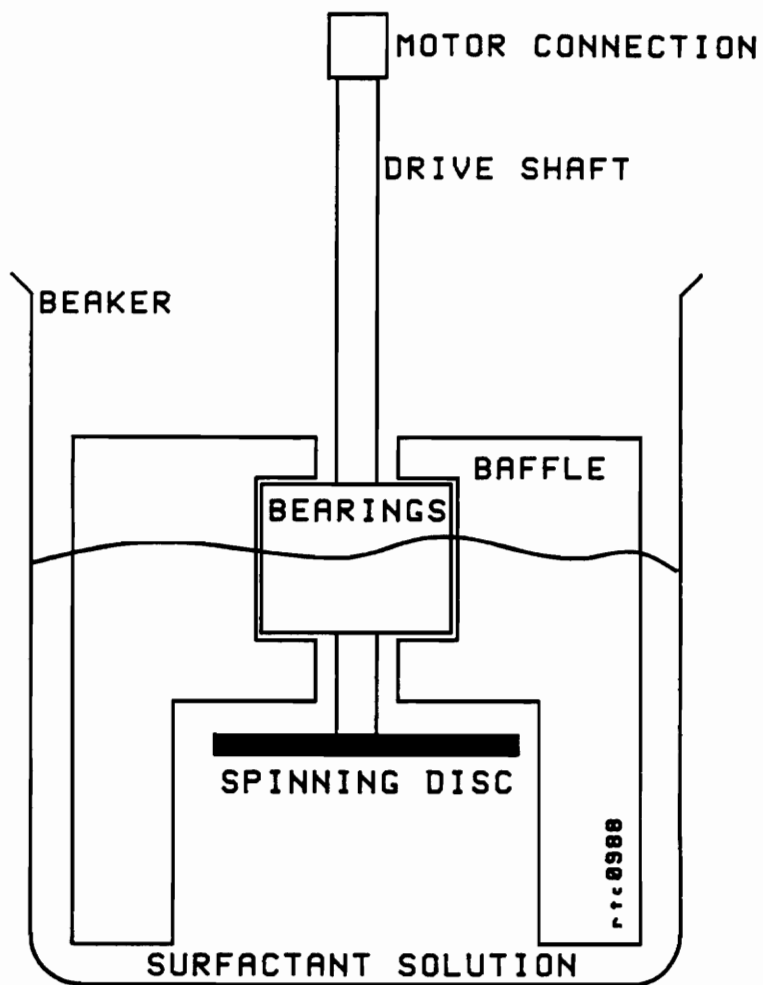


Figure 6. Diagram of the Colloidal Gas Aphron Generator.

4.0 RESIDENCE TIME DISTRIBUTION OF A FLUID IN THE CONTINUOUS POLYAPHRON GENERATOR

Since the development of the current type of continuous polyaphron generator in 1987, the emphasis has been on the fast production of stable polyaphrons. Before 1987, polyaphrons were made solely by hand, a tedious and slow process. The behaviour of the fluid inside the generator was never considered very important as long as good mixing and adequate addition of the two phases, aqueous and organic, were achieved. Since a similar machine with about ten times the capacity of the original one and the scale-down one built for this study are operating successfully, a study of the flow pattern did not become important until it was decided to document the size distribution of polyaphrons and the effect that mixing and flow rates might have on the bubbles' size.

To determine that the size of a particular batch of bubbles made under certain specified conditions was characterized by a specific distribution, one first had to be certain that all the bubbles had indeed been manufactured under such conditions. Polyaphrons were made in a polyaphron generator by first priming the machine with previously made polyaphrons until the tube was approximately one third full. The reason for this was that to produce polyaphrons a large aqueous surface over which the oil was able to spread to a thin film was required. This could not be accomplished with the generator thus it was done by foaming a small volume of aqueous phase in a bottle and then adding oil between shakings. The oil was added first in small quantities, but the amount was increased as the process progressed. This was possible because the globules or aphrons themselves produced additional surface for producing more aphrons. Therefore, once the generator had been primed, it would function continuously for an indefinite time. Naturally, to be certain that all polyaphrons belonging to a batch were made under the same conditions, the operator had to have an idea of how much

of the first made material to discard. For this reason, the residence time distribution of the fluids in the vessel had to be known.

4.1 Experimental Methods

4.1.1 Development of the polyaphron generator

Two polyaphron generators were built to make the polyaphrons used in this study. Both apparatus were constructed similar to the one developed by Bergeron and Sebba (1987). The generators consisted of a cylindrical tube and a rotating shaft centered along the tube axis. Four paddles, perpendicular to the shaft, were attached to the rotating shaft. The paddles were positioned at 90 degree angles with respect to each other. Four entry ports were located on the top of the cylindrical tube; one for the aqueous feed and the other three for the organic feeds. On the bottom of the cylindrical tube and opposite the end where the feed ports were located, an exit port was positioned. A motor with a variable speed drive was used to rotate the shaft which in turn rotated the paddles. The organic and aqueous feeds were added to the system using peristaltic pumps. Figure 7 illustrates a typical continuous polyaphron generator.

The first polyaphron generator was built identical to the one developed by Bergeron and Sebba. The cylindrical tube, tube end plates and paddles were made out of Plexiglas. The 3.5 in. inside diameter tube was 45.7 cm long with a 0.6 cm thick wall. The end plates were approximately 8.9 cm in diameter and fitted inside the tube, sealing the ends. The entry and exit ports were located 3.8, 7.94, 16.0, 26.2, and 43.8 cm from the cylinder end nearest to the feed ports, respectively. All ports were fitted with brass Swagelok fittings to which 5.0 cm long pieces of Tygon special tubing (F-4040-A) were connected. To the opposite end of each tubing, a valve was attached to control the flow of material into and out of the system. The valve leading into the aqueous feed port was directly connected to a Cole-Parmer Masterflex pump

via Tygon tubing. The other three entry port valves were connected to each other with tygon tubing and Y connectors ending in one feed line which was in turn also connected to a Cole-Parmer Masterflex pump via Tygon tubing. A small length of Tygon tubing (5.1 cm) was simply added to the valve positioned in the exit port, allowing the polyaphrons to flow directly into any type of container.

One of the objectives of this study was to try to determine the particle size distribution of the polyaphrons. The polyaphron generator could be operated over a range of feed flowrates and mixing rates. Also, polyaphrons can be made of various phase volume ratios (PVR) and different surfactants can be used to make them. Since all of these parameters could have an effect on the size of the bubbles, polyaphrons made under different conditions had to be manufactured and their bubble sizes determined. This required a large number of different batches of polyaphrons to be made. As the first batch of polyaphrons was being made, it was noticed that a large amount of material was being wasted because the equivalent of at least three times the total void volume of the generator vessel had to be discarded to guarantee that each batch of polyaphrons was indeed representative of a batch made with the specified parameters. In other words, the residence time distribution of the liquids inside the generator had to be considered. This first generator, described in the previous paragraph, had an approximate void volume of 117.2 cu.in. or 1920.6 ml. Therefore, it was considered important to build a smaller apparatus.

Since a new machine had to be constructed, some improvements were made to the older model. The first thing considered was the material with which to construct the cylindrical tube. Previous experience had demonstrated that over time, kerosene, the main component of the polyaphrons used in this study, tended to produce crazing in Plexiglas. The opaqueness of the vessel not only presented a cosmetic problem but also prevented the operator from observing clearly what was going on inside the generator. This can be important, especially during the times in which adverse conditions cause the polyaphrons to break. If this is caught in time, the process can be immediately stopped and avoid the mixing of the broken polyaphrons with the previously collected ones in the sample collector. Also, a clear view

of what is going on inside the vessel allows for observing whether a void volume is forming inside the vessel meaning that the exit flow rate is larger than the total feed flow rates. If insufficient volumes of polyaphrons are inside the generator at any one time, the polyaphrons will immediately break. Another instance in which it is good to be able to see inside the vessel is when it is being washed. Another problem previously observed was that with time, Plexiglas tended to develop stress induced cracks around areas where the tube had been machined to drill feed ports and such. As time went by, these cracks got larger. Eventually the tube could completely crack. Therefore, clear polyvinyl chloride (PVC) was considered a better material to build the generator.

Another problem encountered with the first generator was that its construction made it extremely difficult to take it apart. Occasionally the paddles inside the cylindrical tube became slightly loose on the shaft which resulted in erratic paddle r.p.m. To fix them, the round end caps of the tube had to be removed in order to take out the shaft and paddles. Since the end caps fitted very snugly inside the tube, this was extremely difficult to do. To avoid this problem, the end caps were replaced by end plates. The plates were 8.26 cm squares of polycarbonate with circular grooves drilled on one of the faces of each square. Each groove was large enough to allow for the ends of the PVC tube to fit tightly inside them. Furthermore, another circular groove was drilled inside the first groove to accommodate one O- ring on each end to prevent leaking. The two end plates were secured tightly around the cylinder with four rods that extended from the outer end of one plate to the outer end of the other plate through the four corners of the end plates. Nuts were used to tighten the ends together.

All the polyaphrons used in this study contained LIX-64N, a liquid ion exchange reagent which complexes readily with certain metallic ions such as copper, iron, zinc, and nickel. After making several batches of polyaphrons, all the brass fittings and the valves began to show some degree of discoloration, probably due to leaching. Therefore, the bearings over which the shaft rotated and the shaft itself were replaced with stainless steel bearings and a stainless steel shaft. Oil seals were fitted around the bearings. Also, all the brass fittings were replaced with nylon Swagelok fittings, and the valves removed. The valves had been added

to the apparatus to help control the flow rates but, the aqueous flow rate could be controlled with the pump drive, and the valves used to control the organic flow and the exit flow were not operating adequately. As previously stated, the organic feed line was split into three separate lines before being fed into the vessel. The purpose of the valves was to distribute the organic feed across three feed ports in a predetermined ratio since adding the organic phase too fast through the same point causes the polyaphron matrix to breakdown. It was difficult to achieve this, especially at low flow rates. Therefore, the Tygon tubing at the entrance ports was replaced with nylon tubing. The ends of three pieces of tubing were melted shut and then perforated with a pin. The ends were then attached to the nylon fittings at the entrance ports. The small openings caused the flow to split very well across the three feed ports and as long as too much organic phase did not enter the generator through one of the feed ports, the ratio of the three feeds was found to be unimportant. Finally, the exit valve was also replaced with a long piece of Tygon tubing. The tubing was brought out from under the generator and held at a height above the feed ports with a clamp fixed to a stand. In this manner, gravity took care of regulating the exit flow rate. Lastly, a vent, located on top of the cylindrical tube opposite the exit port, was added to the generator. This vent made it easy to feed seed polyaphrons into the vessel.

This generator, which has a capacity of approximately 865 ml, has been operating for approximately one year and so far has presented no problems and developed no leaks.

4.1.2 Residence Time Distribution

The residence time distribution (RTD) of a system is determined by a stimulus-response technique. The experiment is done by disturbing the system and observing how the system responds to the stimulus. An analysis of the response gives the desired information about the system.

4.1.2.1 Tracer Selection

In any fluid flow system the stimulus is a tracer input into the fluid entering the vessel and the response is a record of the time taken by the tracer to leave the system. Any material that can be detected and which does not disturb the flow pattern of the system can be used as a tracer.

The first material selected as a tracer was bromophenol blue. This chemical dissolves readily in water and very small quantities of it will turn water a deep blue as long as the pH of the water is above 4.6. Deionized or distilled water was used to make the aqueous phase of the polyaphrons; therefore, pH was not a problem. A small batch of colored polyaphrons was successfully made by hand and several samples of them observed under the microscope. The color was not detected under the microscope but at the same time the aphrons did not appear to be affected by the dye. At the time it was thought that the dye concentration could be easily determined with a spectrophotometer using visible light but, this was not possible. Irrespective of the initial concentration of bromophenol blue used, the dye concentration could not be determined because the polyaphrons themselves appeared to absorb all the visible light. Bromophenol blue was obviously the wrong tracer.

The idea of using colorimetry to determine the exit concentration of the tracer was pursued further. A fluorescent dye, fluorescein, was tried next. When the polyaphrons were placed under an ultraviolet lamp, the entire sample glowed, but again, it was impossible to determine dye concentrations using the spectrophotometer. At this point it was decided to try and find a tracer soluble in the organic phase instead of the aqueous one. After all, the volume of the organic phase was several times larger than that of the aqueous phase and if the dye was spread over a larger volume of the aphrons, the colorimetric determination might work. Most importantly, it was decided that a more accurate RTD would be determined by adding the tracer to the larger of the two phases. The first tracer used was waxoline blue, then came waxoline red in various concentrations, and finally UV Ink A946 manufactured by

Polk Corporation, a fluorescent dye. Depending on the dye concentration, different color gradients were detected with the naked eye but it was not possible to find a way to determine actual tracer concentrations. The idea of determining tracer concentration using colorimetry was abandoned.

Finally, it was decided to use copper as a tracer. The polyaphrons needed for this study were to be made with an organic phase containing 10% by volume of LIX-64N in kerosene. The kerosene solution could be previously loaded with copper and the generated polyaphrons could be analyzed for copper content with an atomic absorption spectrophotometer (AAS) if the emulsion could somehow be broken down. This was successfully done by rapidly freezing the polyaphrons to -40°C and then allowing them to warm up to room temperature.

4.1.3 Experimental Procedure

The following experimental scheme was followed for all RTD experiments.

The kerosene solution used as tracer was contacted with an equal volume of a 1g/L copper sulfate solution at pH 2.0 in a stoppered round bottom flask. The two solutions were thoroughly agitated for 10 minutes. The contents of the flask were then poured into a separatory funnel and the organic phase emptied into a bottle. This solution contained a high concentration of copper ions so it was further diluted before feeding it to the generator. A sample of this solution was saved to later determine its copper concentration.

The cylindrical vessel of the polyaphron generator was completely filled with polyaphrons through the vent. The volume of material inside the vessel had to be known to afterwards calculate the RTD. The only way to guarantee no volume change was by maintaining the vessel completely full at all times.

Once the vessel was completely full, the feed lines were removed from the entrance ports and placed inside two different beakers, one containing a LIX/kerosene solution and the other one containing the aqueous solution. The pumps were started and the other end of the feed

lines were inserted in the appropriate beaker in order to recycle the solutions through the feed lines. After letting the pumps run for about 1/2 hour, the flows were adjusted to the desired rates. Flow rates were determined by collecting a certain volume of solution over a timed period.

After adjusting the flow rates, the pumps were quickly unplugged, the feed lines reconnected to the generator, and the pumps restarted. This was done being careful not to touch the dials of the pump drives. Then, a beaker was placed under the exit line to collect the polyaphrons and the motor designed to move the paddles inside the vessel was started. The paddles' r.p.m. was determined and adjusted to the desired rate using a Metek Digital Tachometer.

After everything was adjusted and the generator running smoothly, the feed intakes were measured to make sure the flow rates had not changed appreciably. The system was allowed to run for a few minutes and then the LIX/kerosene feed tank was replaced with a copper/LIX/kerosene tank and a stopwatch started to monitor the time. Samples were taken over time, and the times recorded.

Once all samples were taken, the machine was shutdown, emptied completely, and rinsed out. The samples were then placed in a freezer at -40°C for 3 hours. Afterwards, the frozen samples were removed and allowed to melt at room temperature. If any samples contained unbroken polyaphrons, the freezing routine would be repeated for those samples. Finally, the organic phase of the samples was prepared for analysis and the copper concentration determined with an AAS.

Five RTD tests were conducted under the conditions outlined in Table 2

4.2 Discussion and Results

4.2.1 Tracer Selection

The process of finding an appropriate material to be used as a tracer resulted in more difficulties than had been anticipated. The problem was created by the physical characteristics of polyaphrons. A polyaphron is defined by Sebba (1987) as a high concentration of micrometer-sized oil droplets encapsulated in an aqueous shell. Because of the small size of the individual oil droplets, a sample of LIX/kerosene polyaphrons is not transparent as are the liquids with which they are formed and although a solution of LIX/kerosene is of a pale yellow color, polyaphrons are of a dirty white opaque color. Adding a dye to either the aqueous or organic phases produced colored polyaphrons without any apparent effect on their structure. When the organic phase was colored, the color appeared to be homogeneously distributed through all the aphrons while when the aqueous phase was dyed, the color was not uniformly distributed. This was not surprising since the volume of the aqueous phase was several times less than that of the organic phase and it only encapsulated the oil globules. A color gradient was very apparent when different polyaphron batches were made using different dye concentrations, but the difficulty was in quantifying the color differences. A cell full of polyaphrons acted like a black box which absorbed all the light, visible or ultraviolet, that was transmitted by the spectrophotometer lamp. For this reason, using a dye for tracer was considered impractical.

A material that could be analyzed in some manner other than colorimetry was needed. Copper was an obvious choice since a large part of this study had been devoted to its analysis and at this point kerosene containing copper had been successfully analyzed using an atomic absorption spectrophotometer (AAS). The same problem resurfaced. The sample was no longer kerosene but kerosene aphrons. Samples are suctioned through a very thin tube and passed through an atomizer before entering the burner in an AAS. If the aphrons do not flow

smoothly through the tube, they can cause a pulsating flow through the burner. Variation in sample flow rate is undesirable because it creates fluctuation in the readings. Also, the aphrons were a kerosene/water emulsion and this mixture could possibly produce problems in the burner. Rather than risk damaging the AAS, it was decided to find a way to break the polyaphron matrix.

So as not to complicate the analytical technique, a way of breaking the emulsion without adding other chemicals was sought. First, a sample of polyaphrons was vigorously stirred as it was heated to approximately 35°C. The polyaphrons did not break. Instead of heating the kerosene to higher temperatures, a sample was rapidly frozen to -40°C and left in the freezer for a few hours after which the samples were allowed to warm up at room temperature. After this, most of the matrix broke down. Now it was only a matter of separating the two phases and analyzing for copper. It is conceivable that by breaking the emulsion any of the previously used dyes could have also been used as the tracer.

4.2.2 Operation Difficulties

Other than the tracer problem, the only other problem was created by the Masterflex peristaltic pumps. These pumps were not very accurate and the flow rate tended to vary over a period of time, sometimes quite significantly. Also, although these pumps had a variable speed control drive with a speed control dial, it was practically impossible to set the dial at the same position once it was moved. Anyway, even if this had been possible, from one day to the next without having moved the dial, the pumps would not deliver the same volume of fluid. Therefore, it was useless to try and make a calibration curve for the pumps. As seen from the experimental procedure, every possible step was taken to minimize error. For example, since it was discovered that a greater flow rate fluctuation occurred when the pumps were first started, the pumps were warmed up for at least 1/2 hour. The flow rates were measured before each test even if the same flow rates were required for more than one test.

The flow rates were measured with the feed lines connected to and disconnected from the vessel. By first determining the flow rate with the feed lines disconnected, less material was wasted. Once the desired flow rates were achieved and the feed lines reconnected, a measurement of the fluid intake over time was done to determine whether the flows had changed appreciably.

4.2.3 Residence Time Distribution of the Polyaphron generator

As outlined in Table 2 five RTD experiments were performed. The range of flow rates used, from approximately 2.7 to 30.0 ml/min for the aqueous phase and between 27.0 to 300.0 ml/min for the organic phase, were determined by the upper and lower limits of the pumps. The mixing rate was also determined by the system's limits. 700 r.p.m.'s is the minimum mixing speed needed to form stable polyaphrons and at mixing speeds below 600 r.p.m.'s the polyaphrons will not form. A 1500 r.p.m. upper limit was set because slightly above this speed, the entire generator started to shake uncontrollably. The first four experiments were designed to investigate the fluid behaviour at both the lowest and the highest possible total flow rates (aqueous plus organic) using both the lower and the upper mixing rate limit. A fifth experiment was planned at the center point of all parameters.

The results of these experiments are tabulated in Table 3, Table 4, Table 5, Table 6, and Table 7. Figure 8, Figure 9, and Figure 10 depict a typical downstream signal, called the F curve, in response to an upstream step input signal for an ideal continuous stirred tank reactor (CSTR). For a CSTR,

$$F = \frac{C}{C_T} = 1 - e^{-\theta} \quad (4.1)$$

and,

$$\theta = \frac{t}{\bar{t}}$$

where, F is the F curve, C is the tracer concentration in the exit stream, C_T is the step input tracer concentration, t is the time, and \bar{t} is the holding time which is equal to the ratio of the volume to the volumetric flow rate, $\frac{V_o}{v}$.

Included in the above mentioned figures are also the points that represent the concentration of copper in the exit stream for the experiments done. It is obvious that the behaviour of a fluid inside the continuous polyaphron generator was closely modeled by that of a fluid in a CSTR. This was found somewhat surprising because the fluids were fed into the generator through four different ports at different rates. Behaviour such as that outlined by a tanks-in-series model would have been less surprising. At first it was thought that perhaps the small size of the vessel was responsible for the observed behaviour but later it was concluded that the vigorous mixing that took place inside the generator, even at 700 r.p.m., was probably the one parameter that influenced the fluid behaviour the most. The mixing paddles, constructed long enough so that their outer edges just cleared the generator tube and wide enough so that they extended over the entire length of the tube with a maximum distance of 2.54 cm between any two paddles, and positioned directly under each feed port generated sufficient mixing that the vessel behaved like a CSTR. After concluding this, it came as no surprise that for every RTD test done, the time elapsed between tracer input and tracer response was negligible.

The results obtained from the five original RTD tests planned were sufficient to get a good idea of the fluid behaviour in the generator over the entire range of flow rates, from approximately 2.7 to 30.0 ml/min for the aqueous phase and between 27.0 to 300.0 ml/min for the organic phase, and for mixing rates anywhere between 700 and 1500 r.p.m. From these results it was concluded that for each polyaphron batch generated, a volume equal to four times the total vessel volume of 865 ml would have to be discarded in order to guarantee that all the

polyaphrons belonging to a particular batch had indeed been made under the same conditions.

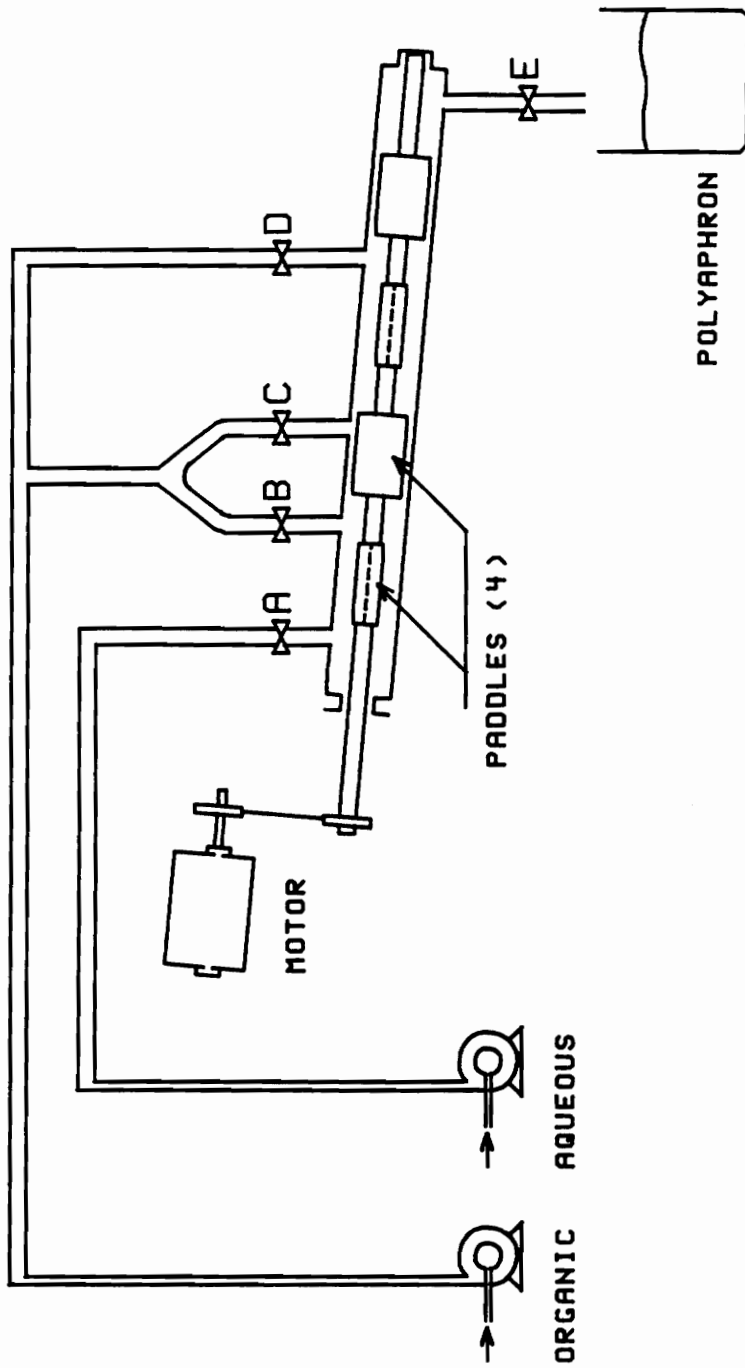


Figure 7. Diagram of a typical Continuous Polyaphron Generator

Table 2. Description of the tests done for the residence time distribution experiments

Test #	Aq. Flow Rate (ml/min)	Org. Flow Rate (ml/min)	Mixing Rate (rpm)	Tracer Conc. (g/L)	V₀ (ml)
1	27.58	273.90	700	0.0820	865
2	27.58	273.90	1500	0.1423	865
3	14.17	151.04	1100	0.5782	865
4	2.70	27.53	700	0.1167	865
5	2.74	27.60	1540	0.0544	865

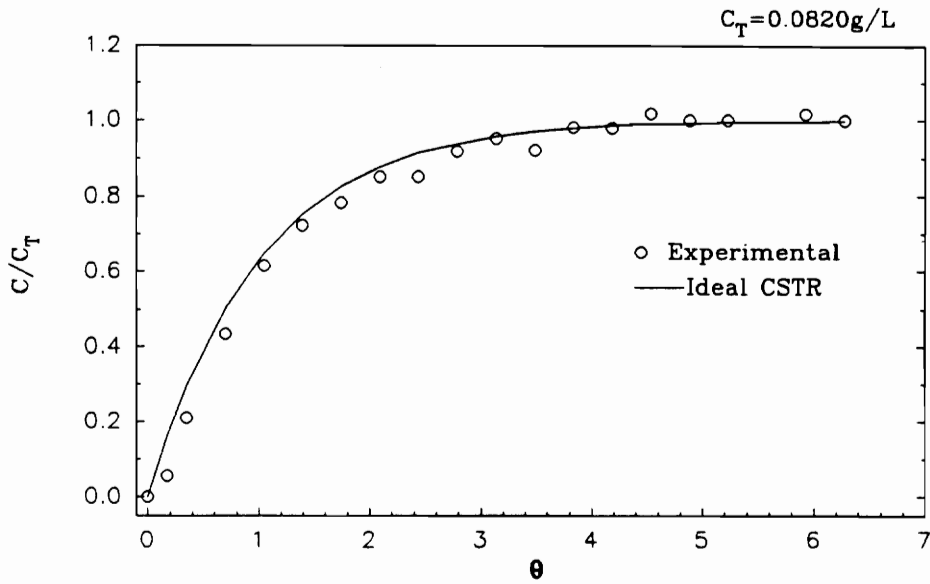


FIGURE (A)

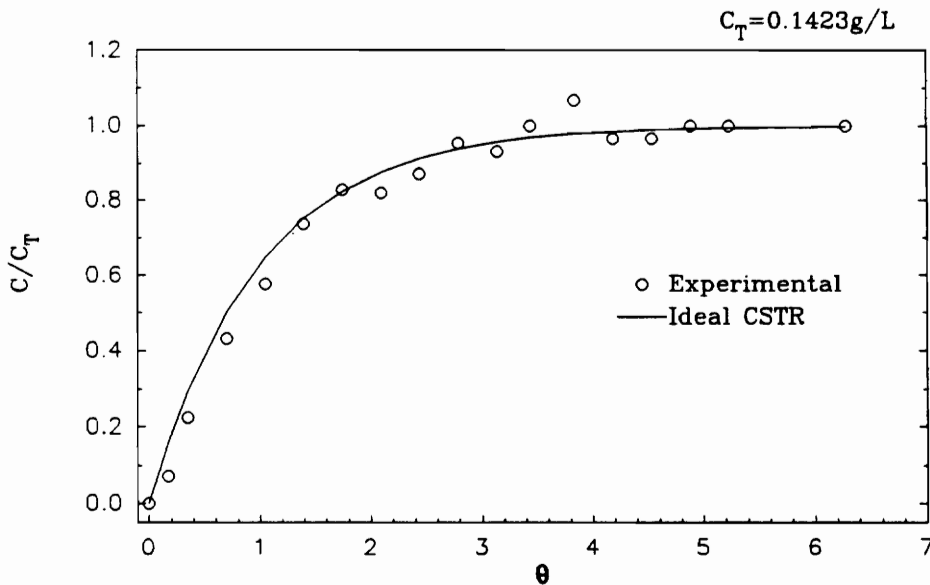


FIGURE (B)

Figure 8. Response to the step input into the polyaphron generator for residence time distribution, (A) Test 1, (B) Test 2.

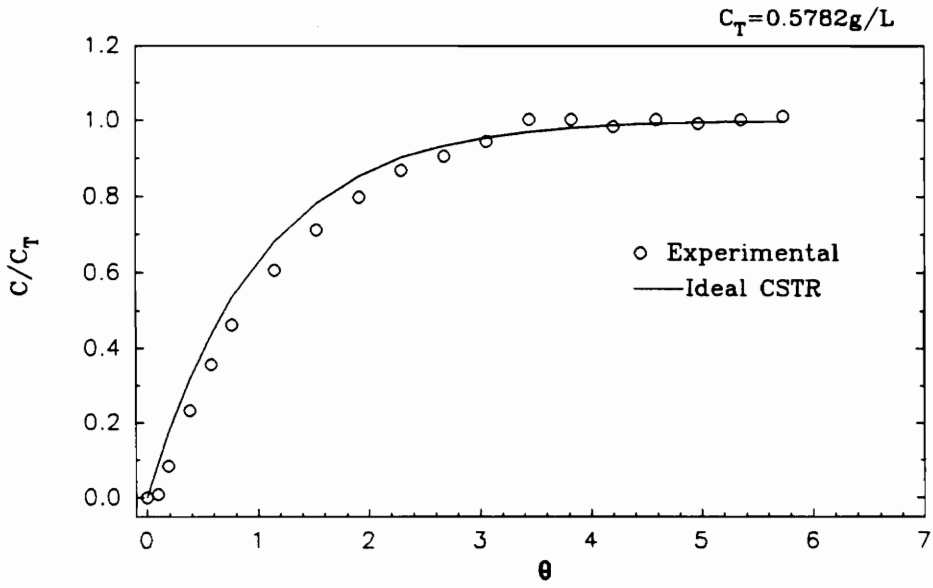


FIGURE (A)

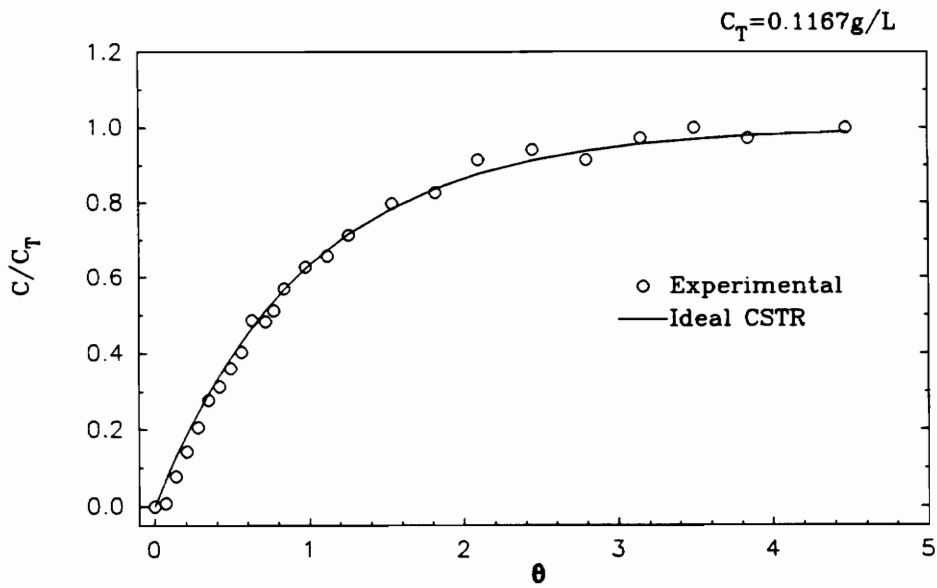


FIGURE (B)

Figure 9. Response to the step input into the polyaphron generator for residence time distribution, (A) Test 3, (B) Test 4.

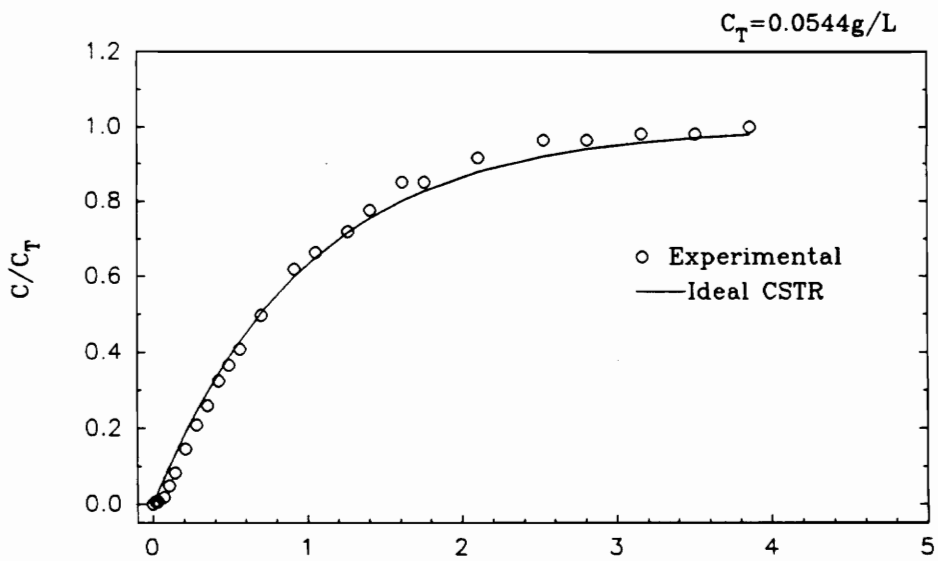


FIGURE (A)

Figure 10. Response to the step input into the polyaphron generator for residence time distribution Test 5.

Table 7. Concentration readings of the continuous response to the step input into the polyaphron generator for residence time distribution Test 5.

Time (min)	C (g/L)	C/C _T	C/C _T (Ideal CSTR)	θ
0.5	0.00036	0.0066	0.0173	0.0175
1.0	0.00035	0.0064	0.0345	0.0351
2.0	0.0010	0.0184	0.0677	0.0702
3.0	0.0027	0.0496	0.0999	0.1052
4.0	0.0045	0.0827	0.1309	0.1403
6.0	0.0079	0.1452	0.1898	0.2105
8.0	0.0114	0.2096	0.2447	0.2806
10.0	0.0141	0.2592	0.2958	0.3508
12.0	0.0177	0.3254	0.3435	0.4209
14.0	0.0199	0.3658	0.3880	0.4911
16.0	0.0222	0.4081	0.4295	0.5612
20.0	0.0270	0.4963	0.5042	0.7015
26.0	0.0337	0.6195	0.5983	0.9120
30.0	0.0361	0.6636	0.6509	1.0523
36.0	0.0391	0.7188	0.7171	1.2627
40.0	0.0422	0.7757	0.7541	1.4030
46.0	0.0463	0.8511	0.8008	1.6135
50.0	0.0463	0.8511	0.8269	1.7538
60.0	0.0493	0.9163	0.8781	2.1045
72.0	0.0524	0.9632	0.9200	2.5254
80.0	0.0524	0.9632	0.9396	2.8060
90.0	0.0534	0.9812	0.9574	3.1598
100.0	0.0534	0.9812	0.9700	3.5075
110.0	0.0544	1.0000	0.9789	3.8583

NOTES: RPM = 1537 - 1549
A_q = 2.74 ml/min
Org = 27.60 ml/min

C_T = 0.0544 g/L
V_o = 865 ml

RESIDENCE TIME DISTRIBUTION OF A FLUID IN THE CONTINUOUS POLYAPHRON GENERATOR

5.0 DETERMINATION OF THE SIZE DISTRIBUTION OF POLYAPHRONS

Although it had not been previously documented, it had been observed in the laboratory that the size of polyaphrons can be dependent on certain variables such as type of surfactant, surfactant concentration, phase volume ratio (PVR), and magnitude of aqueous and organic flow rates and degree of mixing between the aqueous and organic phases during the formation of the polyaphrons. Since transfer of a solute between drops and a continuous phase is affected by the size of the drops, it was important for this study to determine the dependence of the size distribution of polyaphrons on the previously stated variables.

5.1 Experimental Scheme

When doing the residence time distribution tests, a detailed procedure on how to operate the polyaphron generator was developed. To characterize the polyaphrons according to bubble diameter, all that was needed was to decide how many tests to do and how to count and size the individual bubbles.

5.1.1 Design of the Experimental Points

First, the effect of various flow rates and mixing rates were studied. As has been previously explained, the polyaphron generator could be operated over the following range of flow rates: from approximately 2.7 to 30.0 ml/min for the aqueous phase and between 27.0 to 300.0 ml/min for the organic phase. The lower and upper limits for the mixing rate were 700 and 1500 r.p.m., respectively. These boundaries were established by the equipment limitations.

Initially, it was decided to start at the lower end of the flow rate ranges and mixing rate and simply increase these by some factor. Three different batches of polyaphrons were made under the following conditions: one batch with the organic phase fed at a rate of 97.9 ml/min, the aqueous phase fed at 9.7 ml/min, and a 700 r.p.m. mixing rate. From now on this will be represented as (97.9, 9.7, 700). A second batch at (141.6, 19.1, 700), and a third batch at (197.8, 19.8, 700). All aqueous phases were 5 g/L sodium dodecylbenzenesulfonate (NaDBS) in deionized water solutions and all organic phases were 10% LIX-64N in kerosene solutions. The second batch was an error. The organic flow rate was intended to be 197.8 ml/min but afterwards it was determined that an error had been made when calculating the flow rate.

At this point, it came to the author's attention that the number of experiments needed for a particular study can be diminished by using a statistical approach when deciding what experiments to do. First, a design region representing the variables to be studied was drawn. Since there were three variables, two flow rates and one mixing rate, the design region was three dimensional. The boundaries for this design region had to be defined. For this case, these boundaries were the same boundaries previously established by the equipment limitations. Figure 11 (A) depicts an ideal orthogonal design region where the X-axis represents the organic flow rate, the Y-axis represents the aqueous flow rate and the Z-axis represents the mixing rate. With this type of region, the parameters at each corner define the conditions for each test. Also, two or three center runs are defined. The center runs help to establish reproducibility. When it came to generating polyaphrons, the orthogonal design region was impractical because tied to the ratio of the flow rates was the phase volume ratio or PVR. PVR is a useful way to describe polyaphrons and it is the volume ratio of the dispersed oil phase to the continuous aqueous phase. It has become customary to make and study polyaphrons with whole number PVRs, more specifically of PVR 5, 10, and 15. Also, polyaphrons of PVR below 5 and above 15 tend to be less stable, with a substantial amount of the aqueous phase of the ones below PVR 5 separating out of the emulsion matrix within 1 hour or sooner of their having been made. According to the orthogonal design region, polyaphrons of PVR 1.63 and 75 had to be made and polyaphrons of PVR 75 are impossible to make.

A new, non-orthogonal design region shown in Figure 11 (B) was drawn. In this case, a two-dimensional figure was drawn with the organic flow rate on the X-axis and the aqueous flow rate on the Y-axis. A rectangle encasing the design region and lines going through the points where the ratio of the two phases are equal to 5, 10, and 15 were drawn. The points where the lines cross the rectangle represented the tests needed. Since this was a two-dimensional representation of the design region, the mixing rate had not been depicted. Every point represented in the graph was done at 700 and 1500 r.p.m. Also, some center runs were made.

After studying the effect of flow rates, mixing rates, and PVR, a couple of experiments were run to see the effect that surfactants have on the polyaphrons. One polyaphron batch was made with a 5 ml/L of Arquad 12/50 in deionized water solution and an organic phase of 10% LIX-64N in kerosene. The other batch was made with an aqueous solution of 5 g/L NaDBS and an organic solution of 1 ml/L Tergitol 15-S-3 in a 10% LIX-64N in kerosene mixture. In Table 8 all the experimental tests performed to characterize polyaphrons according to size are tabulated.

5.1.2 Analytical Technique

The particle size distribution of foams and biliquid foams is not easily determined. Several apparatus that are supposed to determine the sizes of solid particles exist in the market today. Unfortunately, when it comes to liquid particles, any external forces acting on the particles can easily cause coalescence between the bubbles or breakage of the foam matrix. When considering any technique to determine the size distribution of a batch of polyaphrons, a type of biliquid foam, it was important to consider the possibility that the technique itself might have affected the size of the bubbles.

5.1.2.1 Photo-microscopy

Photo-microscopy is described as the process of photographing a sample through a microscope lens. This is the technique most commonly used to determine size distribution of liquid particles. The advantage of it is that no external forces act on the particles, therefore, it is unlikely that the particle size is affected. The process though is tedious and time consuming.

A Zeiss Axioscope microscope together with a 35 mm Minolta M35W camera and a Zeiss MC63A camera control were used to photograph samples of polyaphrons. The camera control determined the shutter speed based on the light shining through the sample. Two sample holders were fabricated by gluing a sheet of 1/32 in. thick PVC to each of two 75 by 25 mm plain glass microslides. From the center of each PVC sheet a 10 by 10 mm square had been cut out. Samples were prepared as follows. One drop of polyaphrons was transferred from a polyaphron container to the window of one of the microscope slides with a disposable polyethylene pipet. Enough deionized water to fill the cavity in the microslide was added. The solution was carefully stirred with a stainless steel microspatula to spread the polyaphrons on the water. A microslide cover was placed over the sample and the slide placed under a 40 magnification lens attached to the microscope. The image was manually focused and then a picture taken. Sometimes the bubbles would be moving rapidly, probably due to the stirring action, and the picture was not taken until the movement stopped. Several samples were prepared from each batch of polyaphrons. One picture was taken of each sample. Ideally it was intended to take six pictures of each batch, but at times some pictures had to afterwards be discarded because of poor image and other times more pictures were taken from some batches to use all the film. Film could not be left in the camera since other people had access to it. With every roll of film used, two pictures were taken of the scale on an American Optical Company micrometer. The scale was divided into units of 0.01 mm. This scale was used to determine the actual bubble sizes.

After developing the film and printing the pictures, the bubbles on the pictures were counted and their diameter measured with a metric circles template. The diameter of circles in the template ranged from 2 to 30 mm. Every bubble in each picture was sized by placing the template over the bubble and finding the circle that was approximately the same size as that of the bubble. Any bubbles with diameters smaller than 2 mm were counted together. This method of sizing the bubbles was found easier and quicker than measuring the diameter of each bubble with a ruler.

5.1.2.2 Centrifugal Particle Size Analyzer

Since the photo-microscopy method was very time consuming, other methods to determine the bubble sizes were considered. One of these methods was the use of a Shimadzu Centrifugal Particle Size Analyzer model SA-CP3.

The Shimadzu Centrifugal Particle Size Analyzer SA-CP3 utilizes the sedimentation method and detects particle concentration photometrically. The sedimentation method of particle size measurement is widely used because results are reliable, reproducible and operations are comparatively easy. The photometric method is a desirable means of detection since no contact with the particles is required and the sedimenting system is undisturbed. The analyzer was equipped with a rotational mechanism to generate a centrifugal force for accelerated sedimentation but both gravitational and centrifugal sedimentation could be used. Furthermore, size measurement of particles which are lighter than the dispersing liquid was possible by means of the centrifugal lift mode. A built-in microcomputer converted the change in particle concentration detected by the photometric system into the particle size distribution and printed out the result.

This type of analyzer is widely used to determine the size of solid particles but according to the manufacturer it was not developed to size liquid drops. Therefore, Shimadzu was unable to provide the author with information about the reliability of the results, but suggested to try it anyway.

Samples were prepared by pouring 4 ml of distilled water into a 7.4 ml glass vial. One drop of polyaphrons, measured with a polyethylene disposable pipet, was dispersed in the water. The vial was stoppered with a polyethylene cap and the mixture gently shook. The analyzer's glass cell was filled completely with the mixture, and the cell cap carefully inserted in the cell so that no air bubbles remained inside the cell. The excess mixture would spill out of the cell as it was capped and the outside of the cell was afterwards wiped clean with kimwipes making sure that no fingerprints were left on the glass. The cell was then placed inside the cell holder which was positioned in a centrifuge disk mounted inside the measuring chamber of the apparatus. The chamber door was then closed and the machine started. The analyzer was set on the centrifugal lift mode since the polyaphrons were less dense than water. The centrifuge speed was set at an acceleration rate of 120 r.p.m./min. To determine the particle size, the density of the particles had to be entered into the analyzer's computer memory. The density of the polyaphrons was determined by weighing a 5 ml volume of aphrons. Depending on the particle sizes, it took anywhere from 15 minutes to 3 hours to do each sample. A minimum of two tests was done for each of the first 6 polyaphron batches, and 6 tests were done for each of the remaining batches.

5.1.2.3 Dynamic Light Scattering

Another analytical technique considered to determine the particle size of polyaphrons was the use of dynamic light scattering. The instrument consisted of a Brookhaven BI-2030AT digital correlator equipped with 136 channels and a 2 Watt Lexell Argon Ion model 95-2 laser.

The sample preparation required that all solutions be filtered prior to doing the measurements. A sample consisting of two drops of polyaphrons dispersed in distilled water was filtered twice through a 0.5 μm PTFE acrodisc Gelman filter. The solutions were withdrawn with a sterilized plastic disposable syringe and were forced out through the filters placed at the tip of the syringe. The solution had to be filtered to guarantee that it was free of dust particles since these particles are detected and measured by the instrument. When the

polyaphron mixture passed through the filter, the kerosene phase spread on the filter itself breaking down all the bubbles, i.e. all the kerosene was absorbed by the filter. Inspection of the filtered solution under a microscope showed that it contained no bubbles. The idea of using dynamic light scattering to do the particle size analysis was abandoned.

5.1.2.4 Coulter Counter

Coulter counters use the drop in electrical current across the cross-sectional area of a tube to determine particle sizes. At approximately the center of the tube, its cross-sectional area is reduced. A flow of liquid, an electrolyte, moves through the glass tube at a constant velocity. As the fluid passes through the narrowed area of the tube, the electrical current across that area is measured. The amount of current is directly proportional to the volume of electrolyte flowing through the tube. When particles are dispersed in the electrolyte, they displace a volume of liquid equivalent to that of their size. As the liquid flows through the narrowed area of the tube, the current drops according to the size of the particle moving with the electrolyte. The current drop is used to determine the particle size. Depending on the size of the particles, tubes of different diameters are used.

An Electrozone-Celloscope model 112LSDADC-80XY manufactured by Particle Data Incorporated was used to measure the particle size of three polyaphron samples. The samples were prepared by diluting 10 ml of polyaphrons in each of three 50 ml solutions of 1%, 3%, and 4% sodium pyrophosphate, the electrolyte. The Electrozone-Celloscope was interfaced to a computer which gathered the electrical current measurements and converted them to particle sizes.

5.1.2.5 Lasentec's PAR-TEC 100 Laboratory Analyzer

The particle size measurements had been completed when the author came across an advertisement of a particle size analyzer manufactured by Lasentec. When the manufacturer

was contacted, the technical representative claimed that this particular instrument was capable of determining size distribution of emulsions very quickly and without previous sample preparation. A demonstration was scheduled.

The PAR-TEC 100 operates using Scanning Laser Microscope technology which consists in focusing a laser beam at the focal point of a very small beam spot with a light intensity higher than 1,000,000 watts per square inch. The system counts only those particles going through the focal point and not those which are in front of or behind the focal point. The laser beam is scanned at a fixed velocity and the amount of time it takes for the beam to scan across a particular particle is a direct measure of the size of that particle. The laser beam is scanned very rapidly to avoid the effect due to changes in flow. The system is interfaced to a computer that does all the data handling, display, analog outputs, and print-outs.

The measurements were done as follows. After assembling the machine, approximately 200 ml of polyaphrons were poured into a 500 ml beaker. 300 ml of deionized water was added to the beaker. A stirring bar was dropped into the beaker and the beaker placed on a magnetic stirrer. About 2 in. of the end of the probe body, which contains the laser and photo detectors, was placed inside the beaker. After about 5 minutes, a particle size distribution curve was displayed on the computer monitor and the results printed.

5.2 Discussion and Results

5.2.1 Discussion of the Photo-Microscopy Method of Analysis

As mentioned in the experimental section, the microslides used as sample holders were made by gluing a 1/32 in. thick of PVC over the slide. A window cut out of the center of the PVC sheet served as the cavity that contained the polyaphron sample. These microslides were made because slides such as the hanging drop ones were found inadequate. The thinnest hanging drop slides have concavities 0.5 mm deep with the slide itself being some-

where between 1.4 to 1.6 mm thick. When a sample was observed under the microscope, the microscope was focused by adjusting the height of the objective with respect to the lens. Therefore, a sample could be viewed over a range of depths. It is possible that the depth at which the samples were viewed affected the size distribution of the particles because depending on their size, bubbles display different degrees of buoyancy. In order to minimize error, it was decided to build a sample cell with a thinner window. These cells worked adequately.

Irrespective of the size or depth of the cavity in the microslide, the area that was viewed with the microscope lens at one time was much smaller than the sample area. Therefore, each photograph taken represented only a small section of each sample. How representative each photograph was of the entire sample was difficult to assess. Usually, the entire surface of the sample was scanned and the decision of what area to photograph was dependent on the appearance of the bubbles in a particular area. For example, areas that had few bubbles or areas where the bubbles were still agglomerated were automatically discarded. Also, areas where the bubbles were moving were not selected. The movement was typically observed across the entire sample when the sample was first viewed under the microscope, but after two or three minutes most of the bubbles appeared to have stopped moving except for the ones in areas that were close to the edges of the cell cavity. With time, the bubbles must have continued to move, although slowly, because a sample left under the microscope for 30 minutes or longer would start to show a pattern in which the aphrons appeared to be clustered together according to size, with the larger ones positioned in the center of the cell and the smaller ones towards the edges. Since the photographs were taken within the first three or four minutes after the samples were placed in the microslide, each photograph contained bubbles of a variety of sizes. Two typical photographs of aphrons can be seen in Figure 12.

Regardless of the method used to size the bubbles, the polyaphrons were always dispersed in water. Polyaphrons, an aggregate of aphrons, have too much cohesion. A complete description of the forces that operate when aphrons aggregate is not yet known, but at the interfaces the forces are probably the Laplace forces. Due to the high cohesion of the

aphrons, a sample of polyaphrons viewed under the microscope is seen as one continuous body. To see the individual aphrons, the polyaphrons were dispersed in water. Since water was the continuous phase, addition of the polyaphrons to water broke the polyaphrons into individual aphrons.

Photo-microscopy is probably as adequate as any other method which currently exists to do particle size measurements of polyaphrons. The biggest drawback is the time consuming process of counting and measuring the bubbles manually. This problem can be solved with the use of image analyzing. Unfortunately, the instruments needed for image analyzing can be expensive and we lacked the funds to buy them for this project.

5.2.2 Discussion of the Results from the Photo-Microscopy Measurements

Figure 13 (A) to Figure 34 (A) represent the percent of the number of bubbles counted versus the diameter for 19 different polyaphron batches. The data was collected using photo-microscopy. The average diameter for each batch is displayed in each figure. The average diameter was calculated by summing the products of the number of bubbles times their respective diameter and, dividing the summation by the total number of bubbles counted. Figure 13 (B) to Figure 34 (B) represent the weight percent of the aphrons versus the diameter. The weight percent of the aphrons was calculated using the data collected for Figure 13 (A) to Figure 34 (A) and the density of each batch of aphrons. An average diameter for each batch is also displayed in each figure. These diameters were calculated by summing the products of the weight percent times the respective diameter and dividing the summation by 100.

Because of the relatively small size of each sample compared to the volume of polyaphrons in each batch, the bubbles from at least 5 photographs were counted and measured for each batch except for batch D. Each figure in this section represents the summation of all data collected for each batch. Batch D was made at an organic feed flow rate of 300.0

ml/min, an aqueous feed flow rate of 29.7 ml/min and a mixing rate of 715 r.p.m., represented as (300.0, 29.7, 715). The data from only 3 photographs was gathered to determine the size distribution of this batch because each of these photographs contained an unusually large number of bubbles, at least 800, while the photographs of other samples contained on an average around 300 bubbles.

5.2.2.1 Effect of mixing rate

In Table 9 all polyaphron batches made are tabulated, along with the value of the conditions at which they were generated and the average diameter as calculated by photomicroscopy. A comparison of the results obtained for batches D (300.0, 29.7, 715) and G (300.0, 30.0, 1500), which can be seen in Figure 16 (A) and Figure 19 (A), respectively, show that the average diameter for batch D, at 6.72 μm was slightly larger than that for batch G at 6.48 μm . More importantly, batch G, made at the same feed flow rates but at the higher mixing rate of 1500 r.p.m., had a lower percent of bubbles of diameters greater than 14 μm than batch D. Both batches had approximately the same percent of bubbles with diameters less than 5 μm , around 43% for batch G and 44% for batch D. In the weight percent versus diameter data for batches D and G the difference in the number of larger bubbles is more evident. Batch G showed no weight percent contribution from bubbles with diameters greater than 15 μm , while batch D showed a weight percent of 13 for the same diameter range. 49% of the total weight was due to bubbles with diameters between 10 and 15 μm for batch G and 38% was contributed by the same diameter bubbles for batch D.

Inspection of Figure 17 and Figure 18, which represent the data for batches E (49.4, 4.9, 1480) and F (47.2, 4.8, 705), respectively, show the same behaviour. The average diameter of the particles from batch F was 7.39 μm and that for batch E was 6.58 μm . The higher r.p.m. batch, batch E, had approximately 48% of bubbles with diameters lower than 5 μm while for batch F only 41% of the bubbles were below 5 μm . Also, batch E had a smaller percent of bubbles larger than 14 μm than batch F. This again is more evident in the Weight Percent

graphs. From these graphs it is seen that at a diameter above 15 μm the weight percent of batch F was about 46 and that for batch E was about 37.

These same results were made for batches J (150.0, 30.0, 700) and K (150.0, 30.0, 1500) and batches P (47.0, 9.4, 700) and Q (47.0, 9.4, 1500) and batches I (300.0, 20.0, 700) and H (300.0, 20.0, 1500). The data for these batches are represented in Figure 22, Figure 23, Figure 28, Figure 29, Figure 21, and Figure 20 respectively.

From these observations it was concluded that the mixing speed used to generate polyaphrons had a small effect on the size distribution of the bubbles. The average diameter of the bubbles made at lower r.p.m. were slightly smaller than those of the bubbles made at higher r.p.m. Also, for polyaphrons made at higher r.p.m., the number of bubbles with diameters greater than 14 μm was smaller than the number of bubbles greater than 14 μm measured for polyaphrons made at lower r.p.m. This behaviour was probably due to an increase in shear rate as the mixing rate increased. At higher shear rates more of the larger bubbles were broken down into smaller ones. Naturally, the decrease in the number of large bubbles resulted in a lower average diameter. Although the differences observed due to the difference in mixing rate were small, they were consistent throughout all tests.

5.2.2.2 Effect of flow rate

Usually, when studying the effect of several parameters in a process one parameter is changed at a time while keeping all others constant. The effect of feed flow rates on the size distribution of polyaphrons was investigated by changing the two feed flow rates, organic and aqueous, for each test. This was done because changing one flow rate at a time changes the PVR, which is the ratio of the volume of the two phases, and PVR was expected to have a large effect on the size distribution.

Figure 22 and Figure 28 represent the size distribution for batches J (150.3, 30.1, 700) and P (46.9, 9.5, 700), respectively. The average diameter for batch P, which had the lower flow rates, was 9.04 μm and that for batch J was 7.56 μm . The percent of bubbles with diameters

smaller than 5 μm was 27 for batch P and 37 for batch J. The weight percent of the bubbles versus bubble diameter graphs for the same two batches, show that the polyaphrons made with higher flow rates, batch J, had no bubbles with diameters bigger than 20 μm while 27% of the total weight percent of batch P was contributed by bubbles above 20 μm .

The same results described in the previous paragraph were seen with batches K (150.3, 30.1, 1500) and Q (46.9, 9.5, 1500). Batch K had an average diameter of 6.59 μm and batch Q one of 7.86 μm . For batch K 39% of bubbles had diameters less than 5 μm while for batch Q only 23% were in this size range. These results can be observed in Figure 23 and Figure 29.

Up to this point it appeared that polyaphrons made at higher feed flow rates tend to have smaller bubbles than those made at lower flows. But, a look at Figure 16 and Figure 19, which represent the data for batches E (49.4, 4.9, 1500) and G (302.8, 30.0, 1500), respectively, shows that the average diameter of 6.58 μm for batch E was practically the same as that of 6.48 μm for batch G. Also, 48% of all bubbles from batch E had diameters under 5 μm while only 43% of those from batch G fell under 5 μm . The weight percent graphs for the two batches show the same behaviour as before, that is, 15% of the total weight was contributed by bubbles with diameters above 20 μm for batch E while batch G had no bubbles within this range. More important is the fact that 49% of the total weight in batch G and only 35% in batch E were attributed to bubbles with diameters between 10 and 15 μm . This demonstrates that batch G had a larger number of medium sized bubbles. This also explains the small difference between the average diameter of the two batches.

Batches F, A, C, and D, listed in order of increasing feed flow rates, were all generated with a mixing rate of 700 r.p.m. and all had PVRs of 10. The feeds were increased from 47.2 to 300.0 ml/min for the organic phase and from 4.8 to 29.7 for the aqueous phase. As seen in Figure 13, Figure 15, Figure 16, and Figure 18, the average diameters of batches F, A, C, and D were 7.39, 5.0, 6.30, and 6.72 μm , respectively. Also, the percent of bubbles smaller than 5 μm for the same batches in the same order were 41, 56, 46, and 44. The weight percent graphs show that the weight percent attributed to bubbles with diameters between 20 and 30

μm was 14% for batch F, none for batch A, 1% for batch C, and 9% for batch D. Batches F and A followed the same trend observed in previous batches but batches C and D had larger average diameters and a greater number of larger bubbles than A. If each of batches A, C, and D is compared only with batch F, then, the same trends as before are observed.

As the feed flow rates in the polyaphron generator were increased, the residence time decreased. The longer the polyaphrons remained in the vessel, the greater the opportunity for coalescence to occur. After all, the bubbles were being vigorously mixed together as they flowed through the generator. Coalescence of bubbles meant less percent of smaller bubbles and a larger percent of the larger bubbles in the size distribution. This phenomena translates directly to a larger average diameter. Coalescence of the bubbles might possibly not happen easily, especially due to the high stability of polyaphrons, therefore, only when the residence time between two batches was large enough, was this phenomena observed. This was the case for batches F, A, C, and D. The residence time of the fluid inside the vessel was approximately 75 minutes for batch F, 36 minutes for batch A, 18 for batch C, and 12 for batch D. The difference in residence time among the last three batches was not long enough to make a difference. From this it was concluded that when the difference in feed flow rates was large enough, polyaphrons generated at the higher flow rates had a larger number of smaller bubbles.

5.2.2.3 Effect of phase volume ratio (PVR)

Figure 17, Figure 19, Figure 20, Figure 23, and Figure 29 depict the particle size distribution for batches E, G, H, K, and Q, respectively. Batches K and Q had PVRs equal to approximately 5, batches G and E had PVRs of about 10 and batch H was of PVR 15. The mixing rate used to generate all these polyaphron batches was around 1500 r.p.m. The average diameter for these batches was as follows: 6.59 μm for K, 7.86 μm for Q, 6.48 μm for G, 6.58 μm for E and 6.39 μm for H. The average diameter for batch Q was larger than that for the other batches and there was negligible difference among the average diameters of batches

K, G, E, and H. The percent of particles smaller than 5 μm for these same batches was as follows: 39% for batch K, 23% for batch Q, 43% for batch G, 48% for batch E and 47% for batch H. K and Q, the batches of PVR 5, had a lower percent of bubbles with diameters below 5 μm than the rest of the batches. The graphs that represent the weight percent against the diameter of the particles show no appreciable differences for any of the batches. These same observations were made for several other batches of PVR 5, 10, and 15 made at a mixing rate of 700 r.p.m. Namely, batches J and P of PVR 5, batches D, C, A, and F of PVR 10, and batch I of PVR 15. The average diameter of P was 9.04 μm , and that of J was 7.56 μm . All other batches had average diameters that ranged from 5.0 μm to 7.39 μm . The percent of bubbles smaller than 5 μm was 27% for P, 37% for J, and it ranged from 41% to 56% for all the other batches. Again, no appreciable difference was seen in the weight percent graphs of these batches. These results point to the fact that there was no significant difference between the particle size of polyaphrons of PVR 10 and 15. Polyaphrons of PVR 5 did appear to have a smaller percent of bubbles smaller than 5 μm than did the ones of PVR 10 and 15. Perhaps this was because the difference between PVR 10 and 15 was small if one considers that in volume percent, PVR 10 is equal to 91% kerosene and PVR 15 is 94% kerosene. A polyaphron of PVR 5 is equal to 83% by volume of kerosene.

5.2.2.4 Effect of surfactant

To study the effect of surfactant on the particle size distribution of polyaphrons, two batches were made, batch S (267.5, 26.7, 1500) and batch R (259.2, 25.9, 1500). The aqueous phase of batch S was made of 5 g/L NaDBS in deionized water and the organic phase was made of 10% LIX-64N in kerosene and 0.5 ml/L of Tergitol 15-S-3. The aqueous phase of batch R consisted of 5 ml/L of Arquad 12-50 in deionized water and the organic phase was made of 10% LIX-64N in kerosene. Each of these batches was made at approximately the same conditions as batch G (300.0, 30.0, 1500). Batch G was made with a 5 g/L NaDBS in deionized water aqueous phase, and 10% LIX-64N in kerosene. No oil soluble surfactant was added to

the organic phase of the latter two batches. Figure 19 and Figure 31 depict the particle size distribution for batches G and S, respectively. In comparing the two, it is noted that the average diameter of batch G, 6.48 μm , was smaller than that for batch S, 7.15 μm . Also, 43% of the bubbles from batch G were less than 5 μm while only 34% of the ones from batch S were smaller than 5 μm . In the weight percent graphs it can be seen that for diameters between 20 and 30 μm the weight percent for batch S was 17% and that of batch G was 0. At first, these results were surprising because it was expected that the addition of a surfactant to the organic phase would produce smaller polyphrons. In order that an oil will be able to spread in water, the spreading pressure must be greater than the surface pressure produced by the surfactant dissolved in the water. Adding an oil soluble surfactant to the oil phase produces surface pressure. But in this particular case, kerosene is the oil, and kerosene already contains surfactants. A small amount of surfactant added to the kerosene might not make a difference. The differences between the two batches was probably not due to the oil soluble surfactant but to experimental error.

Batch R which was made with Arquad 12/50 as the water soluble surfactant had an average diameter of 7.66 μm and 32% of its particles were smaller than 5 μm . Also, 50% of its total weight was attributed to bubbles larger than 15 μm . This can be observed in Figure 30. When the results of this batch are compared to those of batch G, it can be said that polyphrons made with NaDBS tended to be smaller than polyphrons made with Arquad 12/50.

5.2.2.5 Effect of time

To study what happens to the size of polyphrons when stored over a period of time, the sizes of bubbles from batches A (97.9, 9.7, 700), I (300.0, 20.0, 700), and P (47.0, 9.4, 700) were measured shortly after they were made and four months later. The data collected from batch A soon after being made is presented in Figure 13. The data for the same batch four months later is seen in Figure 32. It was observed that over time the diameter increased from 5.0

μm to $6.23 \mu\text{m}$ and the number of bubbles with diameters less than $5 \mu\text{m}$ decreased from 56% to 43%. Also, the weight percent for bubbles larger than $20 \mu\text{m}$ increased from 0 to 12%. Apparently some degree of coalescence between the bubbles took place over those four months. The average diameter of batch I (300.0, 20.0, 700) increased from 6.80 to $6.86 \mu\text{m}$ and the number of bubbles smaller than $5 \mu\text{m}$ decreased from 47% to 44% over the four month period. The weight percent from bubbles larger than $20 \mu\text{m}$ increased from 0 to 16%. These differences are considered within experimental error except for the weight percent differences. The amount of coalescence that took place in the latter polyaphrons was small compared to the difference observed for batch A. This was probably because batch A had a very large percent of small bubbles to begin with. The data for batch I is depicted in Figure 21 and Figure 33. Batch P (47.0, 9.4, 700) presented a different picture. As observed in Figure 28 and Figure 34, the average diameter for this batch decreased over time from $9.04 \mu\text{m}$ to $7.6 \mu\text{m}$. The number of bubbles smaller than $5 \mu\text{m}$ increased from 27 to 35%. The weight percent of bubbles over $20 \mu\text{m}$ decreased from 27 to 15%. For this particular case it must be considered that this batch had a PVR of 5. Some of the aqueous phase from the lamellae of these aphrons drained over time, forming a separate aqueous phase. The bottle containing the aphrons was shaken vigorously by hand until all the aqueous phase was introduced back into the aphron matrix. It would seem obvious that as the water drained out of the bubbles, some coalescence took place, but it is not understood what happened to the bubbles within the matrix when the aqueous phase was reintroduced with the shaking. Probably some of the water was simply added to the water in the lamella of the matrix but most likely new aphrons were also formed.

5.2.2.6 Reproducibility of results

To determine reproducibility of results, four different polyaphron batches were made under the same conditions and the particle size distribution measured by the photo-microscopy method of analysis. Batches L, M, N, and O were generated at an organic feed flow rate of 175.0 ml/min , an aqueous flow rate of 20.0 ml/min , and a mixing rate of 1100 r.p.m.

Figure 24, Figure 25, Figure 26, and Figure 27 represent the particle size distribution for these batches. The average diameters of batches L, M, and O did not vary much, with L's being 6.63, M's 6.97, and O's 7.50 μm . The percent of bubbles less than 5 μm were 39% for batch L, 37% for M, and 32% for O. Again, only a small variation. The values of these same parameters for batch N showed more difference, with the average diameter being 6.21 μm and 48% of the particles being smaller than 5 μm . But, an overall comparison of all four distributions did not reveal large differences. The weight percent graphs show that the weight percent attributed to bubbles larger than 20 μm was 17% for batch M, 19% for batch O, and 10% for both batches L and N. These were not large differences when considering that one 20 μm diameter bubble will contribute significantly towards the overall weight percent.

5.2.3 Coulter Counter Method of Analysis: Discussion and Results

As was previously stated, the principle of operation of the coulter counter is to measure the electrical current across a sample point. The drop in electrical current is directly proportional to the particle size flowing through the sample point. The electrical current is generated with an electrolyte. The electrolyte used for this study was sodium pyrophosphate. The aphrons were diluted in 3 different solutions of 1%, 3%, and 4% sodium pyrophosphate. Figure 35 depicts the results from these tests. It is obvious that the concentration of the electrolyte made a difference in the results, therefore; it was decided to stop the tests and study under the microscope the behaviour of aphrons diluted in an electrolyte. Regardless of the concentration of sodium pyrophosphate used, dramatic changes occurred to the aphrons. The bubbles coalesced, broke down, and moved continuously. After only a few minutes, no bubbles remained in the sample. Other electrolytes such as sodium chloride were tried, but the same behaviour was observed. The late Professor Sebba was studying a species of aphrons which he called invert aphrons at the time of his death. He used to form them by adding calcium ions to regular aphrons. He described high activity and unusual

behaviour by the aphrons due to the calcium ions. It is possible that the same effect was observed on the polyaphrons due to the electrolyte. The coulter counter method to measure the particle size distribution of polyaphrons was no longer pursued.

5.2.4 Discussion and Results of Particle Analysis with a PAR-TEC 100

Instrument

The PAR-TEC 100 was simple to operate. A beaker with diluted polyaphrons was placed on a magnetic stirrer and the instrument's probe was placed in the beaker. The polyaphrons were diluted because of the high cohesive forces between the bubbles. The mixture was vigorously stirred throughout the testing period. Two sets of data were obtained from the same sample, the first soon after the testing started and the second 8 minutes after the first results had been collected. Figure 36 shows the results obtained for batch H (300.0, 20.0, 1500). The average diameter obtained from the first results was 26.4 μm and the one from the second results was 24.8 μm . The size of the bubbles ranged from below 1.9 μm to around 125 μm . The large number of particles above 22 μm was unexpected. Before testing started a layer of kerosene started to form above the mixture, an indication that the polyaphrons were breaking. During testing, the mixing rate of the sample was increased and the kerosene layer was incorporated into the mixture. The kerosene probably accounted for most of the larger bubbles measured. Whenever polyaphrons are diluted in water, a certain amount of breakage occurs, but during testing with the PAR-TEC 100 an unusual amount of breakage was observed. The stainless steel probe placed in the sample could have contributed to the amount of breakage because it has been observed that the rate of breakage of aphrons in contact with a solid surface increases. This, added to the shearing rate due to mixing would account for the existence of larger bubbles. Since the tests were done during a demonstration of the instrument, this was the only batch tested.

5.2.5 Discussion of Particle Analysis Using the SA-CP3 Centrifugal Particle

Size Analyser

The particle size analyser was easy to use. The measuring conditions were set with a keyboard installed in the machine and the sample was prepared, placed in the sample cell, and positioned in the machine. Depending on the particle sizes in the sample, the measurements took anywhere from 15 minutes to over two hours to complete.

Sample preparation was simple. A drop of polyaphrons was diluted in distilled water and then poured into the sample cell making sure that no air bubbles formed in the cell. The amount of polyaphrons in the sample had to be small because the analyser would show an error message in the CRT display whenever the turbidity of the sample was high.

The accuracy of the measurements using the SA-CP3 Analyser was highly dependent on the accuracy of the density of the particles. To determine the density of each polyaphron batch, 5 ml of polyaphrons were weighed. Polyaphrons, especially the lower PVR ones, tend to encapsulate air within them. Most of this air is released with time which causes the volume to decrease. Therefore, the samples were not weighed until the sample volume stopped decreasing and the void space filled with more aphrons. The densities of all the polyaphron batches are tabulated in Table 10.

5.2.6 Discussion of Results From the SA-CP3 Centrifugal Particle Size

Analyser

The particle size of sixteen different polyaphron batches was measured with the SA-CP3 Centrifugal Particle Size Analyser. The data gathered was displayed by the Analyser as percent weight over various particle diameter ranges. Figure 37 (B) to Figure 53 (B) depict the data collected. To calculate the percent of bubbles from the weight percent data, the median diameter of each diameter range and the density of each polyaphron batch was used. The

percent of number of bubbles versus diameter are shown in Figure 37 (A) to Figure 53 (A). Since the size of the samples tested was small, more than one sample was tested for each polyaphron batch. The results from all samples were averaged for each batch. The figures mentioned represent the total data collected for each batch. The average diameter for each batch calculated from the number of bubbles measured and their respective diameter are tabulated in Table 10 and shown on each figure. An average diameter calculated from the weight percent data is shown on each weight percent graph. These diameters were calculated by summing the products of the weight percent times the respective diameter and dividing the summation by 100.

5.2.6.1 Effect of mixing rate

Figure 40 (A) and Figure 43 (A) depict the percent of bubbles versus diameter for polyaphron batches D (300.0, 29.7, 700) and G (302.8, 30.0, 1500), respectively. Except for the difference in mixing rates, both of these batches were generated under approximately the same conditions. The average diameter of batch D, the one made at a lower mixing rate, was found to be larger at $1.65 \mu\text{m}$ than that of batch G at $0.97 \mu\text{m}$. Batch D had no particles smaller than $0.5 \mu\text{m}$ while for batch G 49% of its particles were smaller than $0.5 \mu\text{m}$. Inspection of Figure 40 (B) and Figure 43 (B) show that for batch D 50% of the weight was attributed to particles between 15 and $20 \mu\text{m}$ and 24% was attributed to particles between 20 and $30 \mu\text{m}$ while for batch G particles between 15 and $20 \mu\text{m}$ had a weight percent of 31 and particles between 20 and $30 \mu\text{m}$ had a weight percent of 32. Although batch G had more bubbles in the 20 to $30 \mu\text{m}$ range, batch D had almost as many bubbles in the 15 to $20 \mu\text{m}$ range as batch G had over both ranges.

The results for batch E (49.4, 4.9, 1500) are represented in Figure 41. Those for batch F (47.2, 4.8, 700) are shown in Figure 42. The conditions under which these batches were generated were also basically the same except for the mixing rate. The same behaviour as before was observed. The average diameter of batch F was found to be larger at $1.87 \mu\text{m}$ than that

of batch E at 1.50 μm . 18% of the particles from batch E had diameters below 0.5 μm and batch F had no particles below this size. The weight percent graphs show that batch E had more bubbles in the 15 to 20 μm range but batch F had more in the 10 to 15 μm range. This set of polyaphron batches and the two described in the previous paragraph had a PVR of 10.

The particle size measurements made for batch J (150.3, 30.1, 700) are shown in Figure 46. Those for batch K (150.3, 30.1, 1500) are depicted in Figure 47. The average diameter for these two batches was found to be the same at 2.54 μm and no appreciable difference was noted in their size distribution. 58% of their particles were below 1.5 μm and although the weight percent of batch K was 10% higher than that of batch J over the 20-30 μm range, the weight percent for both batches was about 80% over the 10 to 30 μm range. This batch had a PVR of 5.

Another set of batches of PVR 5 generated with approximately the same feed flow rates but with different mixing rates were batch P (46.9, 9.5, 700) and batch Q (46.9, 9.5, 1500). The particles in batch P had an average diameter of 2.29 μm and those of batch Q had an average diameter of 2.24 μm . A negligible difference. Figure 49 and Figure 50 show that of the particles in batch Q, 32% were between 0.8 and 1.0 μm , more than the 18% found for batch P in this same range but, for the range of 1.0 to 1.5 μm batch P had 20% more particles than batch Q. Towards the center of the distribution, between 1.5 and 4 μm , is where batch Q had a larger number of bubbles. The weight percent graphs of these two batches show that over a diameter range of 15 to 30 μm , the weight percent of batch P was 66 and that of batch Q was 59. The differences were not considered significant.

The differences between batches H (302.4, 20.3, 1500) and I (302.4, 20.3, 700) were also insignificant. The particles in batch H had an average diameter of 0.36 μm and the ones in batch I had an average diameter of 0.40 μm . Figure 44 shows that 94% of the particles in batch H had diameters smaller than 0.5 μm and Figure 45 shows that 90% of the particles in batch H had diameters smaller than 0.5 μm . The weight percent graphs show that there was little difference in the higher range of the distribution between the two batches. The PVR of these two batches was equal to 5.

From these results it was concluded that the mixing rate had a significant effect only on the polyaphrons of PVR 10. The higher mixing rate of 1500 r.p.m., probably because of the higher shearing rate, produced smaller sized aphrons than the polyaphrons made at a mixing rate of 700 r.p.m. Both polyaphron batches of PVR 15 had 90% or more of their particles smaller than 0.5 μm . It would have been difficult to see a shearing effect in a system that had such small particles to begin with. The PVR 5 polyaphrons were also not affected by the mixing rate. As has been previously said, some of the water from the lamella of this type of polyaphrons tended to drain over time. This probably caused some coalescence, especially among the smaller bubbles. To introduce the water back into the polyaphron matrix, the polyaphrons were always shaken vigorously. The shaking probably formed some aphrons. All this possibly had an effect on the particle size distribution of the bubbles which in turn could have obscured the mixing rate effect.

5.2.6.2 Effect of feed flow rate

As was previously stated, the effect of feed flow rate on the particle size distribution of polyaphrons was studied by comparing the results obtained from polyaphron batches of equal PVR that were made with the same mixing rate. Both feed flow rates were increased simultaneously so as not to change the PVR of the aphrons.

The particle size distribution of polyaphron batches F (47.2, 4.8, 700), A (97.9, 9.7, 700), C (197.8, 19.8, 700), and D (300.0, 29.7, 700), listed in order of ascending flow rates, are depicted in Figure 42, Figure 37, Figure 39, and Figure 40, respectively. The value of the average diameter of the particles from these four batches was as follows: 1.87 μm for batch F, 1.37 μm for batch A, 1.13 μm for batch C, and 1.65 μm for batch D. Batches A, C, and D had average diameters larger than batch F. Also, these same batches had a greater percent of particles with diameters under 0.6 μm than batch F. Batch A had 42%, batch C had 50%, and batch D had 20% while batch F had 0%. The weight percent versus diameter graphs for batches F, A, C, and D show that the weight percent for diameters greater than 15 μm was 62% for batch

F, 47% for A, 55% for C, and 64% for D. Batches A and C had less number of larger bubbles and batches D and F had approximately the same number. Batch D might appear to not be following the trend of batches A and C in relation to F, but a comparison of the weight percent at the 10 to 15 μm range shows that batch D had significantly less particles than the other batches at this range.

The results from batches A, C, and D were all compared against batch F because as was seen with the photo-microscopy measurements the effect of mixing rate was significant only when the difference in the residence time of the fluid inside the polyaphron generator was large enough. The residence time for batch F was 75 minutes, while that for batches A, C, and D was 36, 18, and 12 minutes, respectively.

The results from batches E (49.4, 4.9, 1500) and G (302.8, 30.0, 1500) showed the same trends. The average diameter for batch E, 1.50 μm , was larger than the one for batch G, 0.97 μm . 18% of the particles from batch E and 54% of those from batch G had particles with diameters smaller than 0.6 μm . The weight percent for particles larger than 15 μm was 66% for batch E and 32% for batch G. These results are depicted in Figure 41 and Figure 43. The residence time of batches E and G was 72 and 12 minutes, respectively. The PVR of both batches was 10.

As was explained when discussing the effect of mixing rate on the particle size distribution of the polyaphrons, whenever dealing with polyaphrons of PVR 5 the trends are less obvious. Batch P (46.9, 9.5, 700) had an average diameter of 2.29 μm and batch J (150.3, 30.1, 700) had an average diameter of 2.54 μm although the residence time of P was 72 minutes while that of J was only 22 minutes. In Figure 49 it is seen that 18% of the particles from batch P had diameters between 0.8 and 1.0 μm and 50% had particles between 1.0 and 1.5 μm . Figure 46 shows that 27% of the particles from batch J had diameters between 0.8 and 1.0 μm and 32% had diameters between 1.0 and 1.5 μm . Batch P had less particles in the smaller range but more in the higher range than batch J. The weight percent graphs show that a larger number of bubbles was present in batch P than batch J at the 20 to 30 μm range.

The same type of results were observed when the other set of PVR 5 batches were compared. Batch Q (46.9, 9.5, 1500) had an average diameter equal to 2.24 μm , 33% of its particles were between 0.4 and 0.5 μm , 29% of them were between 1.0 to 1.5 μm . Also, 59% of its weight was contributed by particles larger than 15 μm . Batch K (150.3, 30.1, 1500) had an average diameter of 2.54 μm , 17% of its particles were between 0.4 and 0.5 μm and 41% of them were between 1.0 and 1.5 μm . Particles larger than 15 μm had a weight percent of 30. Figure 47 and Figure 50 show these results.

It is clear that polyaphrons of PVR 10 with significant differences in their residence times, tended to have smaller particles when made at higher flow rates. Polyaphrons of PVR 5, also with large residence time differences, tended to have less particles with diameters above 15 μm when made at higher flow rates. These results were probably a direct effect of coalescence of the bubbles while inside the generator.

5.2.6.3 Effect of the ratio of the volume of the two phases (PVR)

Different polyaphron batches of PVR 5, 10, and 15 at mixing rates of 700 and 1500 r.p.m. were generated. As was previously said, a difference in PVR is invariably tied with a difference in feed flow rates. Since the feed flow rate effect was found to be significant only in cases where the residence time difference was large, the effect observed in different PVR polyaphrons was expected to be mainly a direct consequence of the PVR.

Figure 46 and Figure 49 depict the particle size distribution of batches J (150.3, 30.1, 700) and P (46.9, 9.5, 700). The average diameter for batch J was 2.54 μm and for batch P was 2.29 μm . The smallest particles for both batches were found in the 0.8 to 1.0 μm range. The PVR of both batches was approximately 5. Figure 37, Figure 39, Figure 40, and Figure 42 represent the data for batches A (97.9, 9.7, 700), C (197.8, 19.8, 700), D (300.0, 29.7, 700), and F (47.2, 4.8, 700), respectively. The average diameters of these batches ranged from 1.13 μm to 1.87 μm . The smallest particles found in batch F were in the 0.6 to 0.8 μm range, and the ones in batch D were in the 0.5 to 0.6 μm range. 27% and 19% of the particles from batches A and

C, respectively, had diameters smaller than $0.5 \mu\text{m}$. These last four batches had PVRs of about 10. Figure 45 shows the measurements obtained for batch I (302.4, 20.3, 700). This PVR 15 batch had an average diameter of $0.40 \mu\text{m}$ and 90% of its particles were found to be smaller than $0.5 \mu\text{m}$. Comparison of these results showed that as PVR increased the particle size of the polyaphrons decreased.

The same behaviour was observed with the polyaphrons made at mixing rates of 1500 r.p.m. Batches K (150.3, 30.1, 1500) and Q (46.9, 9.5, 1500) of PVR 5 had larger particles than batches E (49.4, 4.9, 1500) and G (302.8, 30.0, 1500) of PVR 10. Batch H (302.4, 20.3, 1500) of PVR 15 had the smallest average diameter at $0.40 \mu\text{m}$ with 94% of its bubbles smaller than $0.5 \mu\text{m}$. These results were represented in Figure 41, Figure 43, Figure 44, Figure 47, and Figure 50.

The effect of PVR on the particle size distribution of polyaphrons was not unexpected. The main difference between polyaphrons of various PVR was the amount of water soluble surfactant in the system. Since the volume of the aqueous phase was greater in the lower PVR polyaphrons and the surfactant concentration was kept constant for all batches, the amount of water soluble surfactant was greater in the lower PVR systems. For an oil, kerosene in this case, to spread in a surfactant solution, the spreading pressure of the oil must be greater than the surface pressure produced by the surfactant dissolved in the water. The higher the amount of surfactant in the water the higher the surface pressure will be. As the PVR was increased, the difference between the surface and spreading pressures increased as a direct consequence of the smaller amount of surfactant present, and the oil spread easier over the water, causing the formation of smaller bubbles.

5.2.6.4 Effect of surfactant

The nature of the surfactant was naturally expected to have an effect on the particle size distribution of the polyaphrons. All surfactants lower the surface tension of the liquid in which they are dissolved but the degree to which they lower it varies according to the structure of

the surfactant molecule. Since surface tension affects both the spreading and surface pressures of oil and aqueous phases, respectively, different surfactants were expected to affect the size of the individual aphrons in a polyaphron.

Figure 43 and Figure 51 depict the particle size distribution of batches G (302.8, 30.0, 1500) and R (259.2, 25.9, 1500), respectively. Both batches are considered to have been made under approximately the same conditions, but the surfactant used in the aqueous phase of batch G was 5 g/L NaDBS and that used in batch R was 5 ml/L Arquad 12/50. With an average diameter of $0.11 \mu\text{m}$ and almost 100% of its particles with diameters smaller than $0.5 \mu\text{m}$ the particles from batch R were found to be smaller than those from batch G. Batch G had an average diameter of $0.97 \mu\text{m}$ and 49% of its particles were smaller than $0.5 \mu\text{m}$.

Batch S (267.5, 26.7, 1500) was also made under approximately the same conditions as batch G. The same concentration and type of surfactant was used in the aqueous phase of both batches but, 0.5 ml/L of Tergitol 15-S-3 were added to the organic phase. The bubbles from batch S were also found to be smaller than those from batch G. As Figure 52 shows, batch S had an average diameter of $0.42 \mu\text{m}$ and 92% of all its particles were smaller than $0.5 \mu\text{m}$.

5.2.7 Comparison of the Methods Used to Determine the Particle Size

Measurements

The principal methods of analysis used to determine the particle size distribution of the polyaphrons were photo- microscopy and sedimentation. Sedimentation is the method used by the SA-CP3 Centrifugal Particle Size Analyser. The results from each method gave somewhat different particle size distributions for each polyaphron batch.

The sample size used for both methods was small but, while the entire sample was scanned with the Particle Size Analyser only a small portion of the sample was photographed under the microscope. Sample preparation was simple for both methods. The photo-

microscopy method required many hours of tedious bubble counting and measuring while the Analyser, in a maximum of three hours would generate a particle size distribution for one sample. The SA-CP3 Analyser can detect particles between 0.1 μm and 30 μm . With the photo-microscopy method particles smaller than 2.0 μm were not detected. This was probably due to the buoyancy of the particles. The smaller ones were most likely positioned under the larger ones. Also, diffraction might possibly have blurred the image of the smaller particles. Not being able to detect the smaller particles was probably responsible for not detecting an effect due to addition of surfactant to the organic phase. An effect was seen with the SA-CP3 Analyser. On a positive note, the photo-microscopy method did not apply any external forces on the bubbles while the SA-CP3 did. These forces might have affected the bubble size. Also, the SA-CP3 Analyser used the density of the particles to calculate the size distribution. The accuracy of the method was dependent largely on the accuracy of the density.

The PAR-TEC 100 Analyzer was the only other instrument that successfully measured the bubbles of polyaphrons. It was quicker and easier to use than the other two methods, and the sample size was several times larger. The machine could measure particles between 1 and 100 μm . This method calculated a distribution that extended over a range of less than 2.0 μm to 125 μm with more than 50% of the particles between 13 and 44 μm . High degree of polyaphron breakage was noticed during the testing period. Thus, this method probably introduced a larger amount of error.

Table 8. Description of the experimental tests designed to characterize polyaphrons according to size.

Sample ID	Org. Flow Rate (ml/min)	Aq. Flow Rate (ml/min)	Mixing Rate (rpm)	PVR
A	97.9	9.7	700	10.0
B	141.6	19.1	700	7.4
C	197.8	19.8	700	10.0
D	300.0	29.7	700	10.0
E	49.4	4.9	1500	10.0
F	47.2	4.8	700	9.8
G	302.8	30.0	1500	10.0
H	302.4	20.3	1500	15.0
I	302.4	20.3	700	15.0
J	150.3	30.1	700	5.0
K	150.3	30.1	1500	5.0
L	174.5	20.1	1100	8.75
M	174.5	20.1	1100	8.75
N	174.7	20.1	1100	8.75
O	174.7	20.1	1100	8.75
P	46.9	9.5	700	5.0
Q	46.9	9.5	1500	5.0
R	259.2	25.9	1500	10.0
S	267.5	26.7	1500	10.0

Table 9. Average diameter of polyaphron batches determined by photo-microscopy.

Sample ID	Org. Flow Rate (ml/min)	Aq. Flow Rate (ml/min)	Mixing Rate (rpm)	Avg. Diameter (μm)
A	97.9	9.7	700	5.00
B	141.6	19.1	700	6.06
C	197.8	19.8	700	6.30
D	300.0	29.7	700	6.72
E	49.4	4.9	1500	6.58
F	47.2	4.8	700	7.39
G	302.8	30.0	1500	6.48
H	302.4	20.3	1500	6.39
I	302.4	20.3	700	6.80
J	150.3	30.1	700	7.56
K	150.3	30.1	1500	6.59
L	174.5	20.1	1100	6.63
M	174.5	20.1	1100	6.97
N	174.7	20.1	1100	6.21
O	174.7	20.1	1100	7.50
P	46.9	9.5	700	9.04
Q	46.9	9.5	1500	7.86
R	259.2	25.9	1500	7.66
S	267.5	26.7	1500	7.15
A*	97.9	9.7	700	6.23
I*	302.4	20.3	700	6.86
P*	46.9	9.5	700	7.60

Note: * Measurements were made four months after generating the polyaphrons.

Table 10. Density and average diameter of polyaphron batches.

Sample ID	Org. Flow Rate (ml/min)	Aq. Flow Rate (ml/min)	Mixing Rate (rpm)	Density (g/cm³)	Avg. Diameter (μm)
A	97.9	9.7	700	0.8246	1.37
B	141.6	19.1	700	0.7926	1.98
C	197.8	19.8	700	0.8250	1.13
D	300.0	29.7	700	0.8248	1.65
E	49.4	4.9	1500	0.8251	1.50
F	47.2	4.8	700	0.8249	1.87
G	302.8	30.0	1500	0.8254	0.97
H	302.4	20.3	1500	0.8190	0.36
I	302.4	20.3	700	0.8253	0.40
J	150.3	30.1	700	0.7571	2.54
K	150.3	30.1	1500	0.7821	2.54
L	174.5	20.1	1100	0.8212	1.94
P	46.9	9.5	700	0.7794	2.29
Q	46.9	9.5	1500	0.8321	2.24
R	259.2	25.9	1500	0.8218	0.11
S	267.5	26.7	1500	0.8281	0.42
A**	97.9	9.7	700	0.8246	0.42

Notes: * Average Diameter was determined by SA-CP3 Particle Size Analyzer

** Measurements were made four months after generating the polyaphrons.

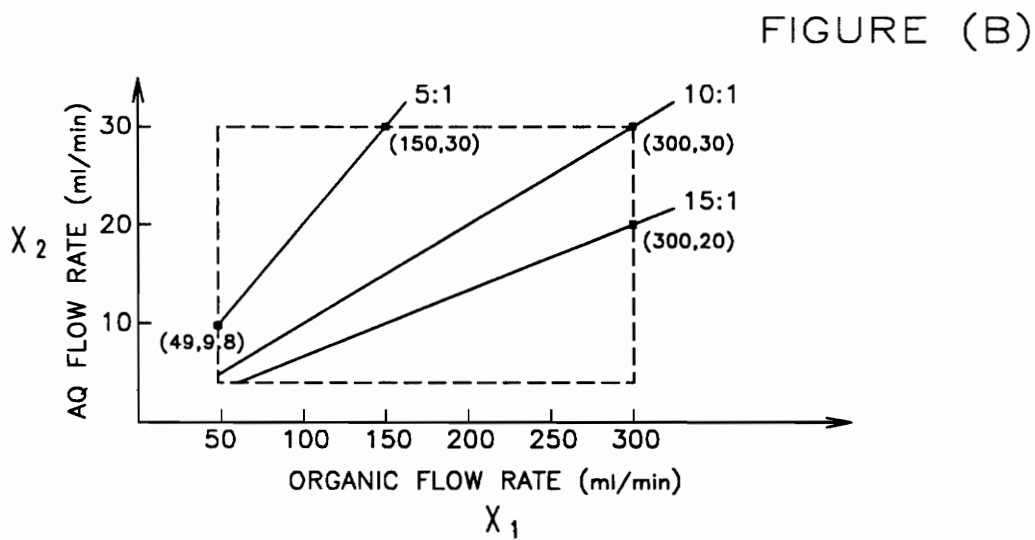
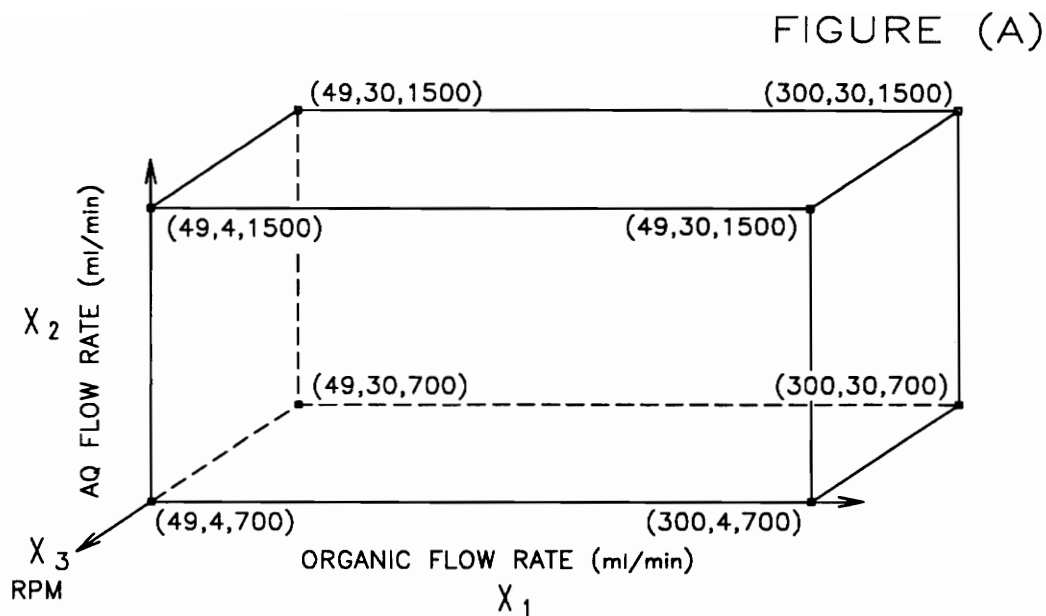


Figure 11. Design region of the experimental tests designed. (A) Orthogonal design, (B) non-orthogonal design.

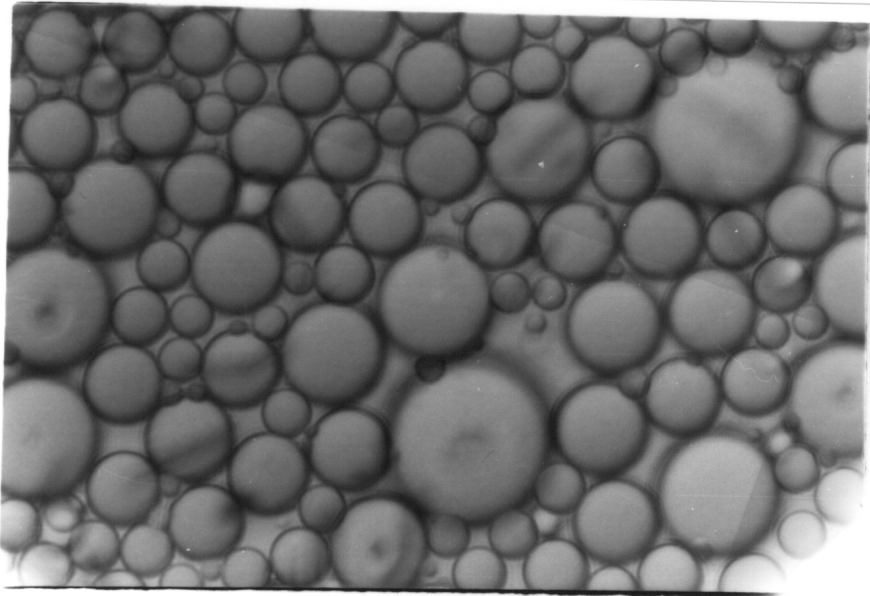


FIGURE (A)

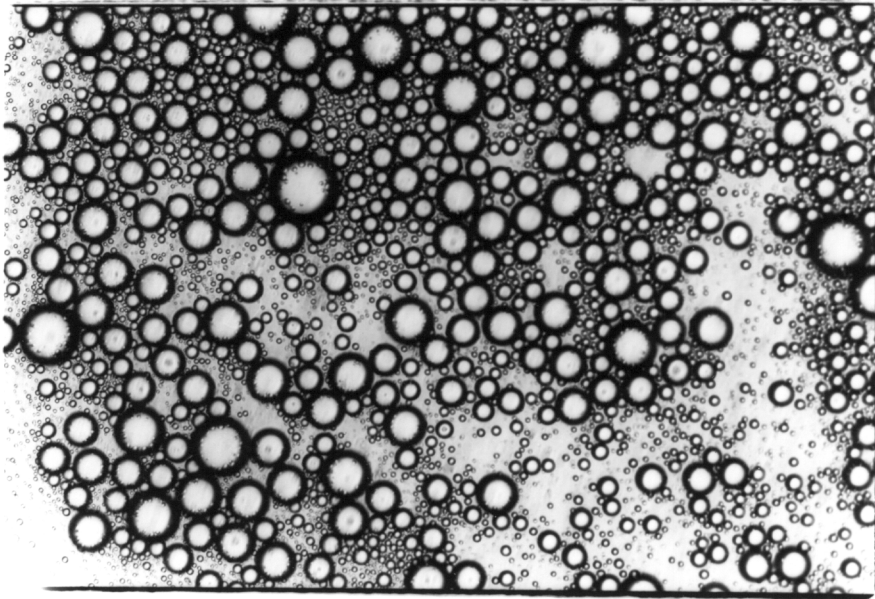


FIGURE (B)

Figure 12. Photographs of polyaphron samples from batches (A) B and (B) D.

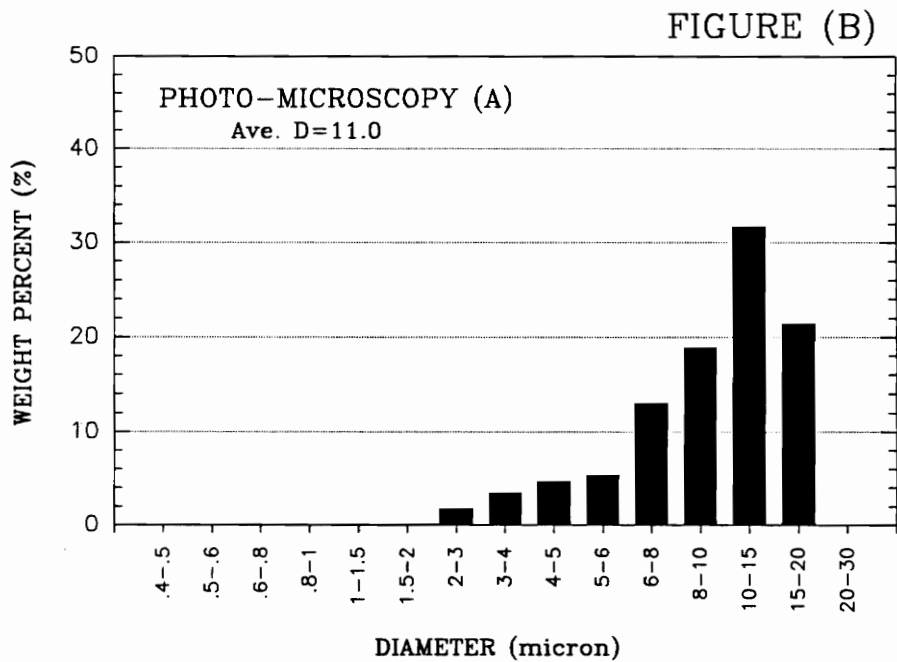
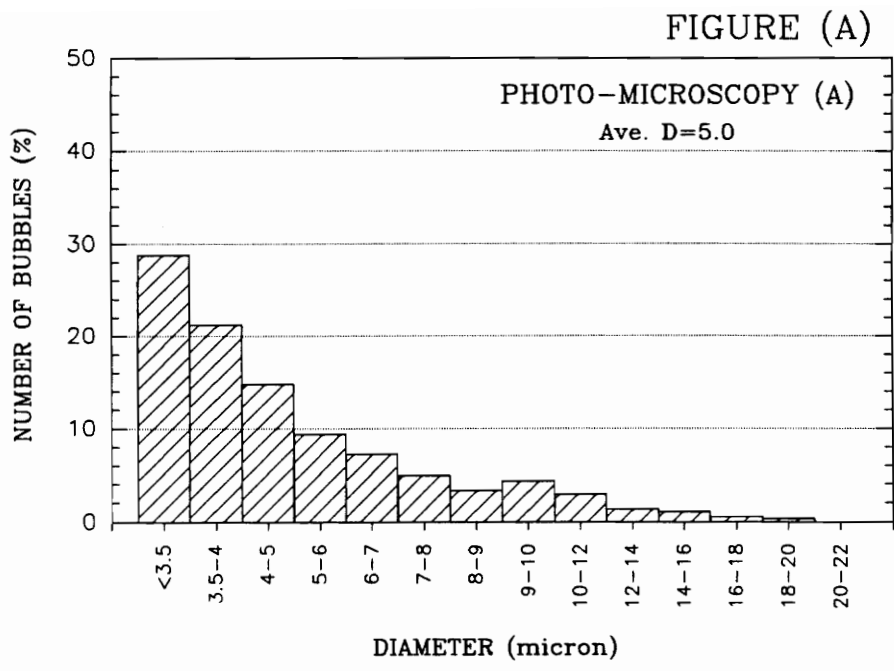


Figure 13. Particle Size Distribution for Batch A (97.9, 9.70, 700), as Determined by Photo-Microscopy. (A) Number of bubbles (%), (B) Weight percent.

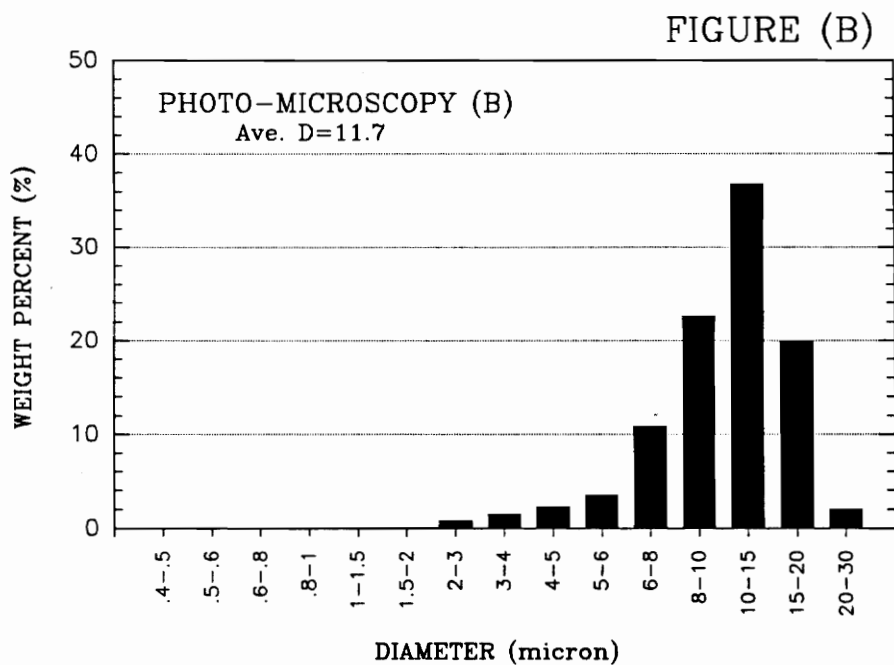
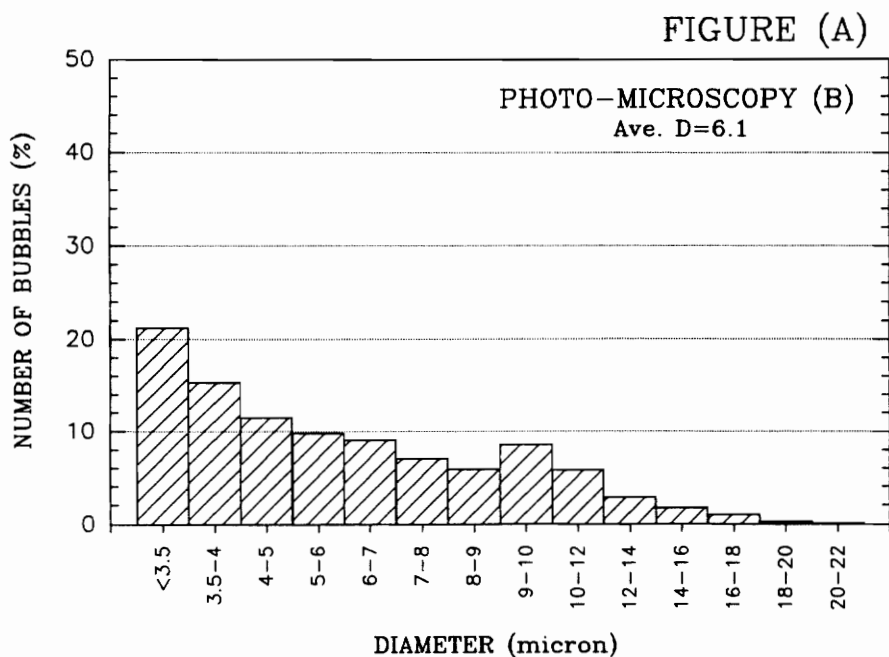


Figure 14. Particle Size Distribution for Batch B (141.6, 19.1, 700), as Determined by Photo-Microscopy. (A) Number of bubbles (%), (B) Weight percent.

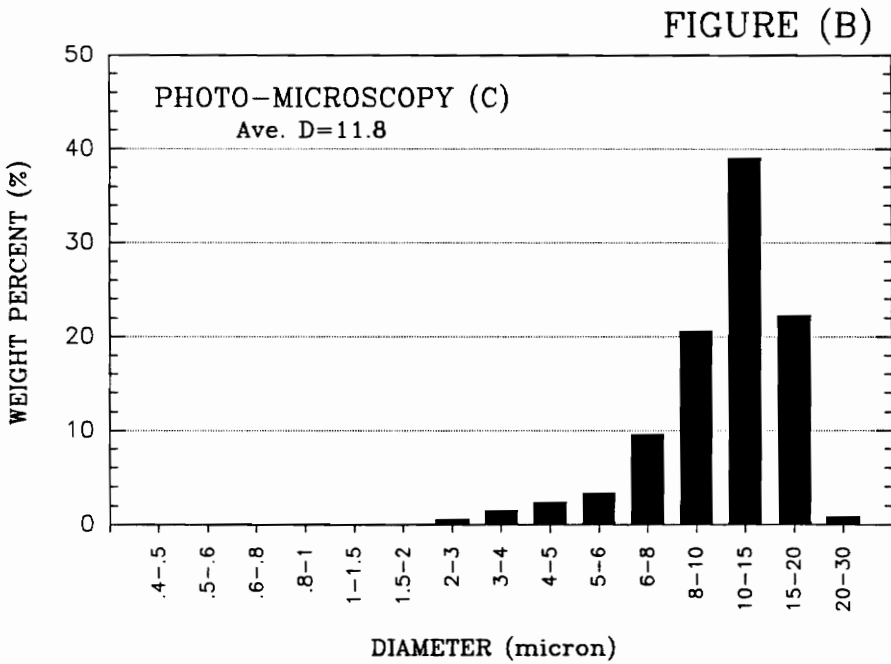
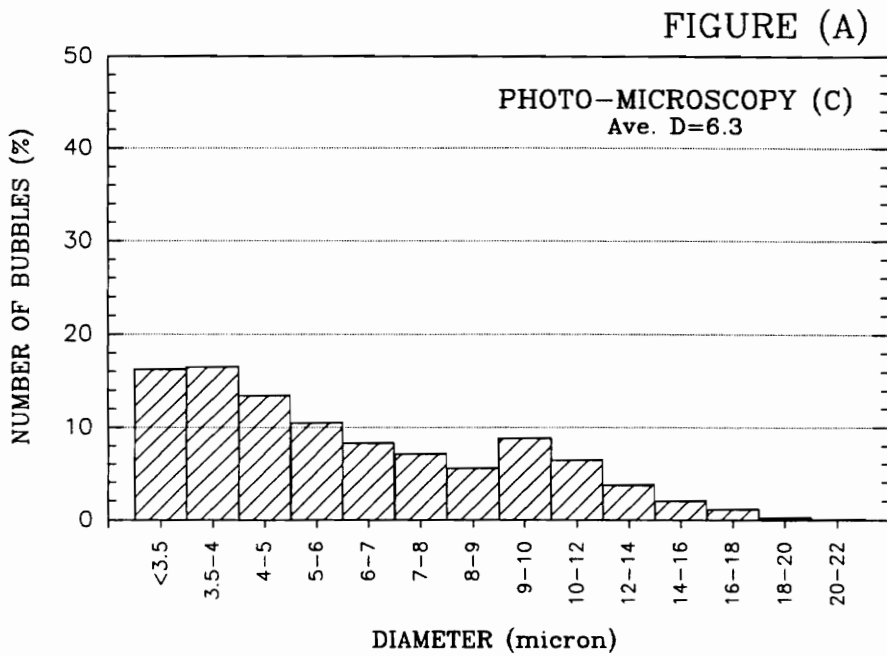


Figure 15. Particle Size Distribution for Batch C (197.8, 19.8, 700), as Determined by Photo-Microscopy. (A) Number of bubbles (%), (B) Weight percent.

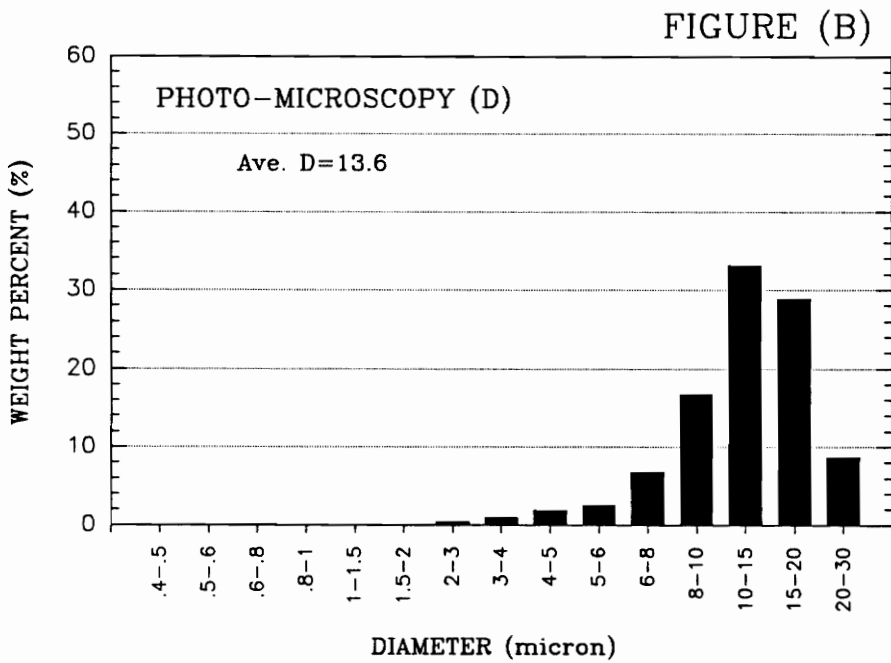
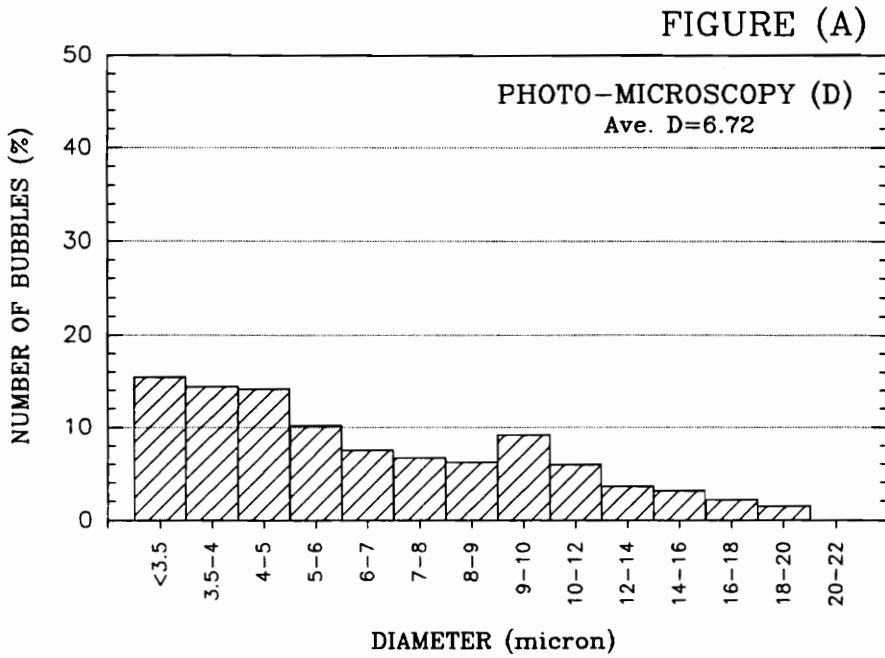


Figure 16. Particle Size Distribution for Batch D (300.0, 29.7, 700), as Determined by Photo-Microscopy. (A) Number of bubbles (%), (B) Weight percent.

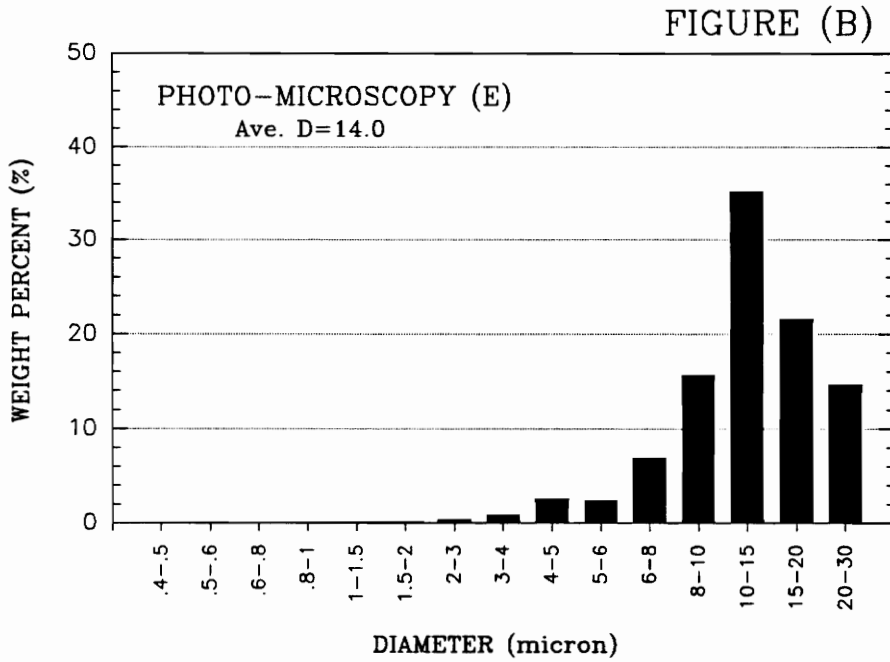
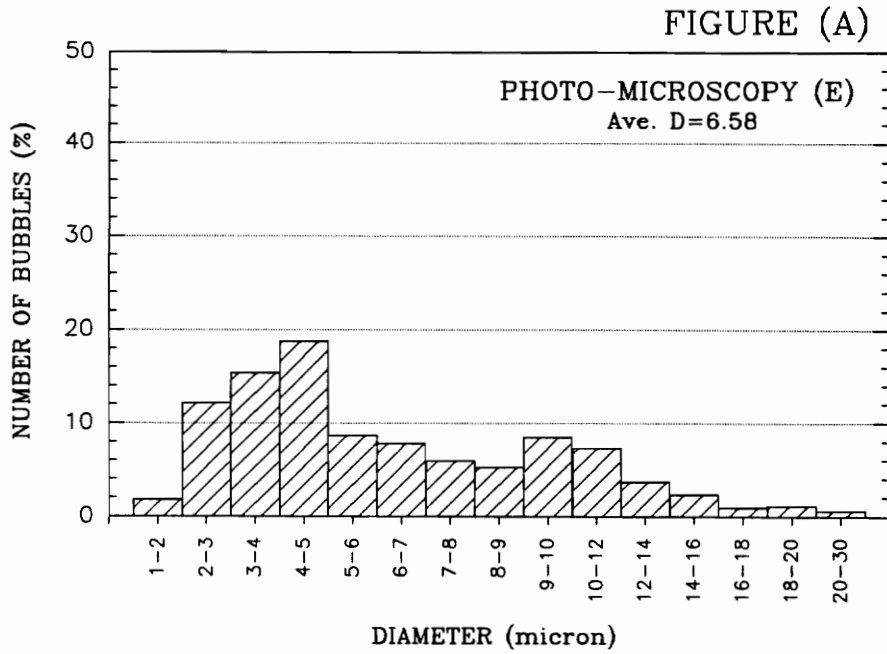


Figure 17. Particle Size Distribution for Batch E (49.4, 4.9, 1500), as Determined by Photo-Microscopy. (A) Number of bubbles (%), (B) Weight percent.

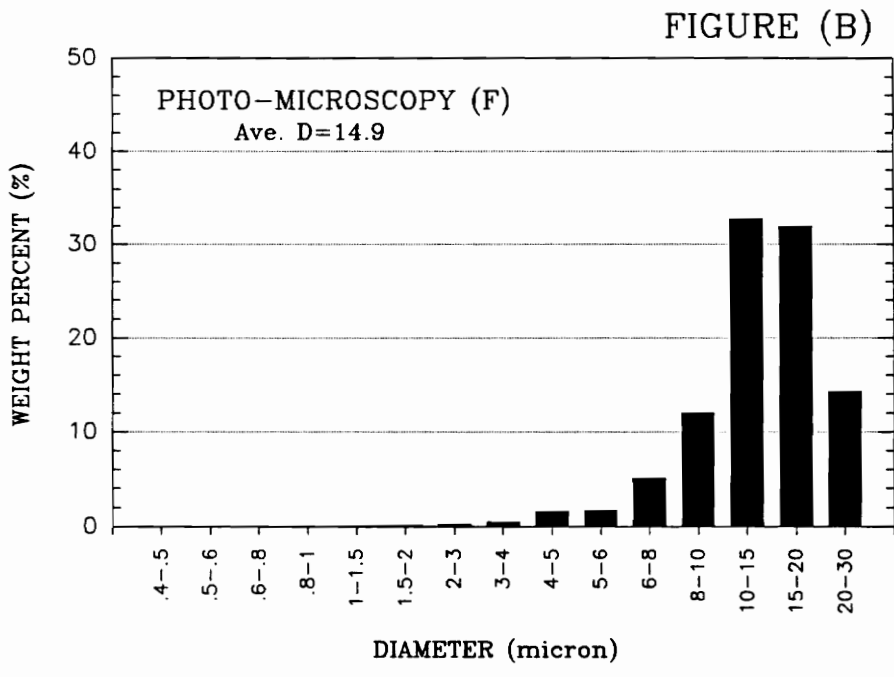
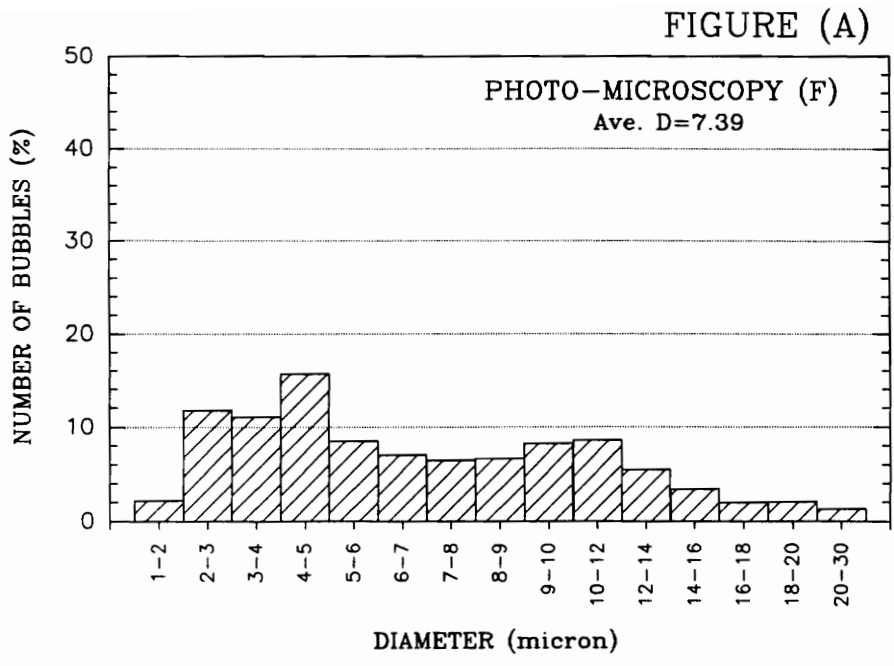


Figure 18. Particle Size Distribution for Batch F (47.2, 4.8, 700), as Determined by Photo-Microscopy. (A) Number of bubbles (%), (B) Weight percent.

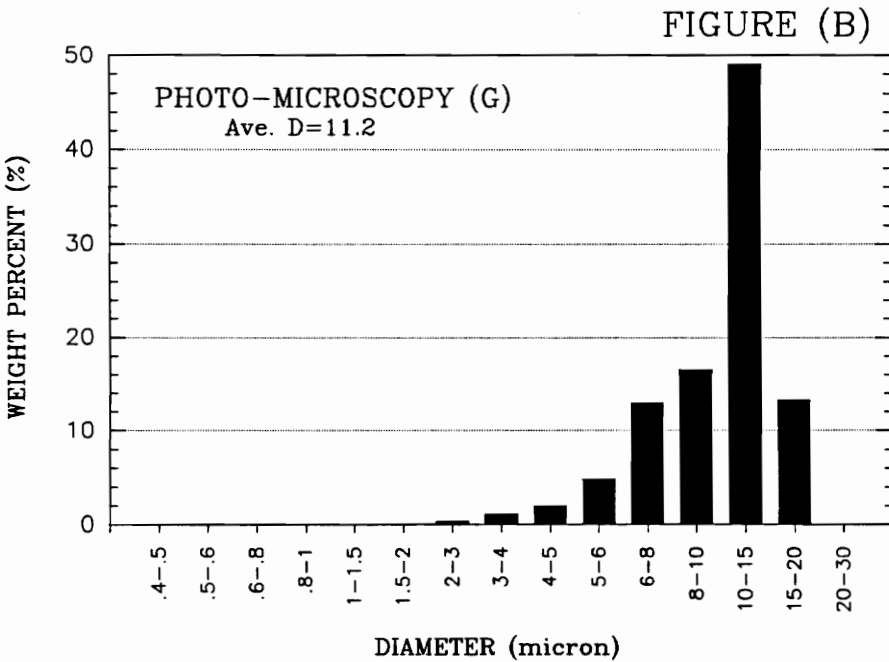
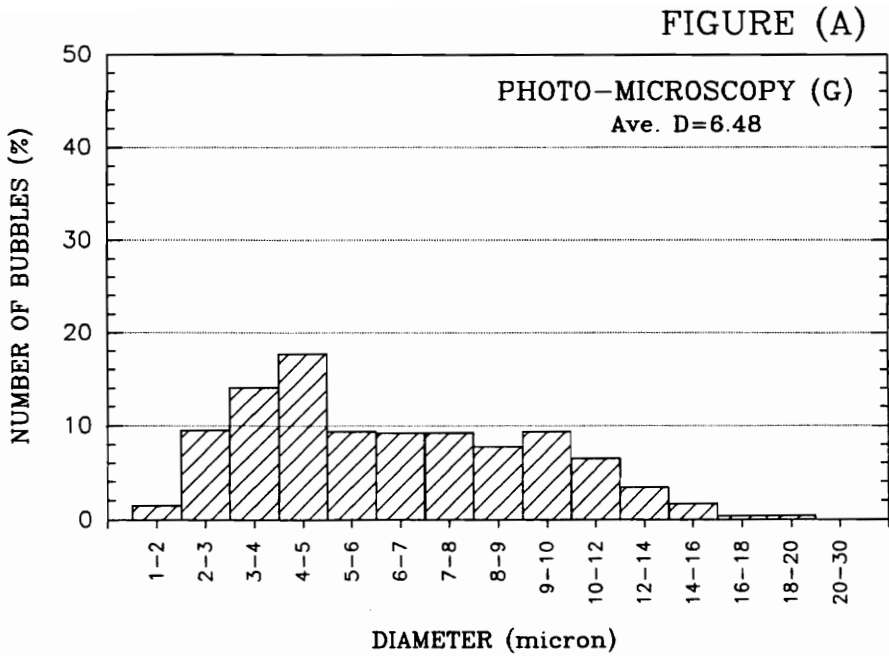


Figure 19. Particle Size Distribution for Batch G (302.8, 30.0, 1500), as Determined by Photo-Microscopy. (A) Number of bubbles (%), (B) Weight percent.

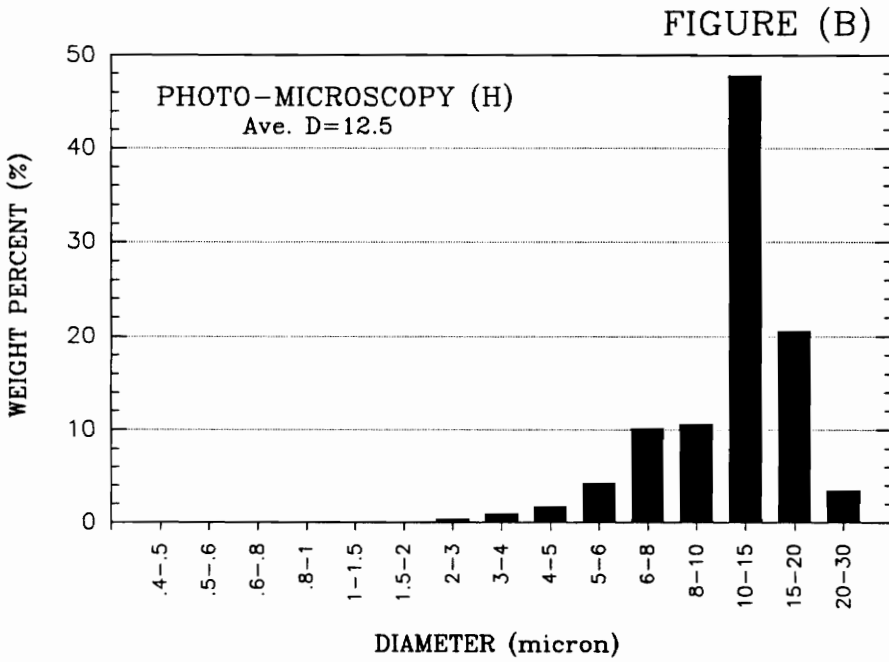
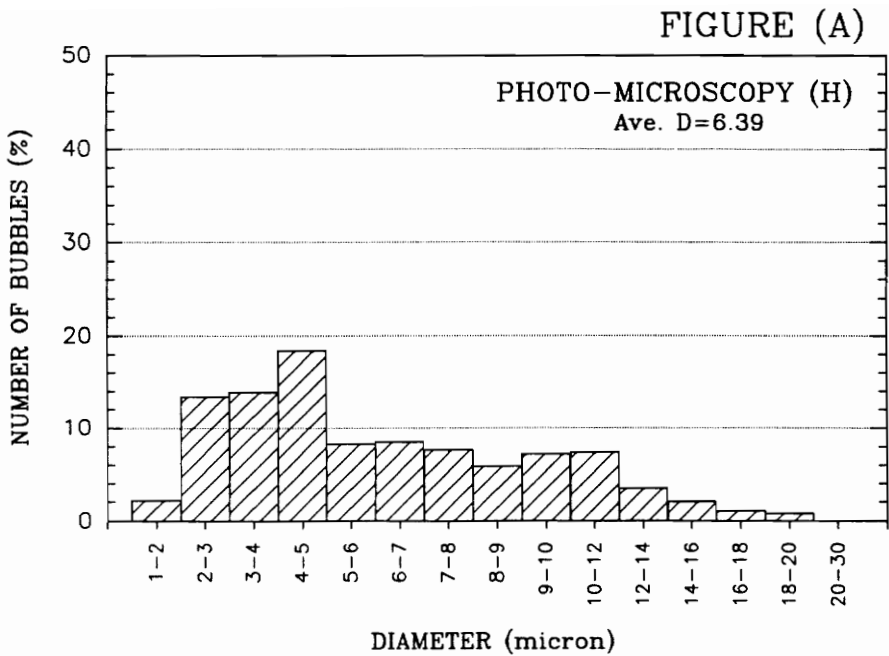


Figure 20. Particle Size Distribution for Batch H (302.4, 20.3, 1500), as Determined by Photo-Microscopy. (A) Number of bubbles (%), (B) Weight percent.

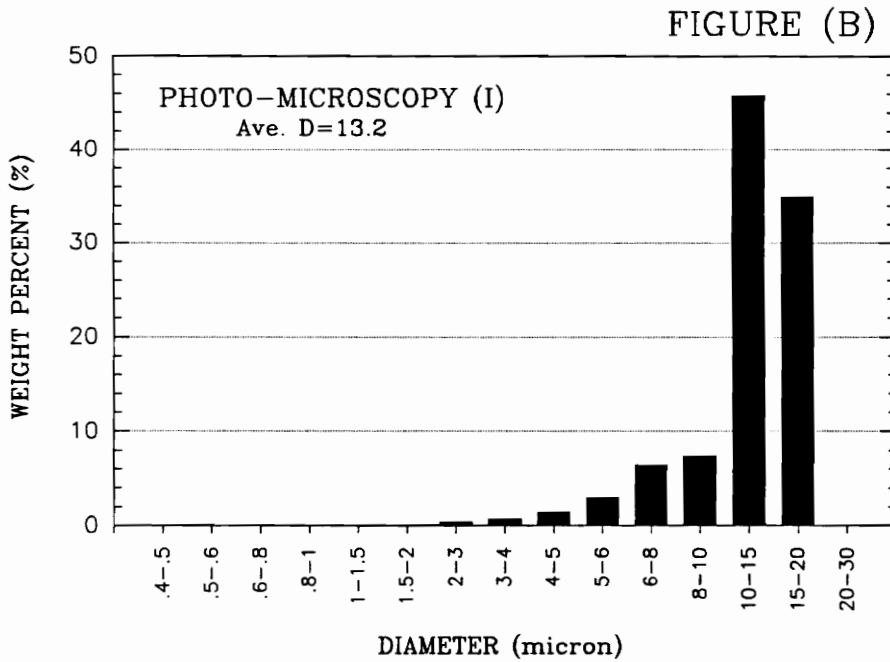
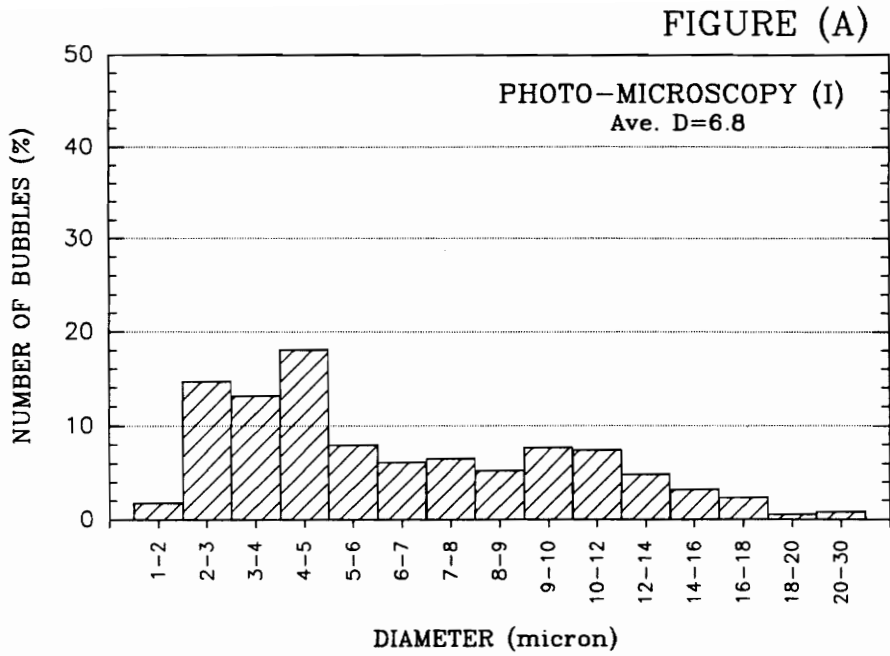


Figure 21. Particle Size Distribution for Batch I (302.4, 20.3, 700), as Determined by Photo-Microscopy. (A) Number of bubbles (%), (B) Weight percent.

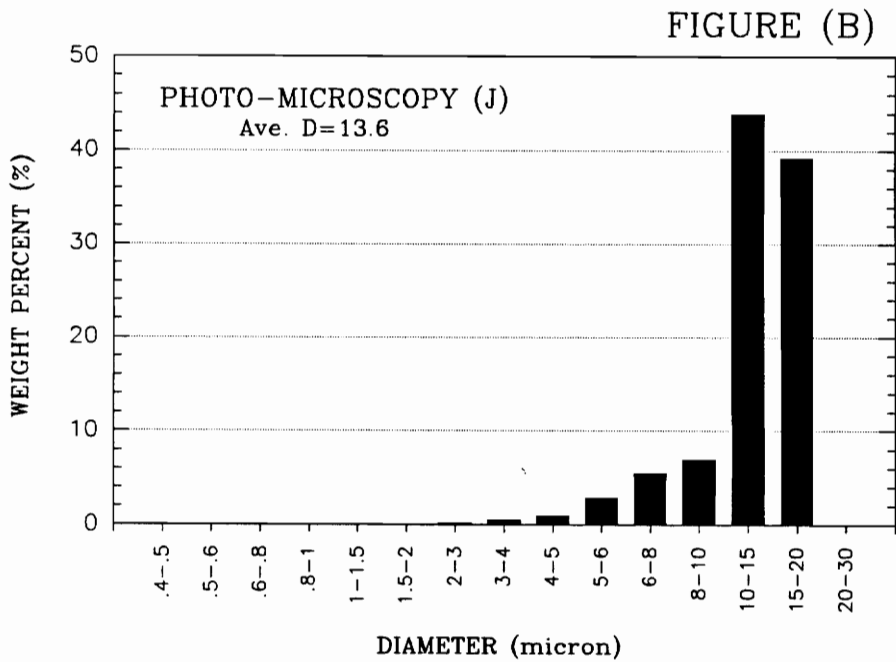
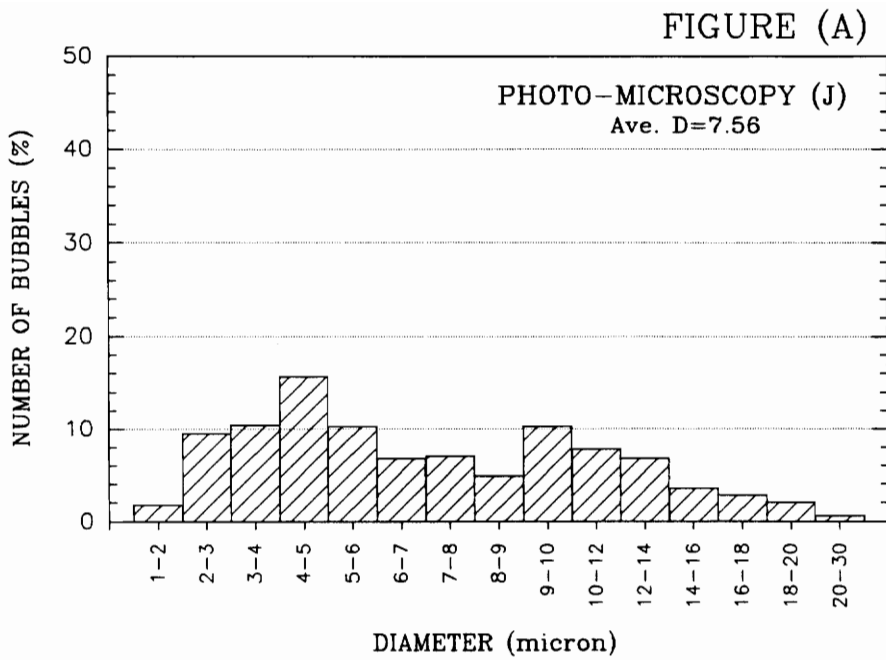


Figure 22. Particle Size Distribution for Batch J (150.3, 30.1, 700), as Determined by Photo-Microscopy. (A) Number of bubbles (%), (B) Weight percent.

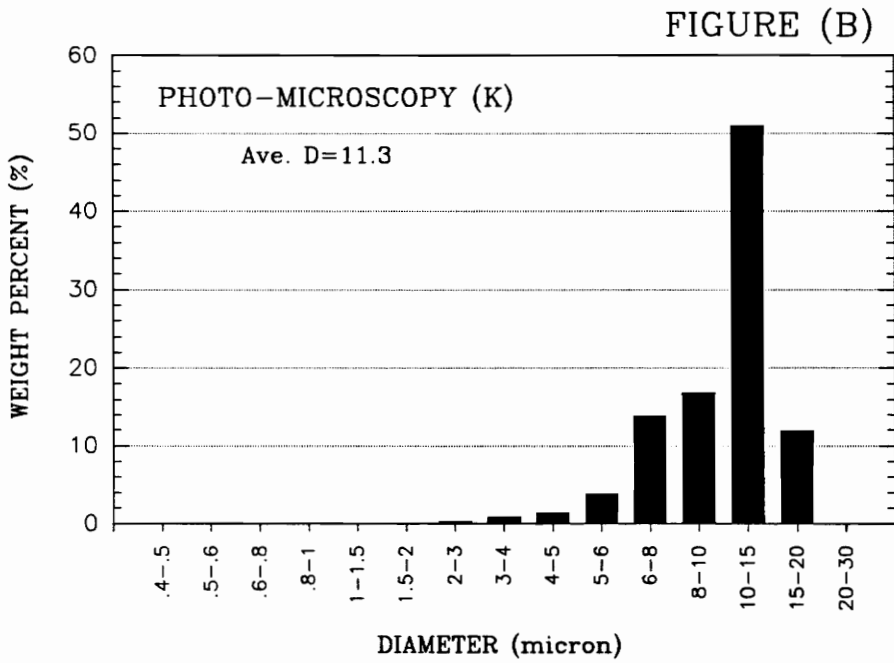
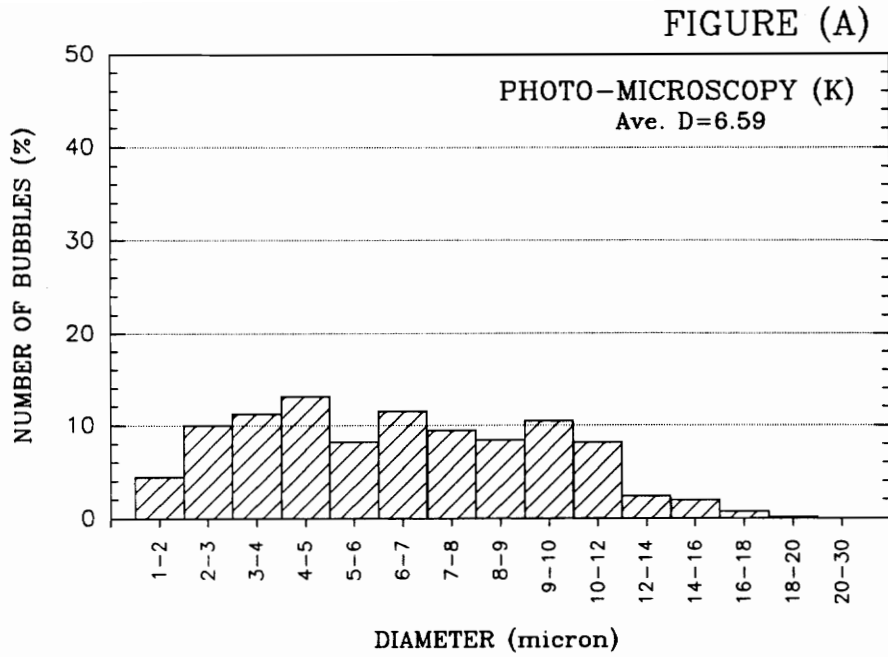


Figure 23. Particle Size Distribution for Batch K (150.3, 30.1, 1500), as Determined by Photo-Microscopy. (A) Number of bubbles (%), (B) Weight percent.

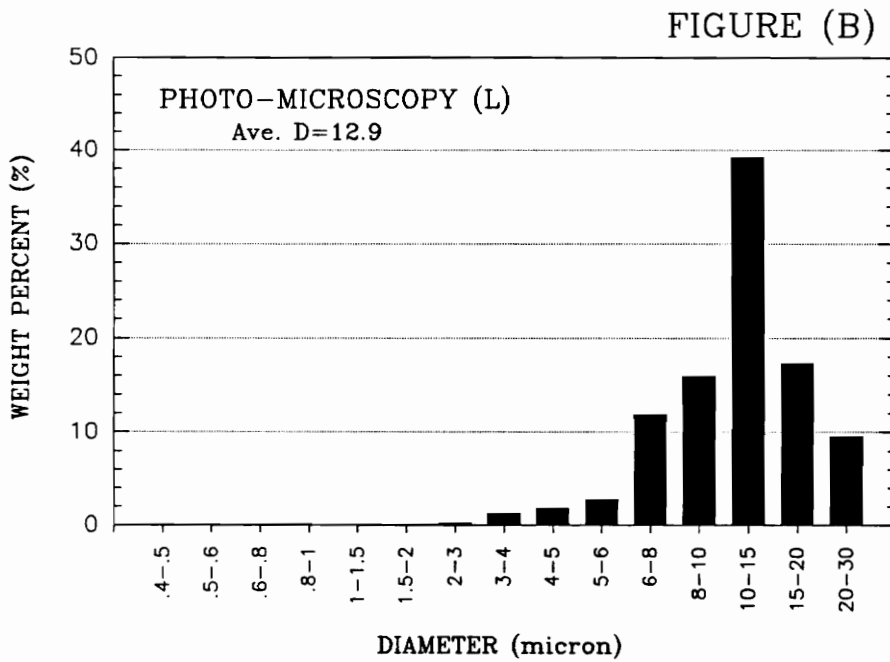
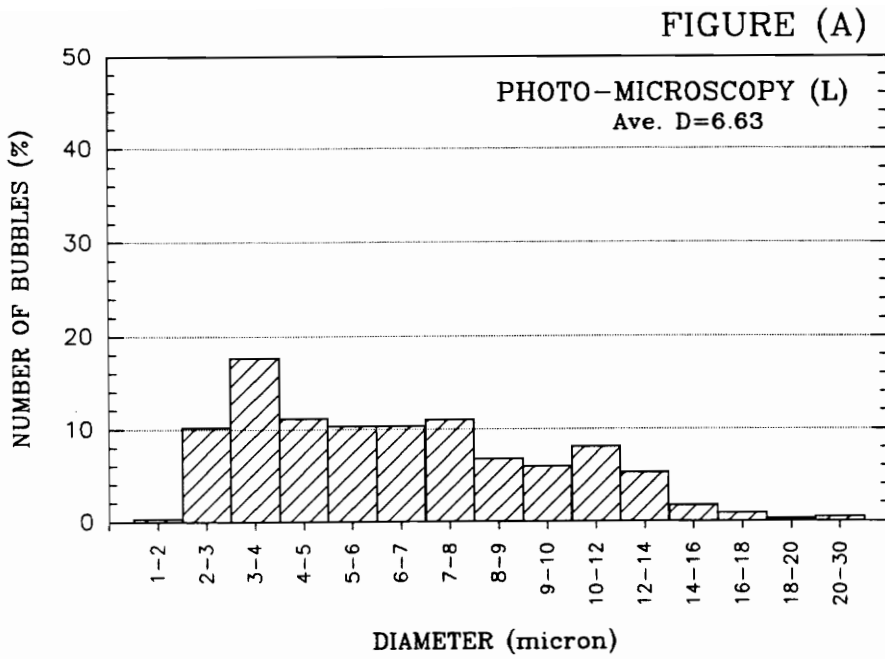


Figure 24. Particle Size Distribution for Batch L (174.5, 20.1, 1100), as Determined by Photo-Microscopy. (A) Number of bubbles (%), (B) Weight percent.

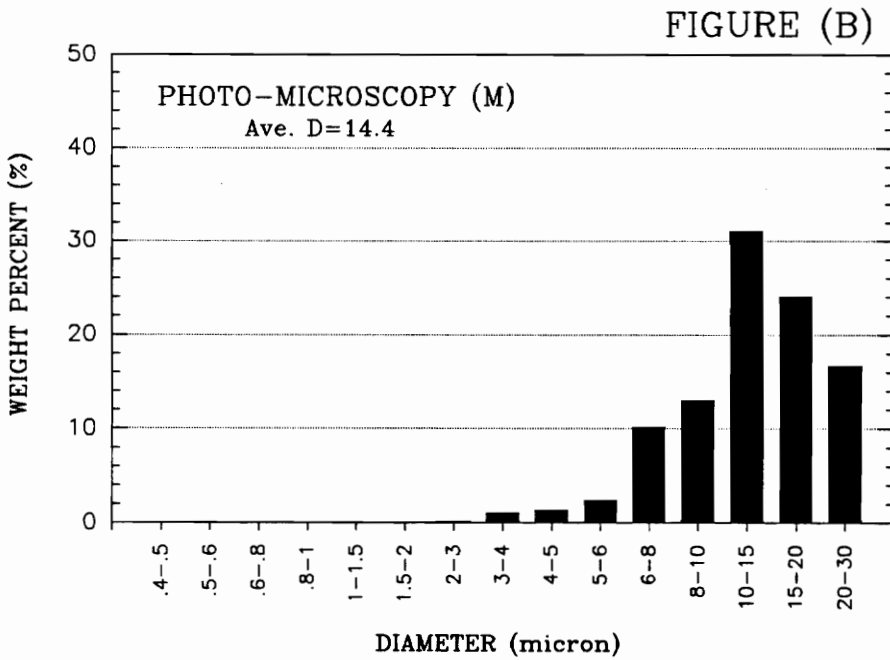
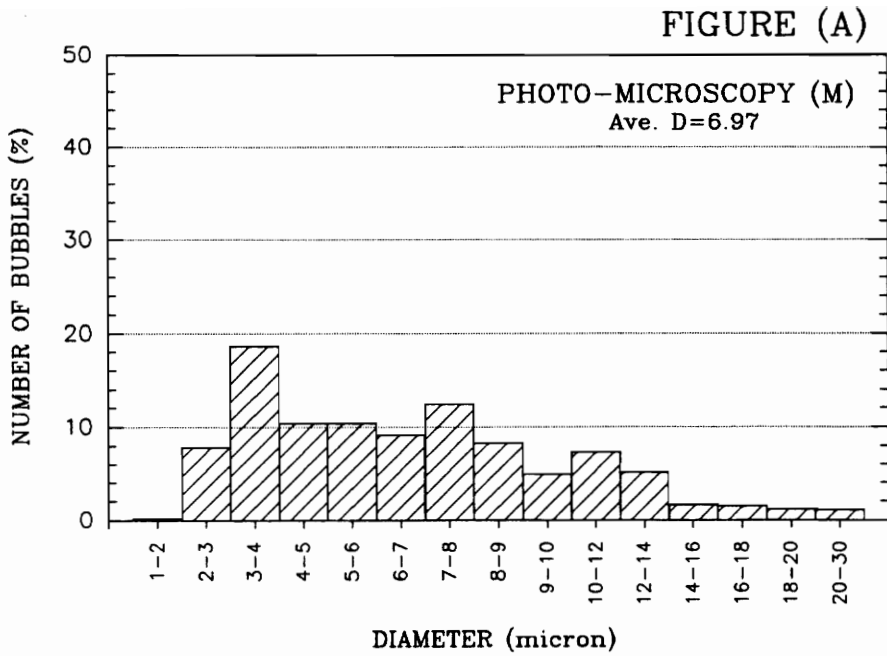


Figure 25. Particle Size Distribution for Batch M (174.5, 20.1, 1100), as Determined by Photo-Microscopy. (A) Number of bubbles (%), (B) Weight percent.

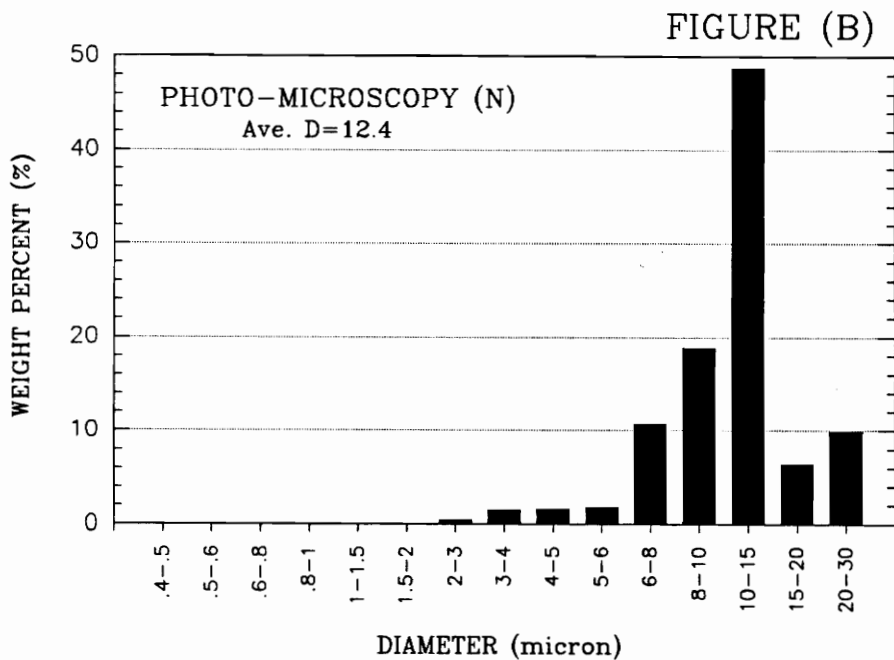
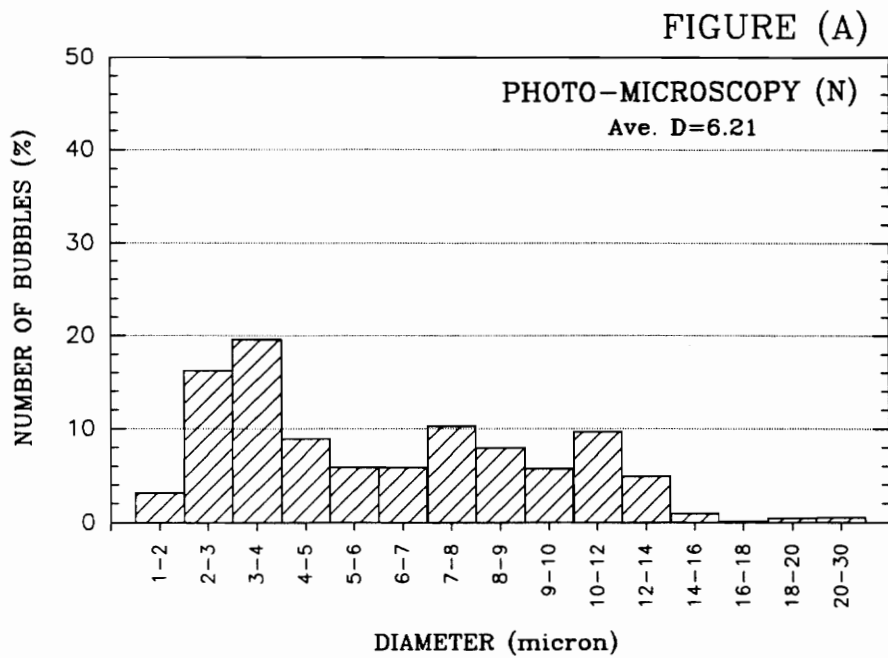


Figure 26. Particle Size Distribution for Batch N (174.7, 20.1, 1100), as Determined by Photo-Microscopy. (A) Number of bubbles (%), (B) Weight percent.

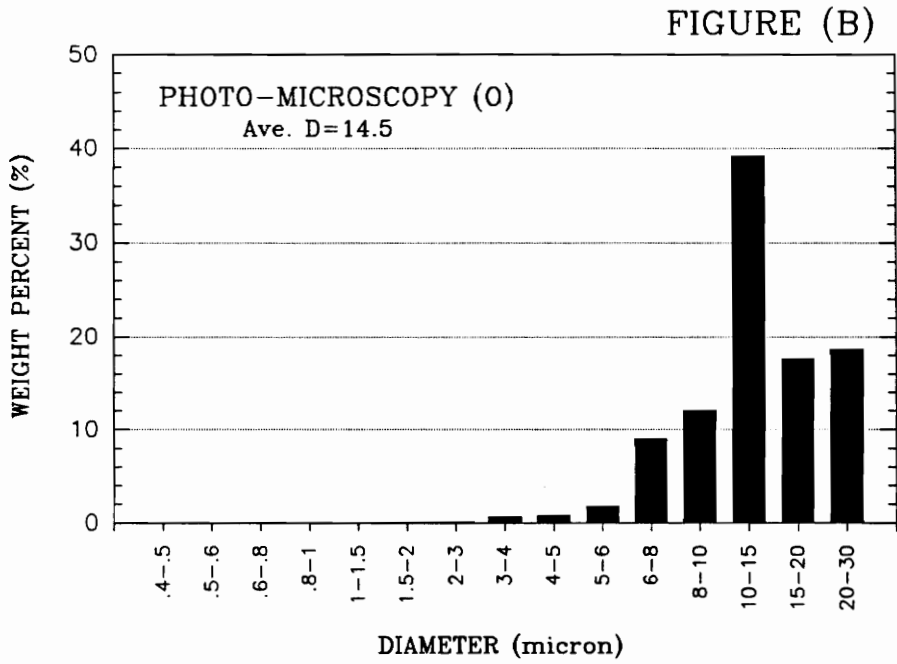
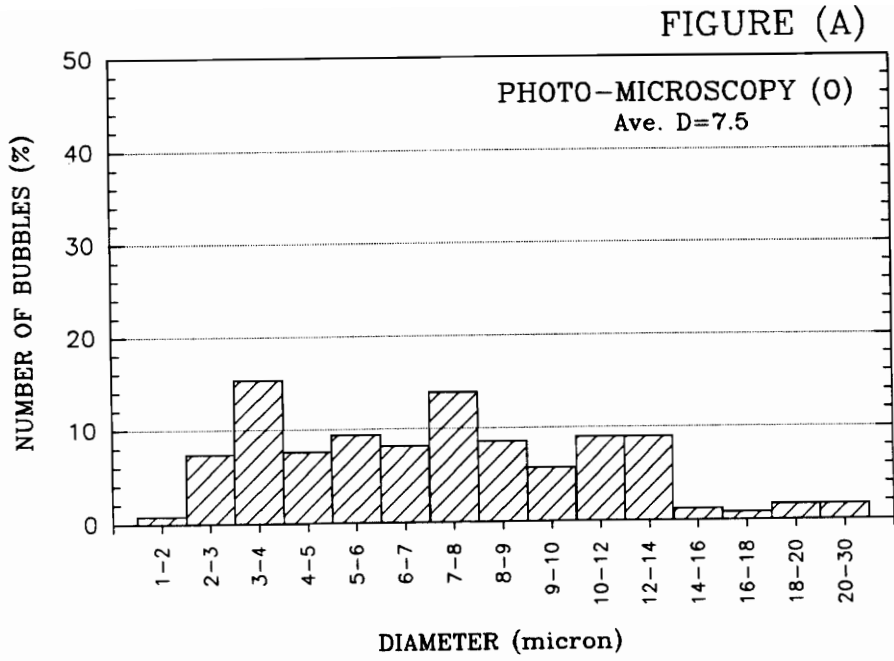


Figure 27. Particle Size Distribution for Batch O (174.7, 20.1, 1100), as Determined by Photo-Microscopy. (A) Number of bubbles (%), (B) Weight percent.

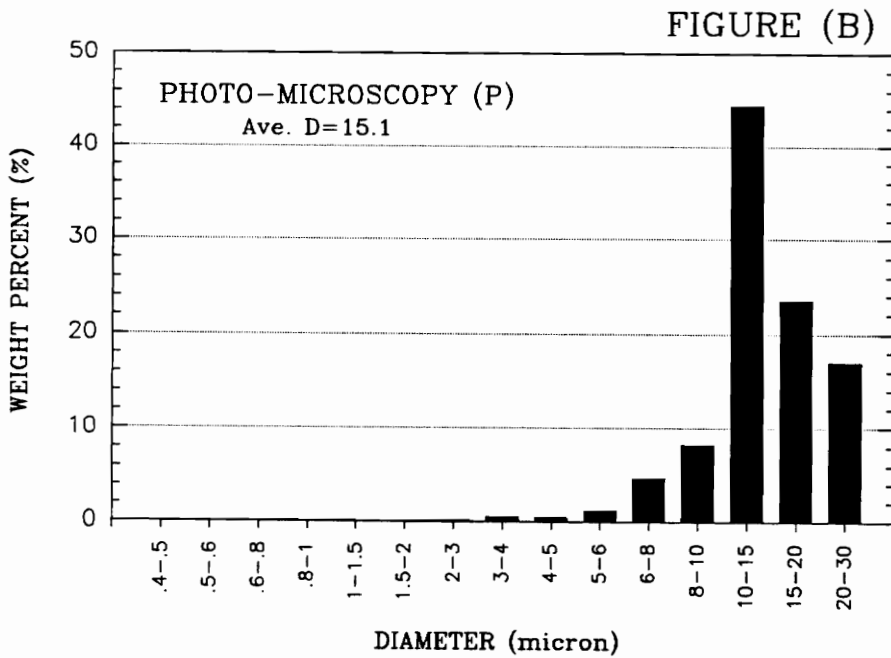
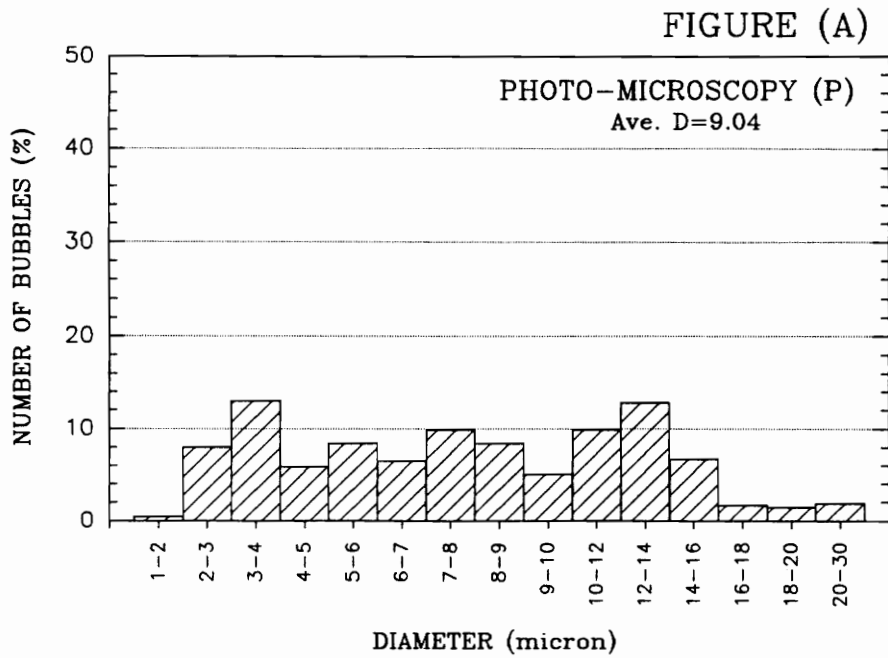


Figure 28. Particle Size Distribution for Batch P (46.9, 9.5, 700), as Determined by Photo-Microscopy. (A) Number of bubbles (%), (B) Weight percent.

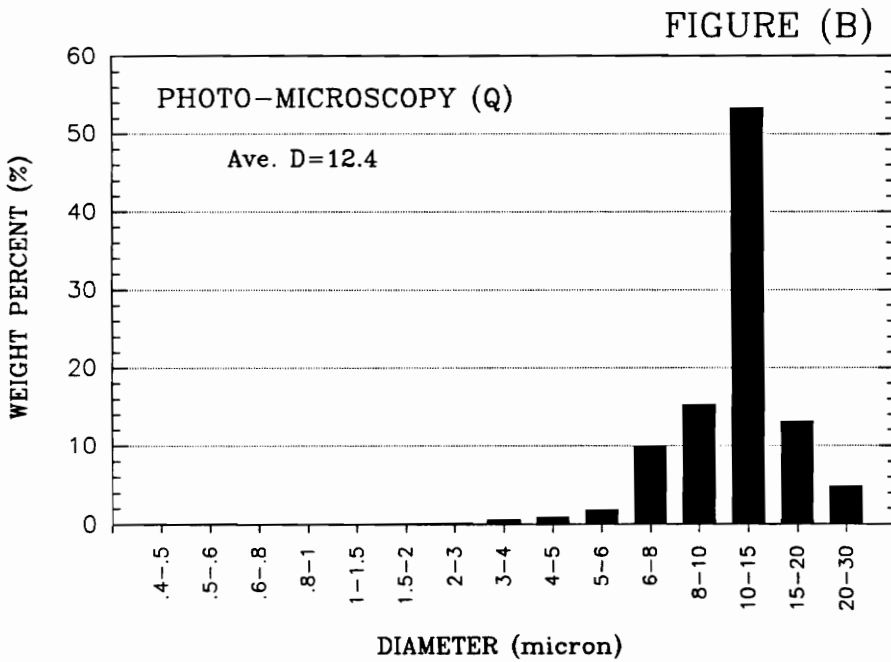
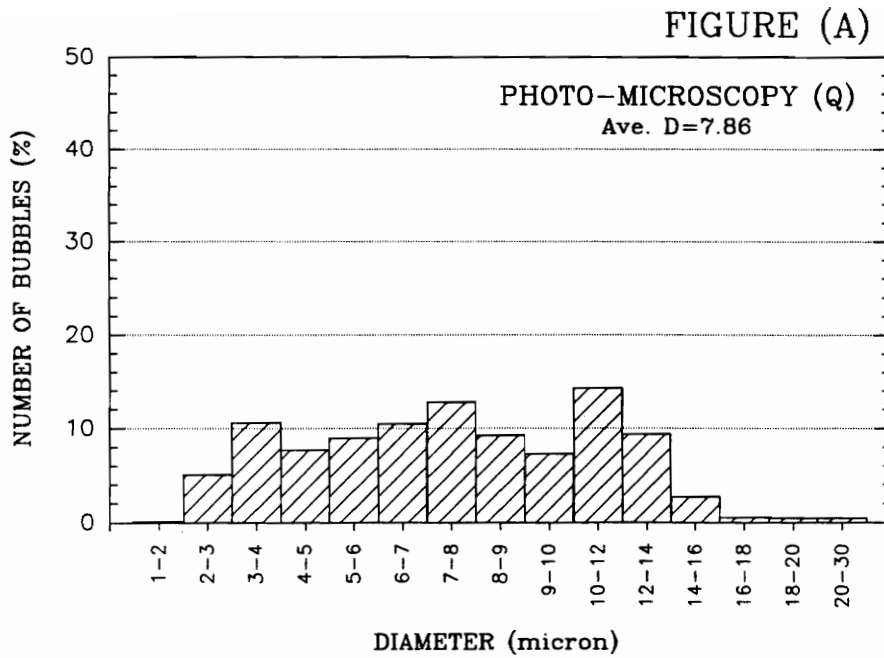


Figure 29. Particle Size Distribution for Batch Q (46.9, 9.5, 1500), as Determined by Photo-Microscopy. (A) Number of bubbles (%), (B) Weight percent.

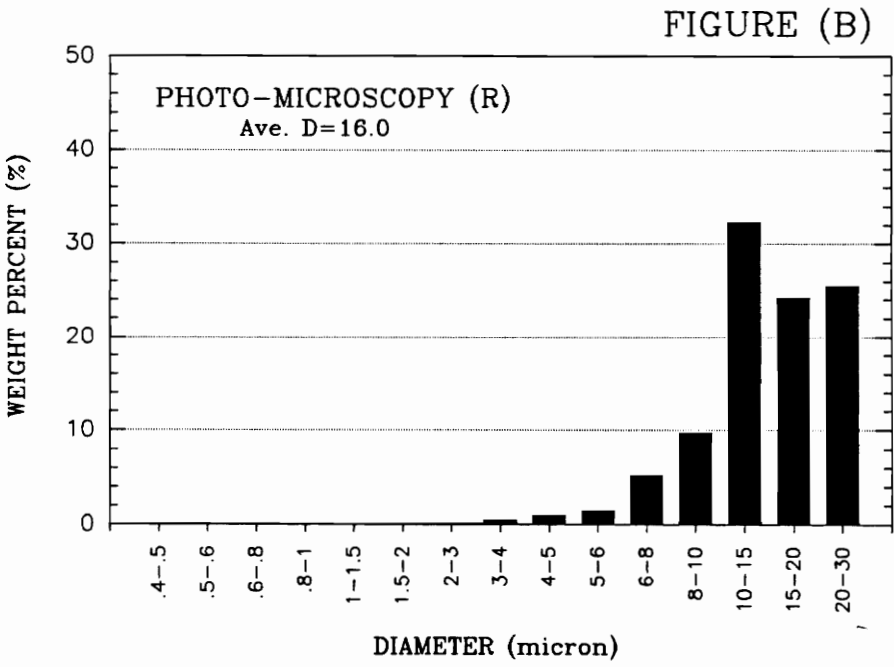
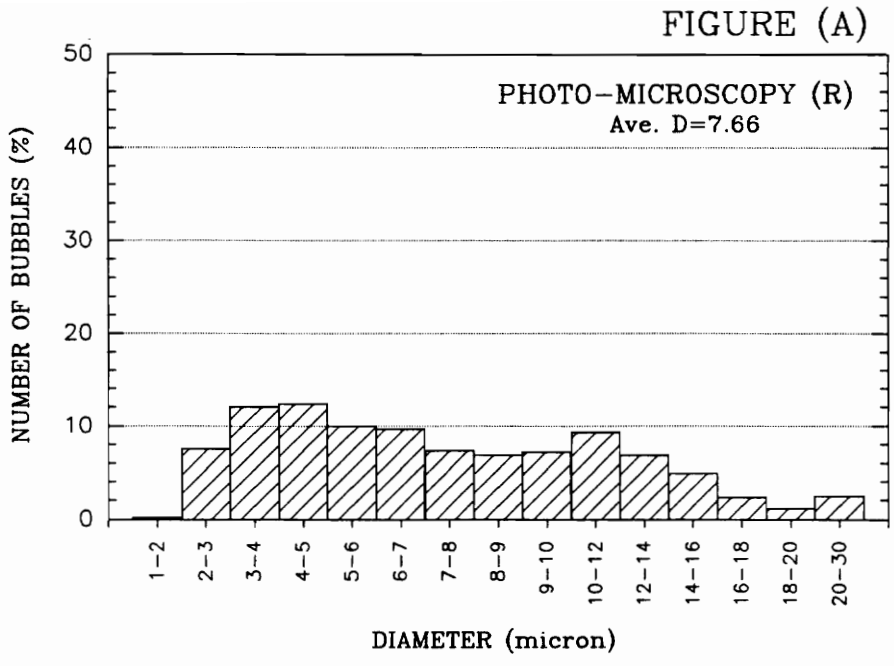


Figure 30. Particle Size Distribution for Batch R (259.2, 25.9, 1500), as Determined by Photo-Microscopy. (A) Number of bubbles (%), (B) Weight percent.

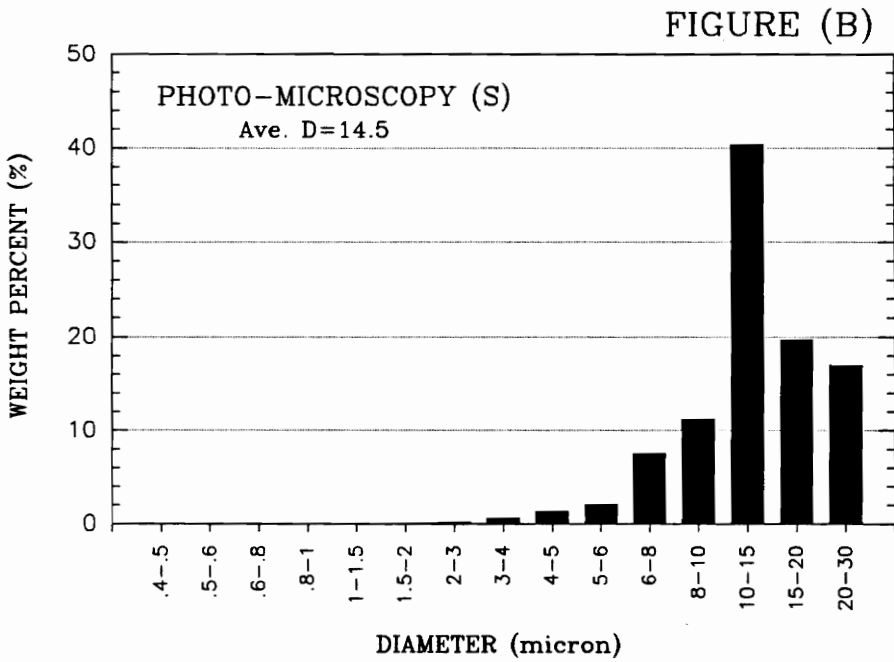
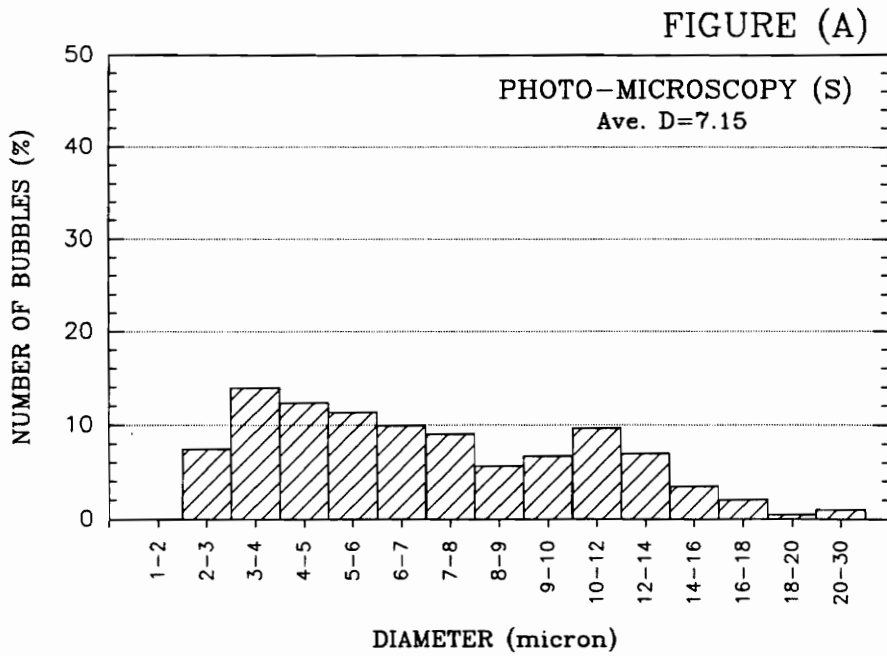


Figure 31. Particle Size Distribution for Batch S (267.5, 26.7, 1500), as Determined by Photo-Microscopy. (A) Number of bubbles (%), (B) Weight percent.

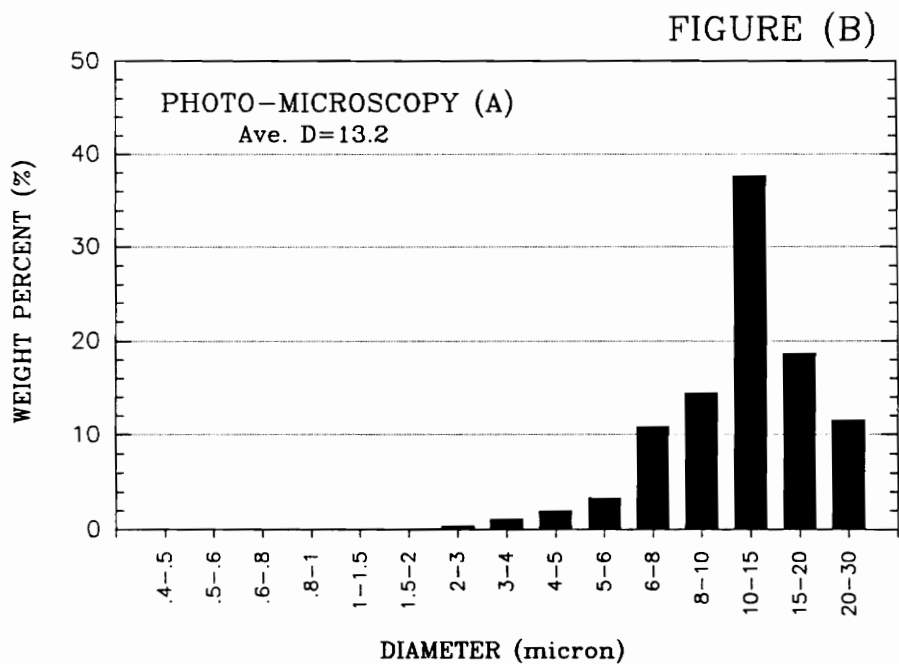
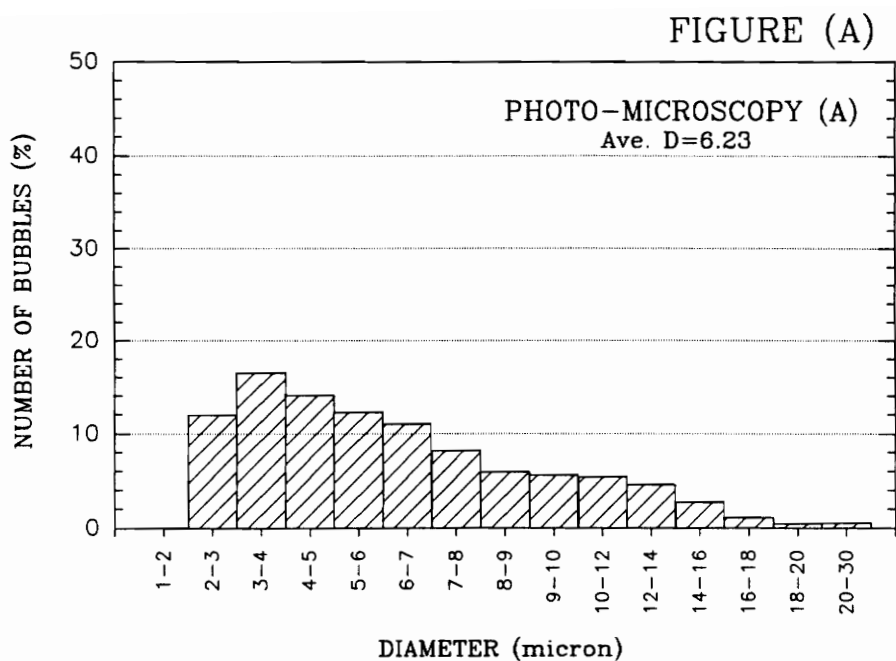


Figure 32. Particle Size Distribution for Batch A (97.9, 9.7, 700), as Determined by Photo-Microscopy Four Months After the Aprons Were Made. (A) Number of bubbles (%), (B) Weight percent.

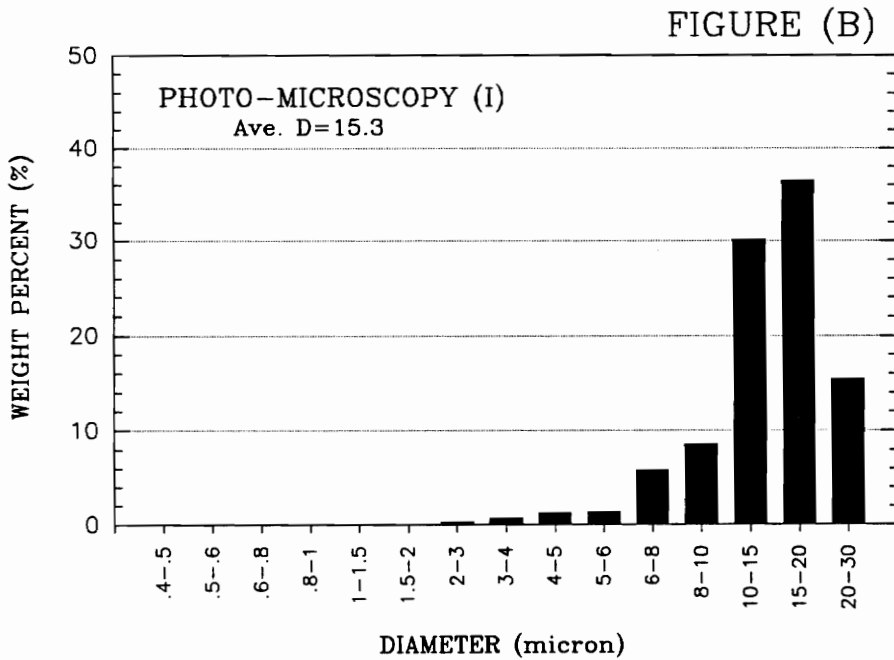
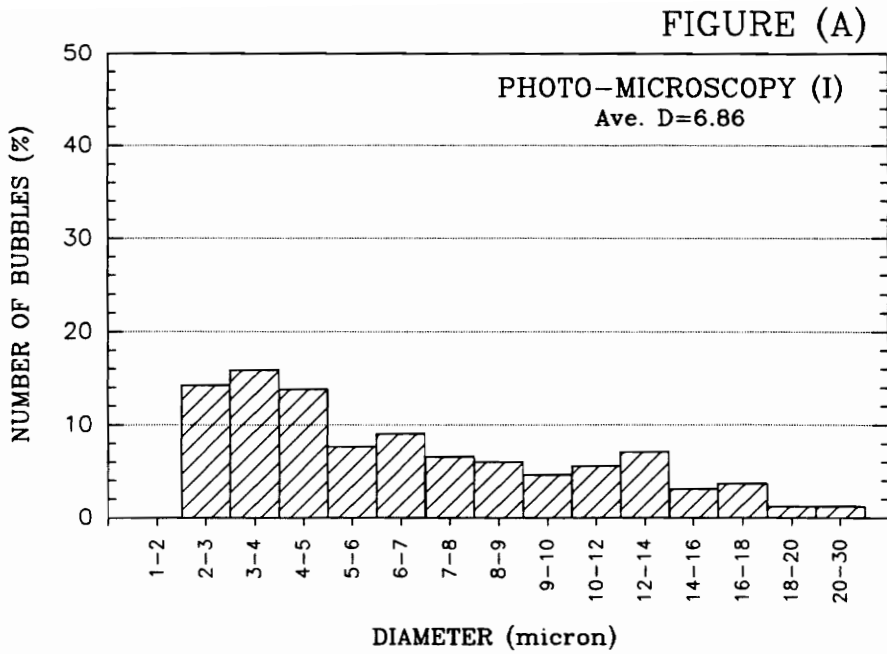


Figure 33. Particle Size Distribution for Batch I (302.4, 20.3, 700), as Determined by Photo-Microscopy Four Months After the Aprons Were Made. (A) Number of bubbles (%), (B) Weight percent.

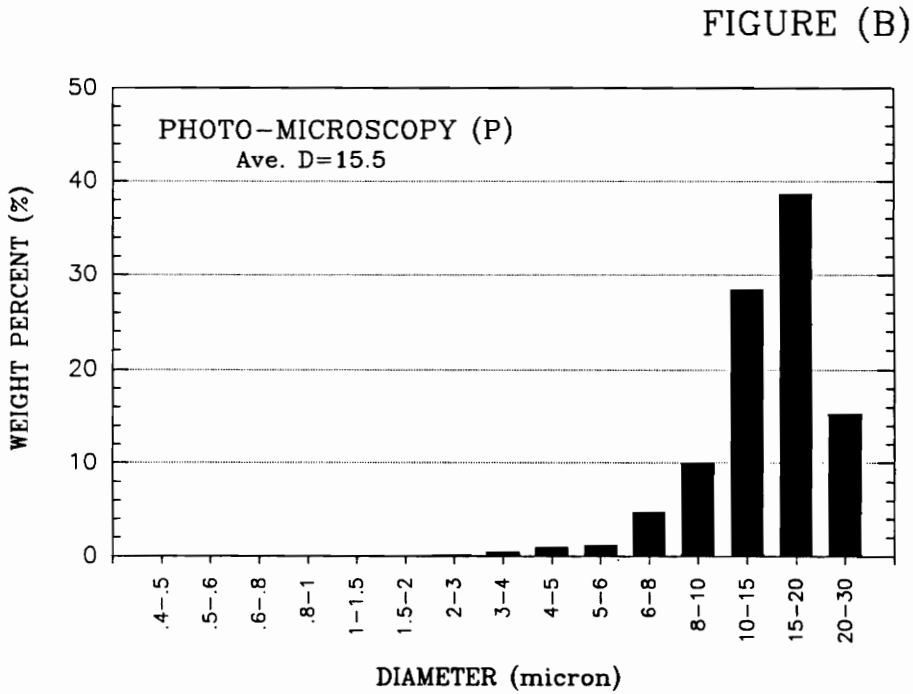
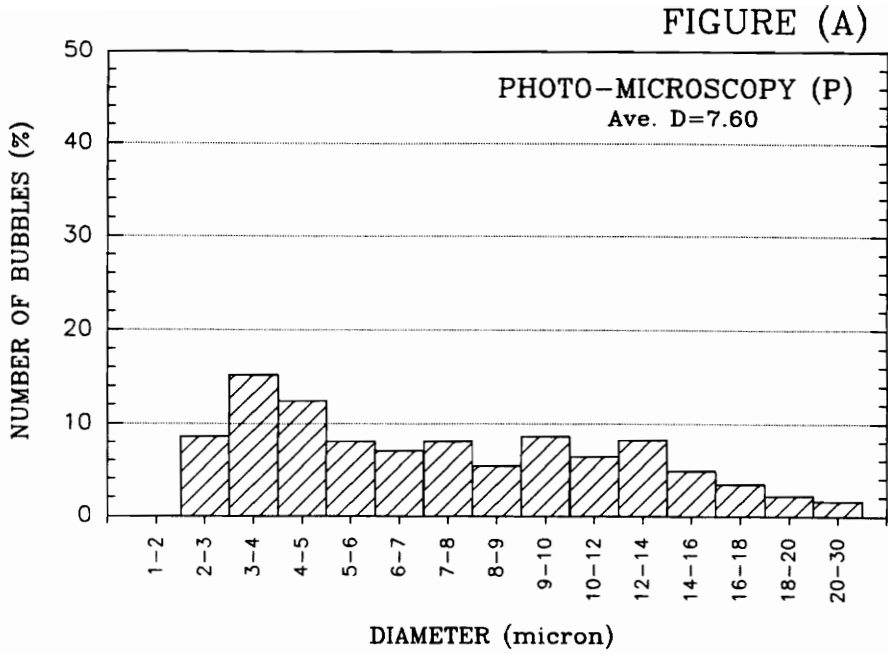


Figure 34. Particle Size Distribution for Batch P (46.9, 9.5, 700), as Determined by Photo-Microscopy Four Months After the Aphrons Were Made. (A) Number of bubbles (%), (B) Weight percent.

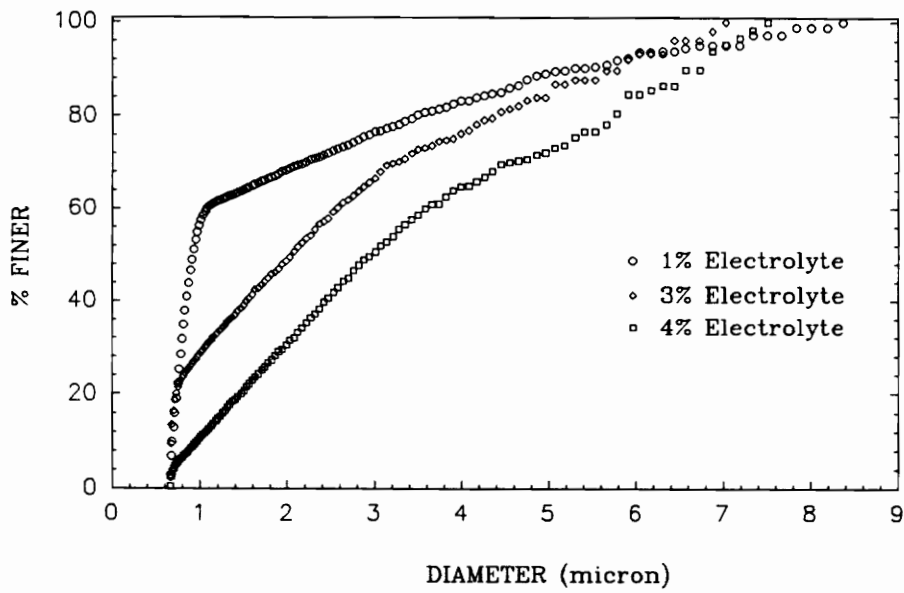


Figure 35. Particle Size of Polyaphrons, Determined with a Coulter Counter

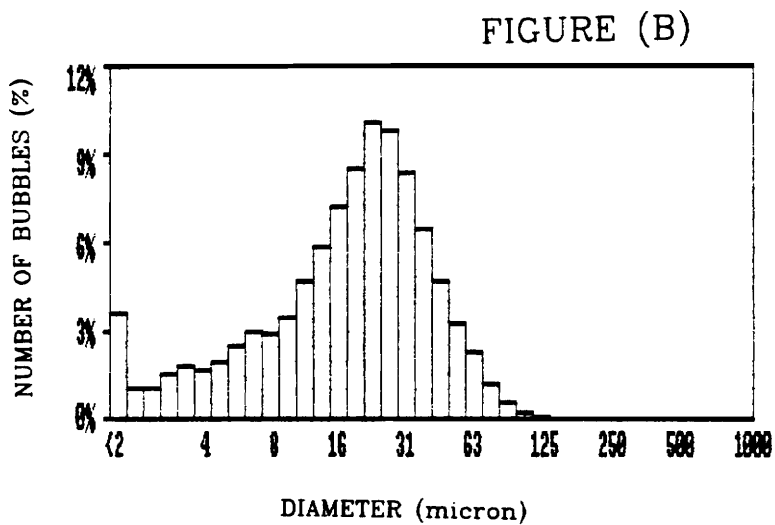
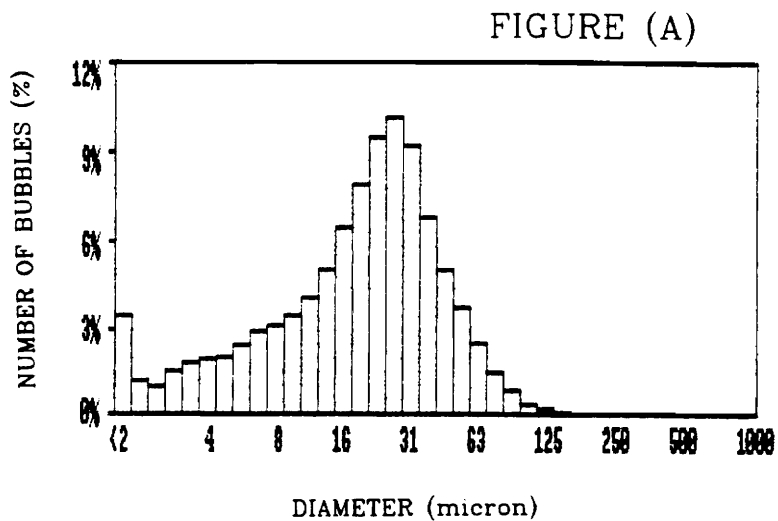


Figure 36. Particle size distribution for Batch H (302.4, 20.3, 1500), as determined by the PAR-TEC 100 Analyzer (A) immediately after testing started, (B) eight minutes.

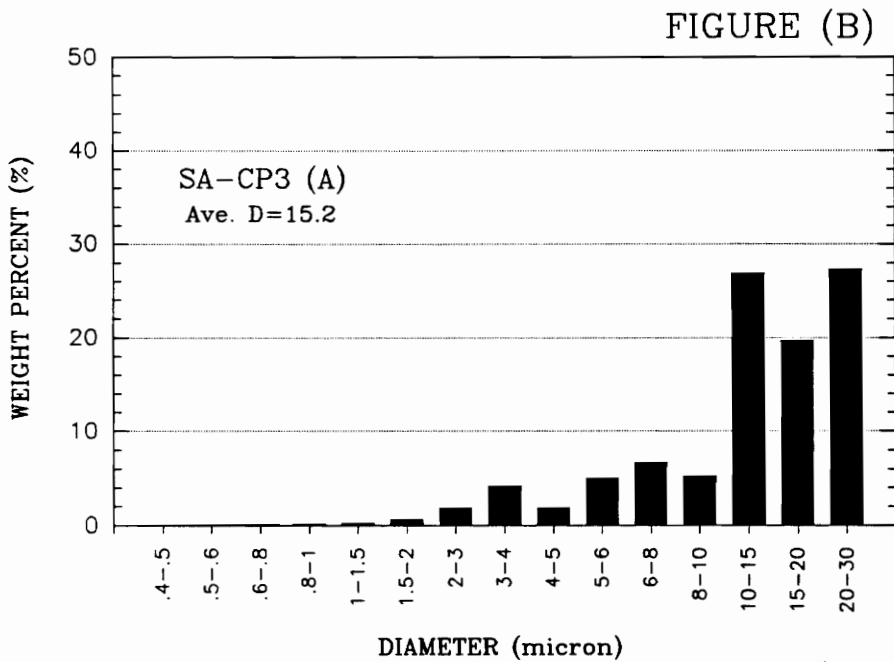
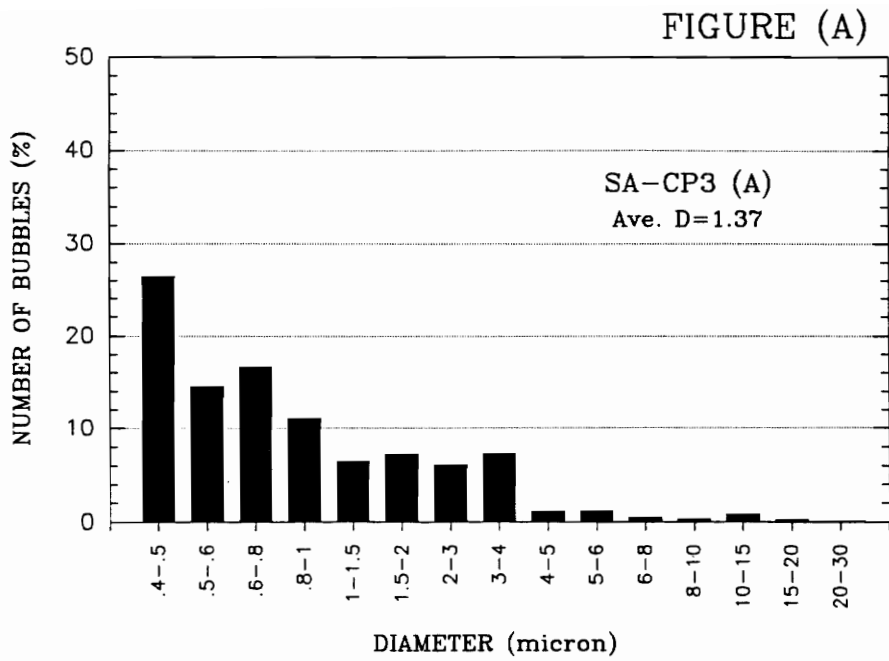


Figure 37. Particle Size Distribution for Batch A (97.9, 9.7, 700), as Determined with the SA-CP3 Analyser. (A) Number of bubbles (%), (B) Weight percent.

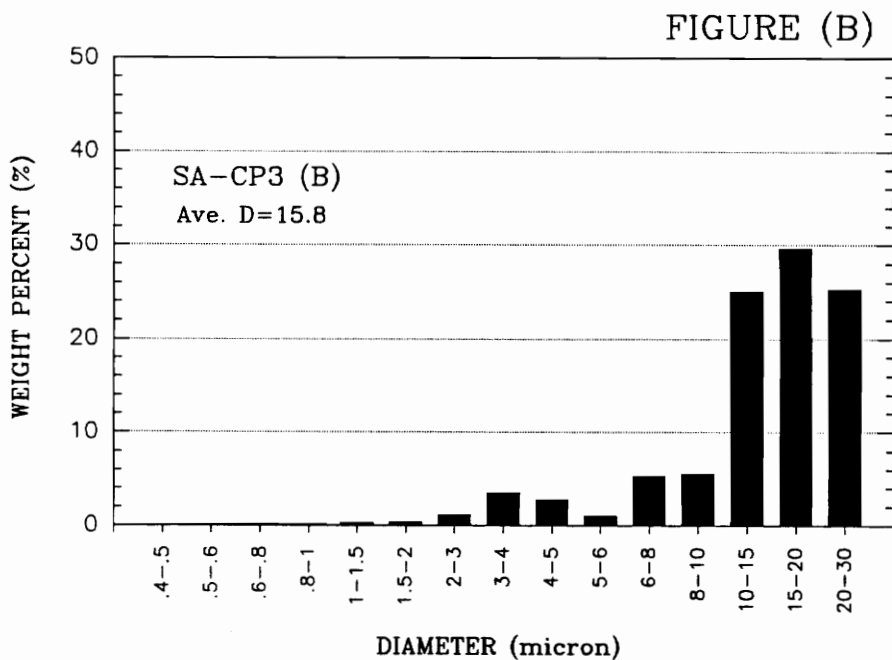
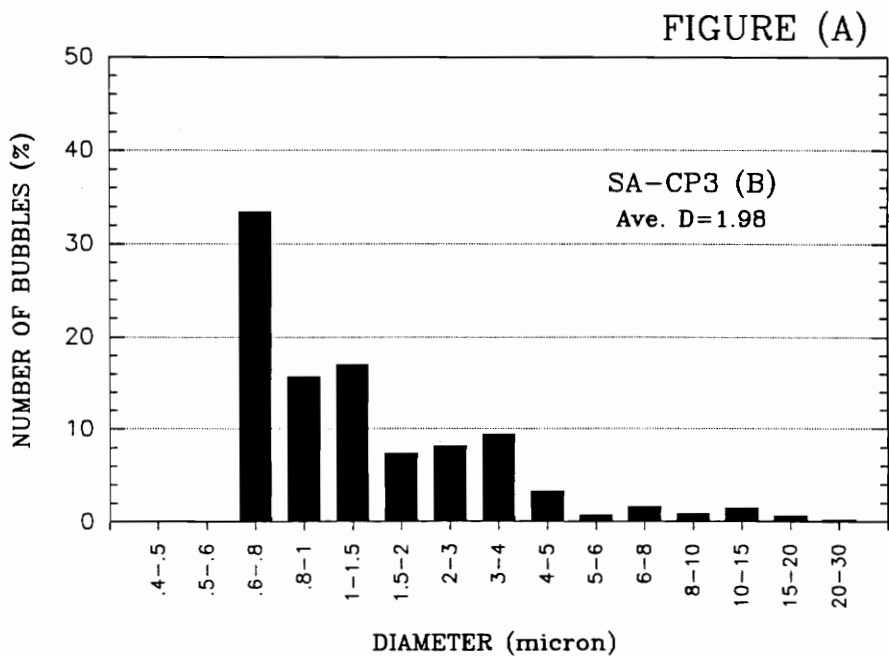


Figure 38. Particle Size Distribution for Batch B (141.6, 19.1, 700), as Determined with the SA-CP3 Analyser. (A) Number of bubbles (%), (B) weight percent.

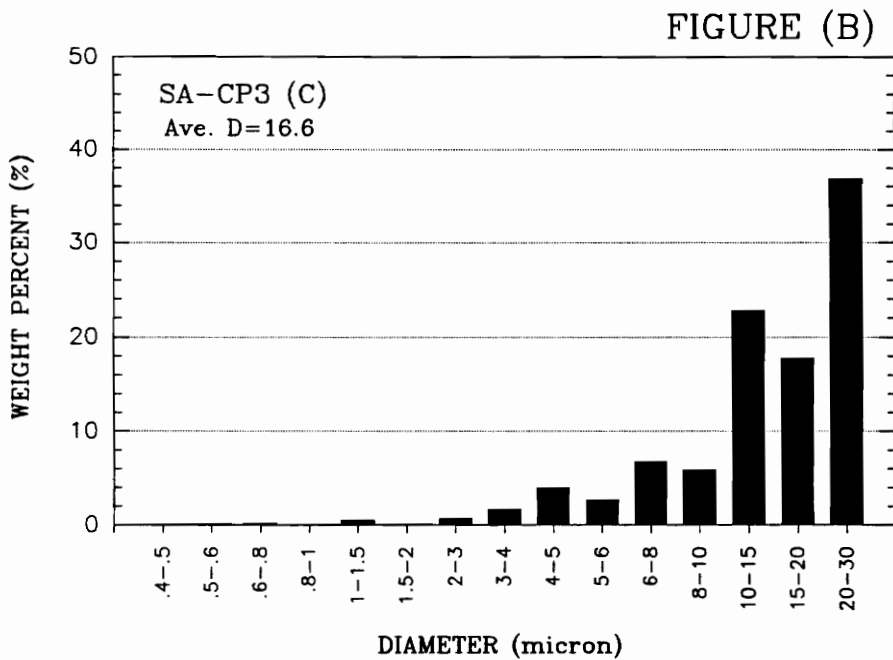
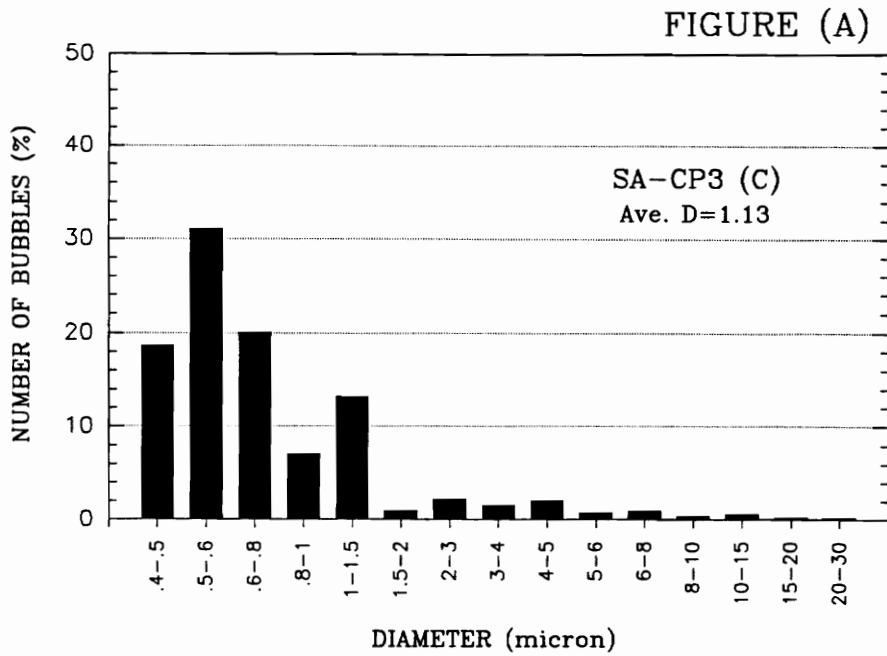


Figure 39. Particle Size Distribution for Batch C (197.8, 19.8, 700), as Determined with the SA-CP3 Analyser. (A) Number of bubbles (%), (B) weight percent.

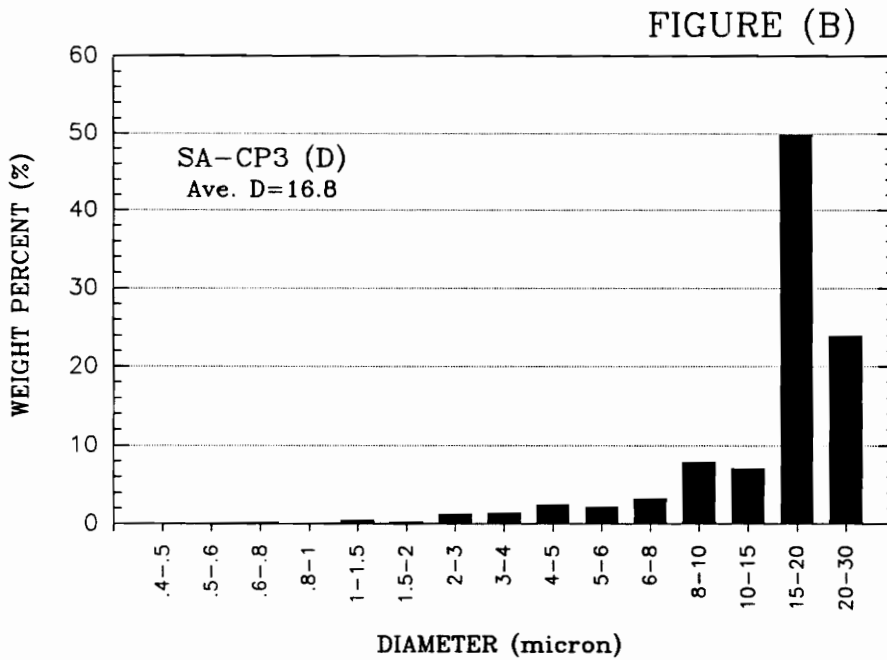
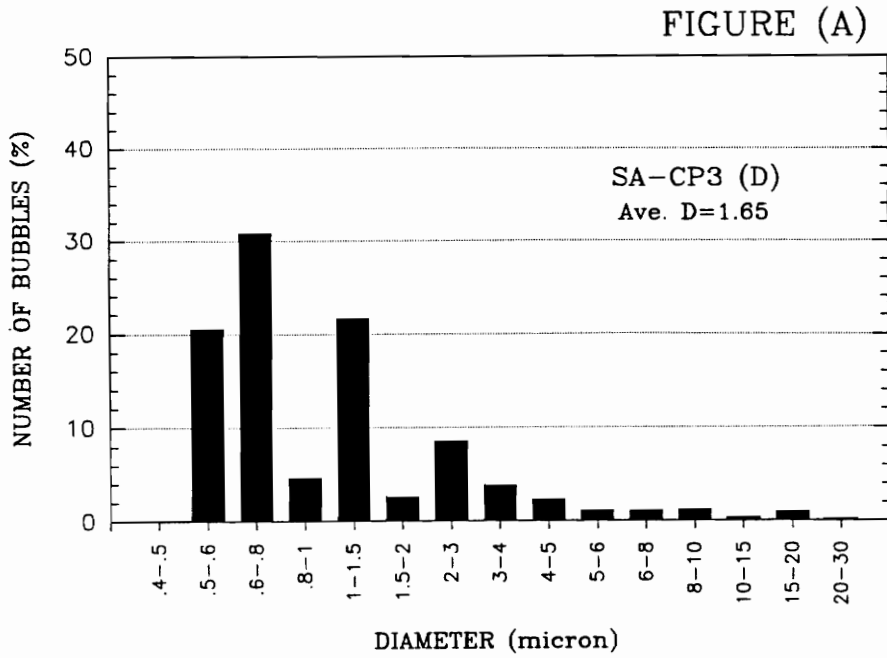


Figure 40. Particle Size Distribution for Batch D (300.0, 29.7, 700), as Determined with the SA-CP3 Analyser. (A) Number of bubbles (%), (B) weight percent.

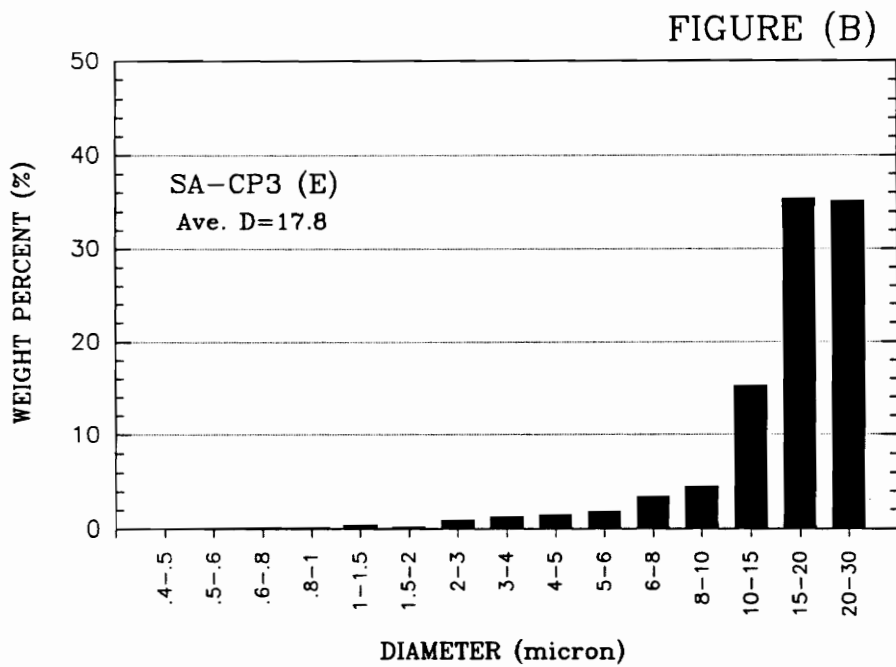
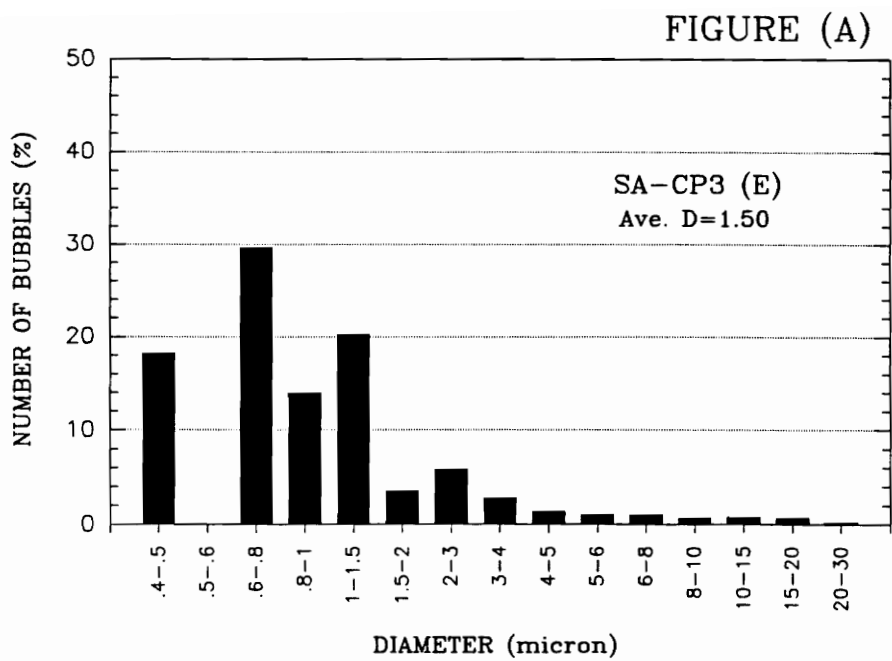


Figure 41. Particle Size Distribution for Batch E (49.4, 4.9, 1500), as Determined with the SA-CP3 Analyser. (A) Number of bubbles (%), (B) weight percent.

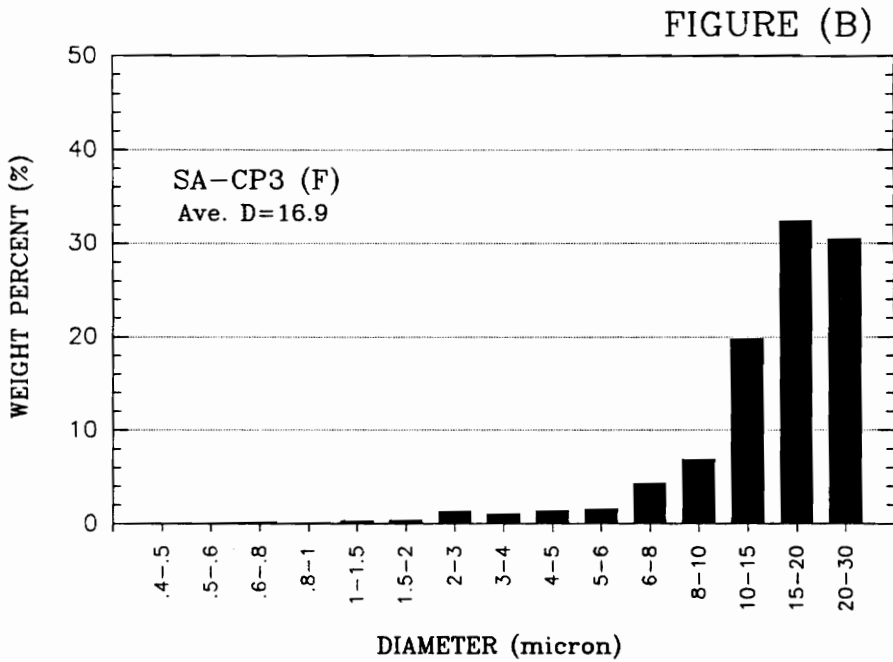
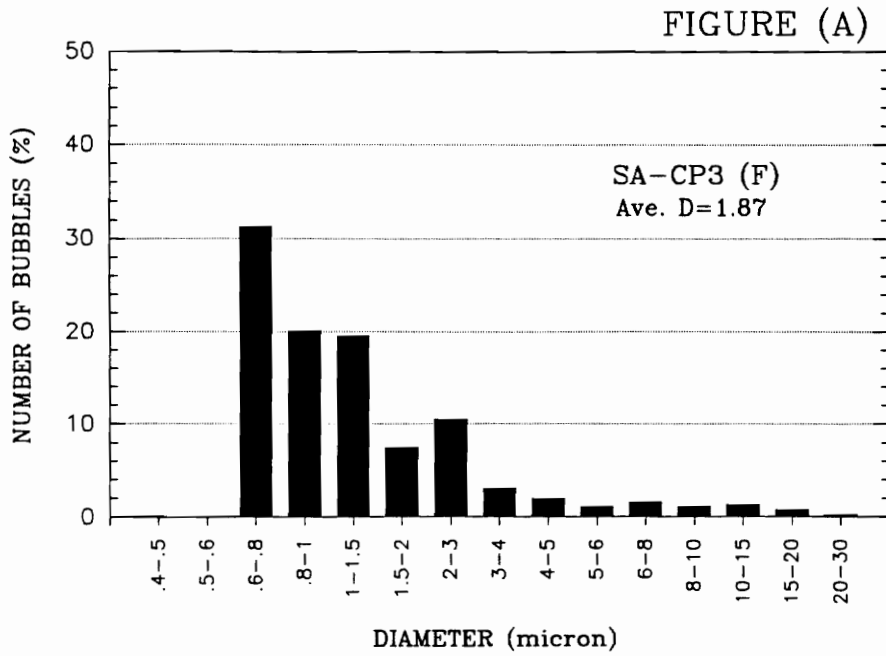


Figure 42. Particle Size Distribution for Batch F (47.2, 4.8, 700), as Determined with the SA-CP3 Analyser. (A) Number of bubbles (%), (B) weight percent.

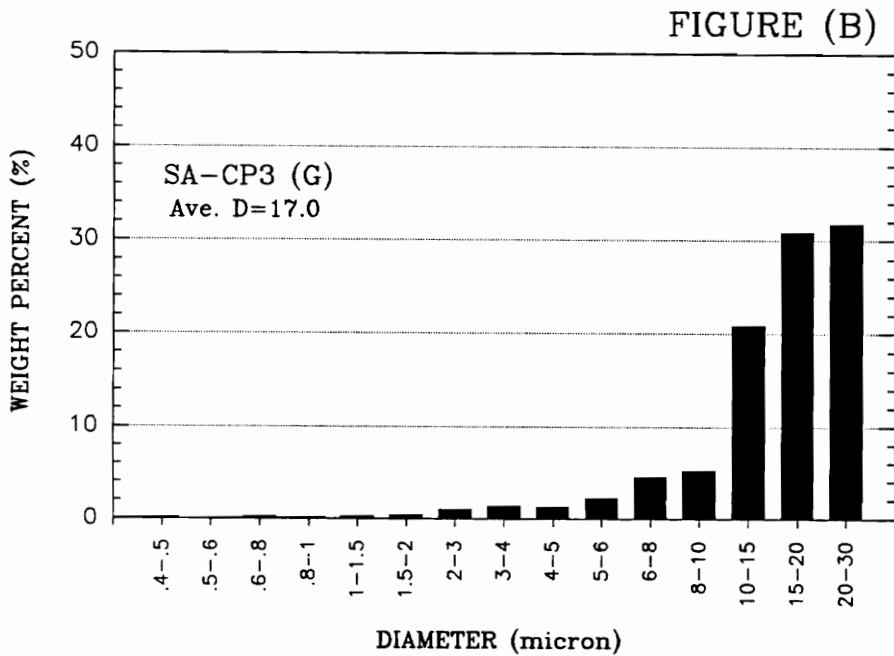
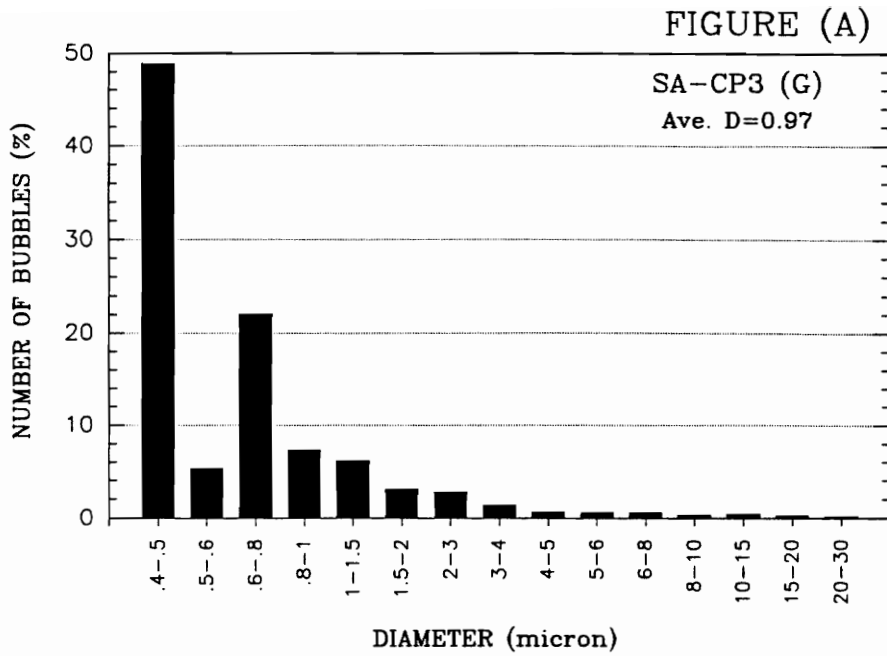


Figure 43. Particle Size Distribution for Batch G (302.8, 30.0, 1500), as Determined with the SA-CP3 Analyser. (A) Number of bubbles (%), (B) weight percent.

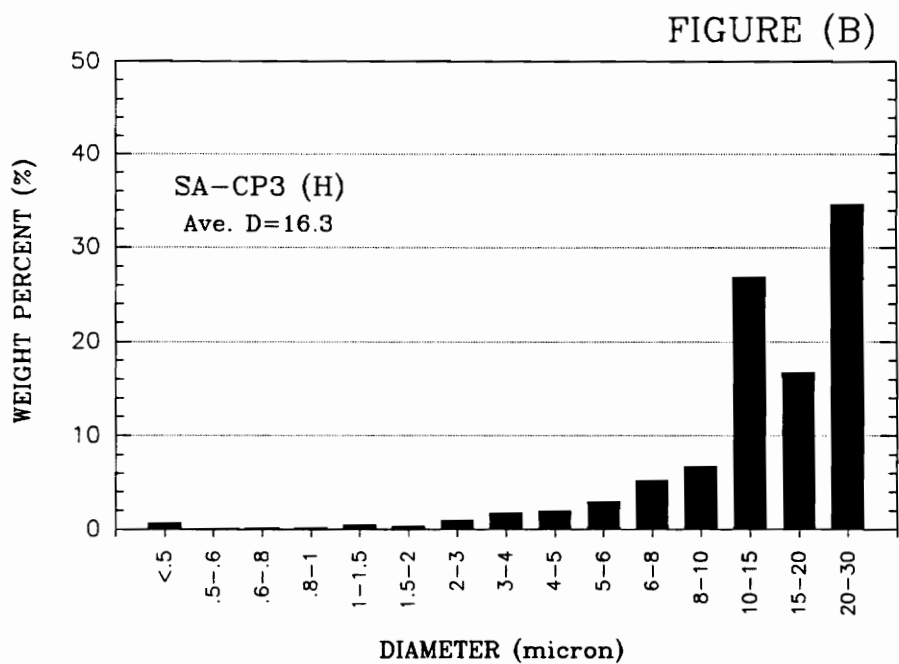
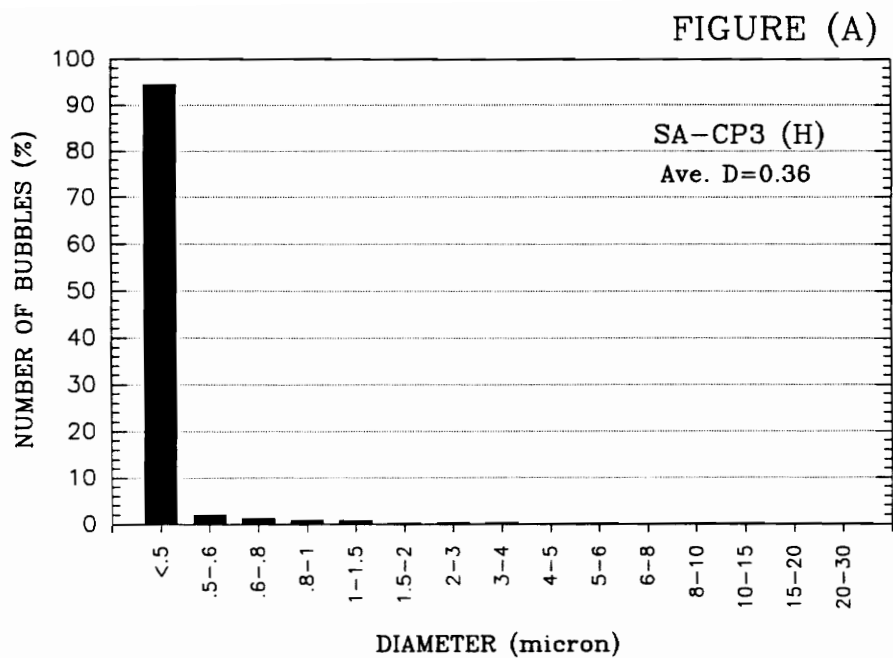


Figure 44. Particle Size Distribution for Batch H (302.4, 20.3, 1500), as Determined with the SA-CP3 Analyser. (A) Number of bubbles (%), (B) weight percent.

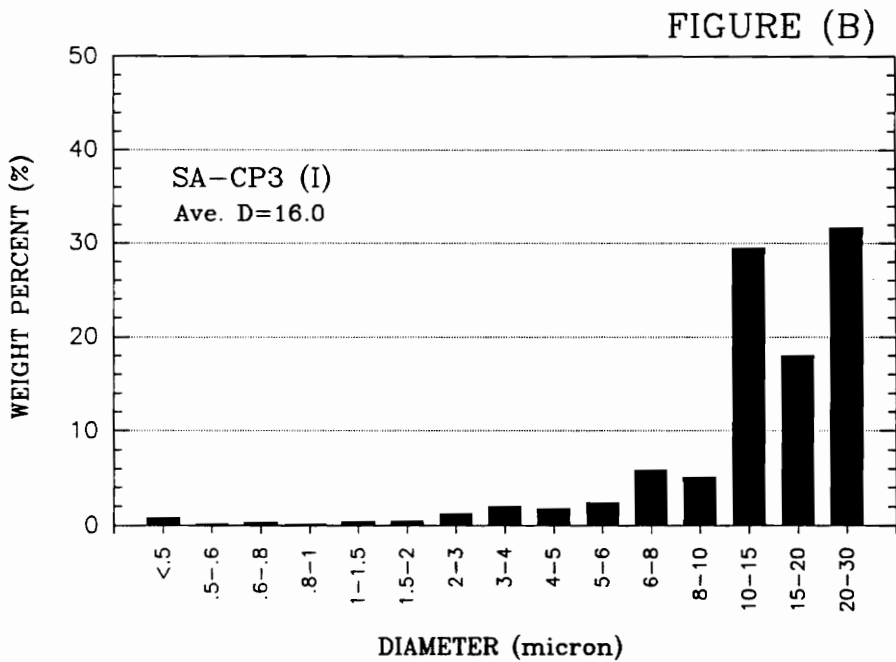
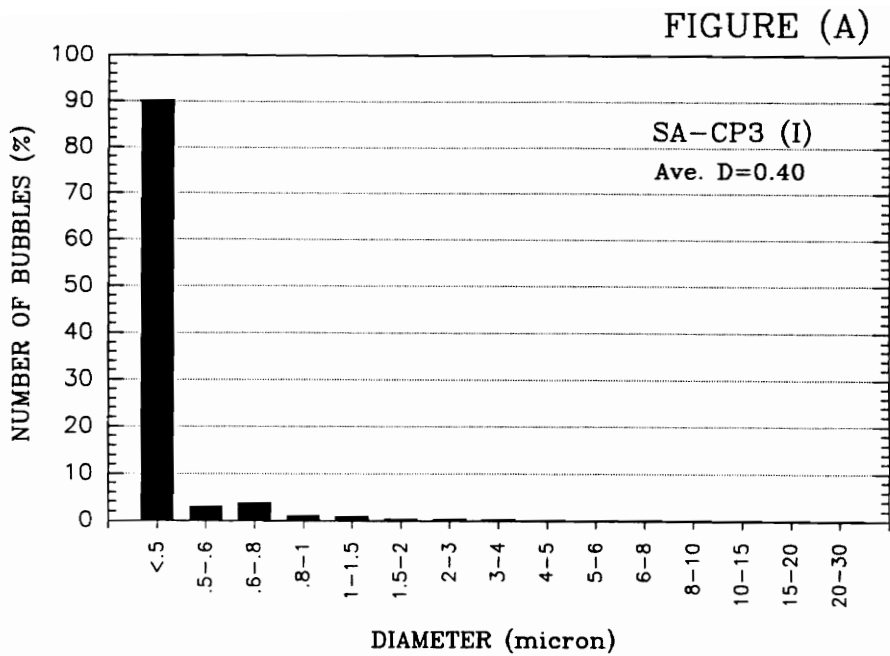


Figure 45. Particle Size Distribution for Batch I (302.4, 20.3, 700), as Determined with the SA-CP3 Analyser. (A) Number of bubbles (%), (B) weight percent.

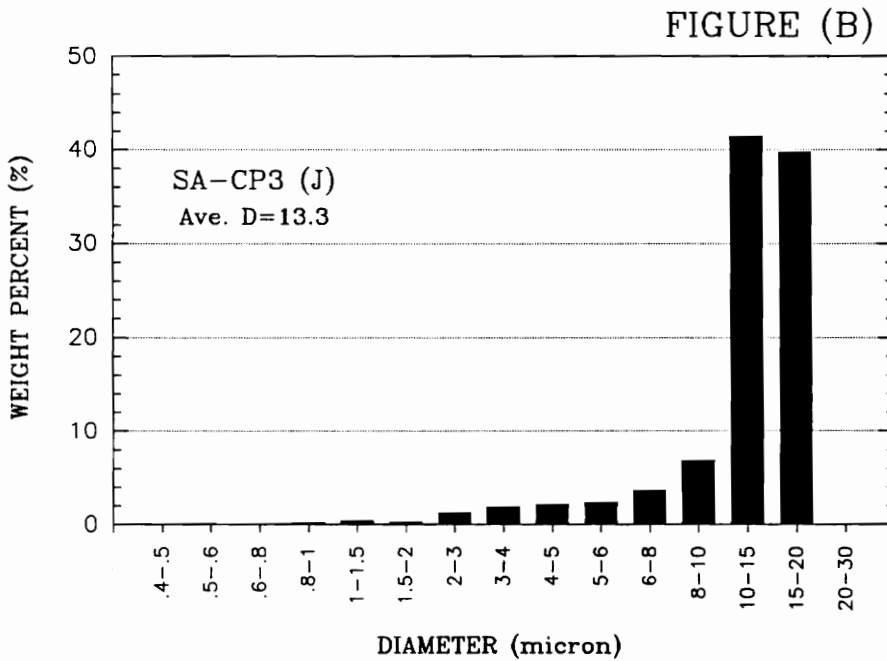
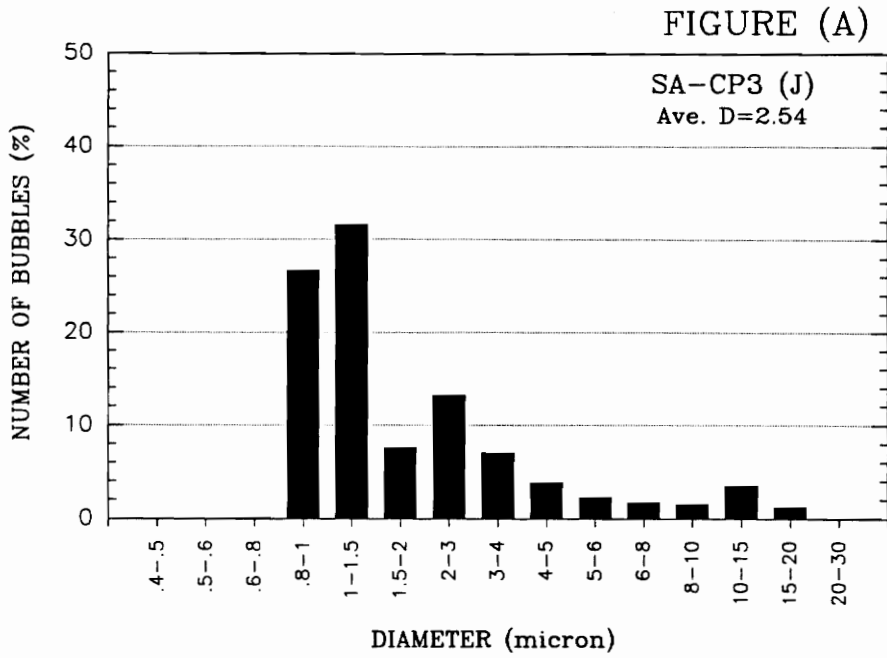


Figure 46. Particle Size Distribution for Batch J (150.3, 30.1, 700), as Determined with the SA-CP3 Analyser. (A) Number of bubbles (%), (B) weight percent.

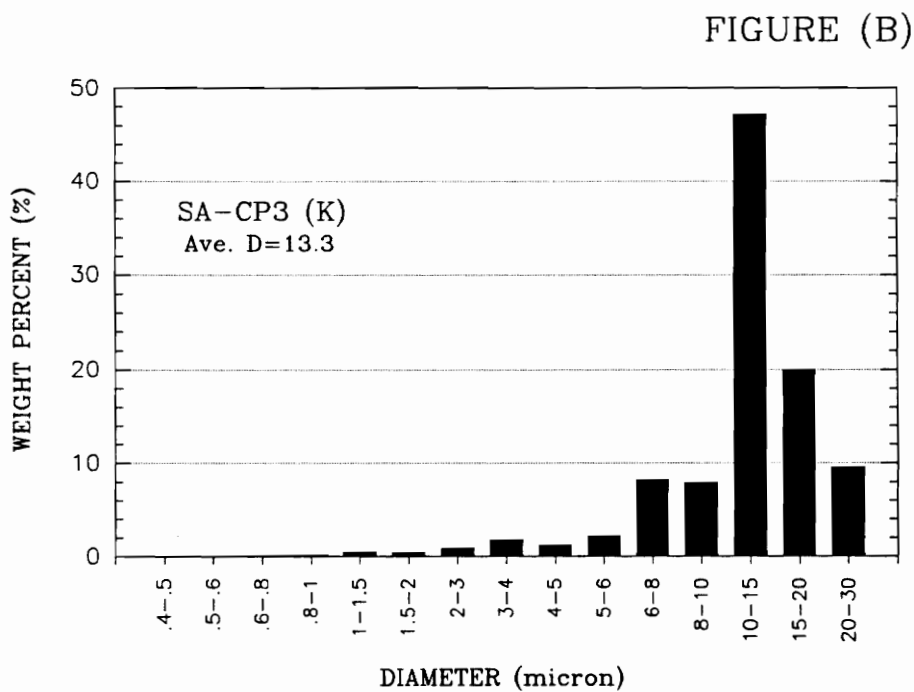
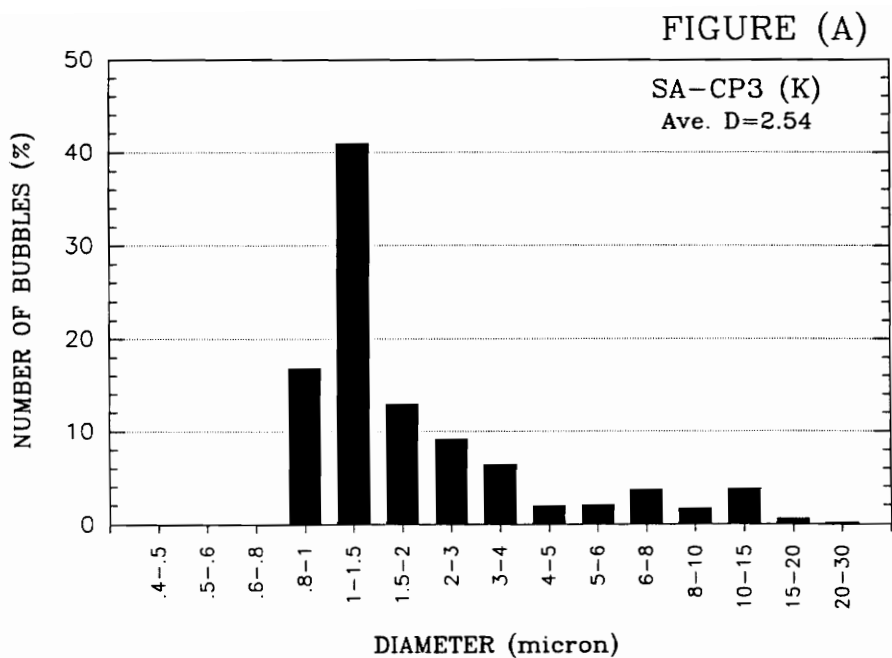


Figure 47. Particle Size Distribution for Batch K (150.3, 30.1, 1500), as Determined with the SA-CP3 Analyser. (A) Number of bubbles (%), (B) Weight percent.

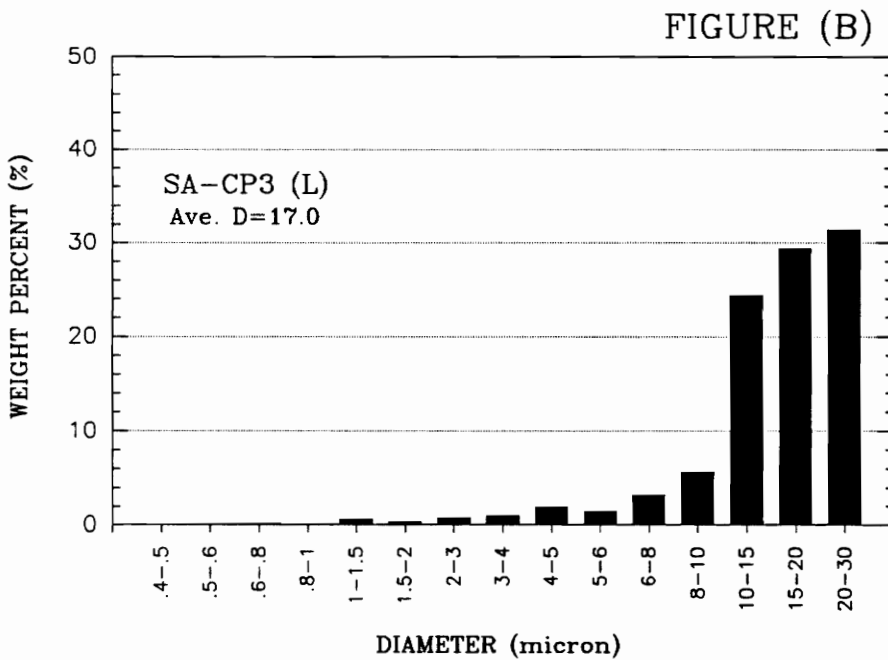
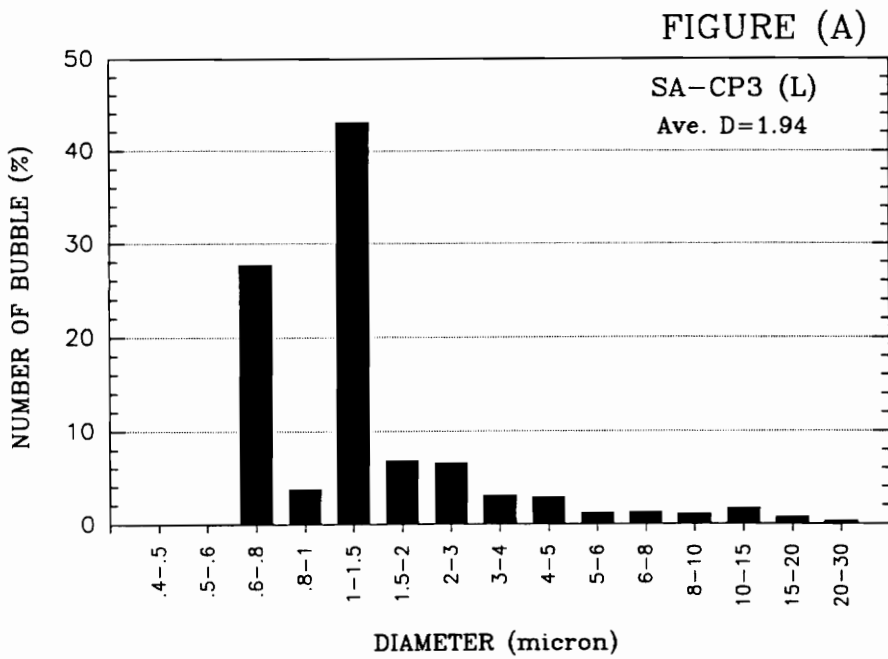


Figure 48. Particle Size Distribution for Batch L (174.5, 20.1, 1100), as Determined with the SA-CP3 Analyser. (A) Number of bubbles (%), (B) weight percent.

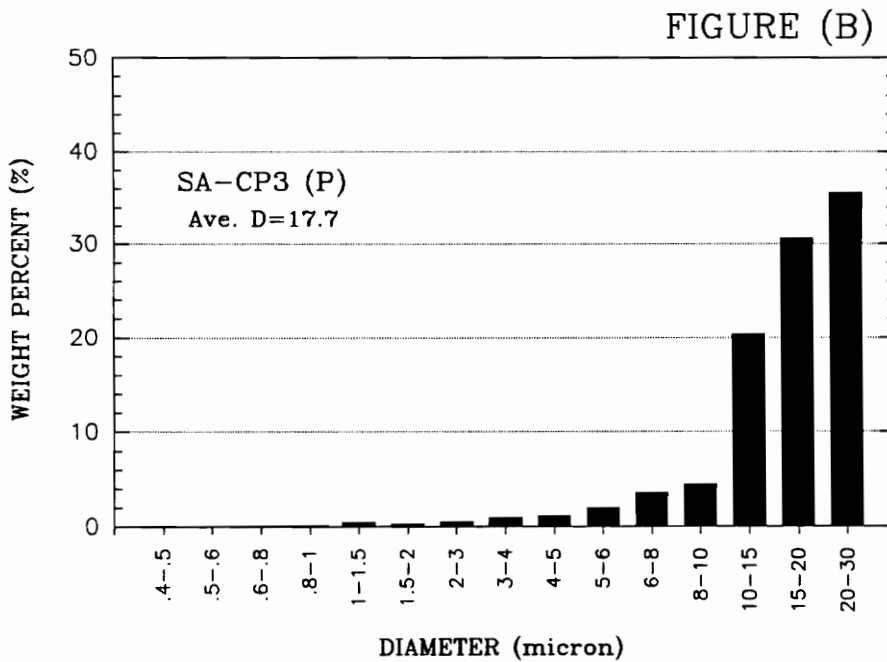
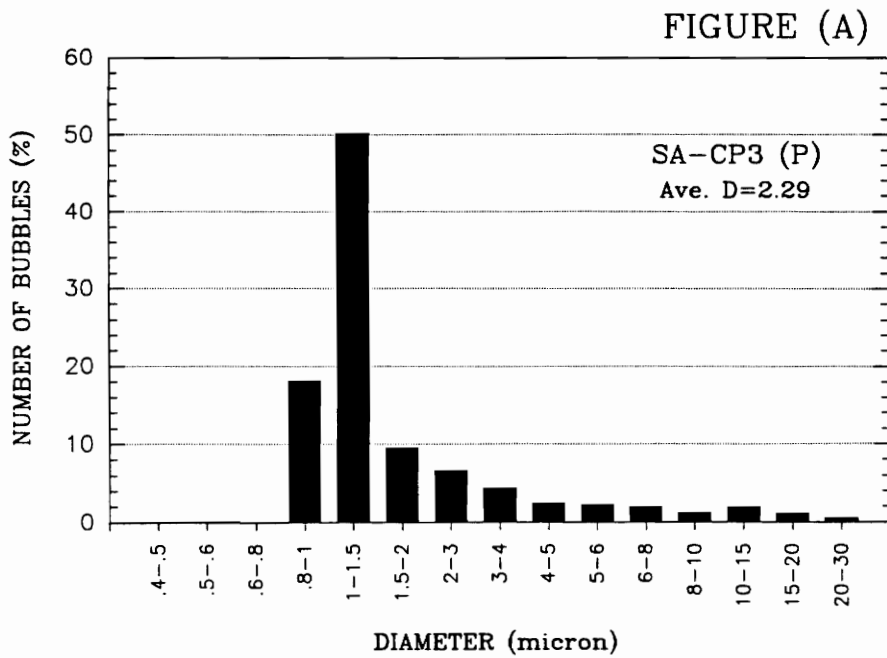


Figure 49. Particle Size Distribution for Batch P (46.9, 9.5, 700), as Determined with the SA-CP3 Analyser. (A) Number of bubbles (%), (B) weight percent.

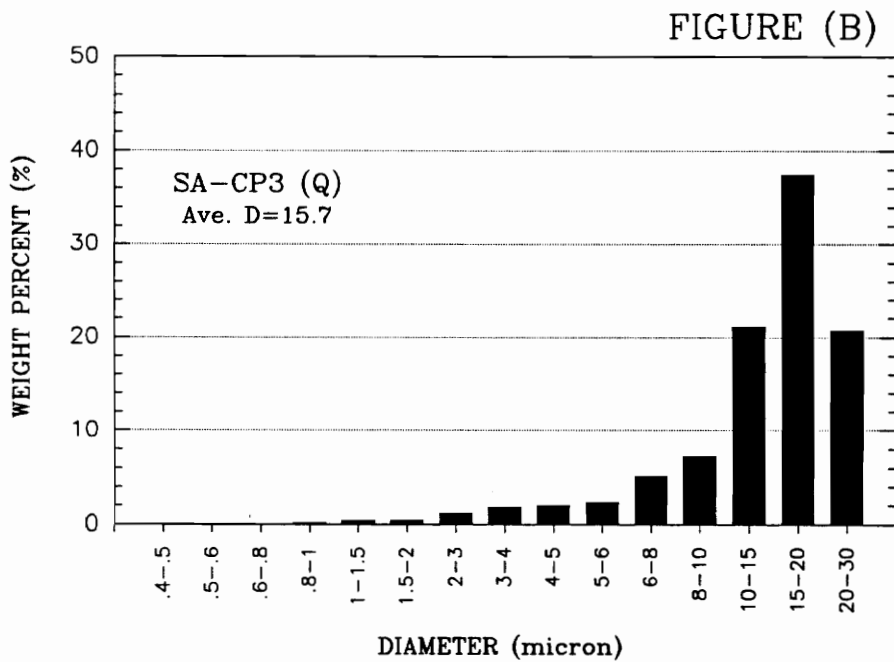
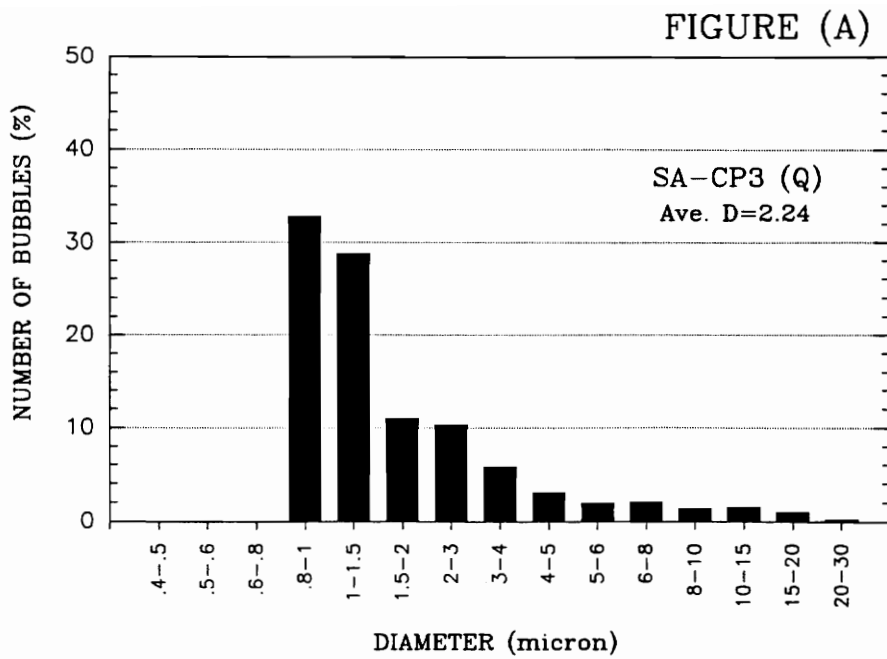


Figure 50. Particle Size Distribution for Batch Q (46.9, 9.5, 1500), as Determined with the SA-CP3 Analyser. (A) Number of bubbles (%), (B) weight percent.

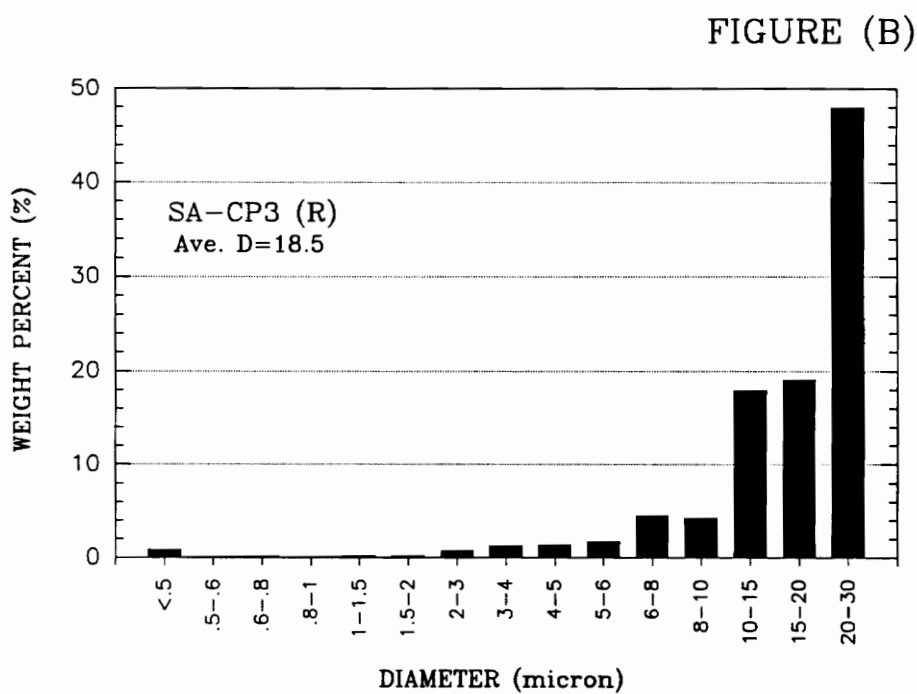
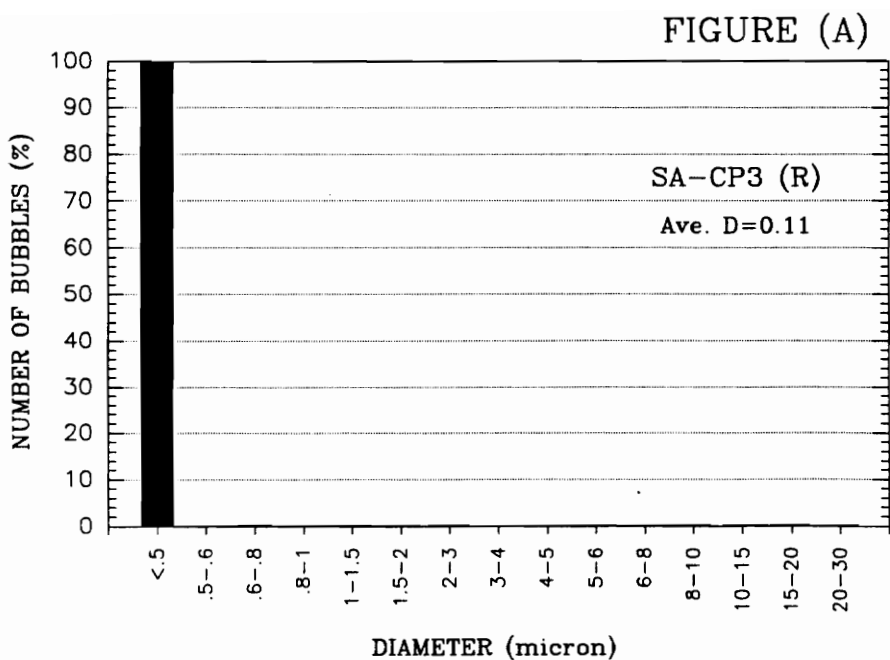


Figure 51. Particle Size Distribution for Batch R (259.2, 25.9, 1500), as Determined with the SA-CP3 Analyser. (A) Number of bubbles (%), (B) weight percent.

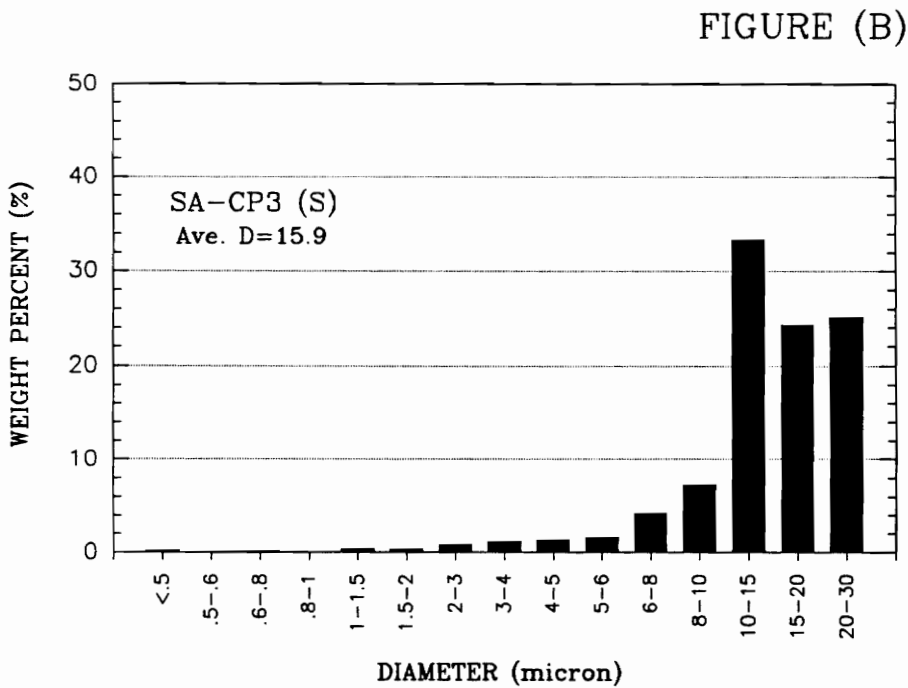
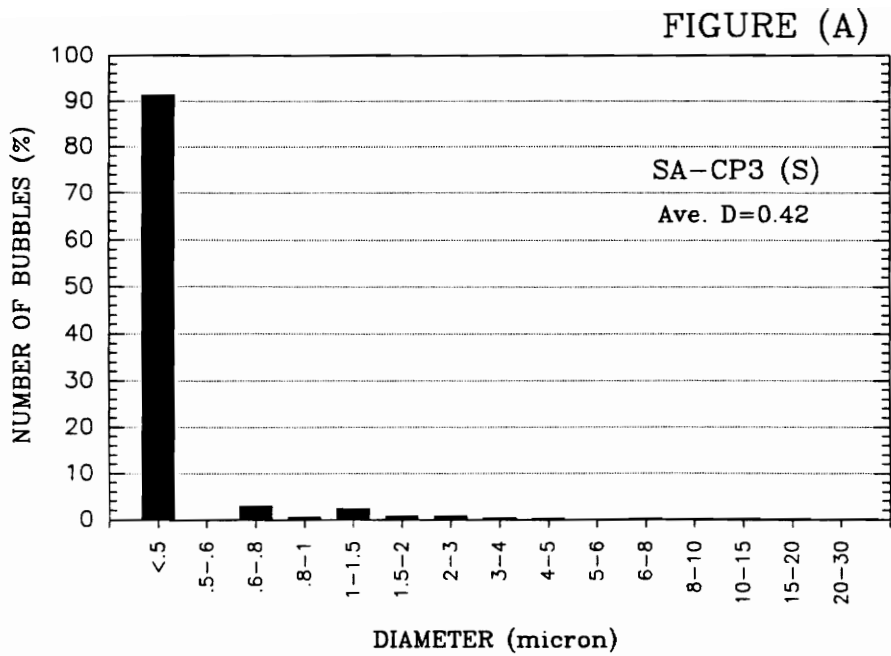


Figure 52. Particle Size Distribution for Batch S (267.5, 26.7, 1500), as Determined with the SA-CP3 Analyser. (A) Number of bubbles (%), (B) weight percent.

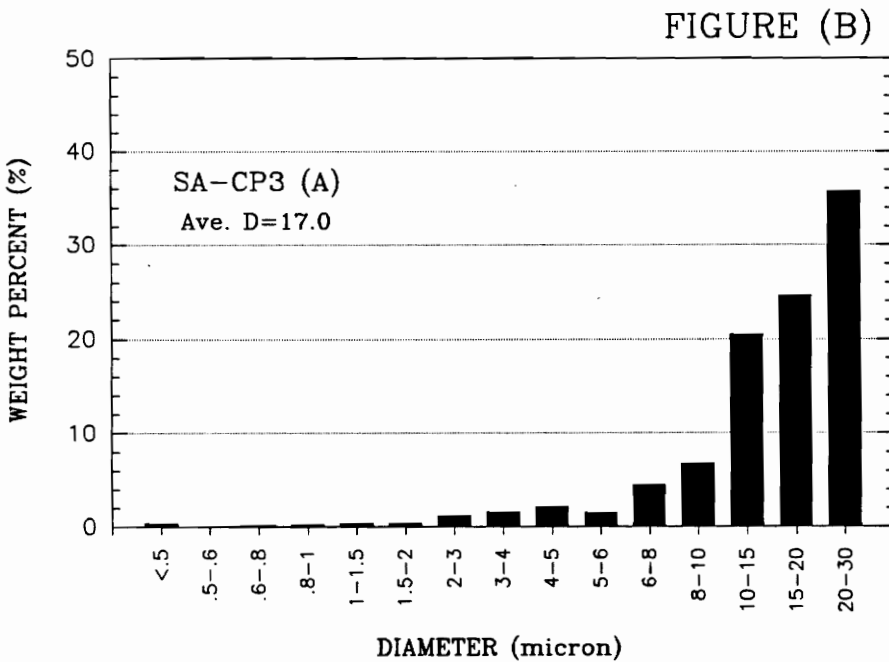
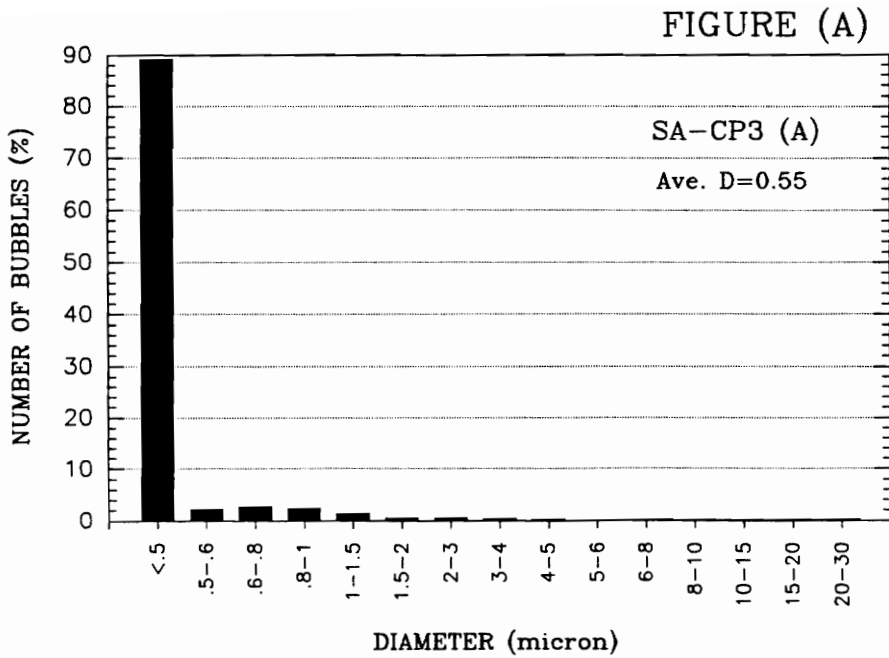


Figure 53. Particle size distribution for Batch A (97.9, 9.7, 700), determined with the SA-CP3 Analyzer, 4 months after aprons were generated. (A) Number of bubbles (%), (B) weight percent.

6.0 CONVENTIONAL VERSUS PREDISPERSED SOLVENT EXTRACTION OF COPPER IN A BATCH REACTOR

In the process of solvent extraction it is important to create a large surface area between the extracting solvent and the feed solution containing the solute in order to achieve rapid approach to equilibrium by facilitating mass transfer of the solute across the interface. Conventional solvent extraction relies on mechanical contactors that employ mechanical energy input to achieve high rates of mass transfer. Contactors can be expensive and energy costs can be significantly high especially for very dilute feed solutions. Predispersed solvent extraction (PDSE), depends on the large surface area created by making the solvent into a polyaphron before contacting the two phases to achieve high rates of mass transfer. The energy costs are low and no special equipment is required to carry out the extraction. In different manners both processes achieve high rates of mass transfer; however, the performance of the two processes under similar conditions had never been compared. To determine whether a higher rate of mass transfer can be achieved with PDSE, batch copper extractions were carried out in a batch reactor operated isothermally.

6.1 Experimental Procedure

Several batch extractions of copper were done to compare the dynamics of conventional solvent extraction to that of predispersed solvent extraction (PDSE). PDSE tests were carried out with aphrons of PVR 5, 10, and 15 at a temperature of about 26°C. The aqueous phase of the aphrons was made of 5 g/L sodium dodecylbenzenesulfonate (NaDBS), in deionized water. The initial concentration of copper in the aqueous phase ranged from about 0.0318 to 3.812 g/L. Another set of extractions was carried out with the same type of PVR 10 aphrons at 5,

15, 35, and 45°C. The initial concentration of copper for these set of extractions was kept at around 3.177 g/L. A set of extractions was also done with PVR 10 aphrons with an aqueous phase of 5 ml/L dodecyltrimethyl ammonium chloride (Arquad 12/50), in deionized water and a temperature of around 26°C. The initial concentration of copper in the aqueous phase for these extractions also ranged from about 0.0318 to 3.812 g/L. All extractions were carried out at a pH of approximately 2.0. Conventional batch extractions were done with various initial concentrations ranging from 3.8124 g/L to 0.0377 g/L and at a temperature of about 26°C. Also, four extractions were carried out over a pH range of 1.0 to 4.38 and five extractions were done over a temperature range of 5 to 45°C and a pH of around 2.0. The initial copper concentration for the last nine extractions was kept between 3.2 and 3.8 g/L. Table 11 and Table 12 outline all the tests done.

Every batch of polyaphrons used for each PDSE extraction was made separately and by hand. This ensured that the volume of solvent used in each extraction was the same. A schematic of the equipment used is shown in Figure 3. The following experimental procedure was followed for all tests.

1. The refrigerator bath was filled with deionized water.
2. The constant temperature circulator and refrigerator bath were turned on.
3. The temperature controller of the circulator was set at the desired temperature and the water temperature in the bath allowed to equilibrate.
4. A solution of 250 ml of 10% LIX-64N in kerosene or a volume of aphrons that contained 250 ml of the same kerosene solution was poured into the two neck round bottle flask. The flask was immersed in the bath water and held in place with a clamp.
5. 250 ml of copper sulfate solution was prepared by diluting a stock solution of copper sulfate to the desired concentration. The pH of the solution was determined with a Fisher

pH meter. The pH was adjusted to about 2.0 with concentrated sodium hydroxide. The solution was poured into a 300 ml erlenmeyer flask which was immersed in the bath water and held in place with a clamp.

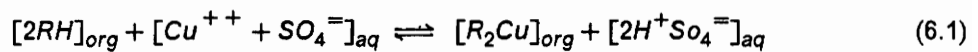
6. After the two solutions, organic and aqueous, had equilibrated to the desired temperature, the stirrer was positioned in the round bottom flask and started.
7. The erlenmeyer flask containing the aqueous solution was removed from the water bath and the solution quickly poured into the round bottom flask. A stopwatch was started.
8. Samples were taken often and the sampling time recorded. Samples were taken by drawing from the extracting vessel and into a test tube about 10 ml of a mixture of aqueous and organic phases. A peristaltic pump was used to remove the samples.
9. In the case of conventional extraction, the two phases in the samples were allowed to separate by gravity. As soon as possible each phase was removed and placed in separate test tubes. The test tubes were sealed with parafilm.
10. In the case of PDSE, immediately after the samples were taken from the extraction vessel, they were centrifuged to separate the two phases. Later, each phase was removed and placed in separate test tubes. The test tubes were sealed with parafilm.
11. All organic and aqueous samples collected were analyzed for copper content with an atomic absorption spectrophotometer.

6.2 Results and Discussion

Copper was extracted from dilute solutions of copper sulphate using a 10% solution of a liquid ion exchanger, LIX-64N, an alpha-hydroxyoxime, in kerosene. The use of LIX in the

hydrometallurgical field has met with considerable success, especially in the area of extraction of metallic ions from solutions. Several LIX reagents exist in the market these days with LIX-84 and LIX-984 considered better copper chelating agents than LIX-64N. When this study started, LIX-64N was the best one in existence and by the time Henkel Corporation started manufacturing LIX-84 and LIX-984 this study was well under way. Since the objective of this study was the dynamics of the PDSE process, it was considered unnecessary to change reagent.

The extraction of copper using LIX-64N involves the contacting of a solvent containing LIX-64N with the copper containing feed, to yield a LIX-copper complex. The chelating action of LIX-64N can be represented in an equation form as:



As can be seen, the reaction is reversible, but for the reverse reaction to be important, the pH has to be in the range of 0.5 to 0.9.

LIX-64N is a viscous amber colored liquid. Before contacting the LIX with the feed solution it is first diluted in a hydrocarbon which is referred to as the carrier. Industrially, kerosene is the carrier of choice because of its low cost. For this study, there was concern that the use of kerosene might present a problem because of its complexity. It is composed of a variety of hydrocarbons and the composition of each lot of kerosene is different. The use of a pure hydrocarbon such as decane was suggested. Unfortunately, even for use at laboratory scale, the cost was high. Therefore, kerosene was used as the carrier but, all the kerosene used for the batch extractions described in this section was bought from the same supplier and the same lot. The kerosene was stored in 5 gallon containers and whenever a container was opened, the surface tension and the viscosity of the kerosene were determined. The surface tension varied from 28.2 to 28.5 dynes/cm and the viscosity was always around 1.63cp.

The LIX concentration used for all tests was 10 volume percent in kerosene. LIX-64N can be used in concentrations up to 30 volume percent. Above this level aqueous entrainment can occur; therefore, it is recommended that LIX-64N not be used in concentrations above 30 percent. 10 volume percent is the recommended concentration for extraction of copper from feed solutions of around 3.0 g/L. Lower LIX concentrations can be used with feeds containing lower copper concentrations but since for this study it was desired to keep the LIX concentration constant, a 10 percent concentration was used throughout.

6.2.1 Conventional Extractions

Figure 54 and Figure 55 show concentration-time curves for the first four copper extractions done. The temperature was kept constant at 26°C for all tests. Temperature variation throughout the entire testing time was negligible. Equal volumes, 250 ml, of each phase were contacted in a 1000 ml two neck round bottom flask. The mixture in the flask was continuously stirred at the same rate for all tests. The pH of the aqueous phase was adjusted with concentrated sodium hydroxide to what at the time was thought to be 2.0. The uncertainty was due to problems that were being experienced with the pH meter. Initially, the response of the meter was slow, but by the time the aqueous solution was being prepared for a fifth test, the pH meter readings were drifting. At this point the electrode was replaced but, there was a large degree of uncertainty as to the actual pH of the four tests already done.

The thing to note from these tests is the amount of time it took for the reaction to reach equilibrium. Equilibrium conditions were expected to be approached in 1 or 2 minutes. Instead, tests 1 and 2 with initial concentrations equal to 3.8124 g/L and 1.5250 g/L, respectively, took up to 60 minutes to reach equilibrium. The other two tests, one with an initial copper concentration of 0.7625 g/L and the other with an initial copper concentration of 0.3177 took 15 and 8 minutes, respectively, to reach equilibrium. This was considerable less time than the first two but, still much longer than expected. The percent of copper extracted with each test

increased as the initial concentration of copper in the aqueous feed decreased. The percent extractions for the four tests were 56.7%, 69.6%, 91.7%, and 99.4%, in order of decreasing initial copper concentration. These results were expected because as the LIX approaches its maximum copper loading capacity, the mass transfer rate decreases.

Since there was uncertainty as to the acidic strength of the feed solutions in the first four tests done, these tests were repeated and two extra tests were done to study the dynamics of the extraction over a range of initial copper concentrations of 3.2215 to 0.0377 g/L. All six tests were done under similar conditions. The temperature was kept at 26°C with negligible temperature variation during and between tests. The pH of the feed solutions was adjusted to around 2.0 with a variation no greater than 0.08 between tests. The mixing rate was also kept constant. Figure 56, Figure 57, and Figure 58 show the concentration versus time curves for these tests. The feed concentration of the first test in this series was 3.2215 g/L, that of the second test was 1.4360 g/L and the last four tests had feed concentrations of 0.7180, 0.3666, 0.0718, and 0.0377 g/L. The percent of copper extracted was 80.3%, 95.3%, 98.3%, 98.3%, 99.3%, and 99.5%, in order of decreasing feed concentrations. The copper recovery was significantly higher than in the first series of tests. An indication that the conditions in the first series of tests were questionable as suspected. As was seen before, the copper recovery increased as the feed concentration decreased, except that in this case, the increase was significant only between the three tests with the higher feed concentrations. For feed concentrations between 0.7180 and 0.0377 g/L the copper recovery ranged from 98.3% to 99.5%. Since these feed concentrations were much lower than the saturation point of a pH 2.0, 10 volume percent LIX-64N solution which is somewhere between 2.8 and 3.0 g/L of copper, close to complete recovery was expected. Another significant difference between this series of tests and the first series was the time required to reach equilibrium. Again, the time was longer than expected but this time it ranged from 15 minutes for the test with the higher feed concentration to 6 minutes for the one with the lower feed concentration. A significant improvement.

A third series of 5 tests was done to observe the effect of temperature on the copper extraction. The feed copper concentrations were between 3.2 and 3.3 g/L for all tests. The pH was kept constant at about 2.0 and equal volumes of the two phases were contacted in the reactor vessel. The mixture was mixed at approximately the same rate during all tests. The temperatures ranged from 5 to 45°C with each test done at 10 degree intervals. Figure 56, Figure 59, and Figure 60 show the concentration versus time curves for these tests. For the test done at 5°C the copper recovery was 70.9% and the reaction took 20 minutes to reach equilibrium. A 75.5% copper extraction was achieved in 15 minutes when the temperature was raised 10° to 15°C. Another 5% increase in copper recovery was achieved by raising the temperature to 26°C but the time required to reach equilibrium remained at around 15 minutes. No appreciable change was observed when the temperature was raised from 26 to 35°C. The percent extraction achieved went from 80.3% to 80.9% and the equilibrium time decreased by two minutes from 15 to 13. A slightly higher recovery of 83.2% was attained at 45°C. The equilibrium time remained at around 12 minutes. Obviously the extraction is enhanced when the temperature is raised from 5 to 26°C but increasing the temperature from 26 to 45° makes little difference. The increase in copper recovery from 80.9% to 83.2% when the temperature was raised from 35 to 45°C might imply that raising the temperature above 45° would again enhance the extraction considerably. This was not investigated further.

As was previously stated, the difference between the results obtained in the first series of tests and the second one demonstrated that there was a difference in the conditions under which the extractions had been carried out. An attempt to shed some light as to the acidic conditions under which these tests had been done led to a fourth series of extractions. These extractions were carried out at pH 1.0, 2.98, 3.93, and 4.38. The pH of the first three solutions was adjusted with concentrated sodium hydroxide while no pH adjustment was done for the last test. The temperature for all tests was kept at 26°C and the feed concentrations were kept somewhere between 3.6 and 3.8 g/L of copper. By the time it was decided to do this series of tests, the extraction apparatus had to be reassembled because it had already been dismantled. Unfortunately, the stirrer that had been used for all previous tests was no longer

available so another one had to be used. It should be noted that the mixing rate achieved with this stirrer was higher than the previous one. Figure 61 and Figure 62 show the concentration versus time curves for these tests. The copper recovery for these four tests was 49.8%, 81.4%, 83.7%, and 81.1%, in order of ascending pH. The increase in copper recovery with a pH increase from 1.0 to 2.98 is higher than 30%. At a pH of 1.0 it took 25 minutes for the reaction to reach equilibrium while for the other three tests equilibrium was reached in only 6.5 minutes. Increasing the pH above 2.98 had an insignificant effect on the extraction. A comparison of these results with those obtained for test 1 from series 2 which was done at pH 2.0, 26°C and with a 3.2215 g/L feed concentration, shows that the copper recovery was similar at 80.3% to the recovery achieved at pH above 2.98. Equilibrium was reached in 15 minutes when the extraction was carried out at a pH of 2.0 while it took 6.5 minutes for all tests carried out at higher pH. This difference in equilibrium time is thought to be more an effect of mixing rate than a pH effect. In effect, the unintentional higher rate at which the tests in this series were mixed demonstrated that the longer than expected times taken to reach equilibrium in all tests was because of relatively low mixing rates. The special contactors used in industry must provide higher contact than that achieved with the stirrer used for this study, explaining the lower equilibrium times reported in the literature. From these results it appears that the pH of the first series of tests was closer to 1.0 than to 2.0. A summary of the results from all preceding tests is shown in Table 11.

6.2.2 Predispersed Solvent Extractions

All batch extractions done with aphrons were carried out in the same manner as the conventional batch extractions. 250 ml of 10 volume percent LIX-64N in kerosene were formed by hand into a polyaphron. The polyaphron was contacted with 250 ml of a copper sulfate solution in a batch reactor. The reactor contents were continuously mixed at a constant rate. Usually, polyaphrons are diluted with water before contacting them with the feed because

the high cohesion forces between the aphrons slows the rate at which they spread through the liquid. However, for all the batch tests done the polyaphrons were not diluted because it was felt that the mechanical mixing would take care of spreading the polyaphrons without resorting to dilution. In a continuous or semi-batch process the polyaphrons are pumped into the system and the movement of the aphrons through the fluid creates sufficient contact so that mechanical mixing is not necessary. In the case of the batch tests done for this study, the copper loaded feed solution was poured into the reactor which already contained the polyaphrons. Without mechanical mixing, the rate of diffusion of the aphrons through the fluid would have been extremely slow.

All samples taken from the reactor had to be centrifuged to separate the two phases quickly. The samples removed were a mixture of raffinate, extract, and polyaphrons because the polyaphrons did not break all at once when contacted with the aqueous phase. The polyaphrons were usually distributed through both the aqueous and the organic phases and it was important to remove the aphrons quickly from the aqueous phase to prevent further transfer of mass.

The first series of six tests were done with polyaphrons of PVR 10. The surfactant used in the aqueous phase of the polyaphrons was 5 g/L sodium dodecylbenzenesulfonate (NaDBS). These tests were comparable to the second series of tests done by conventional extraction. The feed copper concentrations were 2.9228, 1.5250, 0.7815, 0.4244, 0.0820, and 0.04448 g/L. The temperature was kept constant at 26.0°C and the pH was around 2.0 for all tests. The mixture in the reactor was stirred at approximately the same rate as that used in the conventional extraction tests. The copper recoveries were 76.1%, 96.7%, 98.1%, 99.3%, 99.4%, and 99.1%, in order of decreasing feed concentrations. These results are similar to those obtained by conventional extraction. The time required to reach equilibrium was 12.5 minutes for the test with initial feed concentration of 2.9228 g/L. The other five tests reached equilibrium within the first 0.5 minute. A great improvement over conventional extraction. Figure 63, Figure 64, and Figure 65 show concentration versus time curves for these tests.

A second series of tests was done with the same type of polyaphrons as the ones used in the previous tests. Figure 66 and Figure 67 show the concentration versus time curves for these tests. The feed concentration for test 1 was 3.3041 g/L and the extraction was carried out at 5°C. A copper recovery of 76.2% was achieved in 12.5 minutes. The feed concentration of test 2, which was carried out at 10°C, was 3.3041 g/L. It took 7.5 minutes to recover 78.9% of the copper. Tests 3 and 4 also had feed concentrations of 3.3041 g/L but the extractions were carried out at 35°C for test 3 and at 45°C for test 4. The percent extraction for these tests was similar with 84.8% for test 3 and 84.0% for test 4. Both reactions reached equilibrium within 0.5 minute. The pH for all four tests was around 2.0. These tests show that the extraction is enhanced with an increase in temperature. When the temperature was raised from 5 to 15°C the percent extraction increased by almost 3%. An even larger increase of about 6.0% was seen when the temperature was raised from 15 to 35°C. Raising the temperature from 35 to 45°C had no effect on the extraction. More importantly, the time required to reach equilibrium was decreased from 12.5 minutes for test 1 to 0.5 minute for tests 3 and 4. Also, when comparing these results to those of similar tests done with conventional extraction, it is noted that equilibrium conditions are approached much quicker with PDSE.

A third series of six tests were done with PVR 5 polyaphrons. The polyaphrons were again made with an aqueous phase of 5 g/L NaDBS. These tests were comparable with those from series 1. The temperature was kept constant at 26.0°C and the pH was around 2.0. For test 1, with an initial feed concentration of 3.5011 g/L and an 83.8% copper recovery, equilibrium was reached in 0.5 minute. An increase in copper recovery to 96.3% was seen when the feed concentration was decreased to 1.6457 g/L for test 2. For this test equilibrium was also reached within 0.5 minute. By further decreasing the feed concentration, a small increase in copper recovery was noted. The percent extractions for tests of feed concentrations of 0.8769, 0.4022, 0.07625, and 0.03971 g/L were 98.0%, 98.9%, 99.4%, and 99.5%, respectively. Equilibrium was reached in 0.5 minute for all four tests. These results are similar to those obtained with PVR 10 polyaphrons except for the fact that for test 1 done with polyaphrons of PVR

5 equilibrium was reached much faster than for test 1 done with polyaphrons of PVR 10. Figure 68, Figure 69, and Figure 70 show concentration versus time curves for these tests.

A fourth series of six tests comparable to the above six tests was done, except that the polyaphrons used were of PVR 15. Similar results were obtained. The feed concentrations ranged from 3.614 g/L for test 1 to 0.04175 g/L for test 6. The temperature was held constant at 26.0°C. The pH was around 2.0 for all tests and the mixture was stirred at the same rates. The percent of copper extracted increased from 85.3% for test 1 to 99.8% for test 6 as the feed concentration was decreased. Test 1 took 7 minutes to reach equilibrium and all other five tests took only 0.5 minute. Figure 71 through Figure 73 show the concentration-time curves for this series of tests.

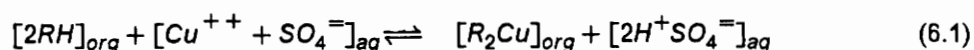
Finally, a fifth and last series of 6 tests was done to observe the effect that using a different water soluble surfactant to make the polyaphrons would have on the extraction. The surfactant used was Arquad 12/50 at a concentration of 5 ml/L. Again, this series of tests was comparable to the previous series. Temperature, pH, and mixing conditions were the same. The feed concentrations ranged from 3.5011 g/L for test 1 to 0.04842 g/L for test 6 and the percent extraction increased from 80.9% to 99.5%. The equilibrium time for test 1 was 7 minutes, that for test 2 was 3 minutes, and all other tests reached equilibrium within the first 0.5 minute. These results are similar to the results obtained for all other series of tests done with polyaphrons of various types. Figure 74 through Figure 76 show the concentration-time curves for these tests. A summary of the results of all the preceding tests is shown in Table 12.

6.2.3 Determination of Equilibrium

The copper concentration in the aqueous and organic phases was plotted over time to determine the ultimate equilibrium concentrations for each experiment. Since there is some experimental error involved in the experimental points, a best fit curve was drawn through the

points. A certain amount of fluctuation was repeatedly observed in the concentration data beyond the time after which the tests were considered to have reached equilibrium, especially with the copper concentration in the organic phase. Whenever this happened, an average of all the concentrations beyond what was estimated to be the equilibrium point was calculated and this was determined to be the ultimate equilibrium concentration for a particular experiment. Figure 54 through Figure 76 show the concentration versus time curves for all the tests.

As has been previously mentioned, the LIX solvents operate by replacing the hydrogen atoms of two solvent molecules with an absorbed copper atom. The general reaction is:



It has been suggested that the equilibrium constant for this reaction can be written as:

$$K_{eq} = \frac{[R_2Cu][H^+]^2}{[Cu^{++}][RH]^2} \quad (6.2)$$

This equation was solved for K_{eq} using the experimental equilibrium data. The concentration of the LIX/copper complex, $[R_2Cu]$, is equal to the ultimate copper equilibrium concentration in the organic phase, C_{org}^* . The concentration of copper ions, Cu^{++} , is equal to the ultimate copper equilibrium concentration in the aqueous phase, C_{aq}^* . The concentration of hydrogen ions at equilibrium was calculated as follows:

$$[H^+]_{eq} = 10^{[-pH]} + 2[C_{org}^*] \quad (6.3)$$

The final LIX concentration was calculated from:

$$[RH]_{eq} = [RH]_{INITIAL} - 2[C_{org}^*] \quad (6.4)$$

Now, in equation 4 the initial LIX concentration was not known because LIX-64N is described by the manufacturer as "a mixture of 2-hydroxy-5-nonylbenzo-phenoneoxime and 5,8-diethyl-7-

hydroxydodecan-6-oxime in kerosene". The density of the mixture was known but not the percentage of each of the components. But, if it is assumed that the amount of LIX initially present is equal to the maximum copper loading capacity achieved with the test from each series done at the highest initial feed concentration, the initial LIX concentration can be estimated. The values of the parameters used to solve equation 2 and the equilibrium constants calculated for two of the series of tests done, one using conventional extraction and one using PDSE, are tabulated in Table 59 and Table 60. The values calculated for the equilibrium constant, which should not be affected by initial feed concentration, decreased with decreasing initial feed concentration. The difference between K_{eq} for the first and second tests of each series is extremely large, with the values for the first tests being surprisingly high. Now, if instead one assumes that the original LIX/kerosene mixture as supplied by the manufacturer contains no kerosene and that the other two components are found in equal quantities, the concentration of LIX in a 10 volume percent solution with kerosene was calculated to be 0.4M. Although this concentration value is unreasonably high, it was noted that by increasing the value of the initial LIX concentration when solving for K_{eq} the difference between the equilibrium constants for each test became smaller. However, the value of the equilibrium constant for test 1 of each series was always higher than the rest.

In the equilibrium expression represented by equation 2, ideal conditions were assumed. If ideal conditions do not hold, the equilibrium expression is no longer a ratio of the concentrations but a ratio of the activities. The acidity of the initial feed solutions used in all tests was very low at pH of about 2.0. Also, the acidity of the solution changed over time since two hydrogen ions were produced for each copper ion that complexed with the LIX. It is noted that the final hydrogen ion concentration calculated for each test decreases with decreasing initial feed concentration and that the difference between test 1 and test 6 of each series can be up to 10 fold. Under such highly variable ionic conditions the ideal assumptions might not hold. Thus, it is possible that the change seen in the equilibrium constant is because the values calculated are factors of K_{eq} and the effect of the activity changes. Since there was no way to determine the separate activities of LIX and the LIX/copper complex, and the initial LIX con-

centration was unknown, it was decided instead to determine only an empirical relationship between C_{aq}^* and C_{org}^* .

The ultimate equilibrium concentrations for each series of reactions done at a temperature of 26.0°C and a pH of 2.0 were used to develop empirical equilibrium isotherms. The isotherms were plotted as the natural logarithm of the copper equilibrium concentration in the organic phase versus the natural logarithm of the copper equilibrium concentration in the aqueous phase for each series of experiments. A best fit curve was drawn through the points. These empirical equilibrium isotherms are depicted in Figure 77 to Figure 79. It should be noted that the first four or five points in all the empirical equilibrium isotherm curves fell in a straight line and the last point or two curved towards an asymptote. For example, the relationship between C_{aq}^* and C_{org}^* for the second series of tests done by conventional extraction can be approximated by the following expression:

$$C_{org}^* = 9.994 \left[\frac{C_{aq}^*}{[7.824C_{aq}^* + 1]} \right]^{0.6508} \quad (6.5)$$

This is represented in Figure 77 (B). The equilibrium curve starts to bend as the LIX approaches its maximum loading capacity or saturation point.

Empirical equilibrium isotherms were not developed for the third and fourth series of tests done by conventional extraction and for the second series of tests done by predispersed solvent extraction. Each test from each of these series was done either at a different temperature or at a different pH to observe the effect of these variables on the ultimate equilibrium concentrations. These fragmented data was not sufficient to make equilibrium isotherms since curves could not be drawn with only one data point.

6.2.4 Correlation of Batch Reactor Data

When doing the batch tests, the copper concentration of each phase was followed over time with the purpose of being able to determine the ultimate equilibrium of each experiment. In doing this several interesting and unexpected observations were made. For example, each experiment was expected to reach equilibrium in three or four minutes but it took some tests almost 60 minutes to do so. Also, the rate of approach to equilibrium was not expected to be affected by initial feed concentration. However, every test done showed that the rate of approach to equilibrium depended on the initial feed concentration. These observations led to a study of the dynamics of each test.

The dynamics of each experiment were modeled according to the film theory. The film theory is based upon a model in which the entire resistance to diffusion is assumed to occur in films at the interface. If, for the specific case of the diffusion of copper ions from the aqueous film to the LIX containing organic film, it is assumed that the organic phase is the one offering resistance to mass transfer; then, the concentration of copper ions in the bulk water, C_{aq} , is equal to the concentration of copper ions in the aqueous phase at the interface of the two phases. Then, for the copper/LIX reaction, the rate equation may be written:

$$\frac{dC_{org}}{dt} = k(C_{org}^* - C_{org}) \quad (6.6)$$

where, C_{org} is the copper concentration in the bulk organic phase, C_{org}^* is the organic copper concentration in equilibrium with C_{aq} , k is the mass transfer coefficient, and t is time.

Equation 6 was used to calculate the mass transfer coefficients for all the batch reactions done at 26°C and a pH of 2.0. The parameters needed in the equation were calculated in the following manner. At any time, t , C_{aq} was determined from the smooth curve drawn through the experimental points in the concentration-time curves. Knowing C_{aq} , C_{org}^* was determined from the equilibrium isotherms developed earlier. C_{org} was determined from the smooth curve

drawn through the experimental points in the concentration-time curves. Now, solving equation 6 for the change in C_{org} and changing the derivative to a discrete change gives,

$$\Delta C_{org} = k(C_{org}^* - C_{org})\Delta T \quad (6.7)$$

This equation was solved by inputting the values of C_{org} and C_{org}^* at 1 minute intervals from time equal to zero to the equilibrium time. A value for k was initially guessed. From the value calculated for the change in C_{org} , C_{org} was calculated and compared to the inputted C_{org} values. The value for the mass transfer coefficient was adjusted to give an optimum fit of the experimental data. All the parameters used to solve the equation and the calculated values of C_{org} for each test done by conventional extraction are tabulated in Table 13 to Table 22. The parameters for the tests done by PDSE are tabulated in Table 31, Table 47, Table 52, and Table 54. This scheme was used to determine k for all reactions that reached equilibrium in three minutes or more. For all the reactions in which equilibrium was reached within 0.5 minute, equation 4 was solved for k directly.

The correlation between the experimental data and the values predicted by the film theory for each test was good. Figure 54 to Figure 58, and Figure 63, Figure 71, and Figure 74. show the calculated and experimental curves. The problem with the model is that for each series of tests, which only differ in the initial copper concentration used, a different mass transfer coefficient was required to fit the data and according to the film theory the mass transfer coefficient should not vary with initial feed concentration. The mass transfer coefficients calculated for each test are tabulated in Table 59 to Table 64. Table 59 and Table 60. demonstrate that for both series 1 and 2 done by conventional extraction, the value of the mass transfer coefficient decreases with decreasing feed concentration. For the series of tests 1, 4 and 5 done by PDSE the mass transfer coefficient increases at first but then it starts to decrease with decreasing feed concentration. For example, from Table 61 it is seen that when the feed concentration decreases from 2.9228 g/L to 1.525 g/L, k increases from 0.535 to 2.654 min^{-1} but as the feed concentration decreases further to 0.7815 g/L, the k de-

creases to 1.380 min^{-1} . The mass transfer coefficient continues to decrease as the feed concentration decreases.

Table 11. Description of copper extraction tests done in a batch reactor using conventional solvent extraction

Series ID	Test ID	C ₀ ^a (g/L)	Temp C	pH	Percent Ext. (%)	t ^b
1	1	3.8124	26.0	?	56.7	60.0
1	2	1.5250	26.0	?	69.6	60.0
1	3	0.7625	26.0	?	91.7	15.0
1	4	0.3177	26.0	?	99.4	8.0
2	1	3.2215	26.0	2.01	80.3	12.0-15.0
2	2	1.4360	26.0	2.01	95.3	13.0
2	3	0.7180	26.0	2.08	98.3	10.0
2	4	0.3666	26.0	2.01	98.3	10.0
2	5	0.0718	26.0	2.03	99.3	9.0
2	6	0.0377	26.0	2.04	99.5	6.0
3	1	3.2088	5.0	2.06	70.9	20.0
3	2	3.3041	15.0	2.03	75.5	15.0
3	3	3.3041	35.0	2.05	80.9	13.0
3	4	3.3041	45.0	2.00	83.2	12.0
4	1	3.6218	26.0	1.00	49.9	25.0
4	2	3.8124	26.0	2.98	81.4	6.5
4	3	3.8124	26.0	3.93	83.7	6.5
4	4	3.8124	26.0	4.38	81.1	6.5

NOTE: ^a C₀ = Initial copper feed concentration

^b t* = Time required for the reaction to reach equilibrium

Table 12. Description of copper extraction tests done in a batch reactor using predispersed solvent extraction

Series ID	Test ID	C ₀ ^a (g/L)	Temp (°C)	pH	Surfactant Used to Make Polyaphron	Surfactant Conc.	PVR	Percent Extraction (%)	t ^b (min)
1	1	2.9228	26.0	2.01	NaDBS ^c	5 g/L	10	76.1	12.5
1	2	1.5250	26.0	2.00	NaDBS	5 g/L	10	96.7	0.5
1	3	0.7815	26.0	2.03	NaDBS	5 g/L	10	98.1	0.5
1	4	0.4144	26.0	2.02	NaDBS	5 g/L	10	99.3	0.5
1	5	0.0820	26.0	2.00	NaDBS	5 g/L	10	99.4	0.5
1	6	0.04448	26.0	2.02	NaDBS	5 g/L	10	99.1	0.5
2	1	3.3041	5.0	2.06	NaDBS	5 g/L	10	76.2	12.5
2	2	3.3041	15.0	2.03	NaDBS	5 g/L	10	78.9	7.5
2	3	3.3041	35.0	2.05	NaDBS	5 g/L	10	84.8	0.5
2	4	3.3041	45.0	2.00	NaDBS	5 g/L	10	84.0	0.5
3	1	3.5011	26.0	2.05	NaDBS	5 g/L	5	83.8	0.5
3	2	1.6457	26.0	2.05	NaDBS	5 g/L	5	96.3	0.5
3	3	0.8769	26.0	2.03	NaDBS	5 g/L	5	98.0	0.5
3	4	0.4022	26.0	2.05	NaDBS	5 g/L	5	98.9	0.5
3	5	0.07625	26.0	2.04	NaDBS	5 g/L	5	99.4	0.5
3	6	0.03971	26.0	2.00	NaDBS	5 g/L	5	99.5	0.5

NOTES:

^aC₀ = Initial copper feed concentration

^bt_c = Time required for the reaction to reach equilibrium

^cNaDBS = Sodium dodecylbenzenesulfonate

^dArquad 12/50 = Dodecyltrimethyl ammonium chloride

Table 12. (Continued)

Series ID	Test ID	C ₀ ^a (g/L)	Temp (°C)	pH	Surfactant Used to Make Polyaphron	Surfactant Conc.	PVR	Percent Extraction (%)	t ^b (min)
4	1	3.6154	26.0	2.01	NaDBS	5 g/L	15	85.3	7.0
4	2	1.5567	26.0	2.01	NaDBS	5 g/L	15	96.7	0.5
4	3	0.7879	26.0	2.00	NaDBS	5 g/L	15	98.4	0.5
4	4	0.4225	26.0	2.05	NaDBS	5 g/L	15	98.9	0.5
4	5	0.08387	26.0	2.06	NaDBS	5 g/L	15	99.6	0.5
4	6	0.04175	26.0	2.02	NaDBS	5 g/L	15	99.8	0.5
5	1	3.5011	26.0	2.06	Arquad 12/50 ^d	5 ml/L	10	80.9	7.0
5	2	1.5059	26.0	2.06	Arquad 12/50	5 ml/L	10	96.3	3.0
5	3	0.8006	26.0	2.05	Arquad 12/50	5 ml/L	10	98.0	0.5
5	4	0.4035	26.0	2.00	Arquad 12/50	5 ml/L	10	98.9	0.5
5	5	0.08387	26.0	2.02	Arquad 12/50	5 ml/L	10	99.6	0.5
5	6	0.4842	26.0	2.01	Arquad 12/50	5 ml/L	10	99.5	0.5

NOTES:

^aC₀ = Initial copper feed concentration

^bt_c = Time required for the reaction to reach equilibrium

^c NaDBS = Sodium dodecylbenzenesulfonate

^d Arquad 12/50 = Dodecyltrimethyl ammonium chloride

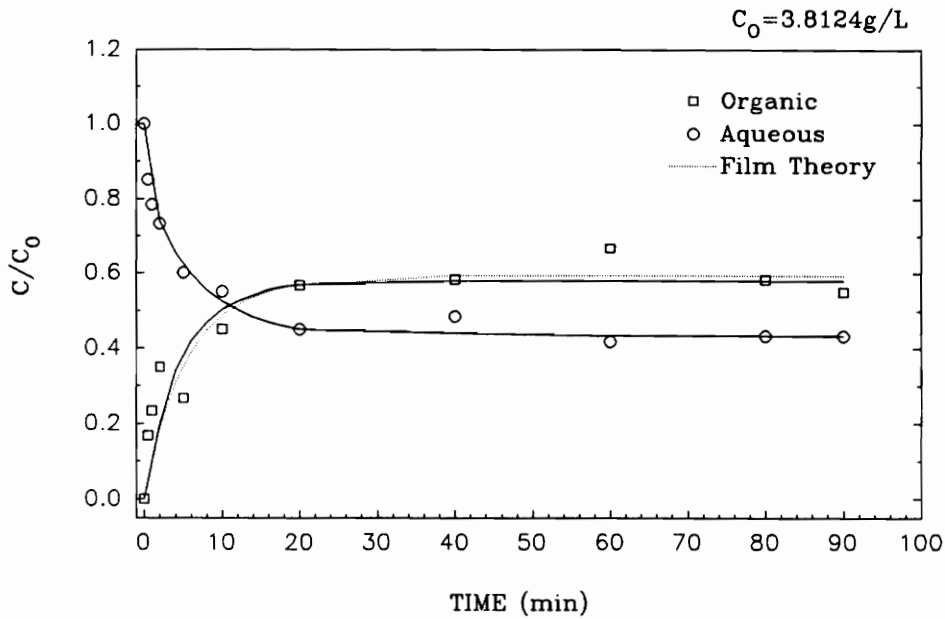


FIGURE (A)

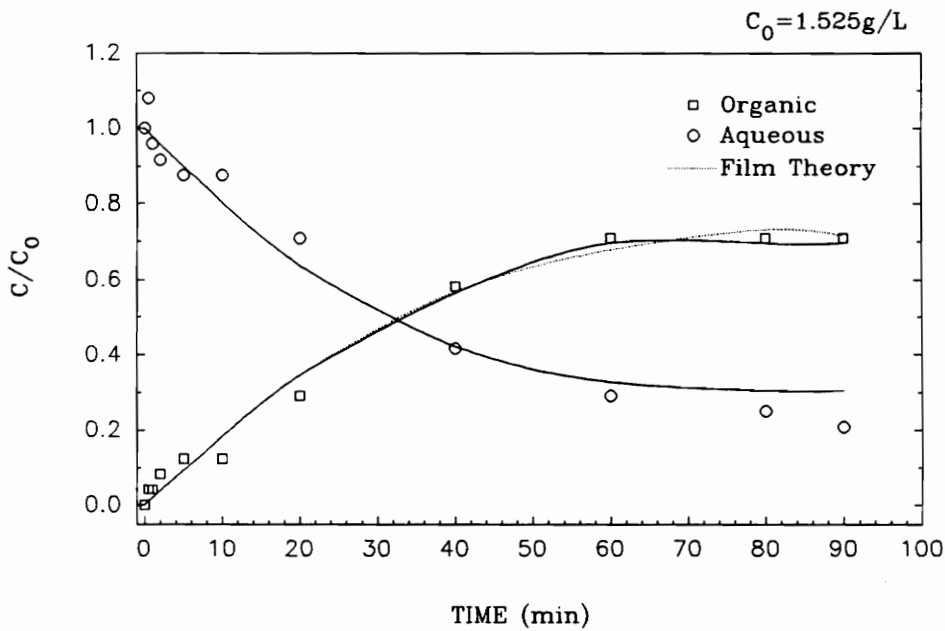


FIGURE (B)

Figure 54. Concentration versus time curves of the experimental and film theory values for the conventional solvent extraction of copper in a batch reactor at $T = 26.0^\circ\text{C}$.: Data found Table 13 and Table 14.

Table 13. Concentration values determined experimentally and calculated from film theory for the conventional solvent extraction of copper in a batch reactor at $C_o = 3.8124$ g/L, and $T = 26.0^\circ\text{C}$.

Time (min)	C_{aq}^a (g/L)	C_{org}^b (g/L)	C_{aqs}^c (g/L)	C_{orgs}^d (g/L)	C_{orgs}^e (g/L)	C_{org}^f (Calc)
0	3.8124	0.0	3.8124	2.25	0.00	0.0
0.5	3.2405	0.6354	-	2.25	-	-
1.0	2.9864	0.8896	-	2.25	-	-
2.0	2.7958	1.3343	2.825	2.25	0.74	0.71
4.0	-	-	2.489	2.25	1.30	1.18
5.0	2.2874	1.0166	-	2.25	-	-
6.0	-	-	2.275	2.25	1.60	1.49
8.0	-	-	2.113	2.25	1.78	1.70
10.0	2.0968	1.7156	2.000	2.25	1.92	1.85
12.0	-	-	1.913	2.25	2.00	1.96
14.0	-	-	1.838	2.25	2.06	2.04
16.0	-	-	1.788	2.23	2.12	2.10
18.0	-	-	1.750	2.23	2.15	2.14
20.0	1.7156	2.1604	1.713	2.22	2.17	2.16
40.0	1.8427	2.2239	1.675	2.21	2.21	2.26
60.0	1.5885	2.5416	1.652	2.21	2.21	2.26
80.0	1.6520	2.2239	1.652	2.21	2.21	2.26
90.0	1.6520	2.0968	1.652	2.21	2.21	2.26

- NOTES:
- ^a C_{aq} = Aqueous copper concentration (experimental points)
 - ^b C_{org} = Organic copper concentration (experimental points)
 - ^c C_{aqs} = Smooth curve drawn through C_{aq}
 - ^d C_{org}^* = Organic copper concentration in equilibrium with C_{aq}
 - ^e C_{orgs} = Smooth curve drawn through C_{org}^*
 - ^f C_{org} (Calc) = values calculated from film theory

Table 14. Concentration values determined experimentally and calculated from film theory for conventional solvent extraction of copper in a batch reactor at $C_o = 1.5250$ g/L, and $T = 26.0^\circ\text{C}$.

Time (min)	C_{aq}^a (g/L)	C_{org}^b (g/L)	C_{aqs}^c (g/L)	C_{orgs}^{*d} (g/L)	C_{orgs}^e (g/L)	C_{org}^f (calc)
0	1.525	0.0	1.525	2.45	0.0	0.0
0.5	1.644	0.075	1.510	2.44	0.0150	0.0150
1.0	1.443	0.061	1.490	2.42	0.0300	0.0298
2.0	1.423	0.102	1.460	2.40	0.0590	0.0589
5.0	1.378	0.183	1.370	2.38	0.143	0.143
10.0	1.345	0.196	1.223	2.31	0.280	0.280
20.0	1.089	0.440	0.972	2.15	0.528	0.528
40.0	0.648	0.872	0.645	1.80	0.860	0.867
60.0	0.465	1.061	0.500	1.57	1.061	1.034
80.0	0.395	1.061	0.464	1.52	1.061	1.115
90.0	0.287	1.050	0.464	1.52	1.061	1.089

- NOTES:
- ^a C_{aq} = Aqueous copper concentration (experimental points)
 - ^b C_{org} = Organic copper concentration (experimental points)
 - ^c C_{aqs} = Smooth curve drawn through C_{aq}
 - ^d C_{org}^{*} = Organic copper concentration in equilibrium with C_{aqs}
 - ^e C_{orgs} = Smooth curve drawn through C_{org}^{*}
 - ^f C_{org} (Calc) = values calculated from film theory

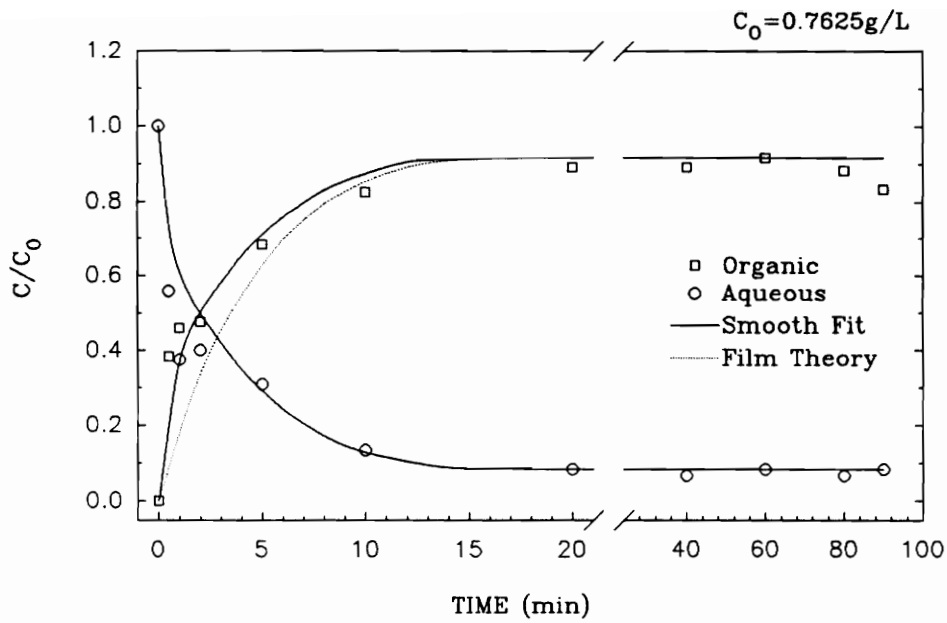


FIGURE (A)

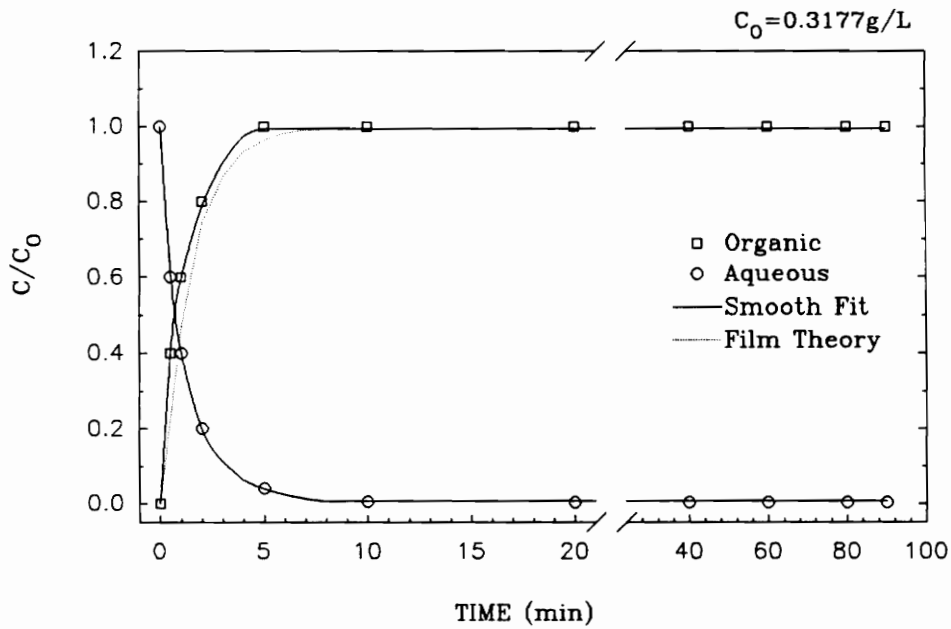


FIGURE (B)

Figure 55. Concentration versus time curves of the experimental and film theory values for the conventional solvent extraction of copper in a batch reactor at $T = 26.0^\circ\text{C}$.: Data found in Table 15 and Table 16.

Table 15. Concentration values determined experimentally and calculated from film theory for the conventional solvent extraction of copper in a batch reactor at $C_o = 0.7625$ g/L, and $T = 26.0^\circ\text{C}$.

Time (min)	C_{aq}^a (g/L)	C_{org}^b (g/L)	C_{aqs}^c (g/L)	C_{orgs}^{*d} (g/L)	C_{orgs}^e (g/L)	C_{org}^f (Calc)
0	0.7625	0.0	0.7625	2.250	0.0	0.0
0.5	0.426	0.292	0.540	-	0.220	-
1.0	0.286	0.349	0.465	-	0.280	-
2.0	0.305	0.362	0.380	1.700	0.3825	0.255
4.0	-	-	0.265	1.450	0.4975	0.417
5.0	0.235	0.521	0.222	-	0.542	-
6.0	-	-	0.185	1.220	0.577	0.531
8.0	-	-	0.130	1.020	0.633	0.605
10.0	0.102	0.629	0.097	0.910	0.666	0.350
12.0	-	-	0.079	0.850	0.690	0.679
14.0	-	-	0.067	0.733	0.696	0.693
16.0	-	-	0.065	0.714	0.698	0.697
18.0	-	-	0.064	0.704	0.699	0.699
20.0	0.0635	0.6990	0.0635	0.699	0.699	0.699
40.0	0.0509	0.6799	0.0635	0.699	0.699	0.699
60.0	0.0635	0.6990	0.0635	0.699	0.699	0.699
80.0	0.0509	0.6354	0.0635	0.699	0.699	0.699
90.0	0.0635	0.6354	0.0635	0.699	0.699	0.699

NOTES:

- ^a C_{aq} = Aqueous copper concentration (experimental points)
- ^b C_{org} = Organic copper concentration (experimental points)
- ^c C_{aqs} = Smooth curve drawn through C_{aq}
- ^d C_{orgs}^* = Organic copper concentration in equilibrium with C_{aq}
- ^e C_{orgs} = Smooth curve drawn through C_{orgs}^*
- ^f C_{org} (Calc) = Values calculated from film theory

Table 16. Concentration values determined experimentally and calculated from film theory for the conventional solvent extraction of copper in a batch reactor at $C_o = 0.3177$ g/L, and $T = 26.0^\circ\text{C}$.

Time (min)	C_{aq}^a (g/L)	C_{org}^b (g/L)	C_{aqs}^c (g/L)	C_{orgs}^d (g/L)	C_{orgs}^e (g/L)	C_{org}^f (Calc)
0	0.3177	0.0	0.3177	1.580	0.0	0.0
0.5	0.1906	0.1271	0.1950	-	0.130	-
1.0	0.1271	0.1906	0.1275	1.250	0.190	0.150
2.0	0.0635	0.2542	0.0625	0.693	0.250	0.236
3.0	-	-	0.0360	0.528	0.286	0.275
4.0	-	-	0.0200	0.429	0.309	0.296
5.0	0.0127	0.3159	0.0125	0.382	0.316	0.306
6.0	-	-	0.0075	0.351	0.316	0.312
7.0	-	-	0.0040	0.330	0.316	0.315
8.0	-	-	0.0018	0.316	0.316	0.316
9.0	-	-	0.0018	0.316	0.316	0.316
10.0	0.0018	0.3159	0.0018	0.316	0.316	0.316
20.0	0.0012	0.3159	0.0018	0.316	0.316	0.316
40.0	0.0012	0.3159	0.0018	0.316	0.316	0.316
60.0	0.0012	0.3159	0.0018	0.316	0.316	0.316
80.0	0.0006	0.3159	0.0018	0.316	0.316	0.316
90.0	0.0006	0.3159	0.0018	0.316	0.316	0.316

- NOTES:
- ^a C_{aq} = Aqueous copper concentration (experimental points)
 - ^b C_{org} = Organic copper concentration (experimental points)
 - ^c C_{aqs} = Smooth curve drawn through C_{aq}
 - ^d C_{orgs}^* = Organic copper concentration in equilibrium with C_{aqs}
 - ^e C_{orgs} = Smooth curve drawn through C_{orgs}^*
 - ^f C_{org}^f (Calc) = Values calculated from film theory

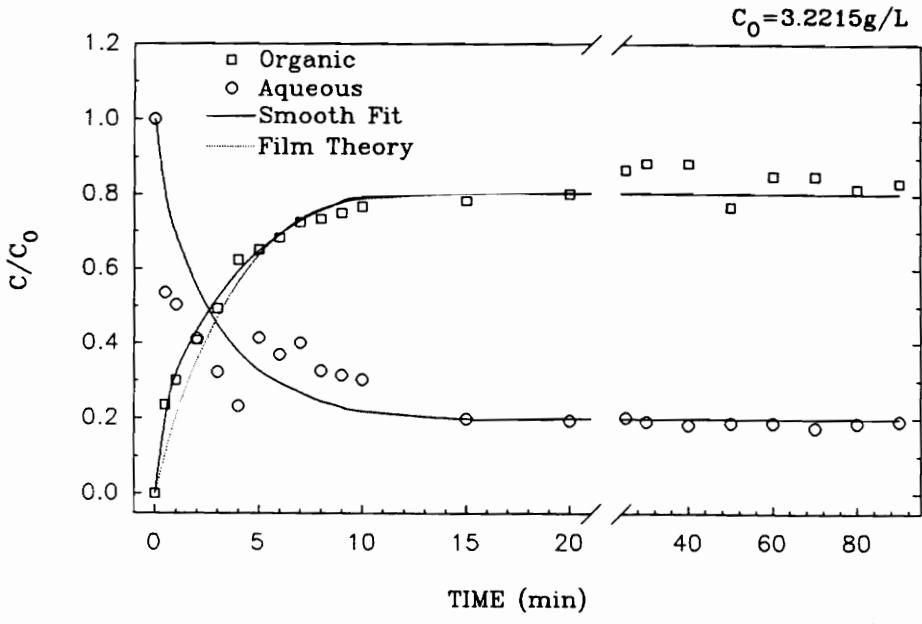


FIGURE (A)

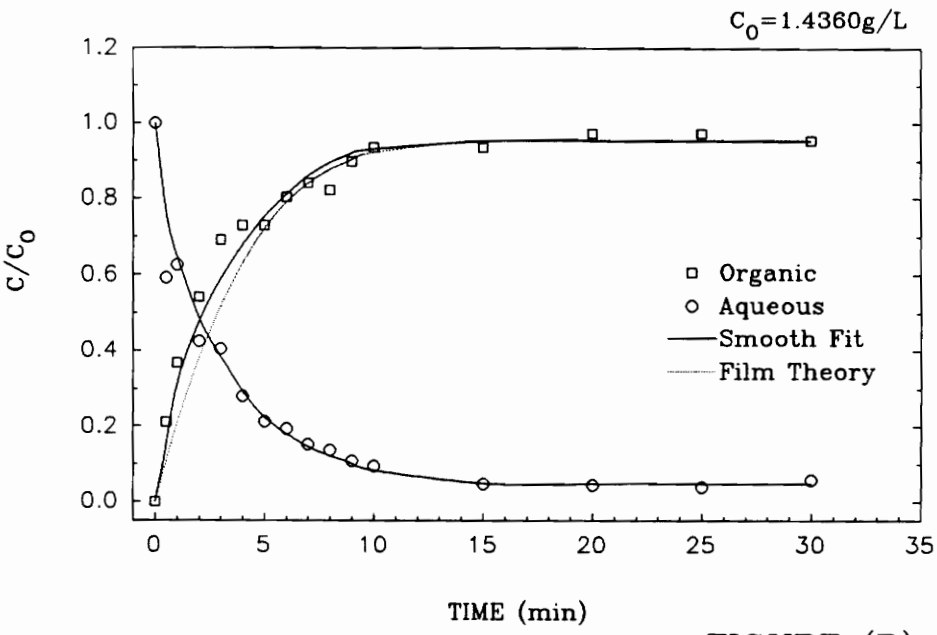


FIGURE (B)

Figure 56. Concentration versus time curves of the experimental and film theory values for the conventional solvent extraction of copper in a batch reactor at $T = 26.0^\circ\text{C}$ and $\text{pH} = 2.0$.: Data found in Table 17 and Table 18.

Table 17. Concentration values determined experimentally and calculated from film theory for the conventional solvent extraction of copper in a batch reactor at $C_o = 3.2215$ g/L, $T = 26.0^\circ\text{C}$, and $\text{pH} = 2.01$.

Time (min)	C_{aq}^a (g/L)	C_{org}^b (g/L)	C_{aq}^c (g/L)	C_{org}^{*d} (g/L)	C_{org}^e (g/L)	C_{org}^f (Calc)
0	3.2215	0.0	3.2215	3.00	0.0	0.0
0.5	1.7219	0.7561	2.577	3.00	0.644	-
1	1.6203	0.9658	2.225	3.00	1.025	0.657
2	1.3280	1.3153	1.775	3.00	1.400	1.129
3	1.0357	1.5885	1.450	2.975	1.675	1.511
4	0.7498	2.0079	1.215	2.915	1.910	1.816
5	1.3343	2.0968	1.050	2.860	2.085	2.051
6	1.1882	2.1985	0.945	2.810	2.225	2.230
7	1.2899	2.3319	0.863	2.760	2.350	2.361
8	1.0484	2.3637	0.788	2.710	2.440	2.151
9	1.0103	2.4145	0.737	2.660	2.515	2.506
10	0.9722	2.4717	0.700	2.630	2.550	2.536
15	0.6354	2.5226	0.635	2.5861	2.5861	2.589
20	0.6227	2.5797	0.635	2.5861	2.5861	2.589
25	0.6481	2.7894	0.635	2.5861	2.5861	2.589
30	0.6163	2.8466	0.635	2.5861	2.5861	2.589
40	0.5909	2.8466	0.635	2.5861	2.5861	2.589
50	0.6036	2.4717	0.635	2.5861	2.5861	2.589
60	0.6036	2.7386	0.635	2.5861	2.5861	2.589
70	0.5655	2.7386	0.635	2.5861	2.5861	2.589
80	0.0636	2.6306	0.635	2.5861	2.5861	2.589
90	0.6227	2.6814	0.635	2.5861	2.5861	2.589

- NOTES:
- ^a C_{aq} = Aqueous copper concentration (experimental points)
 - ^b C_{org} = Organic copper concentration (experimental points)
 - ^c C_{aq}^c = Smooth curve drawn through C_{aq}
 - ^d C_{org}^{*d} = Organic copper concentration in equilibrium with C_{aq}
 - ^e C_{org}^e = Smooth curve drawn through C_{org}
 - ^f C_{org}^f (Calc) = Values calculated from film theory

Table 18. Concentration values determined experimentally and calculated from film theory for the conventional solvent extraction of copper in a batch reactor at $C_o = 1.4360$ g/L, $T = 26.0$

Time (min)	C_{aq}^a (g/L)	C_{org}^b (g/L)	C_{aq}^c (g/L)	C_{org}^{*d} (g/L)	C_{org}^e (g/L)	C_{org}^f (Calc)
0	1.4360	0.0	1.4360	2.975	0.0	0.0
0.5	0.8514	0.3050	1.100	-	0.215	-
1	0.9023	0.2574	0.930	2.800	0.450	0.298
2	0.6100	0.7815	0.700	2.635	0.685	0.544
3	0.5782	0.9912	0.550	2.485	0.848	0.744
4	0.4003	1.0484	0.420	2.315	0.975	0.907
5	0.3050	1.0484	0.320	2.150	1.080	1.036
6	0.2796	1.1564	0.260	2.000	1.165	1.135
7	0.2160	1.2073	0.210	1.825	1.235	1.207
8	0.1970	1.1818	0.175	1.750	1.285	1.259
9	0.1525	1.2899	0.145	1.650	1.325	1.297
10	0.1334	1.3407	0.120	1.540	1.350	1.322
15	0.0699	1.3407	0.070	1.3732	1.368	1.371
20	0.0629	1.3979	0.068	1.3680	1.368	1.372
25	0.0566	1.3979	0.068	1.3680	1.368	1.372
30	0.0826	1.3725	0.068	1.3680	1.368	1.372

NOTES:

- ^a C_{aq} = Aqueous copper concentration (experimental points)
- ^b C_{org} = Organic copper concentration (experimental points)
- ^c C_{aq}^c = Smooth curve drawn through C_{aq}
- ^d C_{org}^{*d} = Organic copper concentration in equilibrium with C_{aq}
- ^e C_{org}^e = Smooth curve drawn through C_{org}
- ^f C_{org}^f (Calc) = Values calculated from film theory

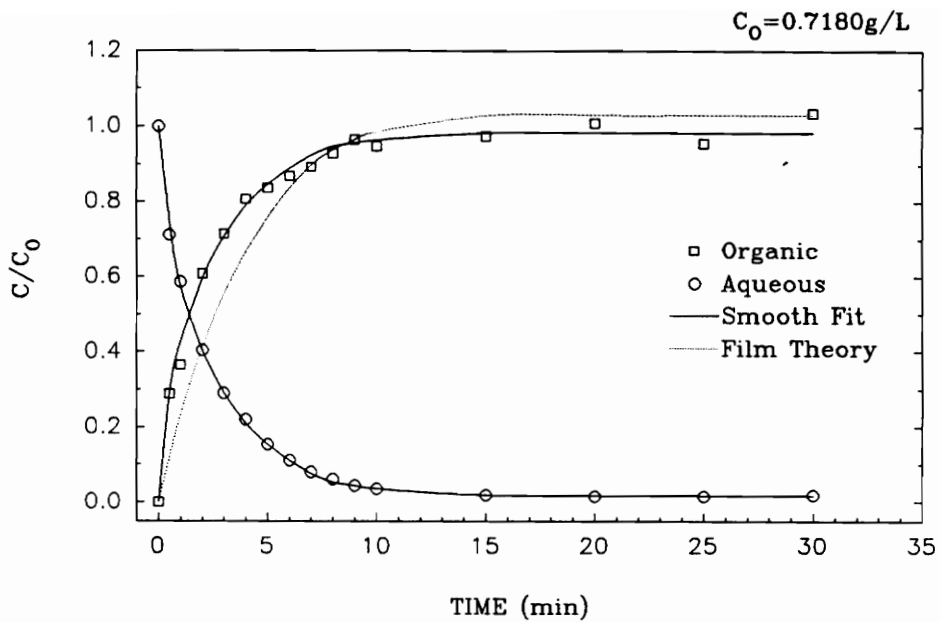


FIGURE (A)

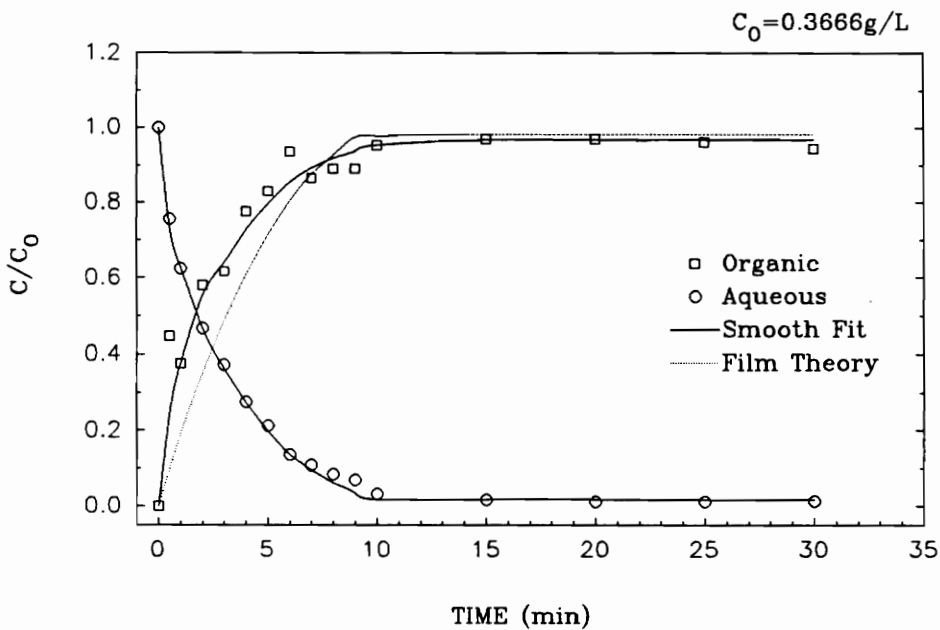


FIGURE (B)

Figure 57. Concentration versus time curves of the experimental and film theory values for the conventional solvent extraction of copper in a batch reactor at $T = 26.0$ °C and $\text{pH} = 2.0$.: Data found in Table 19 and Table 20.

Table 19. Concentration values determined experimentally and calculated from film theory for the conventional solvent extraction of copper in a batch reactor at $C_o = 0.7180$ g/L, $T = 26.0^\circ\text{C}$, and $\text{pH} = 2.08$.

Time (min)	C_{aq}^a (g/L)	C_{org}^b (g/L)	C_{aq}^c (g/L)	C_{orgs}^d (g/L)	C_{orgs}^e (g/L)	C_{org}^f (Calc)
0.0	0.7180	0.0	0.7180	2.65	0.0	0.0
0.5	0.5115	0.2071	0.5115	-	0.2065	-
1.0	0.4213	0.2618	0.4125	2.313	0.3055	0.165
2.0	0.2904	0.4372	0.2904	2.088	0.4276	0.294
3.0	0.2084	0.5140	0.2084	1.825	0.5096	0.398
4.0	0.1576	0.2795	0.1500	1.650	0.5680	0.480
5.0	0.1106	0.6011	0.1100	1.450	0.6080	0.546
6.0	0.0394	0.6240	0.0794	1.3973	0.6386	0.601
7.0	0.0585	0.6418	0.0550	1.2132	0.6630	0.645
8.0	0.0445	0.6672	0.0380	1.0106	0.6800	0.674
9.0	0.0318	0.6926	0.0318	0.9368	0.6862	0.693
10.0	0.0261	0.6799	0.0261	0.8688	0.6919	0.707
15.0	0.0133	0.6989	0.0133	0.7164	0.7047	0.738
20.0	0.0114	0.7244	0.0124	0.7056	0.7056	0.740
25.0	0.0114	0.6862	0.0124	0.7056	0.7056	0.740
30.0	0.0133	0.7423	0.0124	0.7056	0.7056	0.740

NOTES: ^a C_{aq} = Aqueous copper concentration (experimental points)
^b C_{org} = Organic copper concentration (experimental points)
^c C_{aq} = Smooth curve drawn through C_{aq}
^d C_{orgs}^d = Organic copper concentration in equilibrium with C_{aq}
^e C_{orgs}^e = Smooth curve drawn through C_{org}
^f C_{org}^f (Calc) = Values calculated from film theory

Table 20. Concentration values determined experimentally and calculated from film theory for the conventional solvent extraction of copper in a batch reactor at $C_o=0.3666$ g/L, $T=26.0^\circ\text{C}$, and $\text{pH}=2.01$.

Time (min)	C_{aq}^a (g/L)	C_{org}^b (g/L)	C_{aqs}^c (g/L)	C_{orgs}^{*d} (g/L)	C_{orgs}^e (g/L)	C_{org}^f (Calc)
0.0	0.3666	0.0	0.3666	2.2215	0.0	0.0
0.5	0.2770	0.1639	0.2688	-	0.0896	-
1.0	0.2287	0.1379	0.2300	1.93	0.138	0.070
2.0	0.1716	0.2129	0.1713	1.75	0.203	0.128
3.0	0.1366	0.2262	0.1325	1.60	0.235	0.179
4.0	0.1010	0.2847	0.1000	1.45	0.267	0.223
5.0	0.0782	0.3044	0.0725	1.3796	0.292	0.262
6.0	0.0496	0.3431	0.05	1.1536	0.313	0.295
7.0	0.0400	0.3171	0.035	0.9749	0.327	0.321
8.0	0.0311	0.3266	0.0225	0.8260	0.337	0.340
9.0	0.0254	0.3266	0.0125	0.7068	0.344	0.354
10.0	0.0121	0.3495	0.0063	0.3603	0.350	0.360
15.0	0.0057	0.3558	0.0063	0.3603	0.355	0.360
20.0	0.0044	0.3558	0.0063	0.3603	0.355	0.360
25.0	0.0044	0.3526	0.0063	0.3603	0.355	0.360
30.0	0.0051	0.3463	0.0063	0.3603	0.355	0.360

- NOTES:
- ^a C_{aq} = Aqueous copper concentration (experimental points)
 - ^b C_{org} = Organic copper concentration (experimental points)
 - ^c C_{aqs} = Smooth curve drawn through C_{aq}
 - ^d C_{orgs}^* = Organic copper concentration in equilibrium with C_{aqs}
 - ^e C_{orgs} = Smooth curve drawn through C_{orgs}^*
 - ^f C_{org} (Calc) = Values calculated from film theory

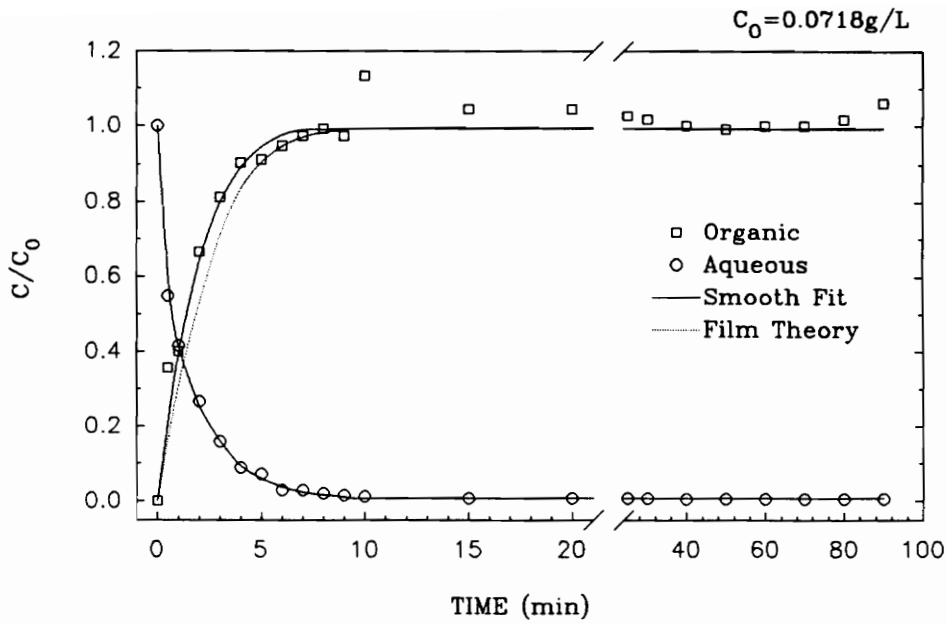


FIGURE (A)

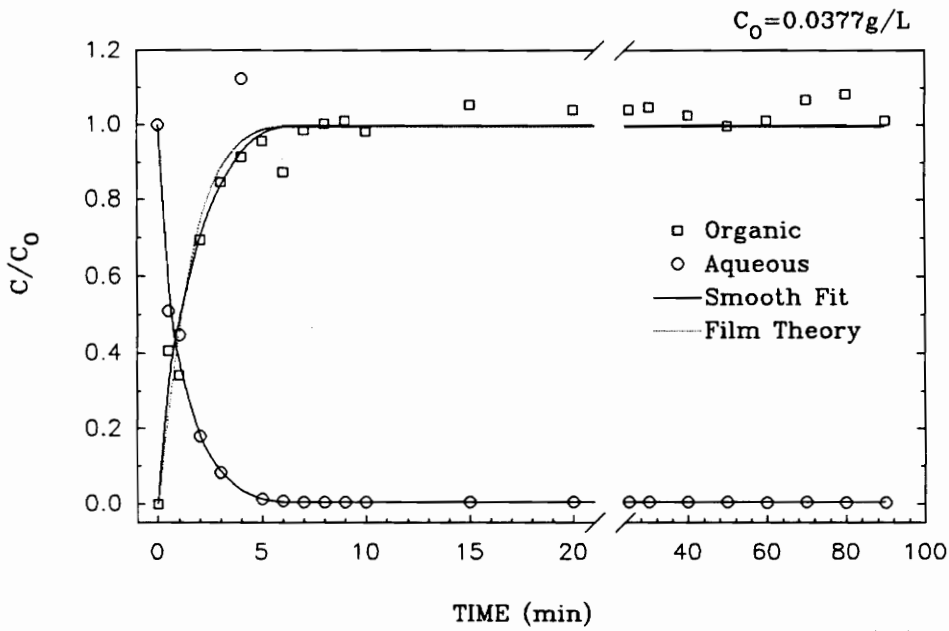


FIGURE (B)

Figure 58. Concentration versus time curves of the experimental and film theory values for the conventional solvent extraction of copper in a batch reactor at $T = 26.0^\circ\text{C}$ and $\text{pH} = 2.0$.: Data found in Table 21 and Table 22

Table 21. Concentration values determined experimentally and calculated from film theory for the conventional solvent extraction of copper in a batch reactor at $C_o = 0.0718$ g/L, $T = 26.0^\circ\text{C}$, and $\text{pH} = 2.03$.

Time (min)	C_{aq}^a (g/L)	C_{org}^b (g/L)	C_{aq}^c (g/L)	C_{org}^{*d} (g/L)	C_{org}^e (g/L)	C_{org}^f (Calc)
0.0	0.0718	0.0	0.0718	1.3778	0.0	0.0
0.5	0.0394	0.0255	0.0431	1.0273	0.015	-
1.0	0.0299	0.0287	0.0296	0.9105	0.0283	0.0221
2.0	0.0191	0.0477	0.0182	0.7747	0.0460	0.0379
3.0	0.0114	0.0582	0.0115	0.6547	0.0572	0.0509
4.0	0.0064	0.0648	0.0067	0.3830	0.064	0.0599
5.0	0.0051	0.0654	0.0043	0.2607	0.0678	0.0649
6.0	0.0020	0.0680	0.0027	0.1809	0.070	0.0679
7.0	0.0022	0.0699	0.0017	0.1311	0.071	0.0696
8.0	0.0015	0.0712	0.0012	0.1062	0.0711	0.0705
9.0	0.0011	0.0699	0.0008	0.0863	0.0712	0.0710
10.0	0.00083	0.0813	0.0005	0.0713	0.0713	0.0712
15.0	0.00050	0.0750	0.0005	0.0713	0.0713	0.0712
20.0	0.00043	0.0750	0.0005	0.0713	0.0713	0.0712
25.0	0.00048	0.0737	0.0005	0.0713	0.0713	0.0712
30.0	0.00046	0.0731	0.0005	0.0713	0.0713	0.0712
40.0	0.00044	0.0718	0.0005	0.0713	0.0713	0.0712
50.0	0.00044	0.0712	0.0005	0.0713	0.0713	0.0712
60.0	0.00039	0.0718	0.0005	0.0713	0.0713	0.0712
70.0	0.00044	0.0718	0.0005	0.0713	0.0713	0.0712
80.0	0.00045	0.0731	0.0005	0.0713	0.0713	0.0712
90.0	0.00044	0.0762	0.0005	0.0713	0.0713	0.0712

NOTES: ^a C_{aq} = Aqueous copper concentration (experimental points)
^b C_{org} = Organic copper concentration (experimental points)
^c C_{aq} = Smooth curve drawn through C_{aq}
^d C_{org}^* = Organic copper concentration in equilibrium with C_{aq}
^e C_{org} = Smooth curve drawn through C_{org}
^f C_{org} (Calc) = Values calculated from film theory

Table 22. Concentration values determined experimentally and calculated from film theory for the conventional solvent extraction of copper in a batch reactor at $C_o=0.0377$ g/L, $T=26.0^\circ\text{C}$, and $\text{pH}=2.04$.

Time (min)	C_{aq}^a (g/L)	C_{org}^b (g/L)	C_{aq}^c (g/L)	C_{orgs}^d (g/L)	C_{orgs}^e (g/L)	C_{org}^f (Calc)
0.0	0.0377	0.0	0.0377	0.875	0.0	0.0
0.5	0.0194	0.0155	0.0220	0.730	0.012	-
1.0	0.0170	0.0130	0.0143	0.600	0.0183	0.0172
2.0	0.0069	0.0265	0.0069	0.450	0.0265	0.0279
3.0	0.0032	0.0323	0.0033	0.215	0.0316	0.0334
4.0	0.0043	0.0349	0.0014	0.1125	0.0350	0.0360
5.0	0.00053	0.0365	0.0005	0.650	0.0368	0.0372
6.0	0.00028	0.0333	0.00019	0.0375	0.0375	0.0375
7.0	0.00020	0.0386	0.00019	0.0375	0.0376	0.0375
8.0	0.00018	0.0383	0.00019	0.0375	0.0376	0.0375
9.0	0.00017	0.0386	0.00019	0.0375	0.0376	0.0375
10.0	0.00017	0.0374	0.00019	0.0375	0.0376	0.0375
15.0	0.00018	0.0402	0.00019	0.0375	0.0376	0.0375
20.0	0.00017	0.0396	0.00019	0.0375	0.0376	0.0375
25.0	0.00017	0.0396	0.00019	0.0375	0.0376	0.0375
30.0	0.00017	0.0399	0.00019	0.0375	0.0376	0.0375
40.0	0.00017	0.0386	0.00019	0.0375	0.0376	0.0375
50.0	0.00016	0.0376	0.00019	0.0375	0.0376	0.0375
60.0	0.00015	0.0381	0.00019	0.0375	0.0376	0.0375
70.0	0.00018	0.0403	0.00019	0.0375	0.0376	0.0375
80.0	0.00014	0.0408	0.00019	0.0375	0.0376	0.0375
90.0	0.00014	0.0381	0.00019	0.0375	0.0376	0.0375

NOTES: ^a C_{aq} = Aqueous copper concentration (experimental points)
^b C_{org} = Organic copper concentration (experimental points)
^c C_{aq}^c = Smooth curve drawn through C_{aq}
^d C_{orgs}^d = Organic copper concentration in equilibrium with C_{aq}
^e C_{orgs}^e = Smooth curve drawn through C_{orgs}^d
^f C_{org}^f (Calc) = Values calculated from film theory

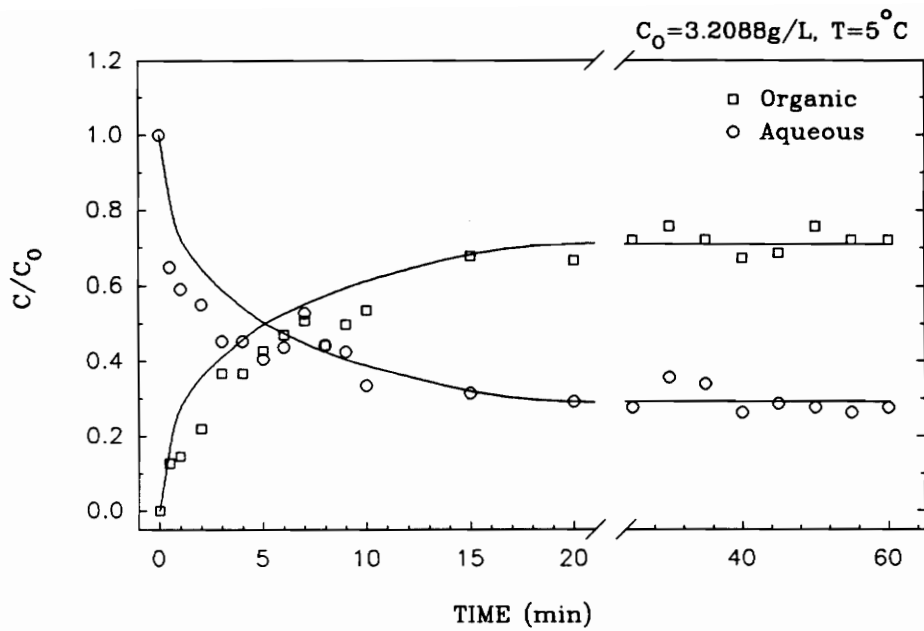


FIGURE (A)

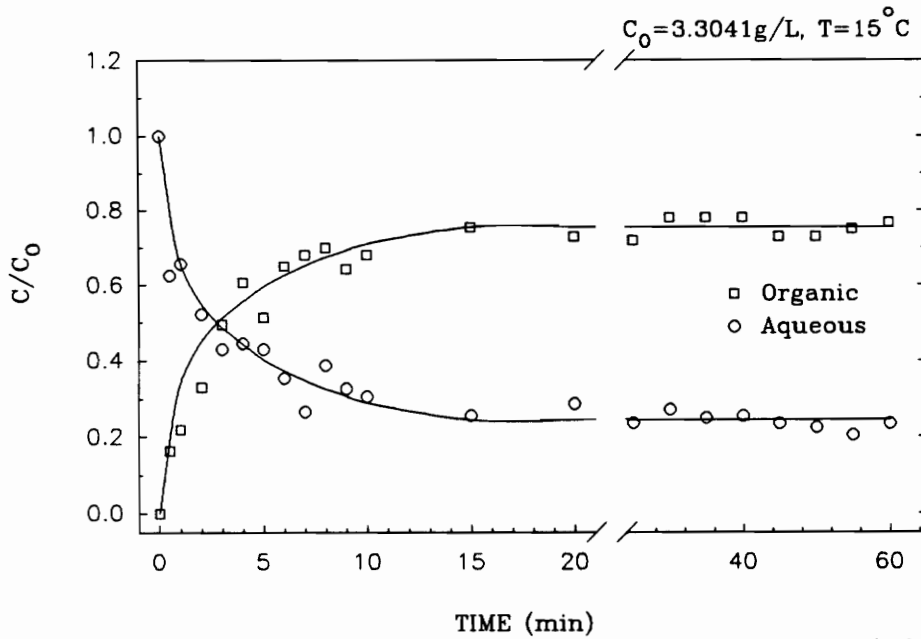


FIGURE (B)

Figure 59. Experimental values of the concentration versus time curves for the conventional solvent extraction of copper in a batch reactor at pH=2.0.: Data found in Table 23 and Table 24.

Table 23. Experimental concentration values for the conventional solvent extraction of copper in a batch reactor at $C_o=3.2088$ g/L, $T=5.0^\circ\text{C}$, and $\text{pH}=2.06$.

Time (min)	C_{aq} (g/L)	C_{org} (g/L)
0	3.2088	0.0
0.5	2.0778	0.4067
1.0	1.8998	0.4702
2.0	1.7664	0.7053
3.0	1.4551	1.1767
4.0	1.4551	1.1767
5.0	1.3026	1.675
6.0	1.4042	1.5098
7.0	1.6965	1.629
8.0	1.4233	1.4169
9.0	1.3661	1.549
10.0	1.0738	1.7156
15.0	1.0039	2.170
20.0	0.9340	2.1349
25.0	0.8832	2.3129
30.0	1.1374	2.4272
35.0	1.0802	2.313
40.0	1.8387	2.1551
45.0	0.9213	2.1987
50.0	0.8896	2.4272
55.0	0.8387	2.313
60.0	0.8896	2.313

Table 24. Experimental concentration values for the conventional solvent extraction of copper in a batch reactor at $C_o=3.3041$ g/L, $T=15.0^\circ\text{C}$, and $\text{pH}=2.03$.

Time (min)	C_{aq} (g/L)	C_{org} (g/L)
0	3.3041	0.0
0.5	2.0714	0.5401
1.0	2.1731	0.7244
2.0	1.7279	1.0865
3.0	1.4233	1.5186
4.0	1.4678	2.006
5.0	1.4233	1.6965
6.0	1.1691	2.1516
7.0	0.8832	2.2513
8.0	1.2835	2.3115
9.0	1.0802	2.1286
10.0	1.0166	2.2493
15.0	0.8451	2.4908
20.0	0.9467	2.4050
25.0	0.7815	2.5756
30.0	0.8959	2.5758
35.0	0.8260	2.5758
40.0	0.8387	2.5788
45.0	0.7752	2.4050
50.0	0.7371	2.4050
55.0	0.6735	2.475
60.0	0.7752	2.5300

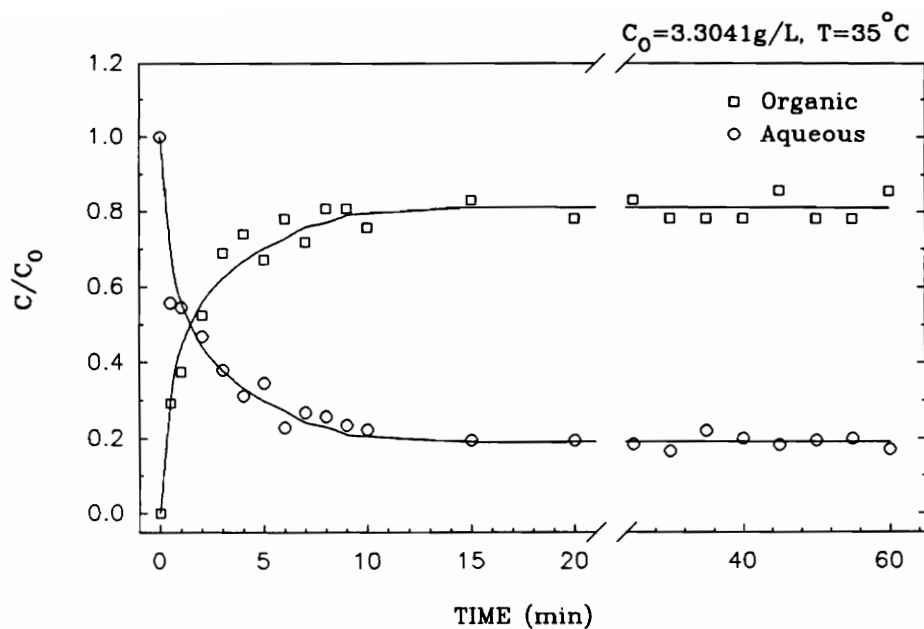


FIGURE (A)

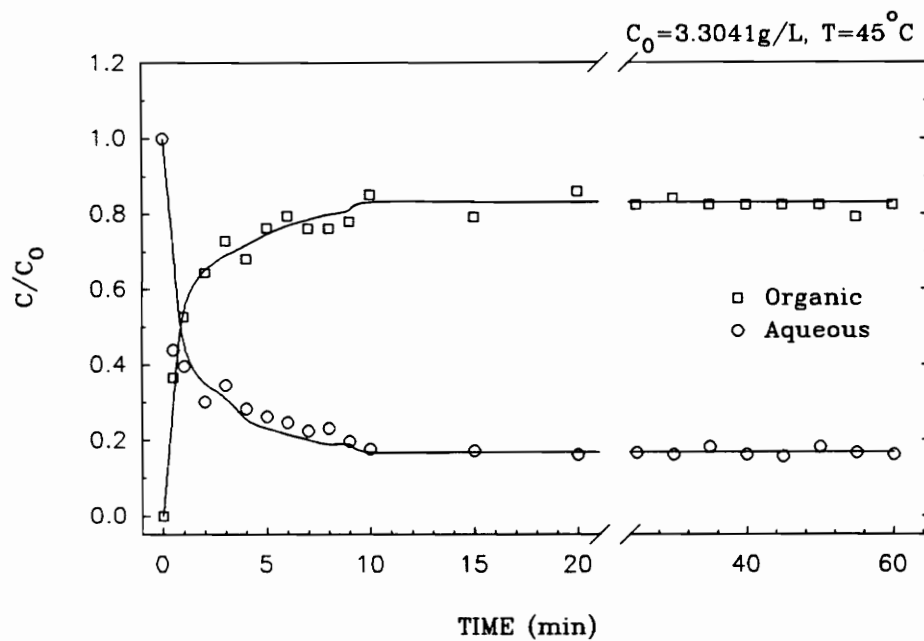


FIGURE (B)

Figure 60. Experimental values of the concentration versus time curves for the conventional solvent extraction of copper in a batch reactor at pH=2.0.: Data found in Table 25 and Table 26.

Table 25. Experimental concentration values for the conventional solvent extraction of copper in a batch reactor at $C_o = 3.3041$ g/L, $T = 35.0^\circ\text{C}$, and $\text{pH} = 2.05$.

Time (min)	C_{aq} (g/L)	C_{org} (g/L)
0	3.3041	0.0
0.5	1.8427	0.9658
1.0	1.8045	1.2390
2.0	1.5504	1.7346
3.0	1.2581	2.2811
4.0	1.0293	2.4463
5.0	1.1437	2.2195
6.0	0.7561	2.5797
7.0	1.8832	2.375
8.0	0.8514	2.6705
9.0	0.7752	2.6703
10.0	0.7371	2.50
15.0	0.6418	2.7436
20.0	0.6418	2.5797
25.0	0.6100	2.7436
30.0	0.5464	2.5797
35.0	0.7244	2.5797
40.0	0.6608	2.5797
45.0	0.6036	2.8275
50.0	0.3418	2.5797
55.0	0.6608	2.5797
60.0	0.5655	2.8275

Table 26. Experimental concentration values for the conventional solvent extraction of copper in a batch reactor at $C_o=3.3041$ g/L, $T=45.0^\circ\text{C}$, and $\text{pH}=2.00$.

Time (min)	C_{aq} (g/L)	C_{org} (g/L)
0	3.3041	0.0
0.5	1.4487	1.2073
1.0	1.3089	1.7410
2.0	0.9976	2.1286
3.0	1.1437	2.4082
4.0	0.9340	2.2506
5.0	0.8641	2.521
6.0	0.8133	2.629
7.0	0.7434	2.5145
8.0	0.7625	2.5145
9.0	0.6545	2.5755
10.0	0.5846	2.8125
15.0	0.5655	2.6173
20.0	0.5337	2.8397
25.0	0.5528	2.7253
30.0	0.2337	2.7825
35.0	0.6036	2.7253
40.0	0.5337	2.7253
45.0	0.5147	2.7253
50.0	0.6036	2.7253
55.0	0.5528	2.6173
60.0	0.5337	2.7253

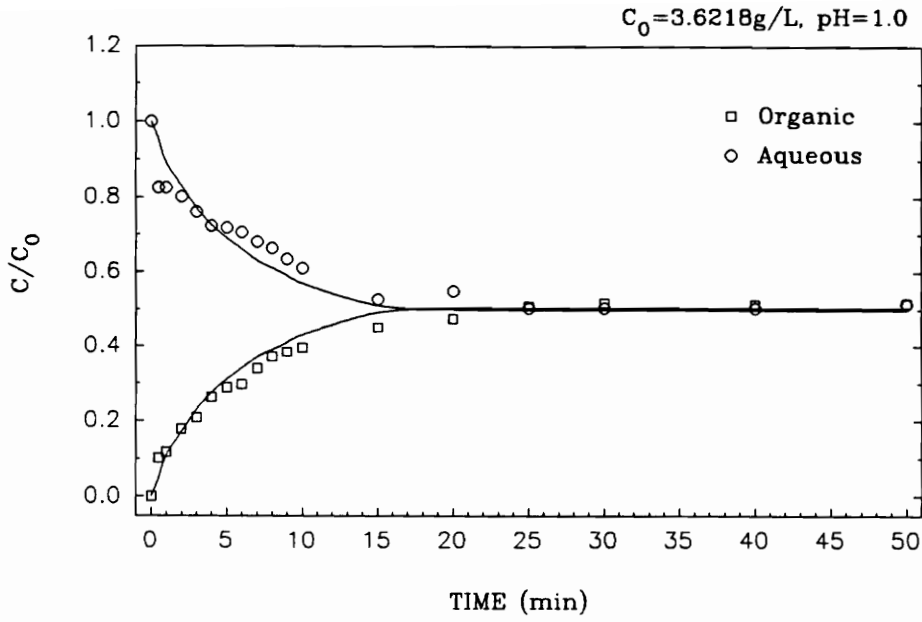


FIGURE (A)

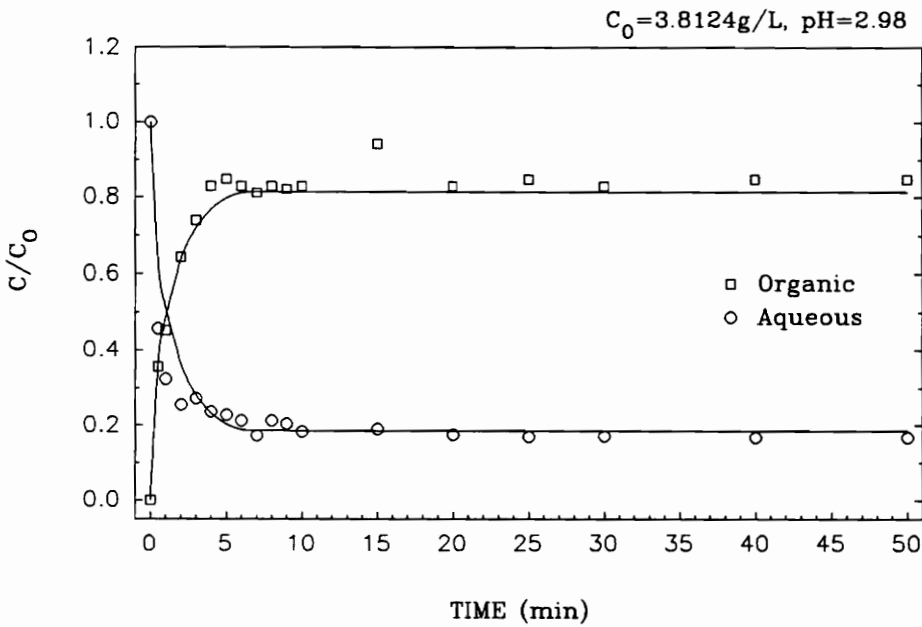


FIGURE (B)

Figure 61. Experimental values of the concentration versus time curves for the conventional solvent extraction of copper in a batch reactor at $T=26.0^{\circ}\text{C}$.: Data found in Table 27 and Table 28.

Table 27. Experimental concentration values for the conventional solvent extraction of copper in a batch reactor at $C_o=3.6218$ g/L, $T=26.0^\circ\text{C}$, and $\text{pH}=1.00$.

Time (min)	C_{aq} (g/L)	C_{org} (g/L)
0	3.6218	0.0
0.5	2.9864	0.3730
1.0	2.9864	0.4244
2.0	2.9038	0.6443
3.0	2.7513	0.7517
4.0	2.6178	0.9531
5.0	2.5988	1.0421
6.0	2.5543	1.0738
7.0	2.4654	1.2263
8.0	2.4018	1.3470
9.0	2.2938	1.3915
10.0	2.2112	1.4297
15.0	1.9062	1.6330
20.0	1.9888	1.7156
25.0	1.8172	1.8427
30.0	1.8172	1.8681
40.0	1.8172	1.8554
50.0	1.8617	1.8681

Table 28. Experimental concentration values for the conventional solvent extraction of copper in a batch reactor at $C_o = 3.8124$ g/L, $T = 26.0^\circ\text{C}$, and $\text{pH} = 2.98$.

Time (min)	C_{aq} (g/L)	C_{org} (g/L)
0	3.8124	0.0
0.5	1.7474	1.3534
1.0	1.2327	0.7283
2.0	0.9722	2.4526
3.0	1.0657	2.8148
4.0	0.9023	3.1643
5.0	0.8705	3.2342
6.0	0.8070	3.1643
7.0	0.6608	3.0944
8.0	0.8070	3.1643
9.0	0.7752	3.1325
10.0	0.6989	3.1643
15.0	0.7244	3.5900
20.0	0.6672	3.1643
25.0	0.6481	3.2342
30.0	0.6545	3.1643
40.0	0.6418	3.2342
50.0	0.6418	3.2342

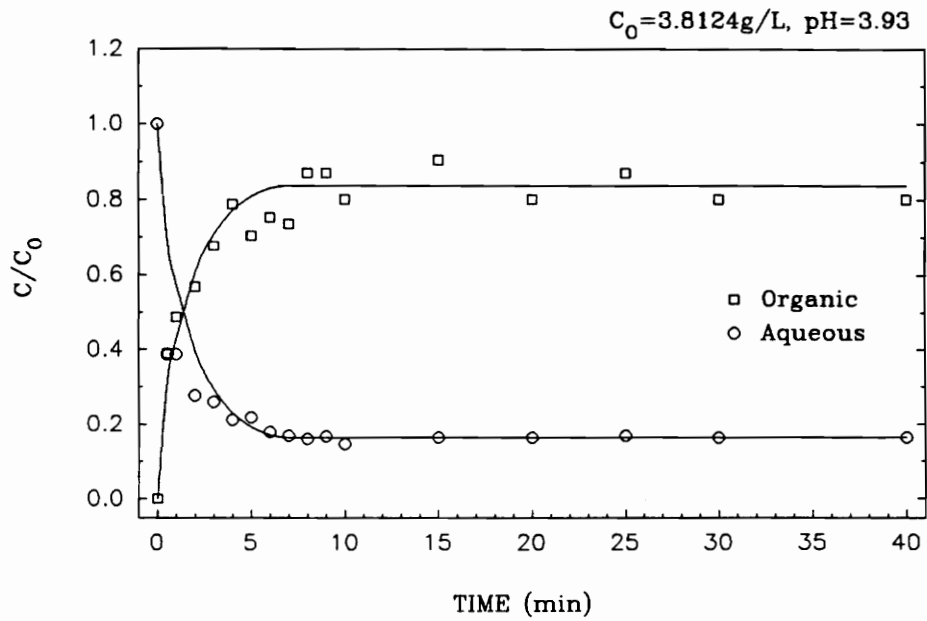


FIGURE (A)

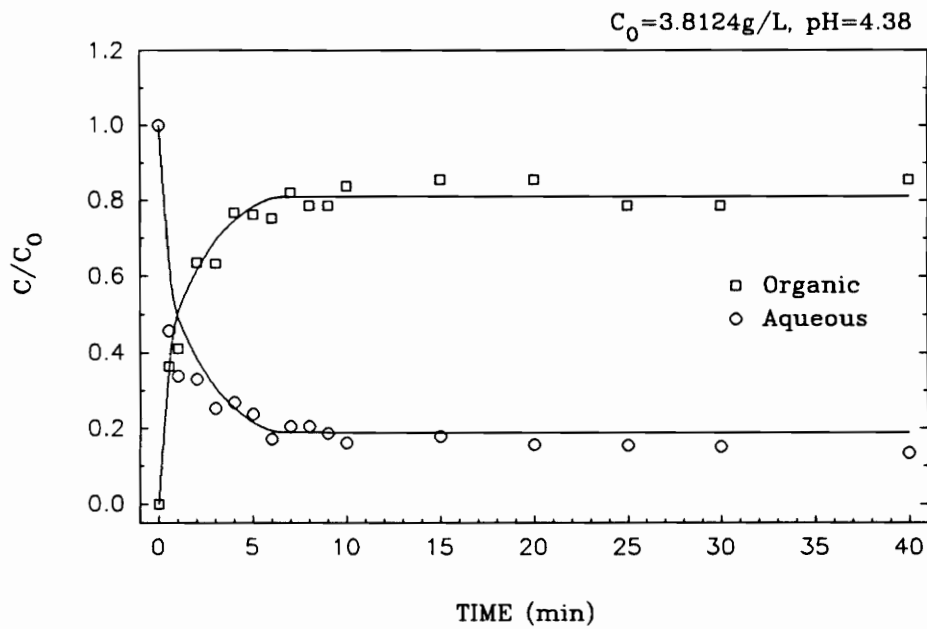


FIGURE (B)

Figure 62. Experimental values of the concentration versus time curves for the conventional solvent extraction of copper in a batch reactor at $T = 26.0^\circ\text{C}$.: Data found in Table 29 and Table 30.

Table 29. Experimental concentration values for the conventional solvent extraction of copper in a batch reactor at $C_o = 3.8124$ g/L, $T = 26.0^\circ\text{C}$, and $\text{pH} = 3.93$.

Time (min)	C_{aq} (g/L)	C_{org} (g/L)
0	3.8124	0.0
0.5	1.1374	1.4830
1.0	1.475	1.8509
2.0	1.0548	2.1623
3.0	0.9912	2.5751
4.0	0.8070	2.9985
5.0	0.8324	2.6819
6.0	0.6799	2.8695
7.0	0.6443	2.8047
8.0	0.6113	3.3219
9.0	0.6360	3.3219
10.0	0.5617	3.0519
15.0	0.6278	3.4509
20.0	0.6278	3.0519
25.0	0.6443	3.3219
30.0	0.6278	3.0519
40.0	0.6278	3.0519

Table 30. Experimental concentration values for the conventional solvent extraction of copper in a batch reactor at $C_o=3.8124$ g/L, $T=26.0^\circ\text{C}$, and $\text{pH}=4.38$.

Time (min)	C_{aq} (g/L)	C_{org} (g/L)
0	3.8124	0.0
0.5	1.7464	1.3903
1.0	1.2930	1.5713
2.0	1.2594	2.4253
3.0	0.9683	2.4171
4.0	1.0274	2.9251
5.0	0.9093	2.907
6.0	0.6551	2.8695
7.0	0.7822	3.1281
8.0	0.7822	3.0009
9.0	0.7142	3.0009
10.0	0.6125	3.1965
15.0	0.6805	3.2571
20.0	0.5960	3.2571
25.0	0.5871	3.0009
30.0	0.5788	3.0009
40.0	0.5109	3.2571

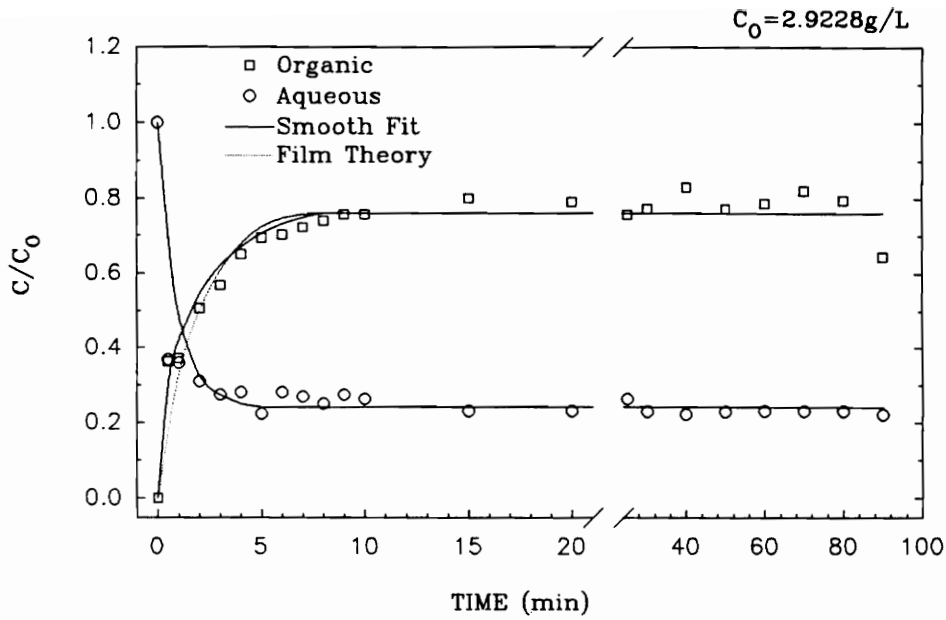


FIGURE (A)

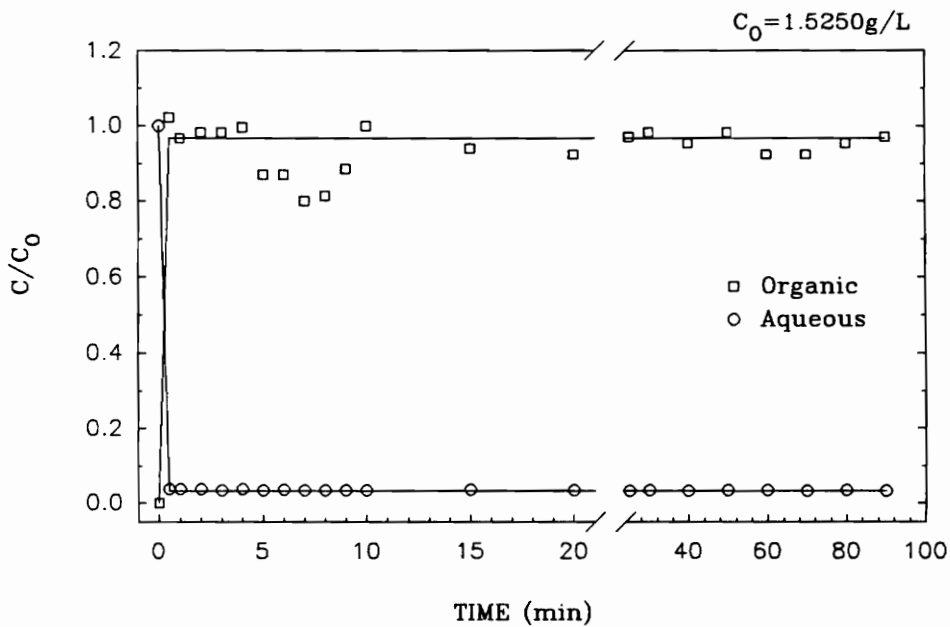


FIGURE (B)

Figure 63. Concentration versus time curves of the experimental and film theory values for the PDSE of copper in a batch reactor at $T=26.0^{\circ}\text{C}$ and $\text{pH}=2.0$.; Polyaphrons made with 5 g/L NaDBS; PVR=10. Data found in Table 31 and Table 32.

Table 31. Concentration values determined experimentally and calculated from film theory for PDSE of copper in a batch reactor at $C_o = 2.9228$ g/L, $T = 26.0^\circ\text{C}$, and $\text{pH} = 2.01$. Polyaphrons made with 5 g/L NaDBS; $\text{PVR} = 10$.

Time (min)	C_{aq}^{a} (g/L)	$C_{\text{org}}^{\text{b}}$ (g/L)	C_{aq}^{c} (g/L)	$C_{\text{org}}^{\text{d}}$ (g/L)	$C_{\text{org}}^{\text{e}}$ (g/L)	$C_{\text{org}}^{\text{f}}$ (Calc)
0	2.9228	0.0	2.9228	2.400	0.0	0.0
0.5	1.0738	1.0611	1.860	2.400	0.940	-
1.0	1.0484	1.0865	1.420	2.400	1.230	0.955
2.0	0.9086	0.4805	0.950	2.320	1.590	1.460
3.0	0.8006	1.6584	0.800	2.275	1.815	4.780
4.0	0.8197	1.8998	0.730	2.250	1.955	1.980
5.0	0.6545	2.0269	0.705	2.230	2.060	2.110
6.0	0.8197	2.0523	0.700	2.223	2.135	2.180
7.0	0.7879	2.1095	0.700	2.223	2.185	2.210
8.0	0.7307	2.1604	0.700	2.223	2.223	2.220
9.0	0.8006	2.2112	0.700	2.223	2.223	2.220
10.0	0.7688	2.2112	0.700	2.223	2.223	2.220
15.0	0.6735	2.3383	0.700	2.223	2.223	2.220
20.0	0.6735	2.3129	0.700	2.223	2.223	2.220
25.0	0.7688	2.2112	0.700	2.223	2.223	2.220
30.0	0.6672	2.2557	0.700	2.223	2.223	2.220
40.0	0.6481	2.4272	0.700	2.223	2.223	2.220
50.0	0.6672	2.2557	0.700	2.223	2.223	2.220
60.0	0.6735	2.3001	0.700	2.223	2.223	2.220
70.0	0.6735	2.4018	0.700	2.223	2.223	2.220
80.0	0.6735	2.3256	0.700	2.223	2.223	2.220
90.0	0.6481	1.8871	0.700	2.223	2.223	2.220

- NOTES:**
- ^a C_{aq} = Aqueous copper concentration (experimental points)
 - ^b C_{org} = Organic copper concentration (experimental points)
 - ^c C_{aq}^{c} = Smooth curve drawn through C_{aq}
 - ^d $C_{\text{org}}^{\text{d}}$ = Organic copper concentration in equilibrium with C_{aq}^{c}
 - ^e $C_{\text{org}}^{\text{e}}$ = Smooth curve drawn through $C_{\text{org}}^{\text{d}}$
 - ^f $C_{\text{org}}^{\text{f}}$ (Calc) = Values calculated from film theory

Table 32. Concentration-time values for the PDSE of copper in a batch reactor at $C_o = 1.5250$ g/L, $T = 26.0^\circ\text{C}$, and $\text{pH} = 2.00$. Polyaphrons made with 5 g/L NaDBS; $\text{PVR} = 10$.

Time (min)	C_{aq} (g/L)	C_{org} (g/L)
0	1.5250	0.0
0.5	0.0566	1.5313
1.0	0.0566	1.4741
2.0	0.0566	1.4741
3.0	0.0515	1.4741
4.0	0.0553	1.4932
5.0	0.0515	1.3280
6.0	0.0527	1.3280
7.0	0.0502	1.2009
8.0	0.0515	1.2200
9.0	0.0496	1.3280
10.0	0.0515	1.4995
15.0	0.527	1.4106
20.0	0.0502	1.3852
25.0	0.0489	1.4551
30.0	0.0502	1.4741
40.0	0.0489	1.4297
50.0	0.0515	1.4741
60.0	0.0502	1.3852
70.0	0.0789	1.3852
80.0	0.0496	1.4297
90.0	0.0789	1.4551

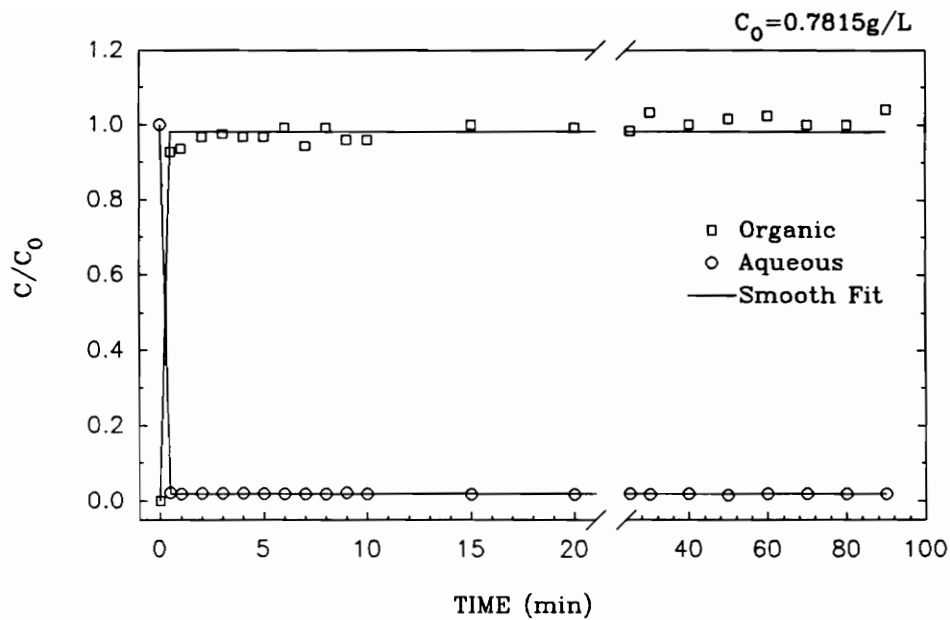


FIGURE (A)

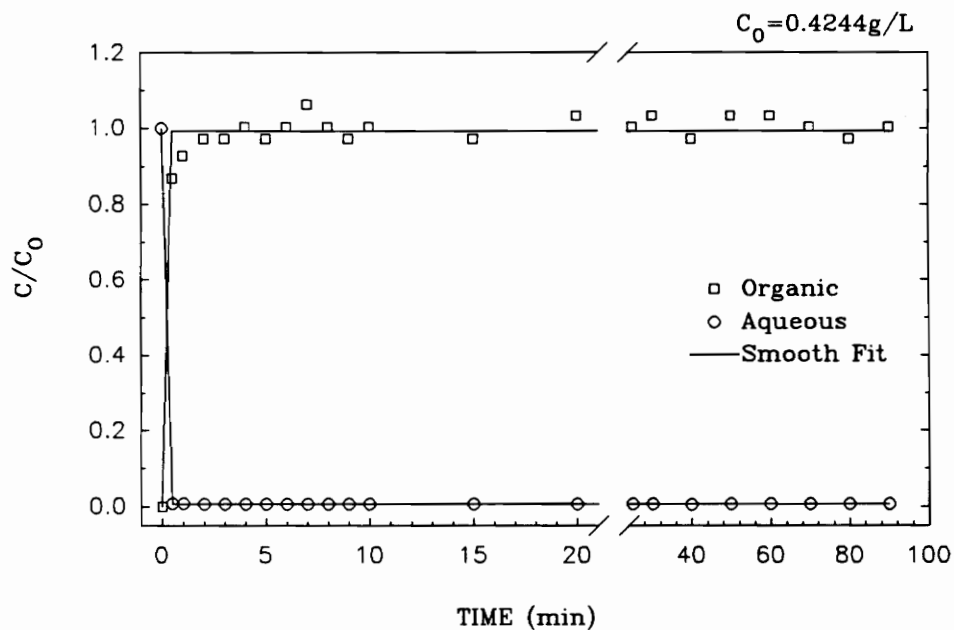


FIGURE (B)

Figure 64. Experimental values of the concentration versus time curves for the predispersed solvent extraction of copper in a batch reactor at $T=26.0^\circ\text{C}$ and $\text{pH}=2.0$.: Polyaphrons made with 5 g/L NaDBS; PVR = 10. Data found in Table 33 and Table 34.

Table 33. Concentration-time values for the PDSE of copper in a batch reactor at $C_o=0.7815$ g/L, $T=26.0^\circ\text{C}$, and $\text{pH}=2.03$. Polyaphrons made with 5 g/L NaDBS; PVR=10.

Time (min)	C_{aq} (g/L)	C_{org} (g/L)
0	0.7815	0.0
0.5	0.0172	0.7244
1.0	0.0152	0.7307
2.0	0.0159	0.7561
3.0	0.0159	0.7325
4.0	0.0159	0.7561
5.0	0.0146	0.7561
6.0	0.0146	0.7752
7.0	0.0146	0.7371
8.0	0.0146	0.7752
9.0	0.0172	0.7498
10.0	0.0146	0.7498
15.0	0.0133	0.7815
20.0	0.0140	0.7752
25.0	0.0146	0.7688
30.0	0.0140	0.8070
40.0	0.0146	0.7815
50.0	0.0127	0.7943
60.0	0.0146	0.8006
70.0	0.0146	0.7815
80.0	0.0146	0.7815
90.0	0.0146	0.8133

Table 34. Concentration-time values for the PDSE of copper in a batch reactor at $C_o=0.4244$ g/L, $T=26.0^\circ\text{C}$, and $\text{pH}=2.02$. Polyaphrons made with 5 g/L NaDBS; $\text{PVR}=10$.

Time (min)	C_{aq} (g/L)	C_{org} (g/L)
0	0.4244	0.0
0.5	0.0034	0.3685
1.0	0.0031	0.3939
2.0	0.0029	0.4130
3.0	0.0029	0.4130
4.0	0.0028	0.4257
5.0	0.0026	0.4130
6.0	0.0027	0.4257
7.0	0.0026	0.4511
8.0	0.0026	0.4257
9.0	0.0026	0.4130
10.0	0.0025	0.4257
15.0	0.0025	0.4130
20.0	0.0025	0.4384
25.0	0.0024	0.4257
30.0	0.0025	0.4384
40.0	0.0024	0.4130
50.0	0.0024	0.4384
60.0	0.0025	0.4384
70.0	0.0025	0.4257
80.0	0.0024	0.4130
90.0	0.0030	0.4257

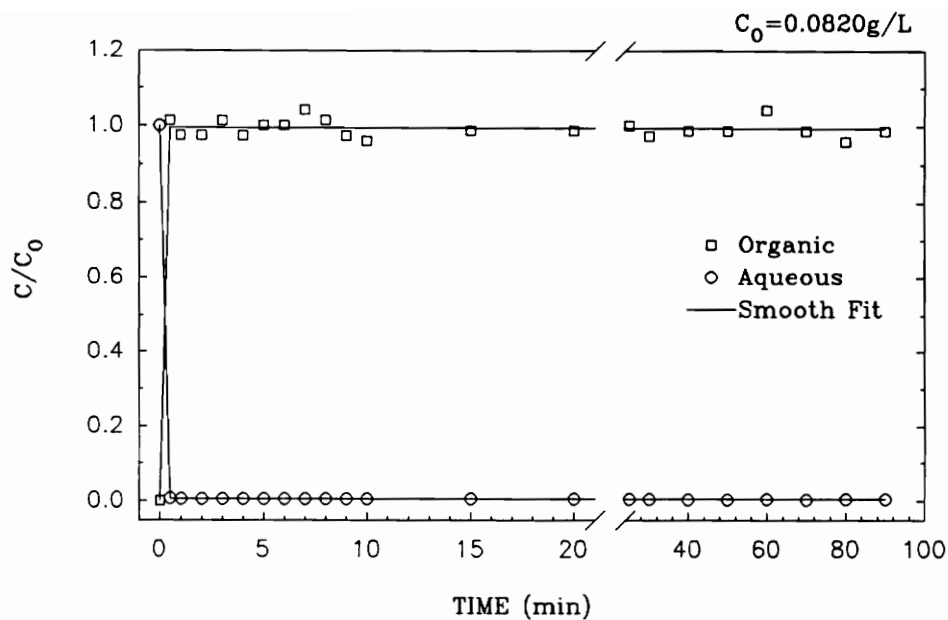


FIGURE (A)

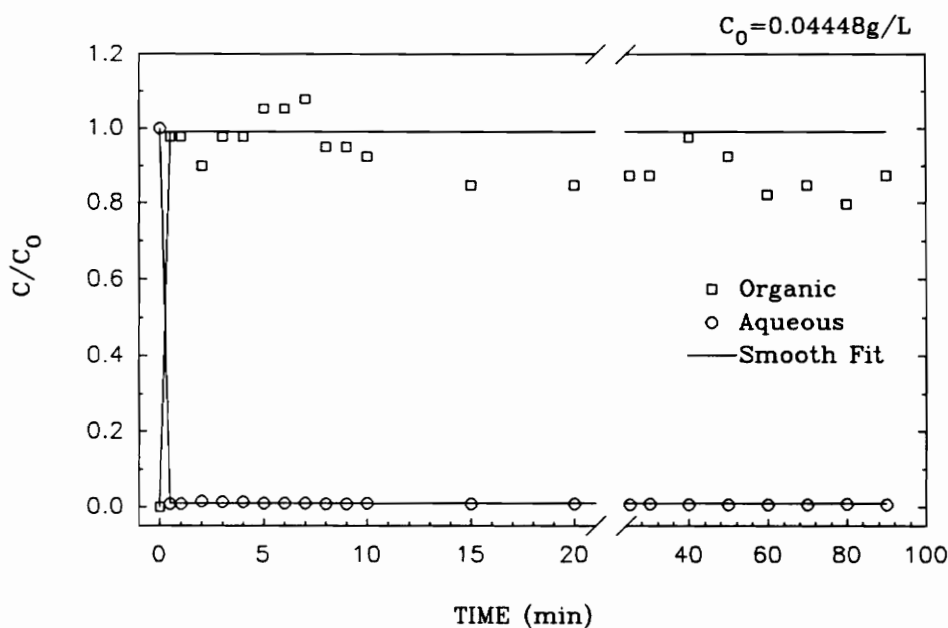


FIGURE (B)

Figure 65. Experimental values of the concentration versus time curves for the predispersed solvent extraction of copper in a batch reactor at $T=26.0^\circ\text{C}$ and $\text{pH}=2.0$.: Polyaphrons made with 5 g/L NaDBS; PVR=10. Data found in Table 35 and Table 36.

Table 35. Concentration-time values for the PDSE of copper in a batch reactor at $C_o=0.0820$ g/L, $T=26.0^\circ\text{C}$, and $\text{pH}=2.00$. Polyaphrons made with 5 g/L NaDBS; $\text{PVR}=10$.

Time (min)	C_{aq} (g/L)	C_{org} (g/L)
0	0.0820	0.0
0.5	0.00057	0.08305
1.0	0.00051	0.07987
2.0	0.00047	0.07987
3.0	0.00043	0.08305
4.0	0.00043	0.07987
5.0	0.00050	0.08216
6.0	0.00046	0.08216
7.0	0.00046	0.08552
8.0	0.00044	0.08324
9.0	0.00044	0.07987
10.0	0.00041	0.07873
15.0	0.00041	0.08101
20.0	0.00043	0.08101
25.0	0.00043	0.08216
30.0	0.00044	0.07987
40.0	0.00037	0.08101
50.0	0.00038	0.08101
60.0	0.00039	0.08552
70.0	0.00037	0.08101
80.0	0.00040	0.07873
90.0	0.00041	0.08101

Table 36. Concentration-time values for the PDSE of copper in a batch reactor at $C_o=0.04448$ g/L, $T=26.0^\circ\text{C}$, and $\text{pH}=2.02$. Polyaphrons made with 5 g/L NaDBS; $\text{PVR}=10$.

Time (min)	C_{aq} (g/L)	C_{org} (g/L)
0	0.04448	0.0
0.5	0.00038	0.04347
1.0	0.00038	0.04347
2.0	0.00064	0.04002
3.0	0.00057	0.04347
4.0	0.00057	0.04347
5.0	0.00044	0.04683
6.0	0.00038	0.04683
7.0	0.00044	0.04797
8.0	0.00032	0.04232
9.0	0.00032	0.04232
10.0	0.00038	0.04117
15.0	0.00032	0.03774
20.0	0.00038	0.03774
25.0	0.00026	0.03887
30.0	0.00034	0.03887
35.0	0.00028	0.04342
40.0	0.00029	0.04115
45.0	0.00029	0.03659
50.0	0.00030	0.03774
55.0	0.00037	0.03546
60.0	0.00030	0.03887

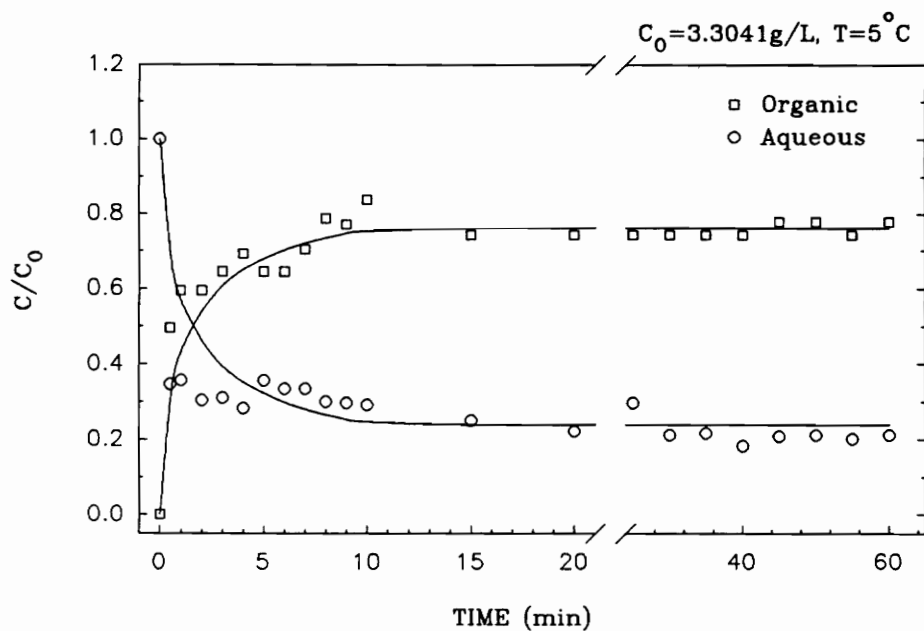


FIGURE (A)

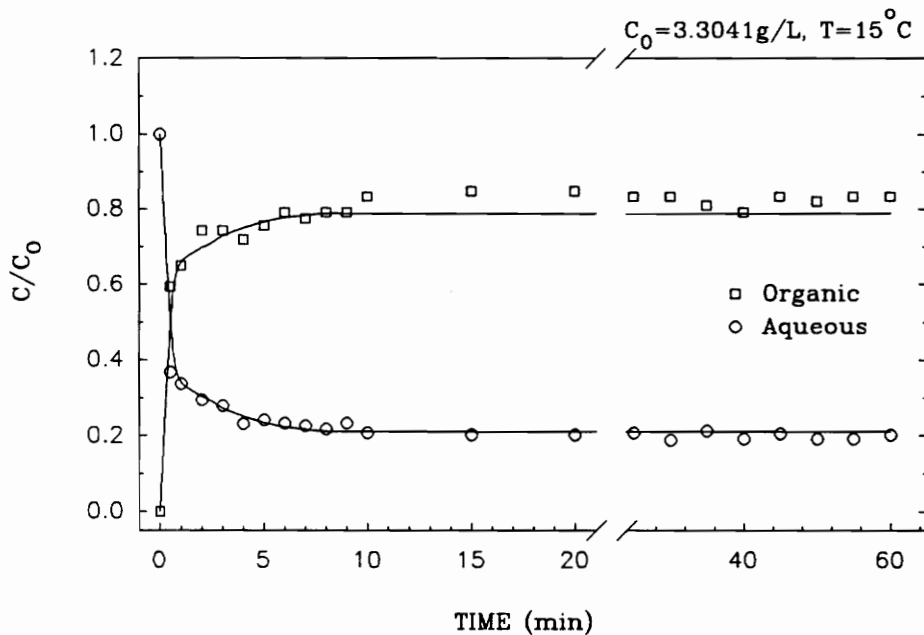


FIGURE (B)

Figure 66. Experimental values of the concentration versus time curves for the conventional solvent extraction of copper in a batch reactor at $\text{pH}=2.0$.: Polyaphrons made with 5 g/L NaDBS; $\text{PVR}=10$. Data found in Table 37 and Table 38.

Table 37. Concentration-time values for the PDSE of copper in a batch reactor at $C_o = 3.3041$ g/L, $T = 5.0^\circ\text{C}$, and $\text{pH} = 2.06$. Polyaphrons made with 5 g/L NaDBS; $\text{PVR} = 10$.

Time (min)	C_{aq} (g/L)	C_{org} (g/L)
0	3.3041	0.0
0.5	1.1437	1.6330
1.0	1.1755	1.9634
2.0	1.0039	1.9634
3.0	1.0230	2.125
4.0	0.9340	2.2874
5.0	1.1755	2.125
6.0	1.1056	2.125
7.0	1.1056	2.3259
8.0	0.9912	2.5991
9.0	0.9785	2.5483
10.0	0.9658	2.7643
15.0	0.8260	2.4567
20.0	0.7307	2.4567
25.0	0.9785	2.4567
30.0	0.6989	2.4567
35.0	0.7180	2.4567
40.0	0.6036	2.4567
45.0	0.6862	2.5755
50.0	0.6989	2.5755
55.0	0.6672	2.4567
60.0	0.6989	2.5755

Table 38. Concentration-time values for the PDSE of copper in a batch reactor at $C_o=3.3041$ g/L, $T=15.0^\circ\text{C}$, and $\text{pH}=2.03$. Polyaphrons made with 5 g/L NaDBS; PVR=10.

Time (min)	C_{aq} (g/L)	C_{org} (g/L)
0	3.3041	0.0
0.5	1.2136	1.9634
1.0	1.1120	2.1477
2.0	0.9722	2.4526
3.0	0.9213	2.4526
4.0	0.7625	2.3750
5.0	0.8006	2.49557
6.0	0.7688	2.6164
7.0	0.7498	2.5593
8.0	0.7180	2.6164
9.0	0.7688	2.6164
10.0	0.6862	2.7435
15.0	0.6672	2.8007
20.0	0.6672	2.8007
25.0	0.6862	2.7435
30.0	0.6227	2.7435
35.0	0.7053	2.680
40.0	0.6354	2.6164
45.0	0.6799	2.7435
50.0	0.6354	2.7118
55.0	0.6354	2.7435
60.0	0.6672	2.7435

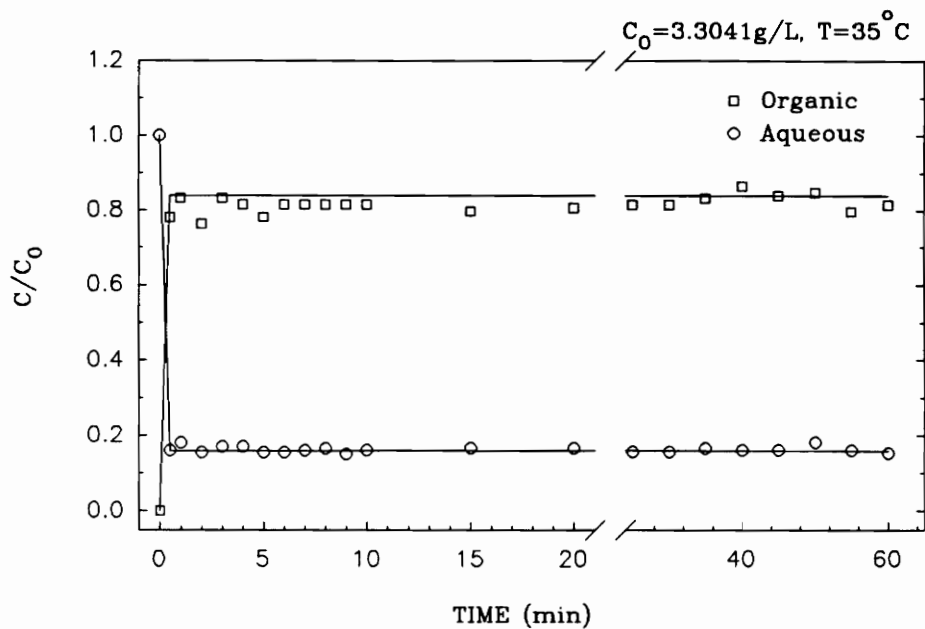


FIGURE (A)

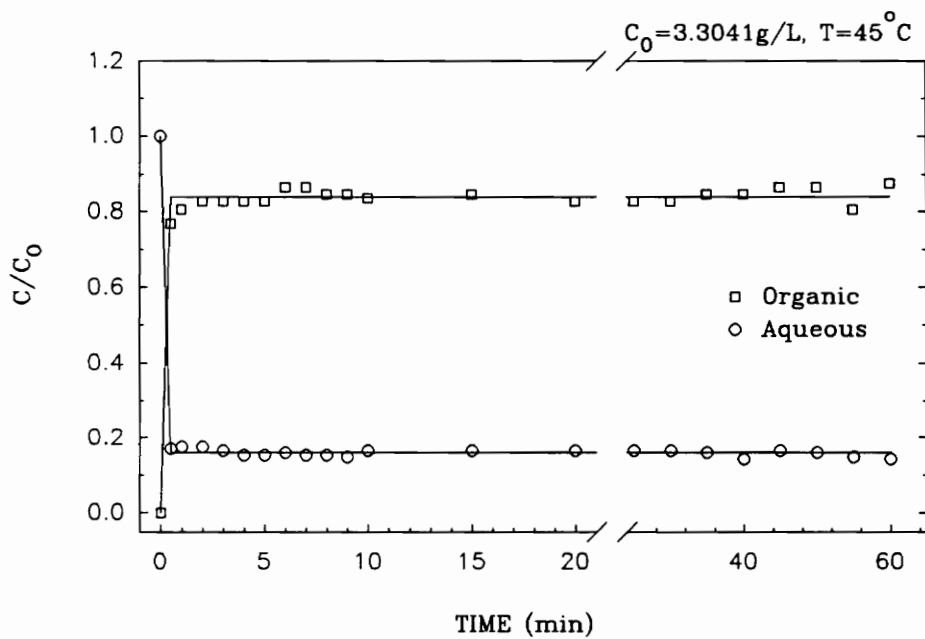


FIGURE (B)

Figure 67. Experimental values of the concentration versus time curves for the conventional solvent extraction of copper in a batch reactor at pH=2.0.: Polyaphrons made with 5 g/L NaDBS; PVR=10. Data found in Table 39 and Table 40.

Table 39. Concentration-time values for the PDSE of copper in a batch reactor at $C_o = 3.30410$ g/L, $T = 35.0^\circ\text{C}$, and $\text{pH} = 2.05$. Polyaphrons made with 5 g/L NaDBS; $\text{PVR} = 10$.

Time (min)	C_{aq} (g/L)	C_{org} (g/L)
0	3.3041	0.0
0.5	0.5306	2.5797
1.0	0.5979	2.7469
2.0	0.5134	2.5245
3.0	0.5642	2.7469
4.0	0.5342	2.6897
5.0	0.5134	2.5817
6.0	0.5134	2.6897
7.0	0.5306	2.6897
8.0	0.5471	2.6897
9.0	0.7962	2.6897
10.0	0.5306	2.6897
15.0	0.5471	2.6325
20.0	0.5471	2.6645
25.0	0.5134	2.6897
30.0	0.5134	2.6897
35.0	0.5471	2.7469
40.0	0.5306	2.8549
45.0	0.5306	2.7723
50.0	0.5979	2.7977
55.0	0.5306	2.6325
60.0	0.5051	2.6897

Table 40. Concentration-time values for the PDSE of copper in a batch reactor at $C_o=3.3041$ g/L, $T=45.0^\circ\text{C}$, and $\text{pH}=2.00$. Polyaphrons made with 5 g/L NaDBS; $\text{PVR}=10$.

Time (min)	C_{aq} (g/L)	C_{org} (g/L)
0	3.3041	0.0
0.5	0.5623	2.5352
1.0	0.5808	2.6623
2.0	0.5808	2.7322
3.0	0.5445	2.7322
4.0	0.5083	2.7322
5.0	0.5083	2.7322
6.0	0.5261	2.8593
7.0	0.5083	2.8593
8.0	0.5083	2.7958
9.0	0.4899	2.7958
10.0	0.5445	2.7610
15.0	0.5445	2.7958
20.0	0.5445	2.7322
25.0	0.5445	2.7322
30.0	0.5445	2.7322
35.0	0.5261	2.7958
40.0	0.4721	2.7958
45.0	0.5445	2.8593
50.0	0.5261	2.8593
55.0	0.4899	2.6623
60.0	0.4721	2.8911

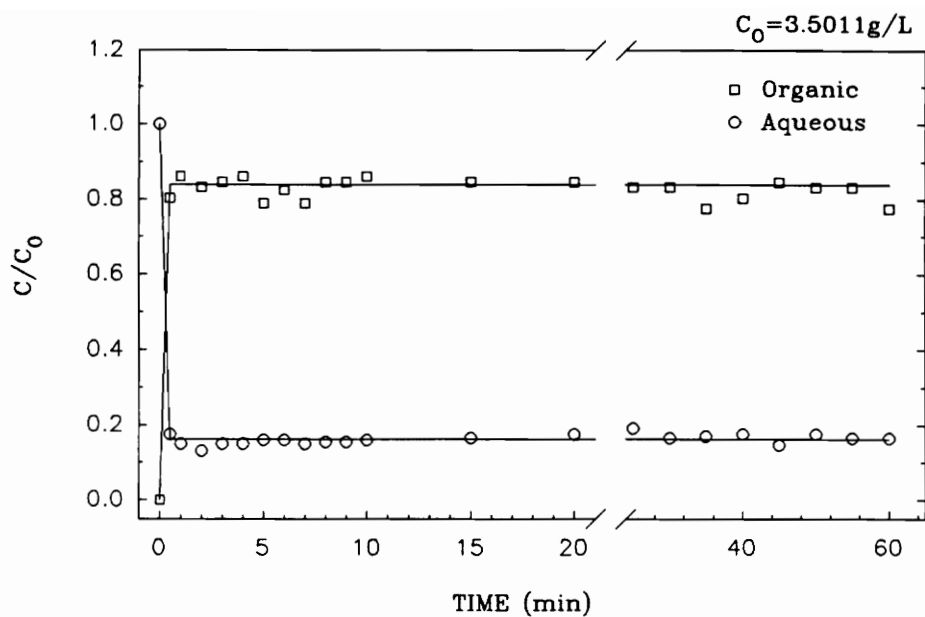


FIGURE (A)

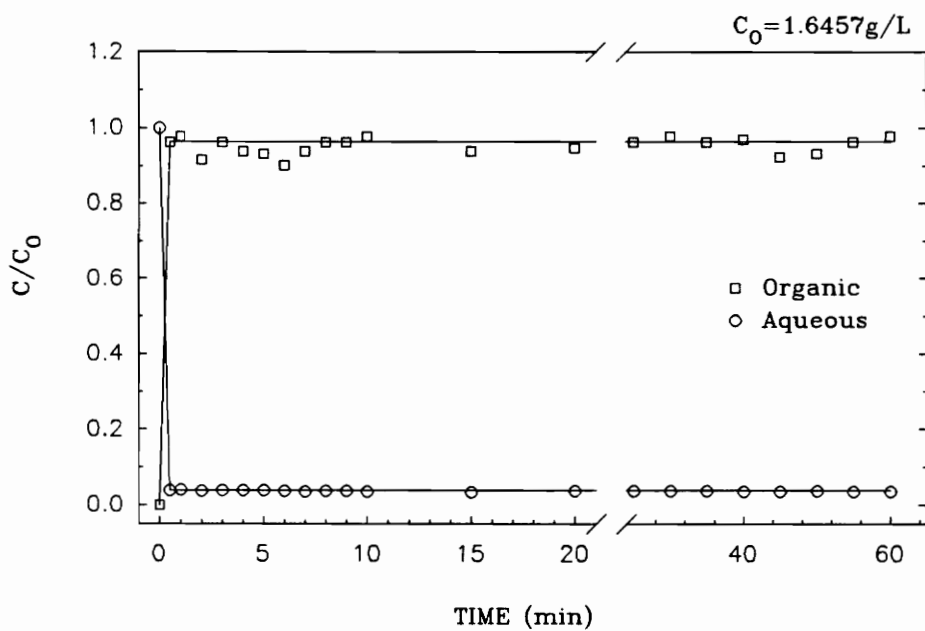


FIGURE (B)

Figure 68. Experimental values of the concentration versus time curves for the conventional solvent extraction of copper in a batch reactor at $\text{pH} = 2.0$.: Polyaphrons made with 5 g/L NaDBS; $\text{PVR} = 5$. Data found in Table 41 and Table 42.

Table 41. Concentration-time values for the PDSE of copper in a batch reactor at $C_o=3.5011$ g/L, $T=26.0^\circ\text{C}$, and $\text{pH}=2.05$. Polyaphrons made with 5 g/L NaDBS; PVR=5.

Time (min)	C_{aq} (g/L)	C_{org} (g/L)
0	3.5011	0.0
0.5	0.6163	2.8085
1.0	0.5287	3.0118
2.0	0.4581	2.9101
3.0	0.5287	2.9610
4.0	0.5287	3.0118
5.0	0.5636	2.7640
6.0	0.5636	2.8847
7.0	0.5287	2.7640
8.0	0.5458	2.9610
9.0	0.5458	2.9610
10.0	0.5636	3.0118
15.0	0.5808	2.9610
20.0	0.6163	2.9610
25.0	0.6691	2.9100
30.0	0.5808	2.9100
35.0	0.5985	2.7132
40.0	0.6163	2.8085
45.0	0.5109	2.9610
50.0	0.6163	2.9100
55.0	0.5808	2.9100
60.0	0.5808	2.7132

Table 42. Concentration-time values for the PDSE of copper in a batch reactor at $C_o=1.6457$ g/L, $T=26.0^\circ\text{C}$, and $\text{pH}=2.05$. Polyaphrons made with 5 g/L NaDBS; PVR=5.

Time (min)	C_{aq} (g/L)	C_{org} (g/L)
0	1.6457	0.0
0.5	0.0630	1.5821
1.0	0.0678	1.6076
2.0	0.0615	1.5059
3.0	0.0630	1.5821
4.0	0.0637	1.5440
5.0	0.0630	1.5313
6.0	0.0615	1.4805
7.0	0.0571	1.5440
8.0	0.0615	1.5821
9.0	0.0607	1.5821
10.0	0.0593	1.6076
15.0	0.0549	1.5440
20.0	0.0615	1.5567
25.0	0.0615	1.5821
30.0	0.0615	1.6076
35.0	0.0607	1.5821
40.0	0.0571	1.5949
45.0	0.0593	1.5186
50.0	0.0622	1.5313
55.0	0.0593	1.5821
60.0	0.0571	1.6076

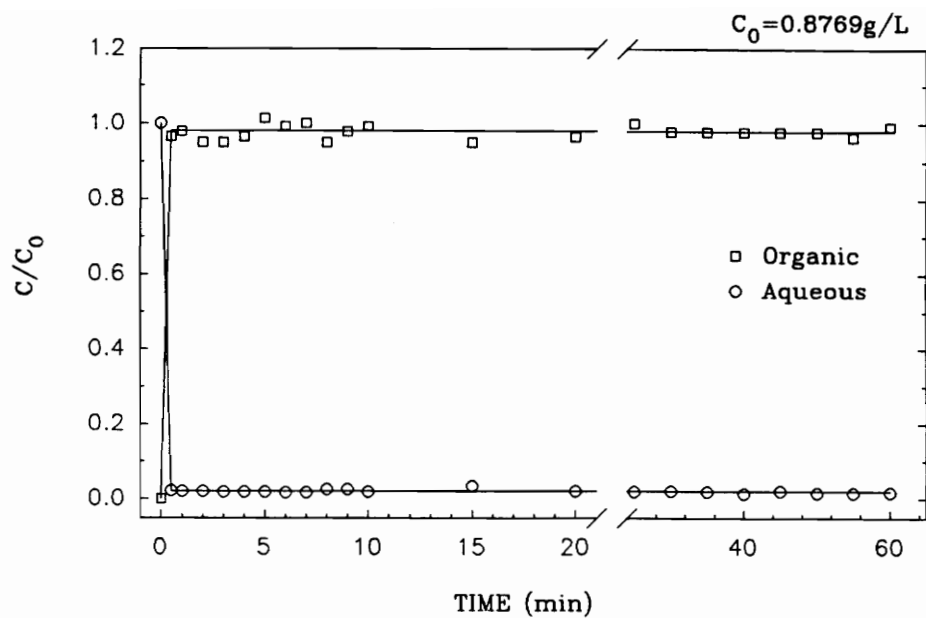


FIGURE (A)

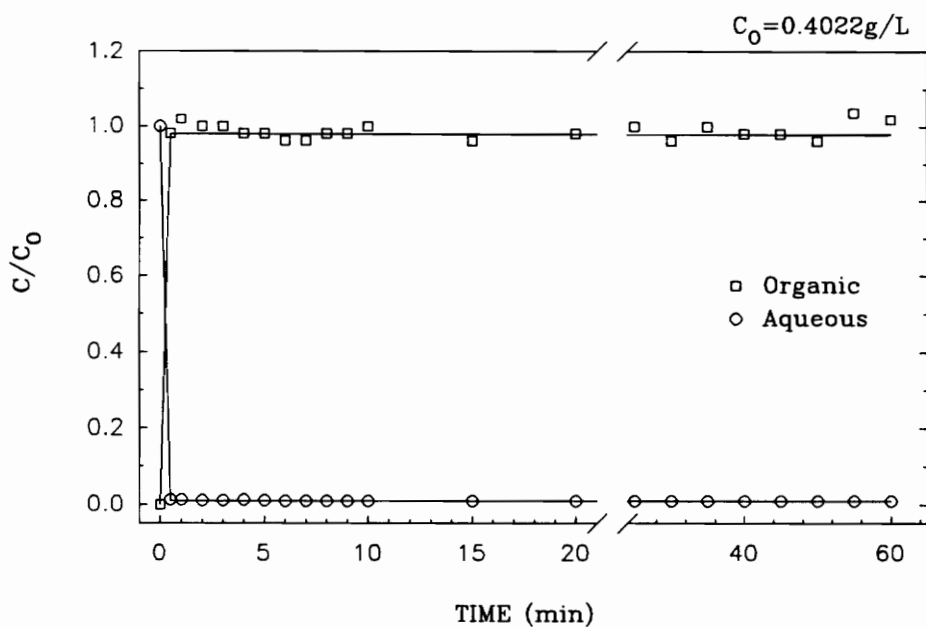


FIGURE (B)

Figure 69. Experimental values of the concentration versus time curves for the conventional solvent extraction of copper in a batch reactor at pH=2.0.: Polyaphrons made with 5 g/L NaDBS; PVR=5. Data found in Table 43 and Table 44.

Table 43. Concentration-time values for the PDSE of copper in a batch reactor at $C_o=0.8769$ g/L, $T=26.0^\circ\text{C}$, and $\text{pH}=2.03$. Polyaphrons made with 5 g/L NaDBS; $\text{PVR}=5$.

Time (min)	C_{aq} (g/L)	C_{org} (g/L)
0	0.8769	0.0
0.5	0.0167	0.8451
1.0	0.0184	0.8578
2.0	0.0178	0.8324
3.0	0.0165	0.8324
4.0	0.0165	0.8451
5.0	0.0172	0.8896
6.0	0.0146	0.8705
7.0	0.0152	0.8769
8.0	0.0229	0.8323
9.0	0.0222	0.8578
10.0	0.0159	0.8705
15.0	0.0305	0.8324
20.0	0.0184	0.8451
25.0	0.0172	0.8769
30.0	0.0187	0.8578
35.0	0.0165	0.8578
40.0	0.0127	0.8578
45.0	0.0178	0.8578
50.0	0.0140	0.8578
55.0	0.0140	0.8451
60.0	0.0152	0.8705

Table 44. Concentration-time values for the PDSE of copper in a batch reactor at $C_o=0.4022$ g/L, $T=26.0^\circ\text{C}$, and $\text{pH}=2.05$. Polyaphrons made with 5 g/L NaDBS; PVR=5.

Time (min)	C_{aq} (g/L)	C_{org} (g/L)
0	0.4022	0.0
0.5	0.0057	0.3946
1.0	0.0051	0.4098
2.0	0.0046	0.4022
3.0	0.0045	0.4022
4.0	0.0053	0.3946
5.0	0.0044	0.3946
6.0	0.0043	0.3870
7.0	0.0041	0.3870
8.0	0.0039	0.3946
9.0	0.0037	0.3946
10.0	0.0041	0.4022
15.0	0.0041	0.3870
20.0	0.0043	0.3946
25.0	0.0037	0.4022
30.0	0.0041	0.3870
35.0	0.0043	0.4022
40.0	0.0043	0.3946
45.0	0.0038	0.3946
50.0	0.0037	0.3870
55.0	0.0036	0.4168
60.0	0.0037	0.4098

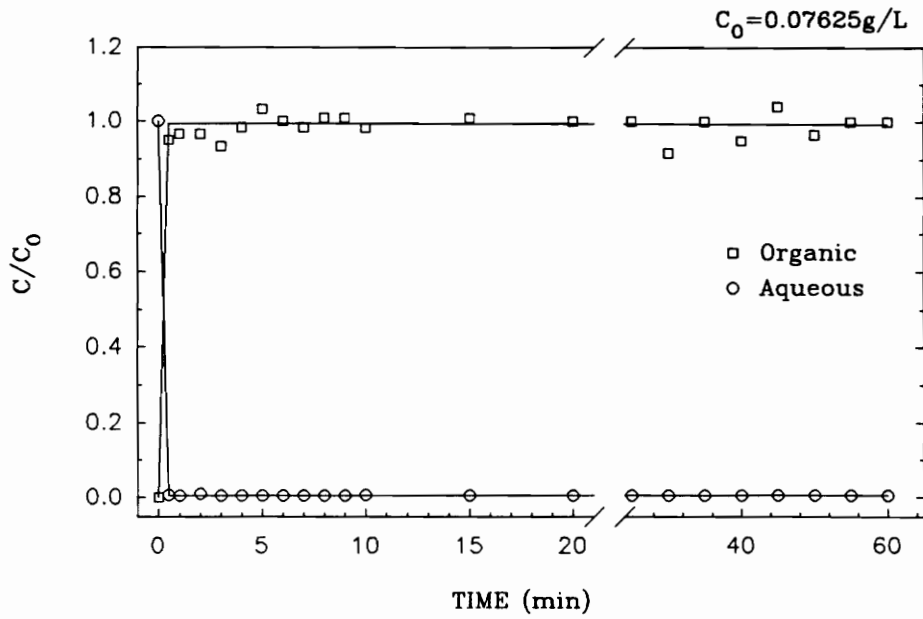


FIGURE (A)

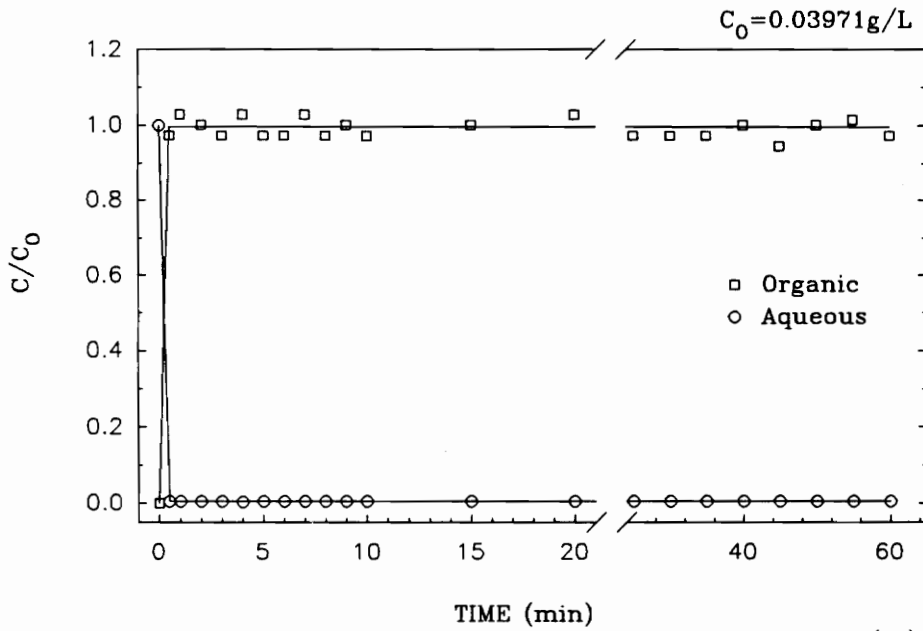


FIGURE (B)

Figure 70. Experimental values of the concentration versus time curves for the conventional solvent extraction of copper in a batch reactor at $\text{pH} = 2.0$.: Polyaphrons made with 5 g/L NaDBS; $\text{PVR} = 5$. Data found in Table 45 and Table 46.

Table 45. Concentration-time values for the PDSE of copper in a batch reactor at $C_o=0.07625$ g/L, $T=26.0^\circ\text{C}$, and $\text{pH}=2.04$. Polyaphrons made with 5 g/L NaDBS; PVR=5.

Time (min)	C_{aq} (g/L)	C_{org} (g/L)
0	0.07625	0.0
0.5	0.00052	0.07244
1.0	0.00044	0.07371
2.0	0.00078	0.07371
3.0	0.00044	0.07116
4.0	0.00043	0.07498
5.0	0.00043	0.07879
6.0	0.00046	0.07625
7.0	0.00041	0.07498
8.0	0.00043	0.07688
9.0	0.00046	0.07688
10.0	0.00050	0.07498
15.0	0.00040	0.07688
20.0	0.00039	0.07625
25.0	0.00037	0.07625
30.0	0.00038	0.06989
35.0	0.00042	0.07625
40.0	0.00042	0.07244
45.0	0.00042	0.07943
50.0	0.00037	0.07371
55.0	0.00041	0.07625
60.0	0.00041	0.07625

Table 46. Concentration-time values for the PDSE of copper in a batch reactor at $C_o=0.03971$ g/L, $T=26.0^\circ\text{C}$, and $\text{pH}=2.00$. Polyaphrons made with 5 g/L NaDBS; $\text{PVR}=5$.

Time (min)	C_{aq} (g/L)	C_{org} (g/L)
0	0.03971	0.0
0.5	0.00018	0.03863
1.0	0.00016	0.04086
2.0	0.00016	0.03978
3.0	0.00016	0.03863
4.0	0.00016	0.04086
5.0	0.00018	0.03863
6.0	0.00016	0.03863
7.0	0.00016	0.04086
8.0	0.00018	0.03863
9.0	0.00018	0.03978
10.0	0.00018	0.03863
15.0	0.00016	0.03978
20.0	0.00019	0.04086
25.0	0.00016	0.03863
30.0	0.00021	0.03863
35.0	0.00021	0.03863
40.0	0.00021	0.03978
45.0	0.00017	0.03755
50.0	0.00021	0.03978
55.0	0.00019	0.04028
60.0	0.00019	0.03863

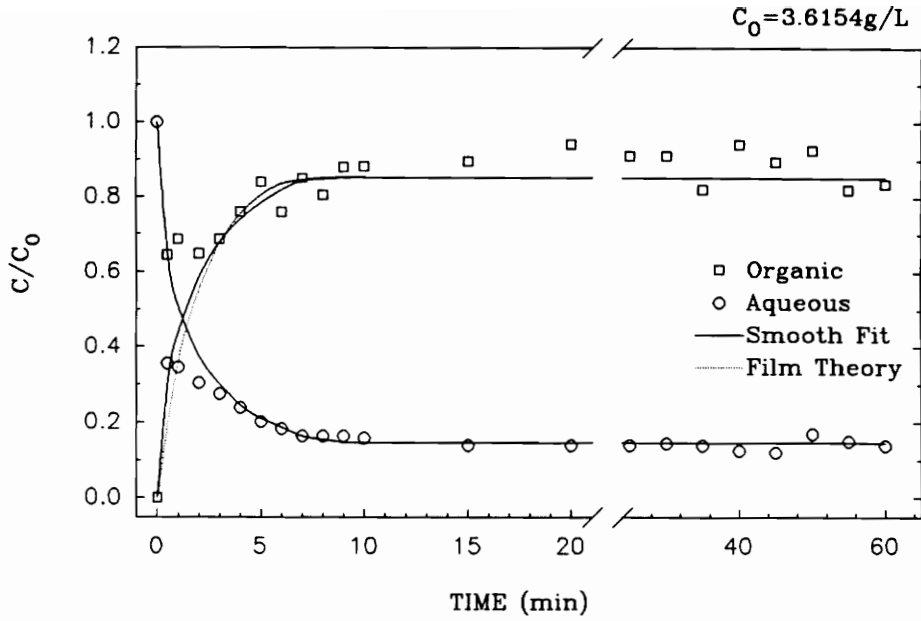


FIGURE (A)

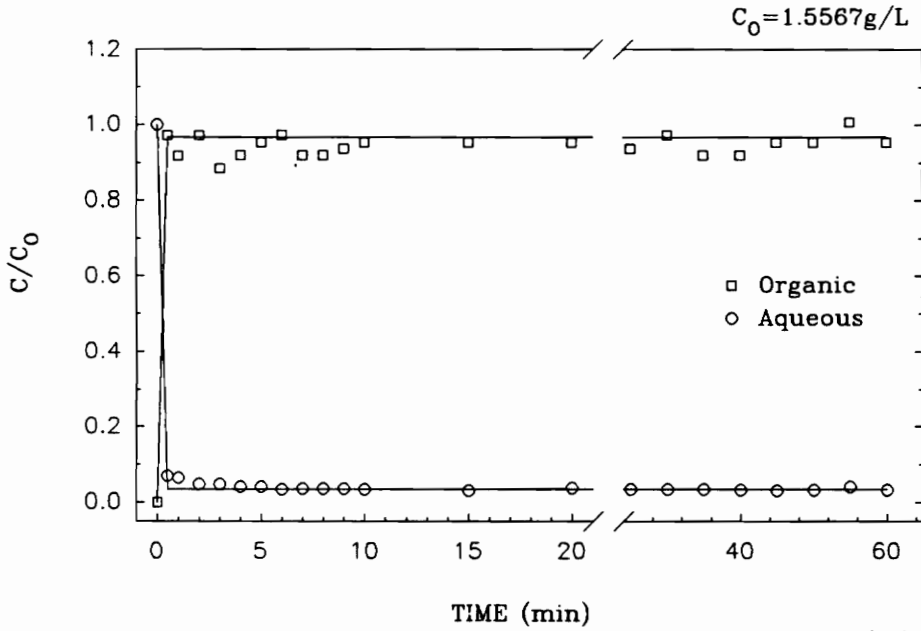


FIGURE (B)

Figure 71. Concentration versus time curves of the experimental and film theory values for the predispersed solvent extraction of copper in a batch reactor at $T = 26.0$ °C and $\text{pH} = 2.0$.: Polyaphrons made with 5 g/L NaDBS; PVR=15. Data found in Table 47 and Table 48.

Table 47. Concentration values determined experimentally and calculated from film theory for PDSE of copper in a batch reactor at $C_o=3.6154$ g/L, $T=26.0^\circ\text{C}$, and $\text{pH}=2.01$. Polyaphrons made with 5 g/L NaDBS; $\text{PVR}=15$.

Time (min)	C_{aq}^a (g/L)	C_{org}^b (g/L)	C_{aq}^c (g/L)	C_{org}^{*d} (g/L)	C_{org}^e (g/L)	C_{org}^f (Calc)
0	3.6154	0.0	3.6154	3.0835	0.0	0.0
0.5	1.2835	2.33	2.350	3.0835	1.175	-
1.0	1.2454	2.4781	1.835	3.0835	1.580	1.29
2.0	1.0992	2.3396	1.350	3.0835	2.110	1.98
3.0	0.9976	2.4781	1.085	3.0835	2.450	2.44
4.0	0.8578	2.7513	0.885	3.0835	2.675	2.73
5.0	0.7244	3.0396	0.760	3.0835	2.835	2.91
6.0	0.6608	2.7513	0.675	3.0835	2.960	3.02
7.0	0.5909	3.0753	0.591	3.0835	3.050	3.06
8.0	0.5909	2.7165	0.560	3.0835	3.070	3.08
9.0	0.5909	3.1897	0.532	3.0835	3.084	3.08
10.0	0.5744	3.1897	0.532	3.0835	3.084	3.08
15.0	0.5064	3.2405	0.532	3.0835	3.084	3.08
20.0	0.5064	3.4057	0.532	3.0835	3.084	3.08
25.0	0.5064	3.2977	0.532	3.0835	3.084	3.08
30.0	0.5236	3.2977	0.532	3.0835	3.084	3.08
35.0	0.5064	2.9673	0.532	3.0835	3.084	3.08
40.0	0.4562	3.4057	0.532	3.0835	3.084	3.08
45.0	0.4391	3.2405	0.532	3.0835	3.084	3.08
50.0	0.6081	3.3486	0.532	3.0835	3.084	3.08
55.0	0.5401	2.9673	0.532	3.0835	3.084	3.08
60.0	0.5064	3.0245	0.532	3.0835	3.084	3.08

- NOTES: ^a C_{aq} = Aqueous copper concentration (experimental points)
^b C_{org} = Organic copper concentration (experimental points)
^c C_{aq}^c = Smooth curve drawn through C_{aq}
^d C_{org}^{*d} = Organic copper concentration in equilibrium with C_{aq}
^e C_{org}^e = Smooth curve drawn through C_{org}
^f C_{org}^f (Calc) = Values calculated from film theory

Table 48. Concentration-time values for the PDSE of copper in a batch reactor at $C_o=1.5567$ g/L, $T=26.0^\circ\text{C}$, and $\text{pH}=2.01$. Polyaphrons made with 5 g/L NaDBS; $\text{PVR}=15$.

Time (min)	C_{aq} (g/L)	C_{org} (g/L)
0	1.5567	0.0
0.5	0.1080	1.5123
1.0	0.0998	1.4297
2.0	0.0737	1.5123
3.0	0.0737	1.3770
4.0	0.0623	1.4297
5.0	0.0623	1.4868
6.0	0.0527	1.5123
7.0	0.0546	1.4297
8.0	0.0546	1.4297
9.0	0.0546	1.4551
10.0	0.0527	1.4868
15.0	0.0483	1.4868
20.0	0.0578	1.4868
25.0	0.0527	1.4551
30.0	0.0515	1.5123
35.0	0.0515	1.4297
40.0	0.0496	1.4297
45.0	0.0483	1.4868
50.0	0.0496	1.4868
55.0	0.0623	1.5694
60.0	0.0496	1.4868

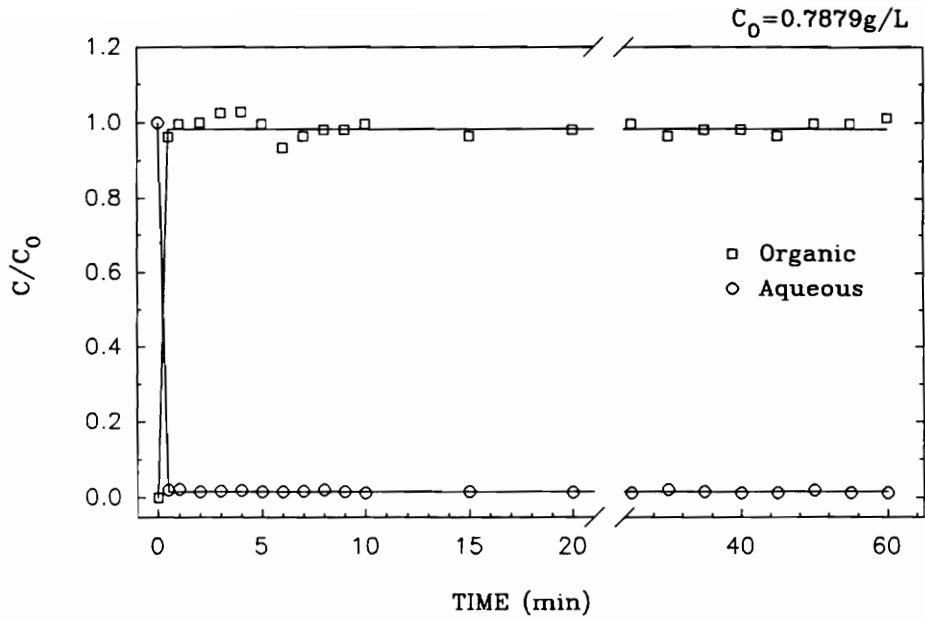


FIGURE (A)

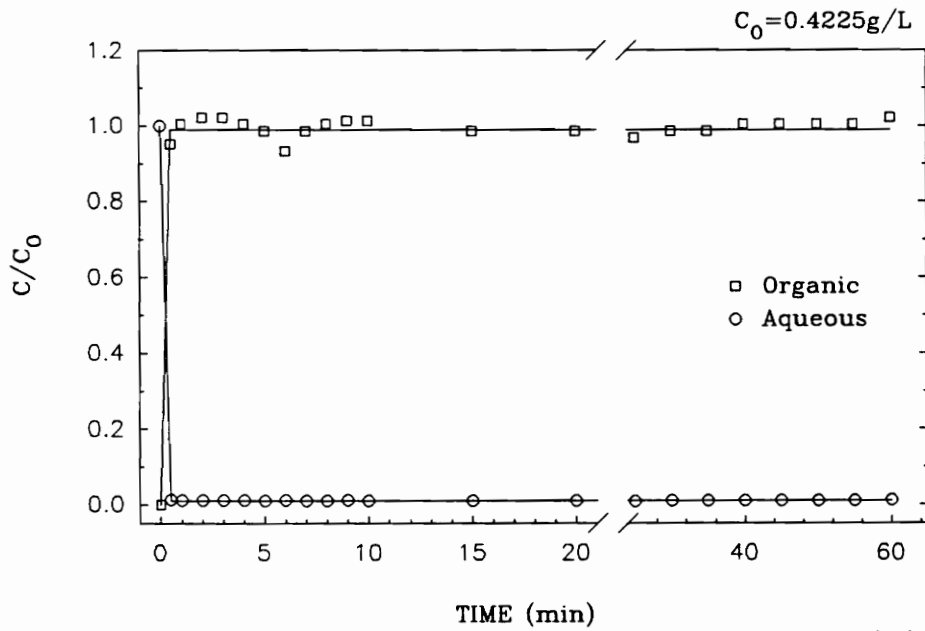


FIGURE (B)

Figure 72. Experimental values of the concentration versus time curves for the conventional solvent extraction of copper in a batch reactor at pH=2.0.: Polyaphrons made with 5 g/L NaDBS; PVR=15. Data found in Table 49 and Table 50.

Table 49. Concentration-time values for the PDSE of copper in a batch reactor at $C_o=0.7879$ g/L, $T=26.0^\circ\text{C}$, and $\text{pH}=2.00$. Polyaphrons made with 5 g/L NaDBS; PVR=15.

Time (min)	C_{aq} (g/L)	C_{org} (g/L)
0	0.7879	0.0
0.5	0.0169	0.7589
1.0	0.0176	0.7579
2.0	0.0124	0.7879
3.0	0.0133	0.8087
4.0	0.0143	0.8133
5.0	0.0129	0.7879
6.0	0.0119	0.7362
7.0	0.0133	0.7625
8.0	0.0162	0.7752
9.0	0.0119	0.7752
10.0	0.0100	0.7879
15.0	0.0119	0.7625
20.0	0.0114	0.7752
25.0	0.0103	0.7879
30.0	0.0157	0.7625
35.0	0.0124	0.7752
40.0	0.0100	0.7752
45.0	0.0100	0.7625
50.0	0.0147	0.7879
55.0	0.0096	0.7879
60.0	0.0100	0.8006

Table 50. Concentration-time values for the PDSE of copper in a batch reactor at $C_o=0.4225$ g/L, $T=26.0^\circ\text{C}$, and $\text{pH}=2.05$. Polyaphrons made with 5 g/L NaDBS; PVR=15.

Time (min)	C_{aq} (g/L)	C_{org} (g/L)
0	0.4225	0.0
0.5	0.0058	0.4022
1.0	0.0047	0.4244
2.0	0.0047	0.4321
3.0	0.0049	0.4321
4.0	0.0047	0.4244
5.0	0.0044	0.4168
6.0	0.0051	0.3946
7.0	0.0043	0.4168
8.0	0.0046	0.4244
9.0	0.0047	0.4283
10.0	0.0038	0.4283
15.0	0.0040	0.4283
20.0	0.0040	0.4168
25.0	0.0036	0.4168
30.0	0.0038	0.4092
35.0	0.0044	0.4168
40.0	0.0043	0.4168
45.0	0.0044	0.4244
50.0	0.0040	0.4244
55.0	0.0044	0.4244
60.0	0.0051	0.4321

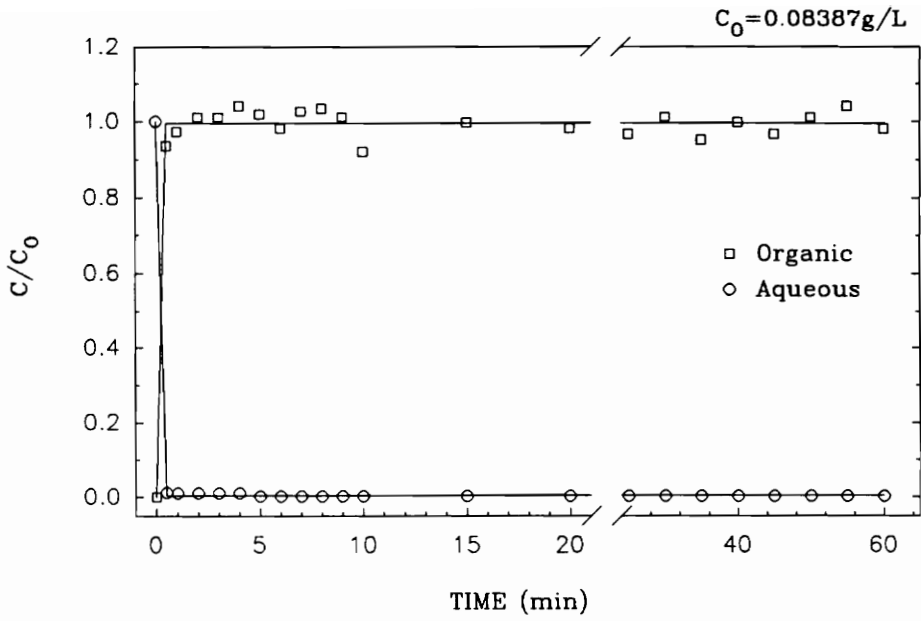


FIGURE (A)

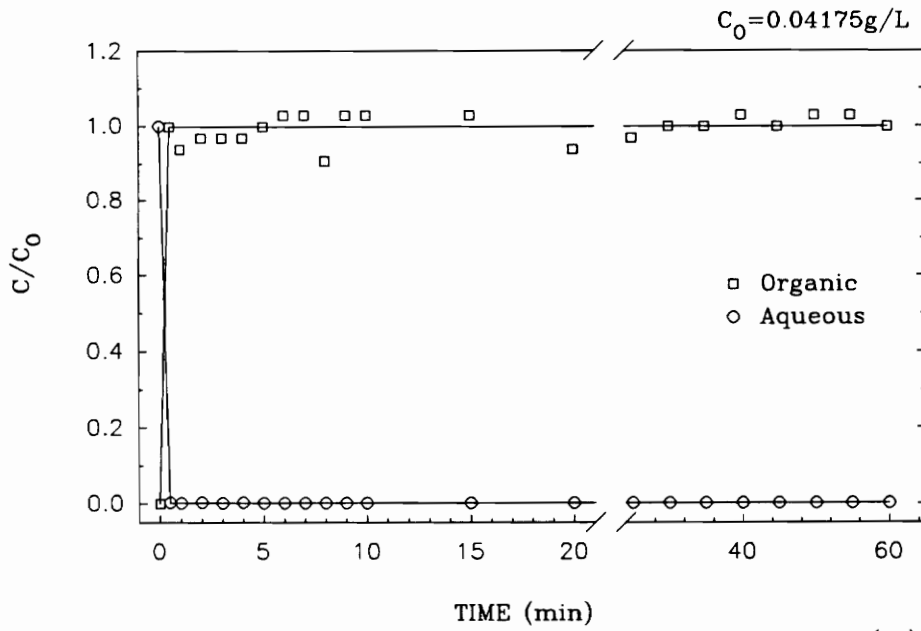


FIGURE (B)

Figure 73. Experimental values of the concentration versus time curves for the conventional solvent extraction of copper in a batch reactor at pH=2.0.: Polyaphrons made with 5 g/L NaDBS; PVR=15. Data found in Table 51 and Table 52.

Table 51. Concentration-time values for the PDSE of copper in a batch reactor at $C_o=0.08387$ g/L, $T=26.0^\circ\text{C}$, and $\text{pH}=2.06$. Polyaphrons made with 5 g/L NaDBS; $\text{PVR}=15$.

Time (min)	C_{aq} (g/L)	C_{org} (g/L)
0	0.08387	0.0
0.5	0.00107	0.07815
1.0	0.00090	0.08197
2.0	0.00084	0.08514
3.0	0.00086	0.08514
4.0	0.00081	0.08769
5.0	0.00018	0.08578
6.0	0.00018	0.08260
7.0	0.00018	0.08641
8.0	0.00021	0.08705
9.0	0.00018	0.08514
10.0	0.00017	0.07688
15.0	0.00017	0.08387
20.0	0.00018	0.08260
25.0	0.00017	0.08070
30.0	0.00017	0.08514
35.0	0.00017	0.07943
40.0	0.00017	0.08387
45.0	0.00017	0.08070
50.0	0.00017	0.08514
55.0	0.00017	0.08769
60.0	0.00020	0.08260

Table 52. Concentration-time values for the PDSE of copper in a batch reactor at $C_o=0.04175$ g/L, $T=26.0^\circ\text{C}$, and $\text{pH}=2.02$. Polyaphrons made with 5 g/L NaDBS; PVR=15.

Time (min)	C_{aq} (g/L)	C_{org} (g/L)
0	0.04175	0.0
0.5	0.00012	0.04168
1.0	0.00010	0.03908
2.0	0.00010	0.04041
3.0	0.00010	0.04041
4.0	0.00010	0.04041
5.0	0.00009	0.04168
6.0	0.00009	0.04295
7.0	0.00008	0.04295
8.0	0.00009	0.03781
9.0	0.00009	0.04295
10.0	0.00008	0.04295
15.0	0.00008	0.04295
20.0	0.00009	0.03908
25.0	0.00009	0.04041
30.0	0.00008	0.04168
35.0	0.00008	0.04168
40.0	0.00008	0.04295
45.0	0.00008	0.04168
50.0	0.00008	0.04295
55.0	0.00008	0.04295
60.0	0.00009	0.04295

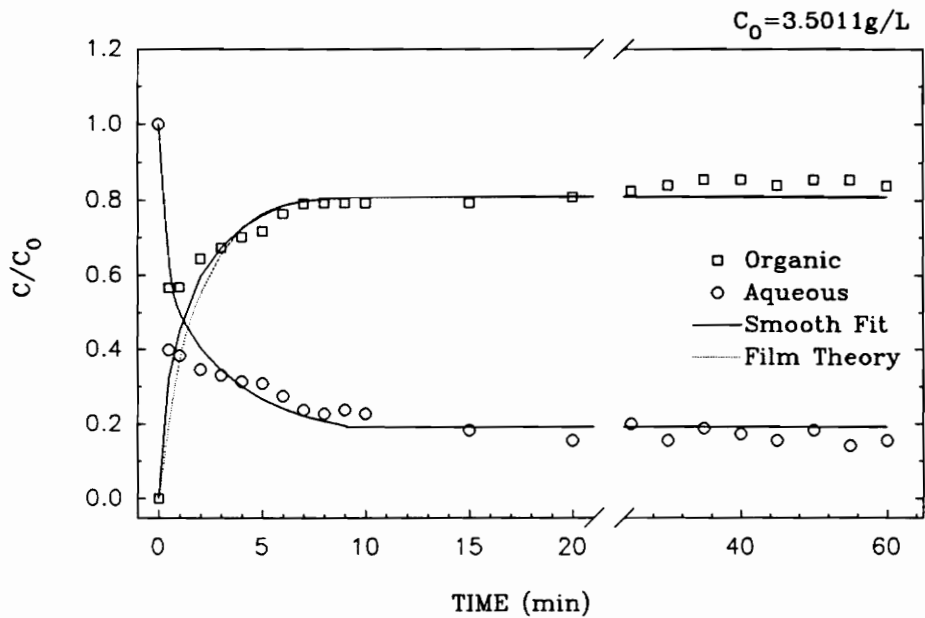


FIGURE (A)

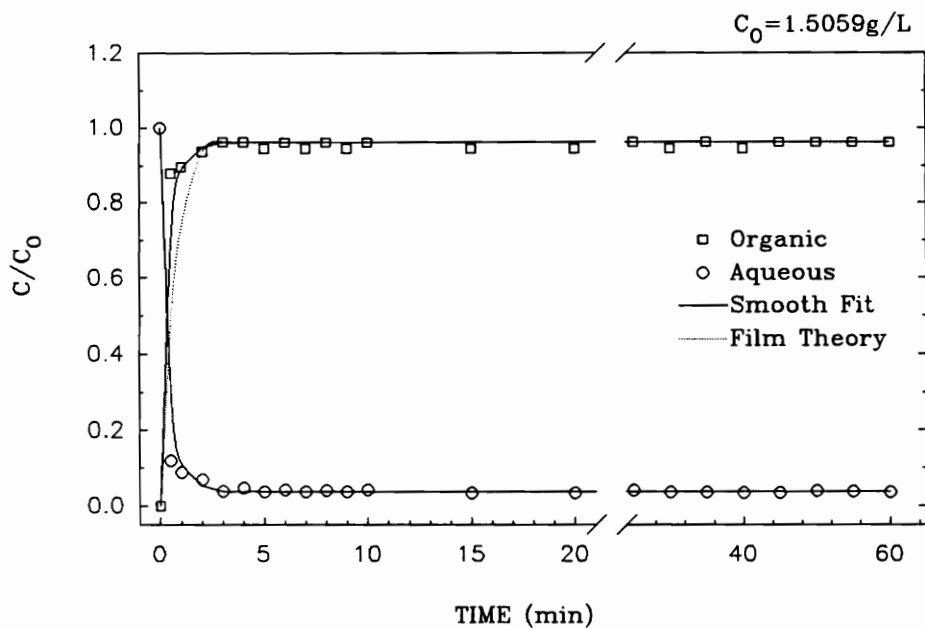


FIGURE (B)

Figure 74. Concentration versus time curves of the experimental and film theory values for the predispersed solvent extraction of copper in a batch reactor at $T = 26.0^\circ \text{C}$ and $\text{pH} = 2.0$: Polyaphrons made with 5ml/L Arquad 12/50; PVR=10. Data found in Table 53 and Table 54.

Table 53. Concentration values determined experimentally and calculated from film theory for PDSE of copper in a batch reactor at $C_o=3.5011$ g/L, $T=26.0^\circ\text{C}$, and $\text{pH}=2.06$. Polyaphrons made with 5 ml/L Arquad 12/50; PVR = 10.

Time (min)	C_{aq}^a (g/L)	C_{org}^b (g/L)	C_{aq}^c (g/L)	C_{org}^{*d} (g/L)	C_{org}^e (g/L)	C_{org}^f (calc)
0	3.5011	0.0	3.5011	2.833	0.0	0.0
0.5	1.3915	1.9791	-	-	-	-
1.0	1.3470	1.9888	1.75	2.833	1.575	1.28
2.0	1.2136	2.2573	1.42	2.833	2.085	1.91
3.0	1.1564	2.3573	1.21	2.833	2.357	2.29
4.0	1.0992	2.4590	1.055	2.833	2.54	2.53
5.0	1.0802	2.5162	0.935	2.833	2.66	2.67
6.0	0.9658	2.6767	0.845	2.833	2.75	2.75
7.0	0.8324	2.7670	0.775	2.833	2.790	2.79
8.0	0.7943	2.7767	0.725	2.833	2.810	2.81
9.0	0.8324	2.7767	0.680	2.833	2.825	2.82
10.0	0.7943	2.7767	0.6681	2.833	2.8330	2.83
15.0	0.6418	2.7767	0.6681	2.833	2.8330	2.83
20.0	0.5464	2.8275	0.6681	2.833	2.8330	2.83
25.0	0.6989	2.8847	0.6681	2.833	2.8330	2.83
30.0	0.5464	2.9355	0.6681	2.833	2.8330	2.83
35.0	0.6608	2.9864	0.6681	2.833	2.8330	2.83
40.0	0.6036	2.9864	0.6681	2.833	2.8330	2.83
45.0	0.5464	2.9355	0.6681	2.833	2.8330	2.83
50.0	0.6418	2.9864	0.6681	2.833	2.8330	2.83
55.0	0.4956	2.9864	0.6681	2.833	2.8330	2.83
60.0	0.5464	2.9355	0.6681	2.833	2.8330	2.83

- NOTES:**
- ^a C_{aq} = Aqueous copper concentration (experimental points)
 - ^b C_{org} = Organic copper concentration (experimental points)
 - ^c C_{aq}^c = Smooth curve drawn through C_{aq}
 - ^d C_{org}^{*d} = Organic copper concentration in equilibrium with C_{aq}^c
 - ^e C_{org}^e = Smooth curve drawn through C_{org}^b
 - ^f C_{org}^f (Calc) = Values calculated from film theory

Table 54. Concentration values determined experimentally and calculated from film theory for PDSE of copper in a batch reactor at $C_o = 1.5059$ g/L, $T = 26.0^\circ\text{C}$, and $\text{pH} = 2.06$. Polyaphrons made with 5 ml/L Arquad 12/50; PVR = 10.

Time (min)	C_{aq}^a (g/L)	C_{org}^b (g/L)	C_{aqs}^c (g/L)	C_{orgs}^d (g/L)	C_{orgps}^e (g/L)	C_{org}^f (calc)
0	1.5059	0.0	1.5059	2.833	0.0	0.0
0.5	0.1785	1.3233	0.3	2.5	1.05	0.733
1.0	0.1341	1.3496	0.14	2.0	1.265	1.11
2.0	0.1048	1.4100	0.065	1.56	1.425	1.41
3.0	0.0585	1.4487	0.0565	1.4494	1.4494	1.45
4.0	0.0624	1.4487	0.0565	1.4494	1.4494	1.45
5.0	0.0566	1.4233	0.0565	1.4494	1.4494	1.45
6.0	0.0635	1.4487	0.0565	1.4494	1.4494	1.45
7.0	0.0566	1.4233	0.0565	1.4494	1.4494	1.45
8.0	0.0616	1.4487	0.0565	1.4494	1.4494	1.45
9.0	0.0566	1.4233	0.0565	1.4494	1.4494	1.45
10.0	0.0635	1.4487	0.0565	1.4494	1.4494	1.45
15.0	0.0502	1.4233	0.0565	1.4494	1.4494	1.45
20.0	0.0515	1.4233	0.0565	1.4494	1.4494	1.45
25.0	0.0604	1.4487	0.0565	1.4494	1.4494	1.45
30.0	0.0534	1.4233	0.0565	1.4494	1.4494	1.45
35.0	0.0534	1.4487	0.0565	1.4494	1.4494	1.45
40.0	0.0502	1.4233	0.0565	1.4494	1.4494	1.45
45.0	0.0502	1.4487	0.0565	1.4494	1.4494	1.45
50.0	0.0585	1.4487	0.0565	1.4494	1.4494	1.45
55.0	0.0566	1.4487	0.0565	1.4494	1.4494	1.45
60.0	0.0534	1.4487	0.0565	1.4494	1.4494	1.45

- NOTES:
- ^a C_{aq} = Aqueous copper concentration (experimental points)
 - ^b C_{org} = Organic copper concentration (experimental points)
 - ^c C_{aqs} = Smooth curve drawn through C_{aq}
 - ^d C_{orgs}^* = Organic copper concentration in equilibrium with C_{aqs}
 - ^e C_{orgps} = Smooth curve drawn through C_{orgs}^*
 - ^f C_{org}^f (Calc) = values calculated from film theory

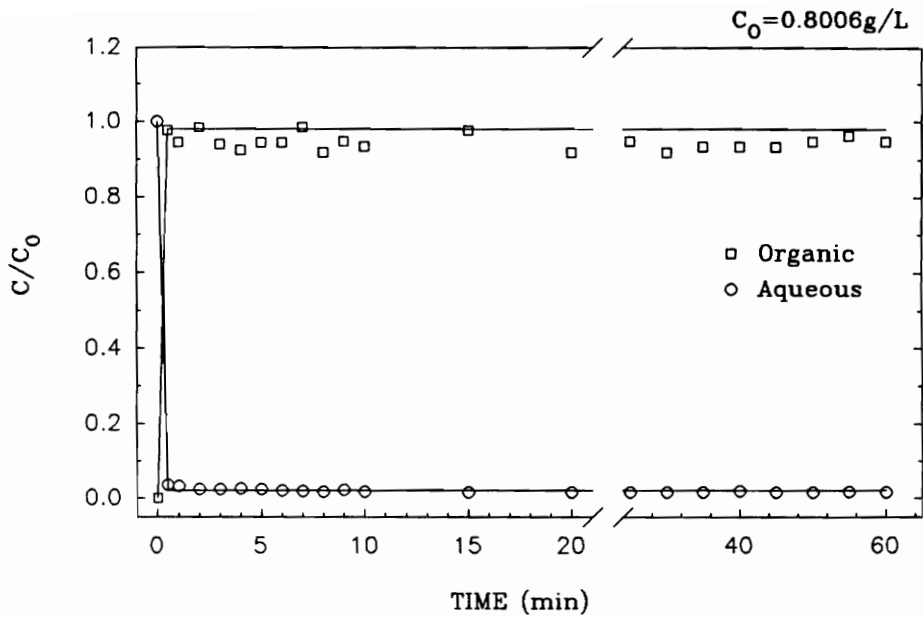


FIGURE (A)

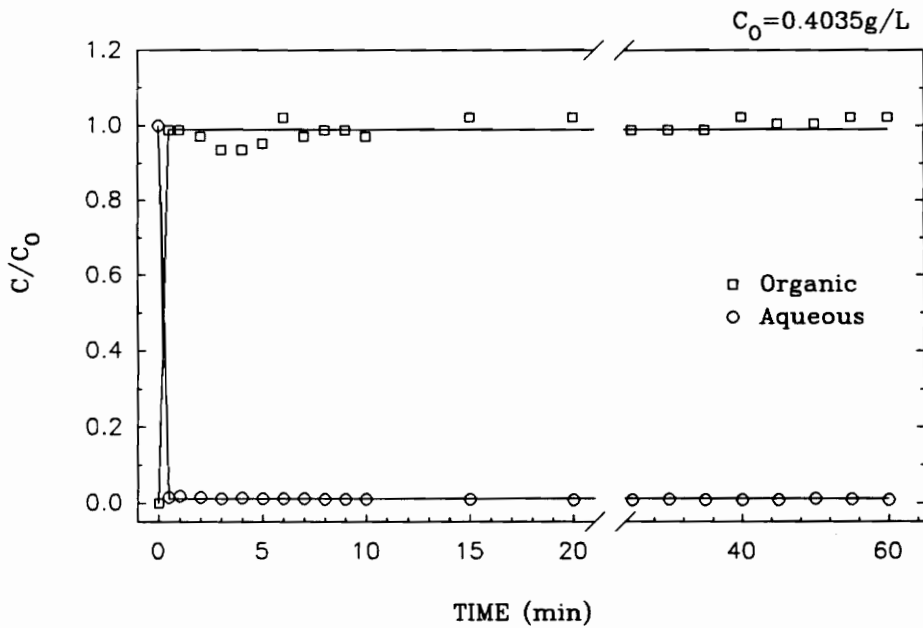


FIGURE (B)

Figure 75. Experimental values of the concentration versus time curves for the conventional solvent extraction of copper in a batch reactor at $\text{pH}=2.0$: Polyaphrons made with 5ml/L Arquad 12/50; $\text{PVR}=10$. Data found in Table 55 and Table 56.

Table 55. Concentration-time values for the PDSE of copper in a batch reactor at $C_o=0.8006$ g/L, $T=26.0^\circ\text{C}$, and $\text{pH}=2.05$. Polyaphrons made with 5 ml/L Arquad 12/50; $\text{PVR}=10$.

Time (min)	C_{aq} (g/L)	C_{org} (g/L)
0	0.8006	0.0
0.5	0.0293	0.7815
1.0	0.0268	0.7561
2.0	0.0195	0.7879
3.0	0.0198	0.7514
4.0	0.0211	0.7387
5.0	0.0191	0.7561
6.0	0.0170	0.7561
7.0	0.0147	0.7879
8.0	0.0139	0.7371
9.0	0.0179	0.7561
10.0	0.0143	0.7498
15.0	0.0130	0.7815
20.0	0.0130	0.7371
25.0	0.0130	0.7561
30.0	0.0125	0.7371
35.0	0.0130	0.7498
40.0	0.0152	0.7498
45.0	0.0120	0.7498
50.0	0.0125	0.7561
55.0	0.0139	0.7688
60.0	0.0130	0.7561

Table 56. Concentration-time values for the PDSE of copper in a batch reactor at $C_o=0.4035$ g/L, $T=26.0^\circ\text{C}$, and $\text{pH}=2.00$. Polyaphrons made with 5 ml/L Arquad 12/50; PVR = 10.

Time (min)	C_{aq} (g/L)	C_{org} (g/L)
0	0.4035	0.0
0.5	0.0060	0.3984
1.0	0.0072	0.3984
2.0	0.0060	0.3914
3.0	0.0050	0.3774
4.0	0.0052	0.3774
5.0	0.0044	0.3844
6.0	0.0050	0.4124
7.0	0.0047	0.3914
8.0	0.0043	0.3987
9.0	0.0041	0.3984
10.0	0.0037	0.3914
15.0	0.0039	0.4124
20.0	0.0034	0.4124
25.0	0.0034	0.3984
30.0	0.0037	0.3984
35.0	0.0034	0.3984
40.0	0.0030	0.4124
45.0	0.0036	0.4054
50.0	0.0045	0.4054
55.0	0.0037	0.4124
60.0	0.0032	0.4124

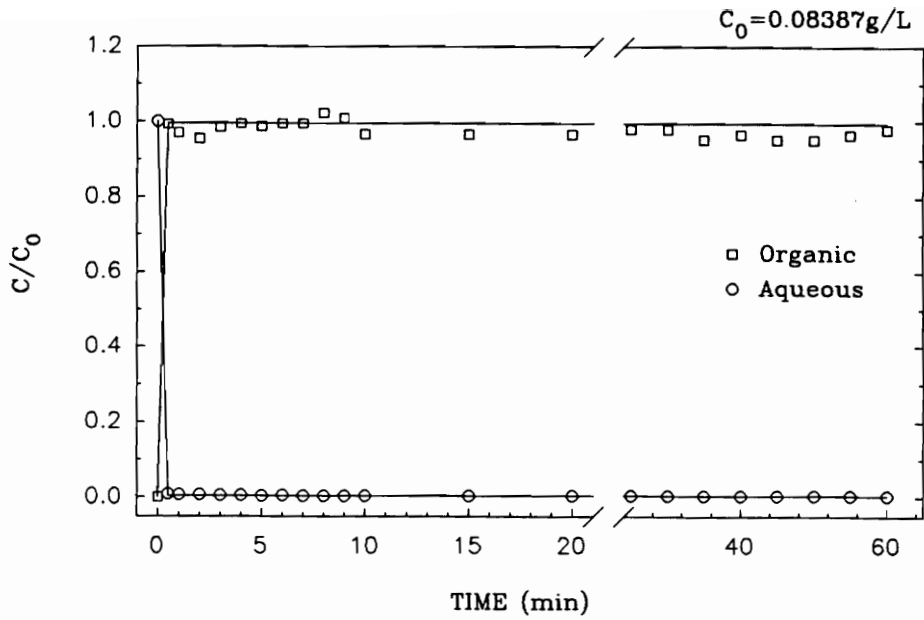


FIGURE (A)

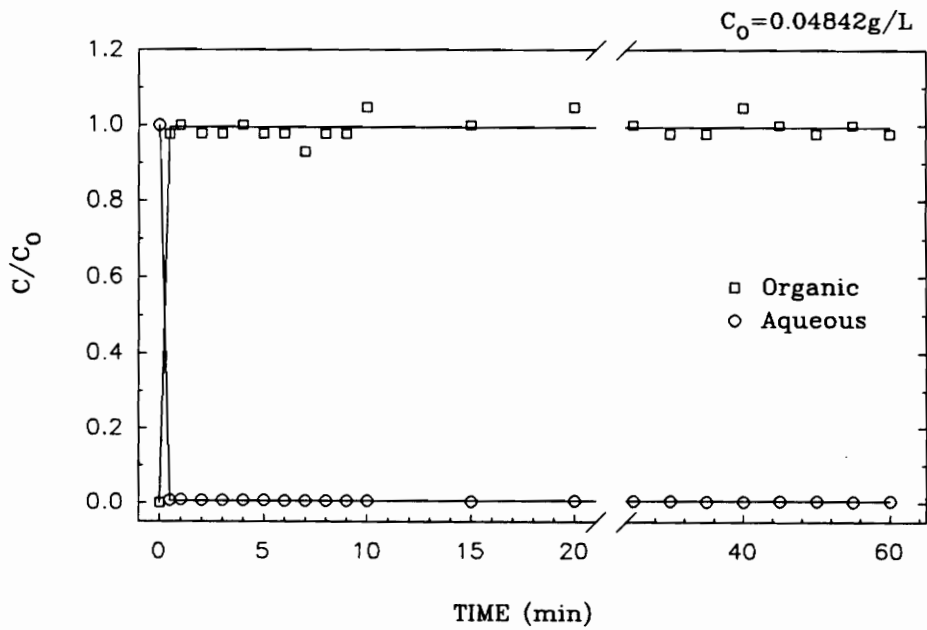


FIGURE (B)

Figure 76. Experimental values of the concentration versus time curves for the conventional solvent extraction of copper in a batch reactor at pH=2.0.: Polyaphrons made with 5 ml/L Arquad 12/50; PVR=10. Data found in Table 57 and Table 58.

Table 57. Concentration-time values for the PDSE of copper in a batch reactor at $C_o = 0.08387$ g/L, $T = 26.0^\circ\text{C}$, and $\text{pH} = 2.02$. Polyaphrons were made with 5 ml/L Arquad 12/50; $\text{PVR} = 10$.

Time (min)	C_{aq} (g/L)	C_{org} (g/L)
0	0.08387	0.0
0.5	0.00078	0.08324
1.0	0.00060	0.08133
2.0	0.00055	0.08006
3.0	0.00046	0.08260
4.0	0.00041	0.08324
5.0	0.00034	0.08260
6.0	0.00040	0.08324
7.0	0.00034	0.08324
8.0	0.00034	0.08578
9.0	0.00033	0.08451
10.0	0.00029	0.08133
15.0	0.00032	0.08133
20.0	0.00027	0.08133
25.0	0.00029	0.08197
30.0	0.00029	0.08197
35.0	0.00029	0.08006
40.0	0.00029	0.08133
45.0	0.00027	0.08006
50.0	0.00032	0.08006
55.0	0.00027	0.08133
60.0	0.00027	0.08197

Table 58. Concentration-time values for the PDSE of copper in a batch reactor at $C_o=0.04842$ g/L, $T=26.0^\circ\text{C}$, and $\text{pH}=2.01$. Polyaphrons were made with 5 ml/L Arquad 12/50; PVR = 10.

Time (min)	C_{aq} (g/L)	C_{org} (g/L)
0	0.04842	0.0
0.5	0.00030	0.04727
1.0	0.00038	0.04842
2.0	0.00030	0.04727
3.0	0.00029	0.04727
4.0	0.00028	0.04842
5.0	0.00029	0.04727
6.0	0.00025	0.04727
7.0	0.00025	0.04499
8.0	0.00021	0.04727
9.0	0.00025	0.04727
10.0	0.00020	0.05077
15.0	0.00019	0.04842
20.0	0.00021	0.05077
25.0	0.00021	0.04842
30.0	0.00020	0.04727
35.0	0.00018	0.04727
40.0	0.00018	0.05077
45.0	0.00020	0.04842
50.0	0.00020	0.04727
55.0	0.00019	0.04842
60.0	0.00020	0.04727

Table 59. Equilibrium concentrations for conventional solvent extraction of copper in a batch reactor at T=26.0°C and pH=2.0. K_{eq} values were calculated from stoichiometry.

Test ID	C_o^a (M)	pH	C_{aq}^{*b} (M)	C_{org}^{*c} (M)	$[H^+]_{eq}^d$ (M)	LIX ^{*c} (M)	K_{eq}^f
1	0.0507	2.01	1.00E-2	0.0507	0.1140	0.00247	10320.7
2	0.0226	2.04	1.07E-3	0.0226	0.0552	0.0587	18.7
3	0.0113	2.08	1.95E-4	0.0113	0.0326	0.0813	9.3
4	0.0058	2.01	9.92E-5	0.0058	0.0215	0.0923	3.2
5	0.0011	2.03	7.87E-6	0.0011	0.0123	0.1016	2.1
6	0.0006	2.04	2.99E-6	0.0006	0.0112	0.1027	2.4

- NOTES:**
- ^a C_o = Initial copper feed concentration
 - ^b C_{aq}^* = Ultimate copper equilibrium concentration in the aqueous phase
 - ^c C_{org}^* = Ultimate copper equilibrium concentration in the organic phase
 - ^d $[H^+]_{eq}$ = Concentration of hydrogen ions at equilibrium
 - ^e LIX^{*} = Concentration of uncomplexed LIX at equilibrium
 - ^f K_{eq} = Equilibrium constant

Table 60. Equilibrium concentrations for the PDSE of copper in a batch reactor at T = 26.0°C and pH = 2.0, (Series 4). Polyaphrons made with 5 g/L NaDBS; PVR = 15. K_{eq} values were calculated from stoichiometry.

Test ID	C_o^a (M)	pH	C_{aq}^{*b} (M)	C_{org}^{*c} (M)	$[H^+]_{eq}^d$ (M)	LIX [*] (M)	K_{eq}^f
1	0.0569	2.01	8.37E-3	3.0835	0.1070	5.222E-4	243612.8
2	0.0245	2.01	8.18E-4	1.5047	0.0574	5.021E-2	37.8
3	0.0124	2.00	2.00E-4	0.7752	0.0344	7.317E-2	13.5
4	0.0066	2.05	7.08E-5	0.4180	0.0232	8.441E-2	7.0
5	0.0013	2.06	5.51E-6	0.08352	0.0126	9.494E-2	4.2
6	0.0007	2.02	1.42E-6	0.04166	0.0113	9.626E-2	6.4

- NOTES:**
- ^a C_o = Initial copper feed concentration
 - ^b C_{aq}^* = Ultimate copper equilibrium concentration in the aqueous phase
 - ^c C_{org}^* = Ultimate copper equilibrium concentration in the organic phase
 - ^d $[H^+]_{eq}$ = Concentration of hydrogen ions at equilibrium
 - ^e LIX^{*} = Concentration of uncomplexed LIX at equilibrium
 - ^f K_{eq} = Equilibrium constant

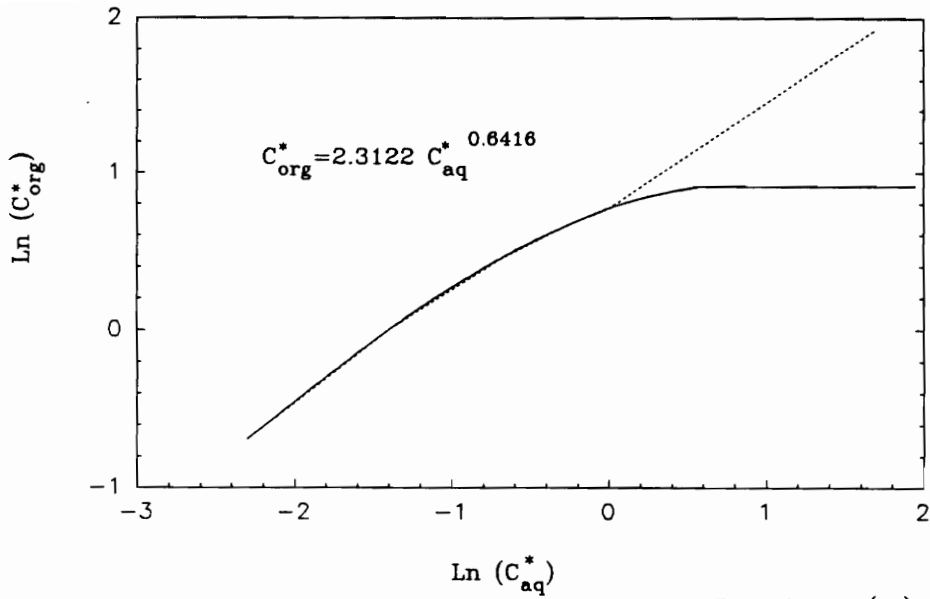


FIGURE (A)

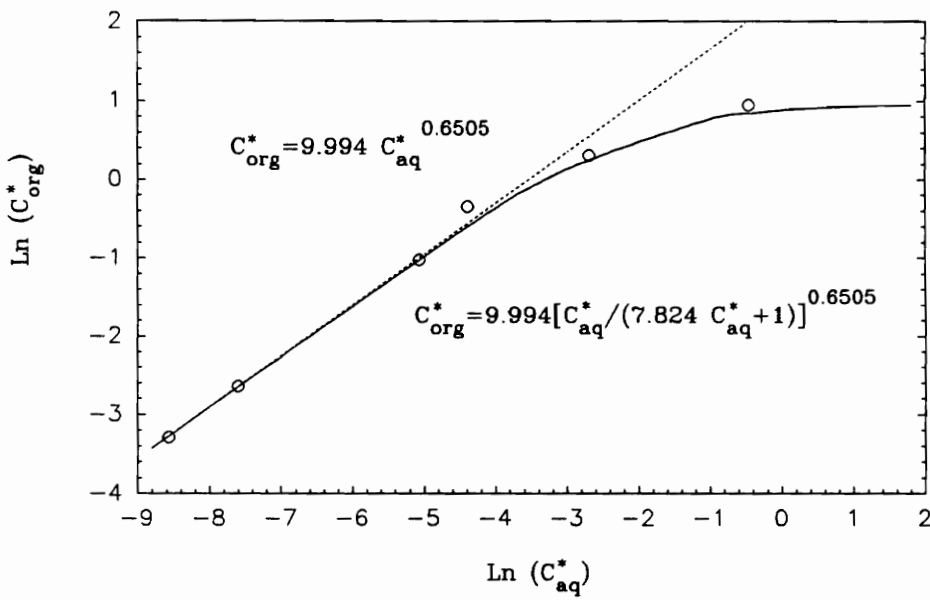


FIGURE (B)

Figure 77. Equilibrium isotherm for the conventional solvent extraction of copper in a batch reactor at $T=26.0^\circ\text{C}$ and $\text{pH}=2.0$.: (A) Data from the literature, (B) data found in Table 62.

Table 61. Equilibrium parameters for the conventional solvent extraction of copper in a batch reactor at T=26.0°C. (Series 1)

Test ID	C_o^a (g/L)	C_{aq}^b (g/L)	C_{org}^c (g/L)	k (min⁻¹)	t^d (min)
1	3.8124	1.6520	2.4500	0.190	60
2	1.5250	0.4640	1.0610	0.0125	60
3	0.7625	0.0635	0.6990	0.0715	15
4	0.3177	0.0018	0.3159	0.114	8

NOTES:

- ^a C_o = Initial feed copper concentration
- ^b C_{aq} = Equilibrium concentration in the aqueous phase
- ^c C_{org} = Equilibrium concentration in the organic phase
- ^d t^d = Time required for the reaction to reach equilibrium

Table 62. Equilibrium parameters for the conventional solvent extraction of copper in a batch reactor at T=26.0°C and pH=2.0. (Series 2)

Test ID	C_o^a (g/L)	C_{aq}^{*b} (g/L)	C_{org}^{*c} (g/L)	k (min ⁻¹)	t^{*d} (min)
1	3.2215	0.6354	2.5861	0.264	12-15
2	1.4360	0.0680	1.3680	0.110	13
3	0.7180	0.0124	0.7056	0.070	10
4	0.3666	0.0063	0.3603	0.0349	10
5	0.0718	0.00050	0.0713	0.0196	9
6	0.0377	0.00019	0.0375	0.020	6

NOTES:

- ^a C_o = Initial feed copper concentration
- ^b C_{aq}^* = Equilibrium concentration in the aqueous phase
- ^c C_{org}^* = Equilibrium concentration in the organic phase
- ^d t^* = Time required for the reaction to reach equilibrium

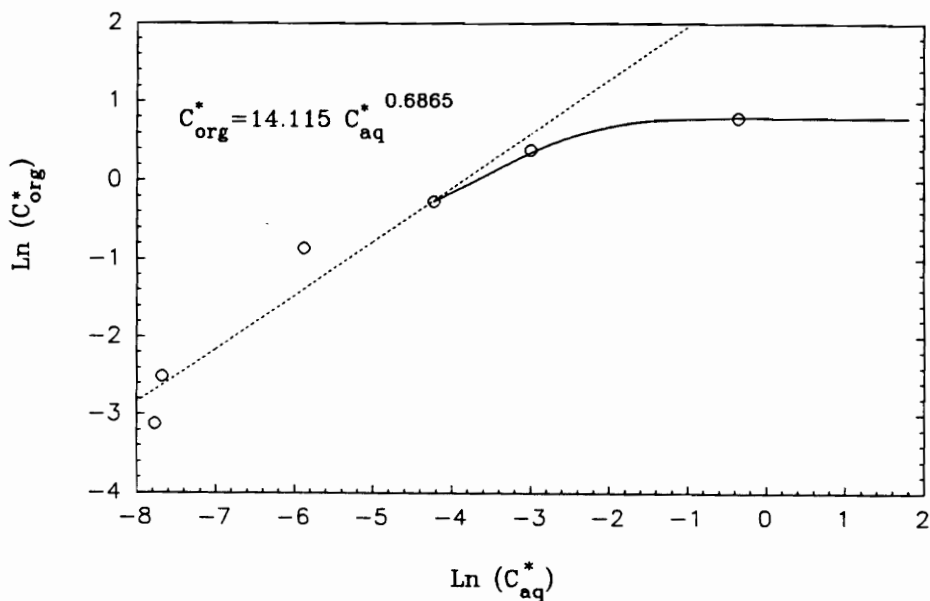


FIGURE (A)

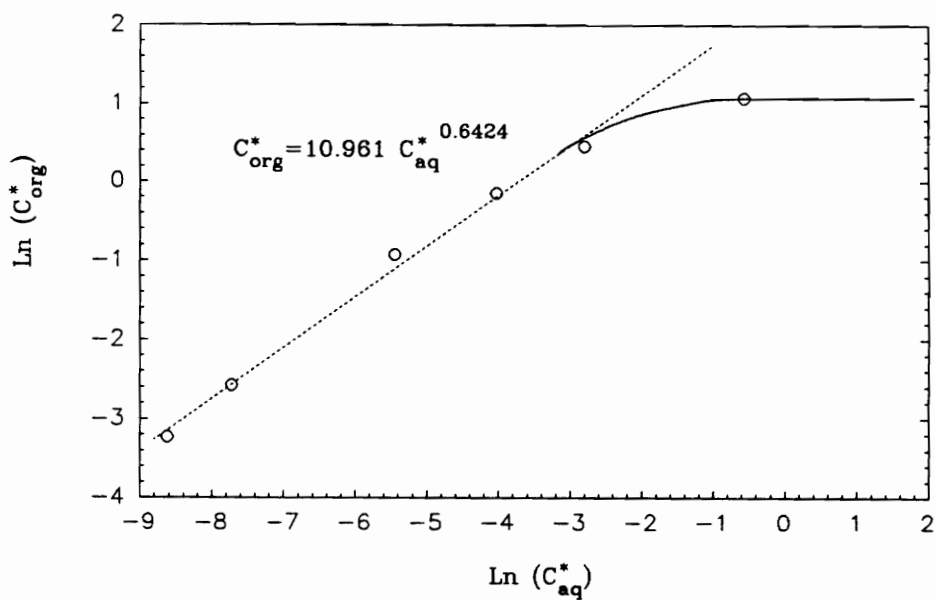


FIGURE (B)

Figure 78. Equilibrium isotherm for the predispersed solvent extraction of copper in a batch reactor at $T=26.0^{\circ}\text{C}$. and a $\text{pH}=2.0$.: Polyaphrons made with 5 g/L NaDBS; and at (A) $\text{PVR}=10$, (Data found in Table 63), (B) $\text{PVR}=5$, (Data found in Table 64).

Table 63. Equilibrium parameters for the PDSE of copper in a batch reactor at T=26°C and pH=2.0. Polyaphrons made with 5 g/L NaDBS; PVR=10. (Series 1)

Test ID	C_o^a (g/L)	C_{aq}^{*b} (g/L)	C_{org}^{*c} (g/L)	k (min ⁻¹)	t ^{*d} (min)
1	2.9228	0.700	2.2228	0.535	12.5
2	1.5250	0.050	1.475	2.654	0.5
3	0.7815	0.0146	0.7669	1.380	0.5
4	0.4144	0.0028	0.4216	0.759	0.5
5	0.0820	0.00046	0.08154	0.147	0.5
6	0.04448	0.00042	0.04406	0.106	0.5

- NOTES:**
- ^a C_o = Initial feed copper concentration
 - ^b C_{aq}^* = Equilibrium concentration in the aqueous phase
 - ^c C_{org}^* = Equilibrium concentration in the organic phase
 - ^d t^{*} = Time required for the reaction to reach equilibrium

Table 64. Equilibrium parameters for the PDSE of copper in a batch reactor at T=26°C and pH=2.0. Polyaphrons made with 5 g/L NaDBS; PVR=5. (Series 3)

Test ID	C_o^a (g/L)	C_{aq}^b (g/L)	C_{org}^c (g/L)	k (min⁻¹)	t^d (min)
1	3.9713	0.5677	2.9334	4.00	0.5
2	1.6457	0.0608	1.5849	2.161	0.5
3	0.8769	0.0177	0.8592	1.172	0.5
4	0.4022	0.0043	0.3979	0.546	0.5
5	0.07625	0.00044	0.07581	0.158	0.5
6	0.03971	0.00018	0.03953	0.115	0.5

NOTES:

- ^a C_o = Initial feed copper concentration
- ^b C_{aq} = Equilibrium concentration in the aqueous phase
- ^c C_{org} = Equilibrium concentration in the organic phase
- ^d t = Time required for the reaction to reach equilibrium

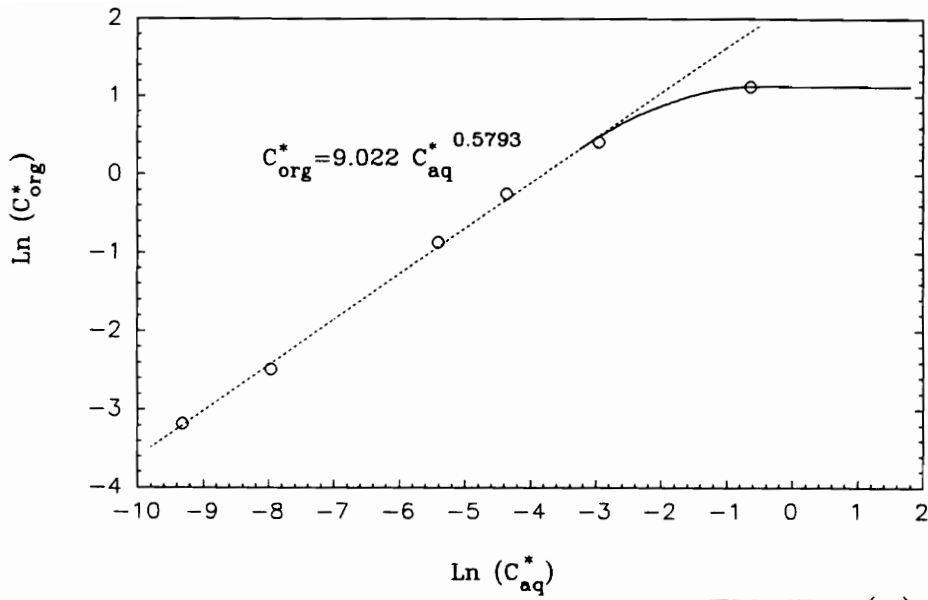


FIGURE (A)

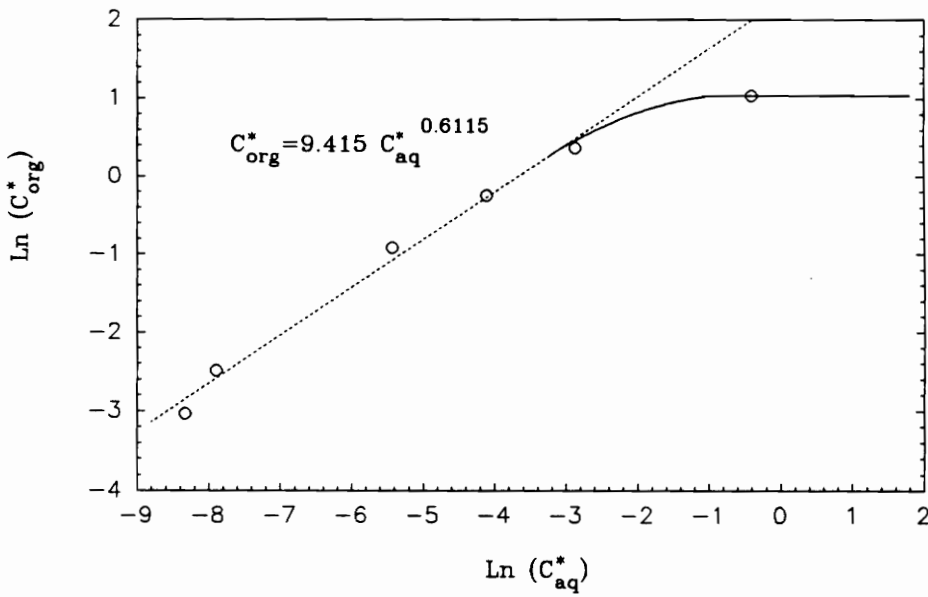


FIGURE (B)

Figure 79. Equilibrium isotherm for the predispersed solvent extraction of copper in a batch reactor at $T=26.0^\circ\text{C}$. and a $\text{pH}=2.0$.: (A) Polyaphrons made with 5 g/L NaDBS; PVR=10. Data found in Table 65, (B) Polyaphrons made with 5ml/L Arquad 12/50; PVR=10. Data found in Table 66.

Table 65. Equilibrium parameters for the PDSE of copper in a batch reactor at T=26°C and pH=2.0. Polyaphrons made with 5 g/L NaDBS; PVR = 15. (Series 4)

Test ID	C_o^a (g/L)	C_{aq}^{*b} (g/L)	C_{org}^{*c} (g/L)	k (min ⁻¹)	t ^{*d} (min)
1	3.6154	0.5319	3.0835	0.562	7.0
2	1.5567	0.0520	1.5047	1.952	0.5
3	0.7879	0.0127	0.7752	1.006	0.5
4	0.4225	0.0045	0.4180	0.581	0.5
5	0.08387	0.00035	0.08352	0.186	0.5
6	0.04175	0.00009	0.04166	0.116	0.5

- NOTES:**
- ^a C_o = Initial feed copper concentration
 - ^b C_{aq}^* = Equilibrium concentration in the aqueous phase
 - ^c C_{org}^* = Equilibrium concentration in the organic phase
 - ^d t^* = Time required for the reaction to reach equilibrium

Table 66. Equilibrium parameters for the PDSE extraction of copper in a batch reactor at T=26°C and pH=2.0. Polyaphrons made with 5 ml/L Arquad 12/50; PVR=10. (Series 5)

Test ID	C_o^a (g/L)	C_{aq}^{*b} (g/L)	C_{org}^{*c} (g/L)	k (min ⁻¹)	t ^{*d} (min)
1	3.5011	0.6681	2.8330	0.625	7.0
2	1.5059	0.0565	1.4494	0.685	3.0
3	0.8006	0.0164	0.7842	1.107	0.5
4	0.4035	0.0044	0.3991	0.598	0.5
5	0.08387	0.00037	0.08350	0.200	0.5
6	0.04842	0.00024	0.04818	0.130	0.5

NOTES: ^a C_o = Initial Feed copper concentration
^b C_{aq}^* = Equilibrium concentration in the aqueous phase
^c C_{org}^* = Equilibrium concentration in the organic phase
^d t^{*} = Time required for the reaction to reach equilibrium

7.0 PREDISPERSED SOLVENT EXTRACTION OF COPPER WITH LIX-64N

The batch extractions carried out by both conventional extraction and predispersed solvent extraction (PDSE) demonstrated the superior contacting capabilities of PDSE. Generally extraction equipment constitutes a mixer-settler assembly or a packed extraction tower. However, the use of aphron technology avoids the need for any mixing devices for contacting the feed with the solvent. In fact, predispersed solvent extraction can be achieved with very simple equipment.

7.1 Experimental Method

7.1.1 Development of Extraction Equipment

The first PDSE tests were performed in batch mode in a glass column 58 cm long and 9.5 cm in diameter with a capacity of about 4 liters. The glass cell had three entry points in the bottom; one for the introduction of the feed solution, one for the introduction of the diluted polyaphrons, and the other for the colloidal gas aphron (CGA) introduction. A schematic of the cell is shown in Figure 80. The extractions were done by first introducing the feed solution into the vessel. Afterwards the diluted polyaphrons were fed into the cell and only after all the polyaphrons had been fed, the CGA were pumped into the system. The mixture inside the cell was allowed to sit undisturbed for a few minutes and then a sample of raffinate was taken and analyzed for copper content. The cell was emptied and cleaned.

The batch cell worked well but like in any other process, it was important to develop an apparatus capable of handling a continuous system. The idea of a column such as that used

for the batch experiments was incorporated into a semi-pilot plant unit. The glass column had a diameter of 12 cm and was 55 cm tall. The cell was mounted on a mobile stand. The feed, diluted polyaphrons, and CGA were introduced into the extraction cell through three entry ports located in the bottom of the cell. The extract was continuously pumped out from the top right hand side of the extraction column, which was open to the atmosphere, via a draw tube. On the left hand side of the cell another draw tube was positioned to continuously pump out the raffinate. Both draw tubes were adjustable so that they could be positioned at various distances from the bottom of the cell. That way, the raffinate and extract could be removed from various points of the extraction column. All solutions were pumped with Masterflex peristaltic pumps. A schematic of the process is shown in Figure 81.

The semi-pilot plant unit never worked to complete satisfaction, mainly because too much solvent was being lost in the raffinate. The mixing generated by the CGA would reintroduce into the raffinate some of the extract that had already separated from it. A unit that allowed the liquids inside the vessel to separate and prevent disturbance to the extract layer was needed. With this in mind, a horizontal trough was built. The trough had a 15 liter capacity and was built out of Plexiglas. The shape of the trough had to permit good distribution of the CGA over the entire area of the vessel; therefore, a V-shaped trough was considered. Unfortunately the V-shape did not allow the experimenter to observe well what happened in the bottom of the cell so the shape of the trough was changed to that of a U. A 3/4 in. diameter Plexiglas tube with both ends closed was placed horizontally on the inside bottom of the cell. The tube was perforated with 3.0 mm diameter holes set approximately 6.0 mm apart, and three entry points positioned equidistant from each other were fitted with swagelok fittings for the introduction of the CGA. On one end of the trough and 7.0 cm above the bottom of the cell, another entry port was made for the introduction of the diluted polyaphrons and the feed solution. The two solutions were fed into the vessel through different lines that joined into one line about 20 cm before entering the cell. On the opposite end from the feed entrance and at the top of the cell, a weir, also made out of Plexiglas, was placed to allow the solvent to overflow. Also, about 2.5 cm below the weir, an exit point was designed to remove the

raffinate. All solutions were pumped with Masterflex peristaltic pumps. A diagram of the apparatus is shown in Figure 82.

One of the major problems encountered with the horizontal trough was the distribution of the CGA. The CGA feed line was divided into three streams and fed through three feed ports. It was impossible to divide the CGA stream equally through the feed ports especially at low flow rates. Even with the installation of valves, most of the time the CGA flow was being pumped in through just one of the ports. Inside the vessel, the CGA would also not distribute evenly throughout the cell. Around 80% of the total flow would distribute itself throughout an area of only about 8.0 cm in diameter. Making the holes smaller in the tube that served as distributor plate did not help. The weir through which the extract overflowed also created problems. Leaks used to constantly form around it and several times the weir completely fell off the vessel. The weir was glued to the vessel but although several different types of adhesives were tried, the kerosene always attacked them. To a lesser degree, leaks were also a problem along the sides of the cell. Another problem with this trough was that all the flow rates were difficult to regulate. As the level of the liquid inside the trough increased, raffinate as well as extract would run off the weir while whenever the level decreased, some of the extract would be removed along with the raffinate.

In an attempt to improve the extraction process and minimize solvent losses, a new trough was designed. The description of the cell is given in the apparatus section of this thesis. The CGA distributor tube was eliminated from the design. Instead, J-shaped feed tubes were designed to feed the CGA just below two straight feed tubes used to feed the copper/polyaphron mixture. In this way it was expected to maximize the use of the CGA as a flotation mechanism. With this change, the shape of the vessel was no longer critical. A U-shaped vessel is more difficult to construct so the vessel was made with the ends shaped like a trapezoid. The weir was also eliminated and the extract was removed from the cell through a stainless steel tube. This allowed better control over the removal of extract. Also, the raffinate was removed from near the bottom of the vessel instead of removing it from the top, close to the extract layer. This prevented the extract layer from being pulled out of the

system with the raffinate. Leaks were greatly minimized by drilling channels on one side of one of two pieces to be glued together. The edge of the undrilled part was fitted snugly into the channel of the other part and then glued. For better control of the flow rates, flowmeters were installed in all lines except the CGA feed line. CGA consist of approximately 60% air and the rest water. Flowmeters have been proven useless when it comes to metering CGA. The process was tested in this cell and then it was decided to add a second cell to the proces to improve solvent recovery. One cell, called the extraction cell, contained the feed solution and the polyaphrons. Gravity alone caused some of the solvent to separate out of the raffinate. This solvent was removed from the system while the raffinate was pumped into a second cell, the flotation cell, to which the CGA was added in the manner previously de-scribed. The extract and raffinate from this cell was separately removed from the system through the exit ports. A diagram depicting the extraction process is shown in Figure 5.

7.1.2 Design of the Experimental Tests

The first four extractions done in the apparatus described in the previous paragraph were designed to test the performance of the extraction cell. The first experiment was done using only one cell. All the materials; copper feed solution, diluted polyaphrons and CGA were fed into the extraction cell. The second test was done using both cells. The CGA was fed only into the flotation cell. Results from these tests demonstrated that the solvent loss was minimized when the second vessel was used so the extractions were carried out using both cells from then on. A third test was done to determine whether the length of the line from the point where the polyaphrons and the copper feed were joined to the entrance of the vessel had an effect on the extraction. The line was extended from 30 cm to 150 cm. No effect on the percent extraction was observed so the line was shortened back to its original size. Another test was carried out to determine whether using water at a pH of 2.0 versus deionized water to dilute

the polyaphrons made a difference in the extraction. The effect was found negligible so all other tests were done with polyaphrons diluted in deionized water.

To optimize the operating conditions of the extraction process in the final apparatus built, the effect of copper feed flowrate, polyaphron feed flowrate, and CGA feed flowrate were studied. As with the tests designed to study the particle size distribution of the polyaphrons, the tests for this part of the study were designed using a statistical approach. A three-dimensional design region was drawn and several tests were planned so as to have an experimental point at each corner of the design region and three points in the center of the region. Figure 83 (A) depicts the design region and the experimental points. The region boundaries were determined by the equipment limitations. The copper feed flow rates ranged from 100 ml/min to 500 ml/min. The polyaphron flow rates ranged from 20 ml/min to 200 ml/min and the CGA flow rates from 10 to 100 ml/min. The results from the first eleven tests showed that the CGA flowrate did not have an effect on the percent of copper extracted; therefore, the three-dimensional design region was converted into two dimensions. To complete the study, four more axial tests were done. The two-dimensional design region is depicted in Figure 83 (B).

Once a statistical model for the above extractions was calculated, two extractions were done and the results compared to those predicted by the model. Also, fourteen other extractions were carried out using several of the different polyaphron batches made for the particle size distribution study.

7.1.3 Experimental Procedure

All the experiments described in the previous three paragraphs, except for the last fourteen, were carried out with polyaphrons from the same batch. The polyaphrons were generated in the continuous polyaphron generator at an organic feed flowrate of 300.0 ml/min, an aqueous feed flowrate of 30 ml/min, and at a mixing rate of 1500 r.p.m.. Also, they were made

from the same batch of kerosene as was used to make the polyaphrons used for the particle size distribution study. The aqueous phase of the polyaphrons was a 5 g/L NaDBS solution and the organic phase consisted of a 10% LIX-64N in kerosene solution.

The following procedure was followed for all extractions except for the test done using only the extraction cell.

1. All the system feed lines were disconnected from the entrance to the vessel and both ends were placed in small buckets containing deionized water. The pumps were turned on and the water allowed to recycle through the feed lines to permit the pumps to warm up.
2. 60,000 ml of a 0.3177 g/L copper sulfate solution was made and stored in three 20,000 ml capacity buckets. The pH of the solution was adjusted to 2.0 with concentrated sodium hydroxide. The buckets were covered until just before being used.
3. A 0.5 g/L NaDBS or a 0.5 ml/L Arquad 12/50 surfactant solution to make the CGA was made and stored in a container. Approximately 10,000 ml were made at a time.
4. The flow rates of the copper sulfate feed pump, the polyaphron feed pump and the surfactant feed pump were adjusted to deliver the desired volume. The flowrate was determined by removing the feed lines from the buckets containing deionized water, placing them in their respective feed tanks, and collecting a volume of liquid over time.
5. The CGA feed flowrate was adjusted to deliver the desired volume of CGA. The CGA flowrate was determined by collecting a volume of CGA over time. The CGA was collected in a graduated cylinder and allowed to break completely. The volume of surfactant solution was measured. This volume had to equal the volume of surfactant solution being fed into the CGA generator.

6. After adjusting all the feed flow rates, the copper sulfate and the diluted polyaphron lines were removed from the feed solutions and the exit ends were quickly attached to the system. The pumps were never stopped during this operation. The entrance end of the lines were then simultaneously placed in their respective feed solutions. 100 ml of polyaphrons were diluted with deionized water at a ratio of 1 volume of polyaphron to 3 volumes of water. The diluted polyaphrons were placed in a beaker, which served as the feed tank, where they were constantly stirred with a magnetic stirrer. Whenever only around 50 ml of polyaphron feed remained in the beaker, another batch of polyaphrons was diluted and poured into it.
7. As soon as the extraction cell filled, the pump used to move the raffinate from the extraction cell to the flotation cell was turned on. The end of the surfactant line, which had been kept in the surfactant tank to recycle the solution, was attached to the CGA generator. The CGA generator was turned on and the feed line was connected to the flotation cell.
8. The flowrate of the raffinate being removed out of the extraction cell and into the flotation cell was adjusted to maintain approximately the same liquid level in the extraction cell. The extract pump was turned on to remove the solvent that separated out of the raffinate.
9. As soon as the flotation cell filled up, the raffinate waste pump and the extract pump were turned on. The flow rates were adjusted to maintain approximately the same liquid level in the flotation cell.
10. The process was run until steady state was reached. Samples of both the extract and the raffinate were taken periodically and later analyzed for copper content with an atomic absorption spectrophotometer.
11. At the end of each test, both cells were completely emptied.

This procedure was also followed for the test done using only the extraction cell, except that the CGA was fed into the extraction cell simultaneously with the copper sulfate and polyaphron feeds.

7.2 Results and Discussion

The results of the extractions carried out to test all the extraction apparatus developed before the final system was designed can be found in the author's masters thesis. The only data presented as part of this study is the data collected from tests done in the final apparatus.

7.2.1 Determination of Equipment Performance

Each extraction apparatus was developed with the intent of improving the effectiveness of the separation of the two phases. The amount of surface area generated by the aphrons is so large, that any type of extraction cell works effectively. The problem of predispersed solvent extraction lies in the small size of the aphrons. Because of this, gravity separation by itself was inadequate since the small bubbles took a long time to rise through the bulk liquid. The separation of the two phases was expedited with the use of colloidal gas aphrons (CGA). CGA are bubbles made up of approximately 60% air and 40% surfactant solution and have diameters of approximately 25 μm . These bubbles are several times larger and more buoyant than the liquid aphrons. Furthermore, the microscopic liquid-core aphrons adhere to CGA bubbles because the surface of the CGA shell is hydrophobic which provides a region where a hydrophobic globule such as a liquid aphron will be comfortable. Thus when CGA were fed into the extraction process, they rose to the surface quickly, carrying the solvent with them. The problem with CGA was that it was very difficult to distribute evenly throughout the extraction cell so as to maximize their flotation effectiveness. Also, when CGA was pumped into the extraction system a large amount of mixing was generated by the bubbles and de-

pending on the extraction equipment, the mixing caused some of the already separated organic layer to be reintroduced into the bulk liquid. This quantity of extract was then carried out of the system together with the raffinate waste stream which translated into a costly loss of solvent. This last problem was the one encountered with the semi-pilot plant unit while the main problem with the trough that was equipped with a distributor tube was the uneven distribution of the CGA. Another problem with the trough was the lack of control of the flow rates and the frequent development of leaks. Both of these units are described in the Development of Extraction Equipment section of this chapter.

The final extraction system was designed as an effort to remedy all the major problems encountered with the previous apparatus. Flowmeters were added to the system to facilitate the determination of the flow rates and allow for better control of them. This was only partially successful. The flowmeters did not measure the flow rates very accurately so one could not depend on the flowmeter readings. The flow rates had to be determined by collecting a volume of liquid over time for each test. However, the flowmeters did help indicate whether a flow started to decrease or increase. The variation of flow delivered over a long period of time by the Masterflex peristaltic pumps could vary considerably at times. One problem that was practically completely eliminated was that of the leaks. The new system rarely leaked. The loss of solvent in the raffinate, although minimized to great extent, was still a problem with the new unit. The first two extractions were done to determine whether the use of two cells over one cell would enhance the solvent recovery. Test 1 was done using only one cell. All materials were fed into the cell simultaneously. The diluted polyaphrons were fed at a rate of 199.8 ml/min. It should be noted that all polyaphrons were diluted at a volume ratio of 1 to 3; thus, whenever diluted polyaphrons are mentioned it should be recognized that the amount of solvent is 1/4 that of the diluted solution. The flowrate of the 0.3177 g/L copper sulfate feed was 501.4 ml/min. and that of the surfactant solution formed into a CGA was 102.0 ml/min. Instead of mentioning the CGA flowrate, the amount of surfactant solution used up during the process will be given. There is no accurate way of measuring the volume of CGA. A volume of CGA cannot be collected over time because as soon as the CGA sits in a container, the

volume decreases as some of the bubbles burst and the air inside them is released into the atmosphere. A flowmeter cannot be used because of the air/water mixture of the CGA. Test 2 was done using the extraction cell and the flotation cell. The CGA was fed only into the flotation cell but some of the solvent separated out in the extraction cell. This extract was continuously removed from the system. The flow rates for this test were 503.3, 199.1, and 102.0 ml/min for the copper sulfate solution, the diluted polyaphrons, and the surfactant solution, respectively. The polyaphrons used for both tests were from the same batch and the surfactant used to make them was NaDBS at a concentration of 5 g/L. The surfactant solution used to make the CGA was Arquad 12/50 at a concentration of 0.5 ml/L. 86.6% of copper was recovered with the first test and 83.1% was recovered with the second test. The differences were considered within experimental error. Addition of the second cell reduced the amount of solvent loss by 5% from 15% to 10%. The second cell became a permanent part of the system.

As was previously mentioned, the diluted polyaphron and the copper sulfate feed lines were connected at a distance of approximately 30 cm from the extraction cell entry port. This line was increased to a length of 150 cm to determine whether the increase in residence time of the mixture would enhance the extraction. The flow rates used for this test were 499.7, 199.3, and 101.3 ml/min for the copper feed, the diluted polyaphrons, and the surfactant solution, respectively. The copper extraction was not enhanced. The amount of copper recovered with this test was 82.0%. The feed line was reduced back to its original length of 30.0 cm.

A fourth test was done to determine whether the pH of the water used to dilute the polyaphrons had an effect on the extraction. From the batch tests it had been determined that an increase in pH enhances the extraction. When the copper sulfate and the diluted polyaphron feed lines were joined, the pH of the copper sulfate solution increased because of the extra volume of water used to dilute the polyaphrons. The polyaphrons for this test were diluted with water that had been adjusted to a pH of 2.0 with concentrated sodium hydroxide. The copper sulfate feed, diluted polyaphrons, and surfactant solution flow rates

were adjusted to 499.2, 200.9, and 99.9 ml/min, respectively. No significant change on the percent of copper recovered was achieved. The percent of copper extracted was 84.5. The change in pH due to the water used to dilute the polyaphrons might become important in an extraction of copper from solutions that contain metal ions other than copper. Under this conditions other ions compete with copper to chelate with the LIX reagent. At a pH of 2.0 LIX-64N chelates preferentially with copper; thus, it would be important to maintain the copper sulfate solution at a pH of 2.0.

All the tests described in the previous paragraphs were done with polyaphrons from the same batch. The polyaphrons were made with 5 g/L NaDBS and 10% LIX-64N in kerosene at a PVR of 10. The surfactant solution used to make the CGA was made of 0.5 ml/L Arquad 12/50 for all tests.

7.2.2 Development of the Statistical Model

The fifteen tests designed to determine the effect of copper sulfate and polyaphron feed flow rates were carried out in the two cell system. All the polyaphrons used in these experiments were from the same batch. The polyaphrons were generated in the continuous polyaphron generator at an aqueous flow of 30 ml/min, an organic flowrate of 300 ml/min, and at a 1500 r.p.m. mixing rate. The organic phase was made of 10% LIX-64N in kerosene and the aqueous phase was made of 5 g/L NaDBS in deionized water. The PVR of the polyaphrons was 10. A description of the conditions for each test and the percent of copper recovery are tabulated in Table 67.

The experimental data from the fifteen tests was used to develop a statistical model for the predispersed solvent extraction process. Initially, the first eleven tests tabulated in Table 67 were performed. The first eight tests represent the corners of a three-dimensional region bound by the equipment limitations. Each axis represents one of three parameters; copper feed flow rate, diluted polyaphron flow rate, or CGA flow rate. The copper feed flow

rates ranged from 100 ml/min to 500 ml/min. The polyaphron flow rates ranged from 20 ml/min to 200 ml/min and the CGA flow rates ranged from 10 to 100 ml/min. Tests 9 to 11 represent the center runs and they were designed around the same point. The parameters used for each test and the percent of copper extracted were used to build a statistical model. The model was built by first assuming the following model:

$$Y = B_0 + B_1X_1 + B_2X_2 + B_3X_3 + B_{12}X_1X_2 + B_{13}X_1X_3 + B_{23}X_2X_3 \quad (7.1)$$

where, $B_{k_{ij}}$ are coefficients, X_1 represents the copper feed flow rate, X_2 represents the diluted polyaphron flow rate, and X_3 represents the CGA flow rate. The values for X_1 , X_2 , and X_3 used were not the actual flow rates. Instead, the flow rates were converted into design parameters by converting each flow rate range into a range between -1 and 1. For example, a copper feed flow rate of 100 ml/min became -1 and one of 500 ml/min became 1 while 300 ml/min was represented by 0. The value of the coefficients in the model were calculated and a statistical analysis on the calculated coefficients was done using SAS programs. The statistical analysis included tests for curvature, and calculation of standard errors, sum of squares, and F- distributions. Preliminary tests on the coefficients indicated that the CGA flow rate, represented by X_3 , was not significant to the model. Thus, all the terms that included only X_3 or the interaction of X_3 with another variable were eliminated from the model. Also, the test for curvature indicated the possible presence of quadratic terms in the model. Therefore, the design was augmented with axial or star points in order to estimate the coefficients of probable quadratic terms. Tests 12 through 14, tabulated in Table 67, were performed to generate these axial points. The new model was represented as follows:

$$Y = B_0 + B_1X_1 + B_2X_2 + B_{12}X_1X_2 + B_{11}X_1^2 + B_{22}X_2^2 \quad (7.2)$$

The coefficients of the variables were again calculated and a statistical analysis on the coefficients was done. The statistical analysis was used to determine which variables contributed significantly to the model and the non-significant terms were once again eliminated. The final model is as follows:

$$Y = -15.735X_1 + 29.745X_2 + 6.778X_1X_2 - 16.333X_2^2 + 78.338 \quad (7.3)$$

and,

$$\begin{aligned} X_1 &= 0.005E_1 - 1.5 \\ X_2 &= 0.01111E_2 - 1.2222 \end{aligned} \quad (7.4)$$

where, Y is the percent of copper extracted, E_1 is the copper sulfate feed flowrate in ml/min, and E_2 is the diluted polyaphron flowrate in ml/min. Figure 84 shows the model's estimated response surface, i.e. a graph of the predicted percent of copper extracted over various diluted polyaphron and copper feed flow rates. Figure 85 depicts the actual data points while Figure 86 depicts the predicted values for the experimental points. The CGA flowrate does not appear in the model because it did not have an effect on the amount of copper extracted. A minimum surfactant flowrate of 10.0 ml/min was found adequate for all tests. Increasing the volume of CGA fed into the system did not increase the solvent recovery any further while at high flow rates such as 100.0 ml/min foam accumulated at the top of the cell.

The extractions carried out with a solvent to aqueous ratio of 1:2 achieved almost complete extraction with 99% of the total copper recovered. The problem with these extractions was that the amount of solvent loss was increased by 10% from 10 to 20% of the total solvent remaining in the aqueous phase. It should be noted though that approximately 95% of the oil in the raffinate separated out within one minute after the raffinate was allowed to sit in a waste bucket. This indicates that perhaps the addition of a settling tank to the system might be effective in eliminating the solvent loss problem. Extractions carried out with a solvent to aqueous ratio of 1:10 resulted in 80 to 85% copper recovery. In conventional extraction a solvent to aqueous ratio of 1:1 or 1:2 is usually used to achieve the same results.

After the design model was developed two more extractions were done to test it. The first test was done with a copper sulfate flowrate of 402.7 ml/min, a diluted polyaphron flowrate of 75.5 ml/min, and a surfactant flowrate of 10.3 ml/min. 57.2% extraction was achieved and the model predicted 55.2%. The second test was done under the following conditions: copper

sulfate flowrate at 199.4 ml/min, diluted polyaphrons flowrate at 128.9 ml/min, and surfactant flowrate at 10.1 ml/min. 95.4% of the copper was recovered and the model predicted a recovery of 90.9%. It is noted that the model predicts the results with good accuracy.

7.2.3 PDSE Using Different Types of Polyaphrons

Fourteen extractions were done using different types of polyaphrons. The polyaphrons used were selected from the ones generated for the particle size study. Polyaphrons made at various feed rates, at different mixing rates, and of different PVR and surfactant were selected for the tests to determine if any of these parameters had an effect on the extraction. A description of the tests along with the type of polyaphrons used is given in Table 68. All tests were carried out under similar conditions. The surfactant solution used was made of 5 g/L NaDBS except for the test where the polyaphrons used were made of 5 ml/L Arquad 12/50. The surfactant used to make the CGA for this test was a 0.5 g/L NaDBS solution. No significant differences were observed among tests except for the one made with the Arquad polyaphrons. The percent of copper extracted with all tests except the Arquad one, ranged from 76 to 84 percent. These differences were considered within experimental error. With the test done with the Arquad polyaphrons only a 60.6% extraction was achieved and a negligible amount of solvent was lost in the raffinate. At this point it is not clear whether the results from this test are in error or whether they indicate that although the amount of copper recovered was less than the amount recovered with the other polyaphrons, the NaDBS CGA showed superior flotation capabilities. This matter needs to be studied further because if NaDBS CGA are indeed superior, then other cationic surfactants other than Arquad 12/50 can be used to make the polyaphrons so as to enhance the extraction. It should be noted that with the batch extractions no decrease in copper recovery was seen when using Arquad polyaphrons.

To complete the copper recovery process the copper must be stripped from LIX-64N. No benefit was found by turning the loaded organic phase into a polyaphron and then stripping

the copper with sulfuric acid. The simplest and most economic system apparently available is the use of a sulfuric acid strip solution, followed by electrowinning of copper. Since the extract from the predispersed solvent extractions is similar to the extract recovered from conventional extraction methods, no problems are foreseen in stripping the copper from the extract by conventional methods. The surfactants used to make the polyaphrons and CGA are all water soluble surfactants; thus, they remain in the raffinate.

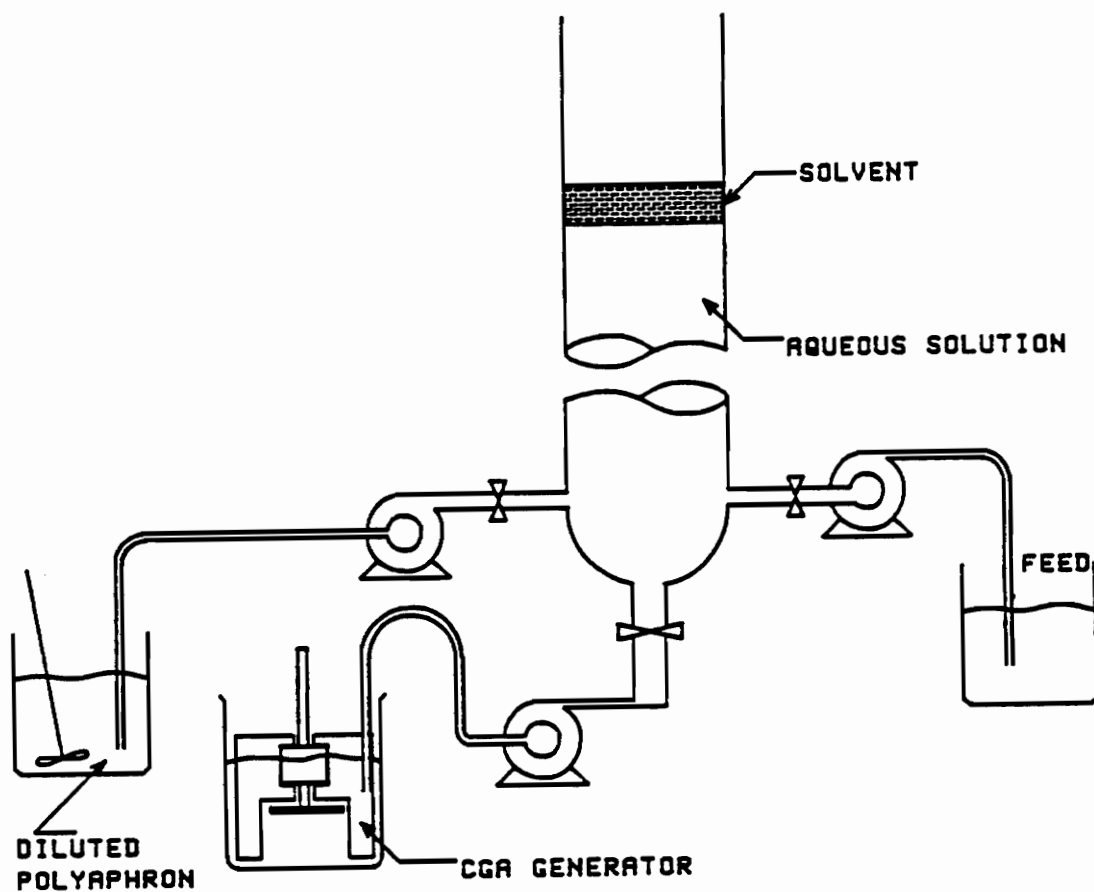


Figure 80. Schematic of the predispersed solvent extraction process in a batch cell.

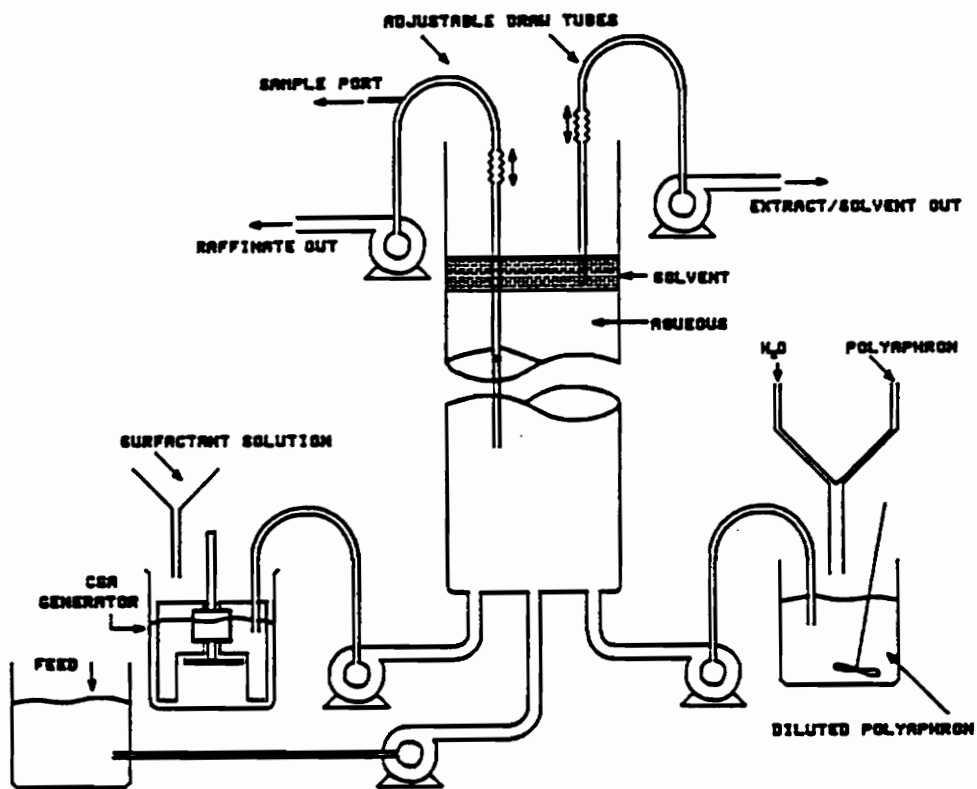


Figure 81. Schematic of the semi-pilot plant unit used for the predispersed solvent extraction experiments.

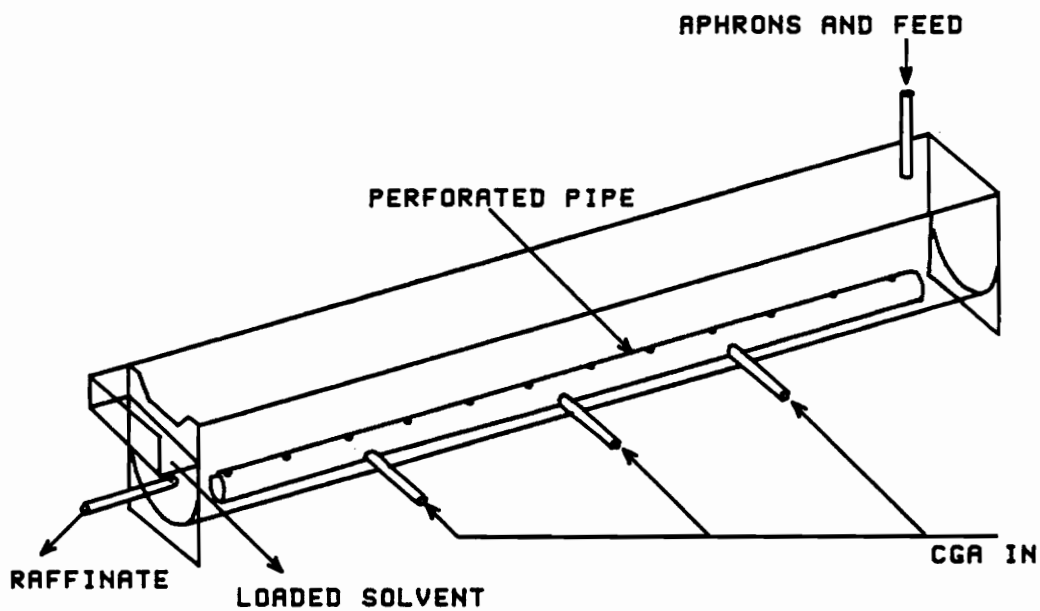


Figure 82. Diagram of the horizontal U-shaped trough used for predispersed solvent extraction tests.

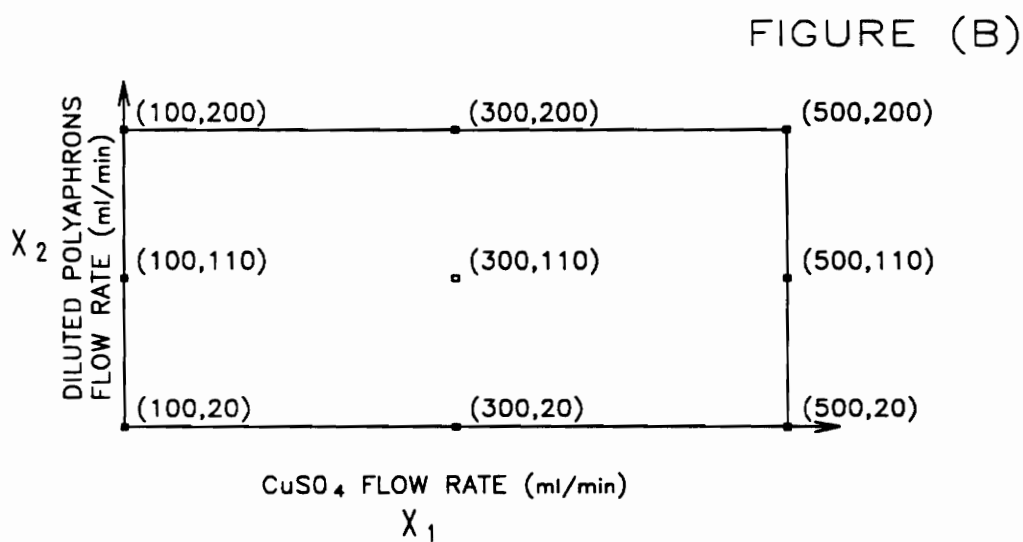
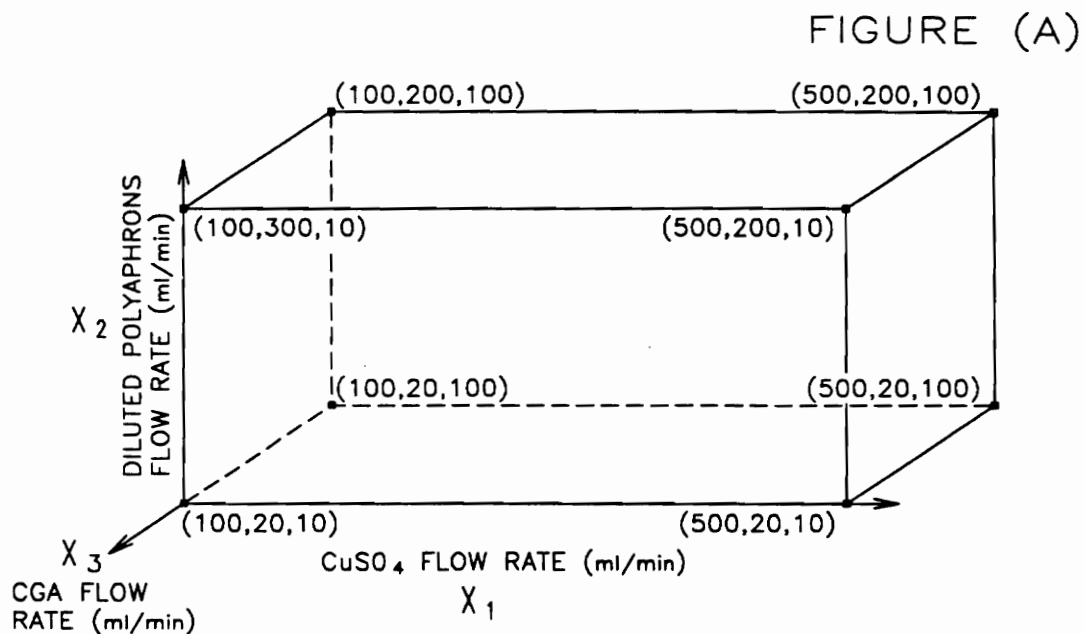


Figure 83. Design region of the experimental tests done for the development of a statistical model that predicts the percent of copper extracted.: (A) 3-Dimensional design region, (B) 2-Dimensional region.

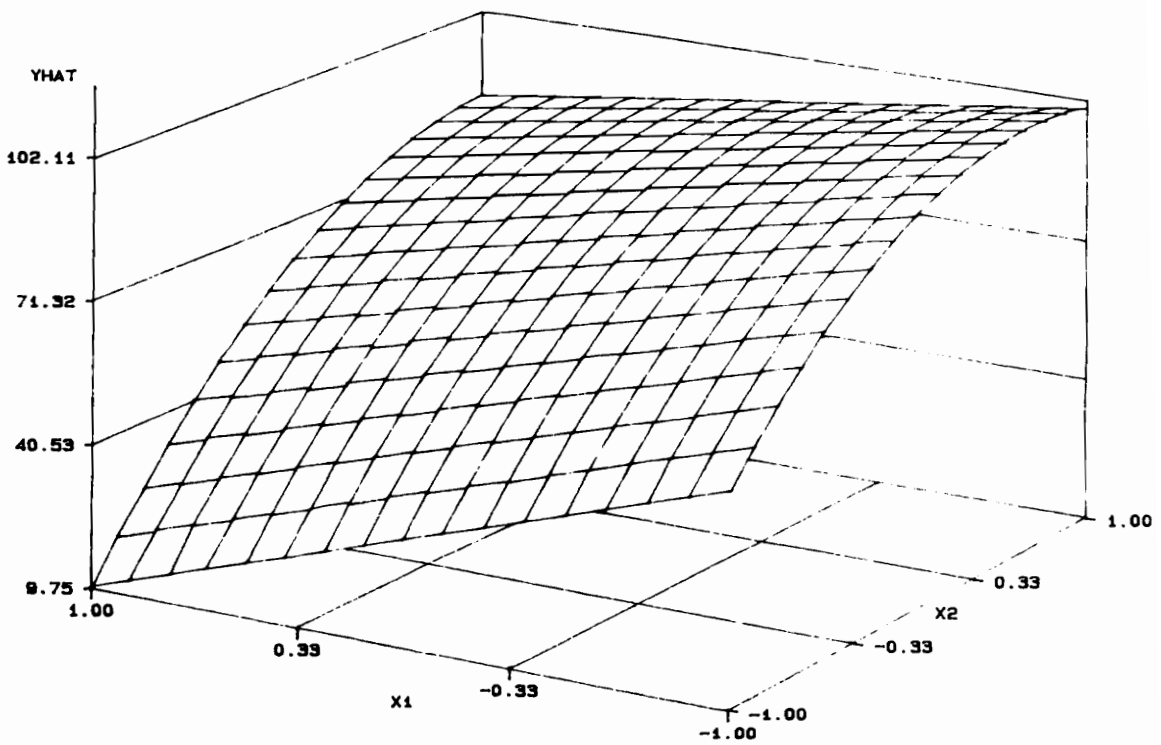


Figure 84. Estimated response surface of the statistical model for the the predispersed solvent extraction process.

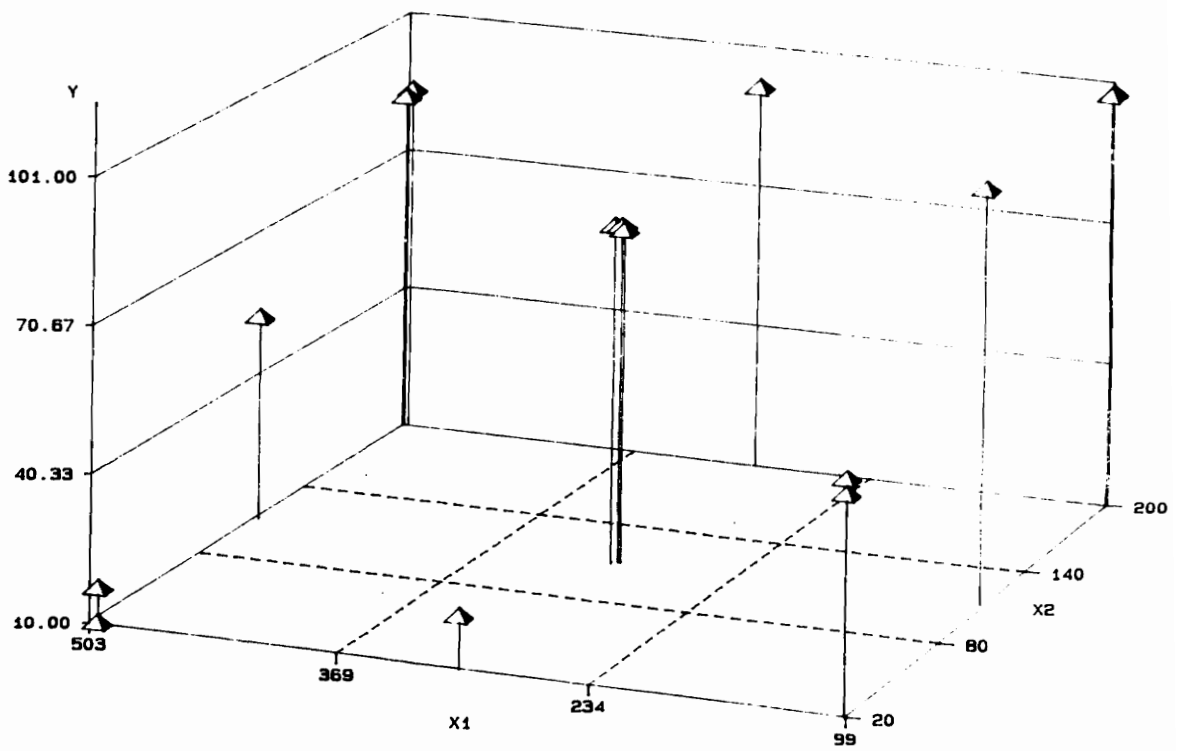


Figure 85. Actual data values for the tests used to develop a statistical model for the predispersed solvent extraction system.

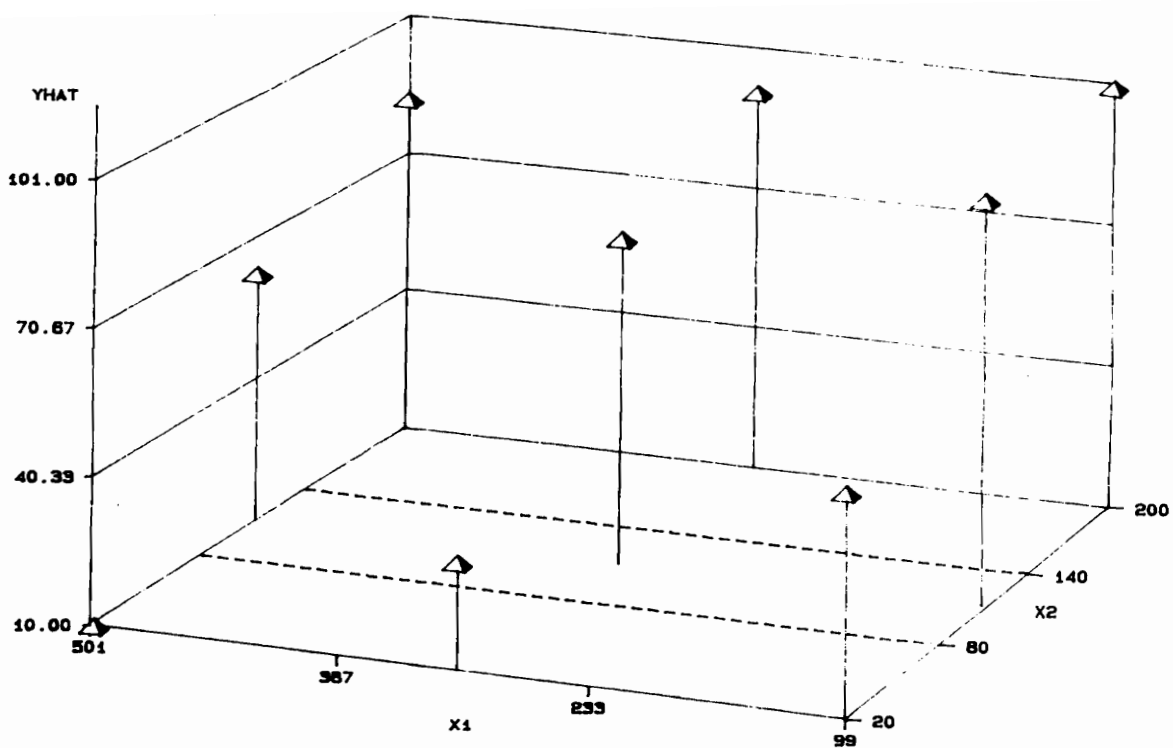


Figure 86. Predicted values from the statistical model for the tests used to develop the model for the predispersed solvent extraction model.

Table 67. Description of the experiments done to determine a statistical model for the predispersed solvent extraction process.

Sample ID	E ₁ (C ₂ SO ₄ Feed) ^a (ml/min)	E ₂ (Diluted Polyaphrons) ^b (ml/min)	E ₃ (CGA) ^c (ml/min)	% Extraction	
				Actual	Predicted
1	100.5	20.2	10.2	57.5	54.8
2	499.0	19.9	10.5	10.5	9.8
3	489.9	20.0	99.3	17.5	9.9
4	100.1	20.0	99.3	54.5	54.8
5	99.1	200.3	9.8	99.2	100.7
6	500.6	199.9	10.2	84.7	82.8
7	503.3	199.1	102.0	83.1	82.6
8	99.9	200.1	100.1	98.8	100.7
9	298.6	110.0	54.9	81.0	78.0
10	297.1	109.9	55.8	80.2	78.5
11	302.1	109.5	55.7	81.0	78.4
12	302.6	19.6	10.1	21.0	31.7
13	500.9	110.6	10.0	53.3	62.8
14	299.8	200.2	10.0	92.8	91.8
15	101.7	111.3	10.0	96.4	94.3
^d 16	402.7	75.5	10.0	57.2	55.2
^d 17	199.4	128.9	10.0	94.5	95.4

- NOTES: ^a Initial concentration of C₂SO₄ feed was 0.3177 g/L. pH = 2.0
^b Polyaphrons were made with 5 g/L N₂DBS. PVR = 10.
^c CGA flowrate is the volume of the surfactant used to make the CGA, (0.5 ml/L Arquad 12/50).
^d These tests were done after the model was developed.

Table 68. Description of the extractions done with different type of polyaphrons.

Sample ID	Polyaphrons Used ^a (X ₁ , X ₂ , X ₃)	Polyaphron PVR	E ₁ (C ₂ SO ₄ Feed) ^b (ml/min)	E ₂ (Diluted Polyaphrons) ^c (ml/min)	E ₃ (CGA) ^d (ml/min)	% Extraction
1	(300, 30, 1500)	10	302.6	112.1	10.7	82.5
2	(99.9, 9.7, 700)	10	300.3	111.2	10.3	81.2
3	(197.8, 19.8, 700)	10	299.7	110.6	10.4	77.4
4	(24.6, 2.4, 700)	10	299.0	111.1	11.5	77.2
5	(150, 30, 700)	5	300.6	119.8	10.8	81.9
6	(150, 30, 1500)	5	300.6	119.8	10.8	84.6
7	(46, 9.4, 1500)	5	300.6	119.8	10.8	84.7
8	(46, 9.4, 700)	5	300.6	119.8	10.8	82.2
9	(300, 20, 1500)	15	299.5	106.3	11.6	78.2
10	(300, 20, 1500)	15	299.5	106.3	11.6	80.5
11	(49.4, 4.9, 1500)	10	301.1	109.4	10.4	76.7
12	(300, 24.7, 1500)	10	300.5	110.0	9.7	76.2
13	(300, 30, 1500)	10	298.4	111.6	10.6	81.7
14	(300, 30, 1500)	10	305.8	111.3	11.9	60.6

NOTES:

- ^a (X₁, X₂, X₃) represents the conditions used to make the polyaphrons. X₁ = Organic phase flowrate (ml/min), X₂ = Aqueous phase flowrate (ml/min), X₃ = mixing rate (rpm).
- ^b Initial concentration of copper sulfate feed was 0.3177 g/L. pH = 2.0.
- ^c All polyaphrons except those used in tests 13 and 14 were made with 5 g/L NDBS in the aqueous phase and 0.5 ml/L Tergitol 15-5-3 in the organic phase. Test 14 polyaphrons were made with 5 ml/L Arquad 12/50.
- ^d CGA flowrate is the volume of the surfactant used to make the CGA. All CGA except for Test 14 were made of 0.5 ml/L Arquad 12/50. Test 14 CGA were made of 0.5 g/L NaDBS.

8.0 CONCLUSIONS AND RECOMMENDATIONS

8.1 Conclusions

The conclusions of this study are divided into sections according to the subjects dealt with in each chapter.

8.1.1 Residence Time Distribution of the Continuous Polyaphron Generator

The residence time distribution of fluids in an 865 ml continuous polyaphron generator was determined using copper as the tracer. The following conclusion was made from the experimental results:

1. The behaviour of a fluid inside the continuous polyaphron generator was closely modeled by that of a fluid in a continuous stirred tank reactor.

8.1.2 Particle Size Distribution Study

The measurement of the particle size distribution of several batches of polyaphrons made with the continuous polyaphron generator led to the following conclusions:

1. Every method or apparatus used to measure polyaphrons gave a somewhat different particle size distribution.

2. Polyaphrons could not be measured with a Brookhaven Instruments dynamic light scattering system or a coulter counter.
3. According to measurements made with the photo-microscope method, higher mixing rates produced smaller aphrons. According to the measurements made with the SA-CP3 Analyser, this effect was seen only in polyaphrons of PVR 10. Mixing rate had no effect on PVR 5 polyaphrons.
4. An increase in feed flow rates produced larger aphrons. This effect was seen only when the residence times differed by at least 30 minutes. These results were observed with the SA-CP3 and the photo-microscopy measurements.
5. According to the results obtained with the SA-CP3 Analyser, as PVR increases the size of the bubbles decreases. No effect was observed with the photo-microscopy measurements for polyaphrons of PVR 10 and 15. Polyaphrons of PVR 5 showed a decrease in size when compared to the higher PVR ones.
6. Bubble measurements done with the SA-CP3 showed that addition of a surfactant to the organic phase of the polyaphrons decreased the size of the aphrons. The photo-microscopy method of analysis showed no difference.
7. The replacement of Arquad 12/50 for NaDBS as the water soluble surfactant affected the particle size distribution of the polyaphrons. The photo-microscopy method showed that the Arquad 12/50 bubbles were bigger while the SA-CP3 measurements showed that they were smaller.
8. According to photo-microscopy measurements some degree of coalescence takes place over time among the aphrons of PVR 10 and 15. No change was seen in polyaphrons of PVR 5.

9. Results can be reproduced, within experimental error, using the photo-microscopy method.

8.1.3 Conventional Versus Predispersed Solvent Extraction of Copper in a Batch Reactor

From the series of tests done to extract copper from dilute aqueous solutions using conventional solvent extraction and predispersed solvent extraction in an isothermal batch reactor, the following conclusions were made:

1. Predispersed solvent extraction is superior to conventional solvent extraction. Under similar conditions equilibrium conditions were approached faster with PDSE.
2. An increase in temperature from 5°C to 26°C enhanced the extraction. This temperature increase increased the copper extraction by about 10% and the time required to reach equilibrium decreased by about 5 minutes. Increasing the temperature above 26°C had little effect on the extraction process.
3. Increasing the pH of the feed solution from 1.0 to 2.0 increased the percentage of copper extracted by 30%. The time required for the extraction to reach equilibrium also decreased by 18.5 minutes. Increasing the pH further only slightly enhanced the extraction process.
4. Using polyaphrons of different PVR had no effect on the copper extraction.
5. Polyaphrons made with NaDBS and Arquad 12/50 produced similar results.
6. The dynamics of the reaction of copper with LIX-64N at a specific feed concentration can be modeled by the film theory.

7. The mass transfer coefficient calculated from film theory varied with initial feed concentration.

8.1.4 Predispersed Solvent Extraction of Copper with LIX-64N

From the extractions done in continuous mode in a system that consisted of two troughs, one to carry out the extraction part of the process and the other to carry out the flotation part, the following conclusions were made:

1. The extraction process was modeled with the following empirical equation:

$$Y = -15.735X_1 + 29.745X_2 + 6.778X_1X_2 - 16.333X_2^2 + 78.338$$

and $X_1 = 0.005E_1 - 1.5$, $X_2 = 0.01111E_2 - 1.222$

where $Y = \% \text{ Cu extracted}$, $E_1 = \text{CuSO}_4 \text{ Feed Flow rate (ml/min)}$, $E_2 = \text{Diluted Polyaphron Flow rate (ml/min)}$.

2. 99% of the copper was recovered with extractions carried out with a solvent to aqueous ratio 1:2. Extractions carried out with a solvent to aqueous ratio 1:10 resulted in 80 to 85% copper recovery.
3. A minimum amount of CGA equivalent to the volume of bubbles that are made with 10ml/min surfactant solution is required to float the liquid aphrons out of the raffinate. Using larger flowrates than this do not improve the solvent recovery.
4. The same amount of copper is recovered regardless of the type of polyaphrons used to extract the copper from the aqueous phase.
5. The final apparatus designed for this study was an improvement over the other apparatus previously designed but the loss of solvent was still a problem.

8.2 Recommendations for Further Study

The following recommendations for further study are made:

1. Several methods were used to determine the particle size distribution of polyaphrons and each method gave a somewhat different distribution. At this point, it is not possible to determine which method was more accurate. Further study needs to be done to determine the accuracy and reproducibility of results of each method. Also, more tests should be done using Lasentec's PAR-TEC 100 Particle Size Analyzer.
2. The dynamics of the approach to equilibrium of the extraction of copper with LIX-64N was modeled according to the film theory. The theory predicted well the results of each test but, the mass transfer coefficients calculated for each test varied with initial feed concentration. Further study needs to be done in this area to determine why the mass transfer coefficient varied. Also, further emphasis should be put into developing a model that predicts the dynamics of the extraction with the same mass transfer coefficient over a range of initial feed concentrations.
3. The calculation of the equilibrium constant raised some interesting questions. If calculated using the ideal equilibrium expression based on the stoichiometry of the reaction, it varied with initial feed concentration. For this study, equilibrium isotherms were drawn and an empirical relationship was derived to relate the equilibrium concentrations of copper in each phase but, this matter should be studied further.
4. The predispersed solvent extraction process in continuous mode was modeled with an empirical equation. A theoretical model based on mass transfer should be studied.
5. The experimental work done for this study has demonstrated that predispersed solvent extraction is superior to conventional extraction. Batch experiments showed that equi-

librium conditions are approached quicker with PDSE than with conventional extraction. Tests performed in continuous mode demonstrated that PDSE needs lower aqueous to solvent ratios than conventional extraction to recover approximately the same amount of copper. The problem with PDSE continuous to be the amount of solvent that remains in the raffinate. It is recommended that a settling tank be added to the process to minimize solvent loss. In fact, with the addition of the settling tank, the flotation cell could possibly be eliminated from the process with the CGA being fed directly into the extraction cell.

9.0 SUMMARY

Predispersed Solvent Extraction (PDSE), was used to extract copper ions from dilute acidic aqueous solution. PDSE is based on the principle that there is no need to comminute both phases. All that is necessary is to comminute the solvent phase prior to contacting it with the feed. This is done by converting the solvent into aphrons, which are micron-sized globules encapsulated in a soapy film. Since the aphrons are so small, it takes a long time for the solvent to rise to the surface under the influence of gravity alone. Therefore, the separation is expedited by piggy-back flotation of the aphrons on especially prepared gas bubbles, which are somewhat larger than aphrons and are called colloidal gas aphrons (CGA).

The predispersed solvent extraction process was studied in both batch and continuous mode. The batch experiments served to compare the two processes under similar conditions. Also, the particle size distribution of polyaphrons was determined.

9.1 Particle Size Distribution of Polyaphrons

A new polyaphron generator was built to manufacture several batches of polyaphrons. The same basic design as the one developed by Bergeron and Sebba (1987), was kept but some improvements on the old design were made. The residence time distribution of a fluid in the generator was studied using copper for tracer. The fluid behaviour was found to be closely represented by that of a continuous stirred tank reactor model.

Five methods were used to try and determine the size distribution of polyaphrons; one of the methods was sedimentation, one was photo-microscopy, two used dynamic light scattering and the last one was conductivity. An SA-CP3 Particle Size Analyzer manufactured by Shimadzu used the sedimentation method to calculate the particle size distribution. The

photo- microscopy method was implemented by photographing with a Minolta 35 mm camera polyaphron samples under a Zeiss Axioscope microscope. The bubbles in the photographs were counted and measured by hand. A Particle Data Incorporated Electrozone-Celloscope used the conductivity method to size the bubbles, and a Brookhaven Instruments system and Lasentec's PAR-TEC 100 Laboratory Analyzer measured the particle size distribution of the bubbles using dynamic light scattering.

Several batches of polyaphrons were made with a continuous polyaphron generator. The generator was operated at different conditions to make each polyaphron batch. Measurements of the bubbles of several polyaphron batches were made to determine what effect, if any, the conditions under which the bubbles were generated had on their size. The aphrons could not be measured with the Brookhaven Instruments Dynamic Light Scattering apparatus and the Electrozone-Celloscope. The Brookhaven instrument is very sensitive and will measure dust particles found in the sample. Thus, the samples had to be filtered before being analyzed. The aphrons broke down completely when filtered. To measure particle sizes with the Electrozone-Celloscope instrument, the aphrons had to be diluted in an electrolyte solution. Different concentrations of electrolyte gave different size distributions. Aphrons diluted in weak sodium chloride and sodium pyrophosphate solutions were observed under the microscope. The electrolyte solution caused the aphrons to become very active, moving rapidly across the viewing area. Also, most of the aphrons broke down after a few minutes. The particle size distribution of the aphrons was measured with the other three instruments. All three methods gave somewhat different distributions. Of all three, the sedimentation method detected a larger number of smaller aphrons. The average diameter of the aphrons calculated by this method ranged from 0.4 to 2.54 μm . With this method, the accuracy of the results is largely dependent on the accuracy of the density of the particles. Since aphrons entrap air easily, it is difficult to measure their density with high accuracy. With the photo- microscopy method the average diameters were calculated to range from 5.0 to around 9.0 μm . It is suspected that the smaller bubbles could not be seen under the microscope because they were hidden under the larger more buoyant ones. Only one sample was analyzed with Lasentec's

PAR-TEC 100 instrument. The average diameter was calculated to be around 26.0 microns. A large amount of aphron breakage in the sample being analyzed was noticed. Further studies need to be done using this technique.

The effect that the conditions under which the aphrons were generated had on their size was small and sometimes the results varied depending on the method used. The feed flowrate was the one variable that seemed to produce the largest effect. When the residence time of the fluid in the polyaphron generator was increased by at least 30 minutes, the aphrons produced were larger.

9.2 Batch Extractions Using Both Predispersed Solvent Extraction and Conventional Extraction

A series of tests were done to extract copper from dilute aqueous solutions using conventional solvent extraction and predispersed solvent extraction in an isothermal batch reactor. Predispersed solvent extraction was found superior to conventional extraction. For most tests using PDSE equilibrium conditions were approached within 0.5 minute. Some tests done by conventional extraction took longer than 30 minutes. Experiments were carried out at various temperatures, pH, and initial copper feed concentrations to observe the effect of these parameters on the extraction process. Increasing the temperature or increasing the pH enhanced the extraction. The concentration of copper in both the organic and the aqueous phases was obtained over time and the results were used to determine the ultimate equilibrium concentration for each experiment. Empirical equations were developed to relate the equilibrium concentration of copper in both phases. The dynamics of each experiment were modeled according to the film theory.

9.3 Predispersed Solvent Extraction of Copper

Copper extractions were done in continuous mode in a system that consisted of two troughs, one to carry out the extraction part of the process and the other to carry out the flotation part. The extraction apparatus was designed to try and eliminate problems encountered with previous apparatus. The main focus of attention was on diminishing the amount of solvent loss in the aqueous phase. This was accomplished to some extent but, solvent loss continues to be a problem. Several tests were done using various combinations of copper sulfate feed flowrate, diluted polyaphrons feed flowrate, and colloidal gas aphrons feed flowrate to determine the effect of these parameters on the extraction process. The results from these tests were analyzed statistically and an empirical model was developed for the extraction process. The CGA flowrate had no effect on the extraction itself, but it did affect the amount of solvent recovery. The statistical model developed was:

$$Y = -15.735X_1 + 29.745X_2 + 6.778X_1X_2 - 16.333X_2 + 78.338$$

. Where $X_1 = 0.005E_1 - 1.5$ and $X_2 = 0.01111E_2 - 1.2222$ and Y is the percent of copper extracted, E_1 is the copper feed flowrate in ml/min, and E_2 is the diluted polyaphron flowrate in ml/min. Tests were also done using the various batches of polyaphrons that had been generated to determine the size distribution of the bubbles to study the effect of bubble size on the extraction process. No significant differences were noticed in the extraction.

Literature Cited

- Aggarwal, A.J., A. Rodarte, and F. Sebba, (1986), *J. Separation Proc. Tech.*,7, pp. 29-33.
- American Dye Manufacturers Institute (1972). "The Contribution of Dyes to the Metal Content of Textile Mill Effluents," *Text. Chem. Color.*, 4, 275-277.
- Barnes, L.J., F.J. Janssen, J. Sherren, J.H. Versteegh, R.O. Koch, and P.J.H. Scheeren (1991). "A New Process for the Microbial Removal of Sulphate and Heavy Metals from Contaminated Waters Extracted by a Geohydrological Control System", *Chemical Engineering Research and Design*, 69, (A3), 184-186.
- Barrett, W.J., Morneau, G.A., and Roden, J.J. III (1974). *Waterborne Wastes of the Paint and Inorganic Pigment Industries*. U.S. Environmental Protection Agency, U.S. Government Printing Office, Cincinnati, Ohio, p.47.
- Caballero, M., R. Cela, and J.A. Perez-Bustamante (1989). "Studies on the Use of Colloidal Gas Aphrons in Coflotation and Solvent Sublation Processes. A comparison with the Conventional Technique", *Separation Science and Technology*, 24 (9&10), 629-640.
- Cohen, J.M. (1977). *Trace Metal Removal by Wastewater Treatment*. EPA Technology Transfer, January, U.S. Government Printing Office, Region 5-11.
- Geckeler, K.E., V.M. Shkinev, and B.Ya. Spivakov (1988). "Liquid-Phase Polymer-Based Retention (LPR) - A New Method for Selective Ion Separation", *Separation and Purification Methods*, 17 (2), 105-140.
- Golomb, A. (1972). "Application of Reverse Osmosis to Electroplating Waste Treatment. II: The Potential Role of Reverse Osmosis in the Treatment of Some Plating Wastes," *Plating*, 59, 316-319.
- Jones, K.C. and Pyper, R.A. (1979), "Copper Recovery from Acidic Leach Liquors by Continuous Ion-Exchange and Electrowinning," *J. Metals*, 31, 19-25.
- Klepac, J., D.L. Simmons, R.W. Taylor, J.F. Scamehorn, and S.D. Christian (1991), "Use of Ligand-Modified Micellar-Enhanced Ultrafiltration in the Selective Removal of Metal Ions from Water", *Separation Science and Technology*, 26(2), 165-173.
- Kocjan, R. and S. Przeszlakowski (1989), "Retention of Heavy Metals and their Separation on Silica Gel Modified with Calconecarboxylic Acid", *Separation Science and Technology*. 24(3&4), 291-301.
- Merchuk, J.C., Shai, R., and Wolf, D. (1980), "Experimental Study of Copper Extraction with LIX-64N by Means of Motionless Mixers," *Ind. Eng. Chem. Process Des. Dev.*, 19, 91-97.
- Murray, K.J. and Bouboulis, C.J. (1973) How to select organic carriers for optimum copper Recoveries. *Engng. Min. J.* 174(7), 74-77.
- Netzer, A. and Beszedits, S. (1979). "Removal of Copper from Wastewaters," *Copper in the Environment*, 124.

- Roman, R.J., Sheffer, H., Stone, W. (1980), "Copper Leaching Practices in the Western U.S.," *U.S. Bur. Min.*
- Sabacky, B.J. and Evans, J.W. (1979), "Electrodeposition of Metals in Fluidized Bed Electrodes. Part II. An Experimental Investigation of Copper Electrodeposition at High Current Density," *J. Electrochem. Soc.*, 126, 1180-1187.
- Sebba, F., (1963), *Nature*, 197, p. 1195.
- Sebba, F., (1984), *Chem. and Ind.*, 10, p.367.
- Sebba, F., (1985a), *Chem. and Ind.*, 4, p. 91.
- Sebba, F., (1985b), *Separation and Purification Methods*, 14, p. 127.
- Sebba, F., (1987), *Foams and Biliquid Foams — Aphrons*, John Wiley & Sons, Great Britain.
- Sebba, F. and S.M. Barnett, *Proc. 2nd. Int. Conf. Chem. Eng.*, 4, Montreal, Canada, pp. 27-31.
- Sheffer, H.W. and Evans, L.G. (1968), *U.S. Bur. Min. Inf. Cir.* 8341.
- Shimizu, K. and Furuhashi, A. (1984). "Solvent Extraction of Copper(II) with 2-(o-Hydroxyphenyl)benzothiazole," *Bull. Chem. Soc. Jpn.*, 57, 3593-3594.
- Srinivasan, V. and M. Subbaiyan (1989), "Electroflotaion Studies on Cu, Ni, Zn, and Cd with Ammonium Dodecyl Dithiocarbamate", *Separation Science and Technology*, 24(1&2), 145-150.
- Stalidis, G.A., K.A. Matis, and .K. Lazaridis (1989), "Selective Separation of Cu, Zn, and As from Solution by Flotation Techniques", *Separation Science and Technology*, 24 (1&2), 97-109.
- Stalidis, G.A., N.K. Lazaridis, and K.A. Matis (1989), "Continuous Precipitate Flotation of CuS/ZnS", *Separation Science and Technology*, 24(12&13), 1033-1046.
- Thurlow and Associates (1977). Literature Review of Wastewater Characteristics and Abatement Technology in the Wood and Timber Processing Industry. Fisheries and Environment of Canada , Rep.EPS 3-WP-77-2, Ottawa, Ont.
- Vijayalakshmi, C.S., Annapragada, A.V., and Gulari, E. (1990), "Equilibrium Extraction and Concentration of Multivalent metal Ion Solutions by Using Winsor II Microemulsions", *Separation Science and Technology*, 25(6), 711-727.
- Warnke, J.E., Thomas, K.G., and Creason, S.C. (1977). "Wastewater Reclamation Systems Ups Productivity, Cuts Water Use," *Chem. Eng.*, 84(7), 75-77.
- Warwick, G.C.I., Schuffham, J.B. and Lott, J.B. (1970) Solvent Extraction - Today's Exciting Process for Copper and Other Metals. *World Mining*, 23(11), 46-52.
- Wodzki, R., A. Wyszynska, and A. Narebska (1990), "Two-Component Emulsion Liquid Membranes with Macromolecular Carriers of Divalent Ions", *Separation Science and Technology*, 25(11&12), 1175-1187.
- Zamzow, M.J., B.R. Eichbaum, R. Sandgren, and D.E. Shanks (1990), "Removal of Heavy Metals and Other Cations from Wastewater Using Zeolites", *Separation Science and Technology*, 25(13- 15), 1555-1569.

Appendix A. Polyaphrons

Polyaphrons or oil core aphrons are a type of biliquid foam which consists of micron-sized oil droplets encapsulated in an aqueous shell. A diagram of the structure of an oil core aphron is depicted in Figure A1. Polyaphrons are made by spreading an oil (internal phase) which contains an oil-soluble surfactant dissolved in it, on the surface of water that has a water-soluble surfactant dissolved in it. As the oil spreads on the water, the oil film becomes so thin that movements of the mixture will allow the water to break through various points of the thin film eventually breaking it up to form minute droplets. When this happens, the water, which has a low contact angle induced by the dissolved surfactant, climbs onto the oil droplets and somehow spreads around it, eventually encapsulating the oil droplet with a soapy shell (Sebba, 1987).

The diameter of polyaphrons will vary from submicrometer to about $100\mu\text{m}$. The size will depend on the type and concentration of surfactants used. The higher the concentration of the surfactant in the oil phase, the smaller the aphrons will be.

It has been found useful to describe polyaphrons in terms of the phase volume ratio (PVR). PVR is the volume ratio of the dispersed oil phase to the continuous phase. Therefore, a polyaphron containing 100 parts of kerosene to 10 parts water, has a PVR of 10. Properly made polyaphrons of PVR 5 to 19 are very stable and can be kept for very long periods of time (two years or more).

Polyaphrons can be made by hand or with a continuous polyaphron generator. If made by hand, all that is needed is a stoppered bottle. The aqueous phase is placed in the bottle and the closed bottle is vigorously shaken to form a foam. Small amounts of oil at a time are added to the foam until all the oil has been added. After each addition of oil, the bottle is shaken to break up the oil film. The quantity of oil that can be added at a time is limited because the environment of the aphrons that have already been formed must remain aqueous.

If not, the aphrons congeal and no longer offer an interface for spreading (Sebba, 1987). Polyaphrons can be made very easy and quickly using the continuous polyaphron generator. The generator must first be seeded with some previously made polyaphrons and then it is just a matter of setting the organic and aqueous phase pumps at the required flow rates. Polyaphrons of PVR 5 to 20 have been made using both techniques.

Polyaphrons, used together with CGA, form the basis for PDSE. In conventional solvent extraction mass transfer of the solute across the interface is achieved by vigorous mixing of the aqueous and solvent phases. On the other hand, in PDSE the solvent phase is aphronized before contacting it with the aqueous phase. The small size of the aphrons generates a tremendous amount of surface area so that when the aphrons are contacted with the aqueous phase the individual aphrons distribute themselves throughout the aqueous phase, eliminating the need of vigorous mixing.

A detailed description of the properties of polyaphrons and its applications can be found in *Foams and Biliquid Foams — Aphrons* (Sebba, 1987).

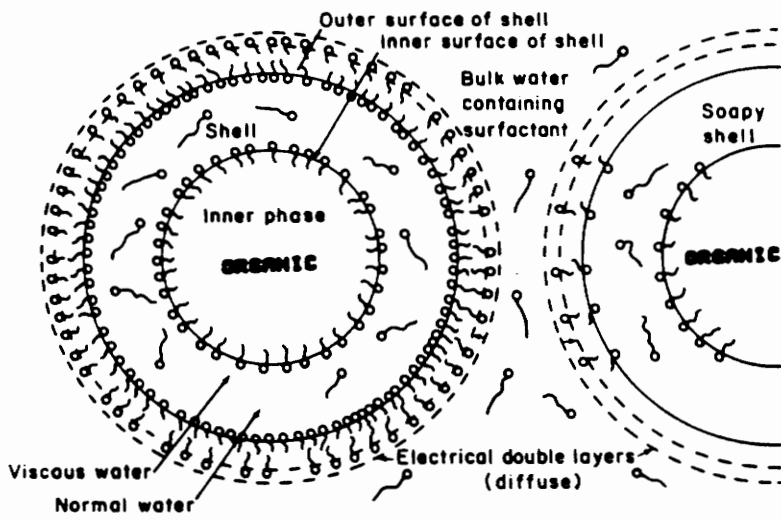


Figure A1. Structure of an oil core aphron

Appendix B. Colloidal Gas Aphrons

Colloidal gas aphrons (CGA), are micron sized gas bubbles encapsulated by a shell of aqueous soapy film. This film introduces such a strong barrier to coalescence that coalescence never occurs as long as the bubbles are completely immersed in water. The structure of a CGA is illustrated in Figure B1. The size of CGA are in the order of 25 - 50 μ m in diameter. CGA with diameters smaller than 25 μ m have never been observed in the laboratory. This might be because they are too small to be seen under a powerful microscope or because the smaller bubbles burst very fast due to the fact that the pressure inside a bubble is inversely proportional to its diameter. Because of the small size of the bubbles, they float to the surface very slowly. Therefore, the CGAs have a long enough life-time that they can be generated in one place and pumped to another.

CGA are made very quickly using a CGA generator and a dilute surfactant solution. The generator works under the principle that when a disc, fixed to a vertical shaft connected to an electrical motor, is made to rotate at a speed of 4,000 r.p.m. or more; strong waves of surfactant solution are produced at the surface. These waves strike the baffles, mounted vertically around the disc; and on re-entering the water they entrain the gas in the form of very small bubbles. CGA containing up to 65% of gas in water are very rapidly and easily made.

CGA have been found useful in many separation processes such as PDSE, ion and precipitate flotation, bubble-entrained floc flotation, and separation of oil from sand (Sebba, 1987). Most of its applications depend upon the following properties:

1. The buoyancy of the encapsulated gas
2. Adherence of particles to the encapsulating shell
3. Low viscosity of the system

4. Large surface area produced by the small size of the bubbles.

Detailed information on CGA properties and applications can be found in *Foams and Biliquid Foams — Aphrons* (Sebba, 1987).

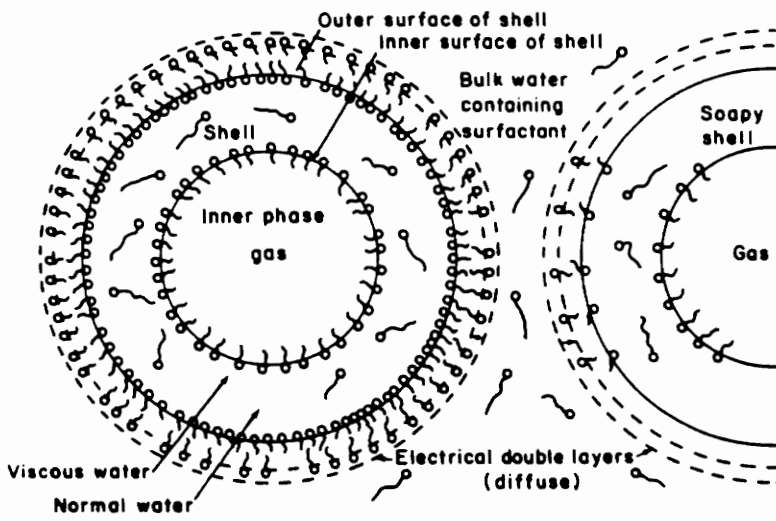


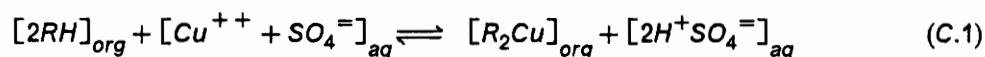
Figure B1. Structure of a colloidal gas aphron

Appendix C. Some Facts About LIX- 64N

LIX 64N is an alpha-hydroxyoxime designed specifically for the extraction of copper from aqueous solutions. The extractant is a mixture of 2 - hydroxy - 5 - nonylbenzo - phenoneoxime, and 5,8 - diethyl - 7 - hydroxydodecan - 6 - oxime in kerosene. The extractant and its copper complex are insoluble in water and are characterized by having a solubility of at least 2 weight percent in the hydrocarbon that constitutes the organic phase. LIX reagents are used by numerous commercially successful metal recovery operations around the world. Figure C1 illustrates some molecular structures of some LIX reagents.

LIX-64N is a dark amber liquid with a kerosene odor. Its boiling point is 240°C and it has a density of 0.980 g/cc.

The chelating action of LIX-64N can be represented in an equation form as:



As can be seen, the reaction is reversible, but for the reverse reaction to be important, the pH has to be in the range of 0.5 to 0.9.

LIX-64N is no longer being manufactured by Henkel Corporation. Instead, they are manufacturing LIX-84 and LIX-894 which they consider to be better copper extractants than LIX-64N.

Appendix D. Sample Calculation for Determination of Percent of Copper Extracted in the Continuous Process.

To determine the percent of copper extracted for a particular test, the dilution factor due to the water from the CGA and the diluted aphrons had to be taken into account. The percent extraction calculation for Test 4 follows.

PVR of polyaphrons:	10
Copper feed flowrate:	298.6 ml/min
Surfactant flowrate:	54.9 ml/min
Diluted aphrons flowrate:	110.0 ml/min
Initial feed concentration:	0.005 mol/L
Final copper concentration:	0.000647 mol/L

Since to 1 volume of aphrons 3 volumes of water were added, of the 110.0 ml/min diluted aphrons, 27.5 ml were aphrons and 82.5 ml were water. But, the aphrons contained some water; therefore,

$$\text{Water in aphrons} = \frac{27.5}{11} = 2.5 \text{ ml} \quad (\text{PVR} = 10)$$

$$\text{Total water added to system by diluted polyaphron flowrate} = 85.0 \text{ ml/min}$$

Then, the copper concentration in the aqueous phase after dilution is,

$$\text{Cu Feed concentration} = \frac{\text{Cu flow rate}}{(\text{Cu flow rate} + \text{surfactant flowrate} + \text{water from diluted aphrons})}$$

$$\frac{(0.005 \text{ mol/L}) \times (298.6 \text{ ml/min})}{(298.6 + 54.9 + 85.0) \text{ ml/min}} = \frac{0.00340 \text{ mol copper}}{L}$$

Thus,

$$\begin{aligned}\% \text{extraction} &= \frac{(\text{Initial Concentration} - \text{Final Concentration})}{(\text{Initial Concentration})} \times 100 \\ &= \left(\frac{0.00340 - 0.000647}{0.00340} \right) \times 100 = 80.97\%\end{aligned}$$

Appendix E. Sample Preparation for Copper Determination with Atomic Absorption Spectrophotometer (AAS)

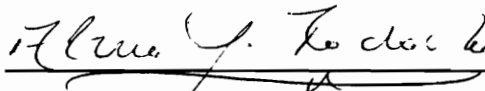
To determine the concentration of copper in the organic and aqueous phases, standards were made. The aqueous standards were made from Fisher copper reference standard solution. The organic standards were made from a 1,000 ppm copper solution prepared in the following way:

A 1,000 ppm copper solution in water was made. Enough ammonium hydroxide was added to the aqueous solution to turn it a deep blue color. The aqueous solution was contacted with an equal volume of a 10% LIX-64N in kerosene solution. The mixture was shaken vigorously for ten minutes. The phases were separated in a separatory funnel. The aqueous phase was analyzed for copper and the organic phase concentration was determined by doing a mass balance.

All the samples analyzed had to contain between 0.1 and 1.0 ppm of copper. Outside this range the copper concentration is no longer linear with respect to the absorbance. Thus, all the samples had to be diluted before being analyzed. The dilution factor sometimes had to be up to 1000. Therefore, mechanical micropipetters with disposable tips were used to do the dilutions.

Vita

Alma Isabel Marín Rodarte, daughter of Gustavo A. and Alma Marín, was born December 17, 1950 in Tiquisate, Guatemala. She received an Associate of Science degree in Engineering and in Business from Tidewater Community College in Virginia Beach, Virginia in June, 1983. Immediately after, she entered Virginia Polytechnic Institute & State University where she received a Bachelor of Science in Chemical Engineering in June, 1985, and a Master of Science in Chemical Engineering in December, 1988. She is married to Walter E. Rodarte and has a daughter, Karla Isabel. Upon completion of this degree, she will begin a career with Texaco at the Port Arthur Research Laboratories in Port Arthur, Texas.



Alma I. Rodarte